

Engineering *Corynebacterium glutamicum* for the Production of Itaconic Acid from an Acetate-Containing Aqueous Sidestream of Fast Pyrolysis

Marc Pascal Schmollack

Vollständiger Abdruck der des TUM Campus Straubing für Biotechnologie und
Nachhaltigkeit der Technischen Universität München zur Erlangung eines

Doktors der Naturwissenschaften (Dr. rer. nat.)

genehmigten Dissertation.

Vorsitz: Prof. Dr.-Ing. Michael Zavrel

Prüfende der Dissertation:

1. Prof. Dr. Bastian Blombach
2. Prof. Dr. rer. nat. Volker Sieber

Die Dissertation wurde am 11.10.2023 bei der Technischen Universität München eingereicht
und durch den TUM Campus Straubing für Biotechnologie und Nachhaltigkeit am 20.02.2024
angenommen.

Motivation

The post-World War II period, also referred to as the “Great Acceleration”, marks the beginning of the Anthropocene, a new geological epoch in which human impact on the Earth exceeds that of natural forces [53, 67]. It is characterized by an instantaneous rapid increase in various socio-economic and Earth-system based indicators used to measure population, economic growth, globalization, use of resources, and human impact on the environment [254]. However, the rapid socio-economic growth of humanity during the Great Acceleration has been accompanied by an enormous consumption of primary energy, mainly provided by burning coal and oil [225, 243, 254]. The resulting increase in the release of the greenhouse gas CO₂, as well as other climate-active gases derived from growing industry and agriculture, has induced rapid global warming and is responsible for the climate crisis we find ourselves in today [157, 308].

Today more than ever, the world's population is suffering the consequences of men-made climate change. Rising global surface temperatures are contributing to the spread of disease [248, 303], more frequent droughts, storms and floods [62, 273], water and food shortages [182], increased global migration [17, 215], and extinction of more and more species [229, 276]. To restrict the negative impacts of climate change, the global community agreed in 2015 in the Paris Climate Agreement to limit the rise of the global temperature to 1.5 °C. To achieve this goal, the major industrialized countries, especially, must overcome their dependence on fossil fuels and reset their economies in favor of greener and more sustainable technologies to reduce greenhouse gas emissions rapidly and effectively [66]. To this end, almost 60 countries self-proclaimed to support a policy oriented towards bioeconomy and to invest in local and macro-regional projects in this field. On the other hand, only 19 countries, most of them in the European Union, have actually implemented national bioeconomy strategies [42], with the European Union itself developed such a strategy in 2012 [5]. In this process of economic transformation biotechnology plays a crucial role by enabling the conversion of renewable resources such as biomass into fuels and platform chemicals, which can replace petroleum-based derivatives in the chemical industry and in our daily lives. With this work, we contribute to the biotechnological production of platform chemicals from organic non-food substrates and thus make a small contribution to achieving the international climate goals and the sustainable preservation of the environment and our planet.

Acknowledgments

First of all, I would like to thank my Ph.D. supervisor Prof. Dr. Bastian Blombach, for giving me the opportunity to work on this exciting project of high socio-economic importance, and whose broad knowledge and encouragement helped me to deepen my scientific expertise in the field of biotechnology. During my time as a Ph.D. student, Bastian Blombach was not only a great supervisor, but his modern leadership style also created a supportive working atmosphere that allowed for fruitful discussions on an equal footing. In this context, I would also like to thank Prof. Dr. Erich Glawischnig, who accompanied me as a mentor throughout my doctoral studies. His fundamental theoretical and practical knowledge, especially in the field of microbiology, helped me to realize this work. Further, I would also like to thank Dr. Daniel Siebert, who introduced me to the practical side of the work and was always available for result-oriented discussions about the project. In particular, I wish to thank all my colleagues from the MIB research group, whom I, unfortunately, cannot name here. They have contributed to a constructive working atmosphere and have become like a second family. I would like to express my thanks to all the students I had the privilege to supervise and who contributed to the progress of this project with the right mixture of fun and seriousness. Further, I am extremely grateful to so many people in my private life, my friends and my family, who have supported me mentally throughout my studies, relieved me in difficult times and helped me whenever I needed it. Only with them could I get this far. Further thank goes to Prof. Dr. Michael Bott from the Research Center Jülich for providing the plasmid “pEKEx2-*malE*_{opt}” and Prof. Dr. Nicolaus Dahmen and Dr. Axel Funke from the KIT Institute for Catalysis Research for providing the acetate-containing sidestream from the bioliq[®] process. I also thank Dr. Richa Bharti and Prof. Dr. Dominik Grimm from the TUM Campus Straubing for processing the raw data of transcriptome analysis, which was performed in the scope of this work. Special thanks go to Manuel Merkel, Dirk Kiefer, Dr. Marius Henkel and Prof. Dr. Rudolph Hausmann from the Department of Bioprocess Engineering at the University of Hohenheim, who performed large-scale cultivations of our strains as part of the “ValProWa” project network. Last but not least, I would like to thank once more Prof. Dr. Bastian Blombach and PD Dr. Katrin Ochsenreither for proofreading and commenting on the first drafts of this work.

Associates and Students Involved in this Work

The present thesis was written by myself. However, within the framework of the project network “ValProWa”, several people were involved in the planning, execution, evaluation and interpretation of the experiments and the data obtained. Listed below are the persons whose participation had a direct impact on the project described in this thesis. Prof. Dr. Bastian Blombach and Dr. Daniel Siebert as supervisors and project and laboratory managers were involved in the planning of the experiments and the interpretation of the results. The maintenance of the equipment and the preparation of the stock solutions was mainly done by Janine Huber, Sebastian Roth and Annette Weiske. Felix Werner was involved in cloning and performing bioreactor experiments. Clarissa Schulze was also involved in the latter. Manuel Merkel, Dirk Kiefer, Dr. Marius Henkel, and Prof. Dr. Rudolph Hausmann of the University of Hohenheim (Hohenheim, Germany) performed large-scale cultivations of the strains generated in this work. The analysis of the transcriptome data was performed by Dr. Richa Bharti and Prof. Dr. Dominik Grim of the TUM Campus Straubing (Straubing, Germany). Raw pyrolysis water was provided by Prof. Dr. Nicolaus Dahmen and Dr. Axel Funke of the KIT (Eggenstein-Leopoldshafen, Germany). The pEKEx2-*malEcad*_{opt} plasmid was provided by Prof. Dr. Michael Bott of the FZ Jülich (Jülich, Germany). In the context of this study, several bachelor theses were carried out by the following students

- **Maria Vogt (2021).**
Expression of Itaconate Transporters and Genomic Integration of *cis*-Aconitate Decarboxylase for Itaconate Production in *Corynebacterium glutamicum*.
- **Paul Derrer (2021).**
Engineering and Characterization of *Corynebacterium glutamicum* Mutant Strains for Improved Metabolization of Acetol.
- **David Jocher (2022).**
Production of Itaconic Acid from Pyrolysis Water with Genetically Engineered *Corynebacterium glutamicum*.

List of Publications

The project work presented in this thesis was funded by the German Federal Ministry of Education and Research (BMBF) under grant number 031B0673C as part of the “ValProWa” project network. In the context of various project meetings and reports, the progress of the project was reported internally. Parts of this project have been made available to the public in the publications listed below and have been incorporated, in part, identically into this thesis.

Peer-Reviewed Journals:

- Merkel, M., Kiefer, D., **Schmollack, M.**, Blombach, B., Lilge, L., Henkel, M., & Hausmann, R. (2022). Acetate-Based Production of Itaconic Acid with *Corynebacterium glutamicum* using an Integrated pH-Coupled Feeding Control. *Bioresource Technology*.
- **Schmollack, M.**, Werner, F., Huber, J., Kiefer, D., Merkel, M., Hausmann, R., Siebert, D. & Blombach, B. (2022). Metabolic Engineering of *Corynebacterium glutamicum* for Acetate-Based Itaconic Acid Production. *Biotechnology for Biofuels and Bioproducts*.

Talks and Presentations:

- **Schmollack, M.**, Siebert, D & Blombach, B. (2021). Production of Itaconic Acid from a Bio-Refinery Sidestream with *C. glutamicum*. *Public University Seminar Talk, Straubing, Germany (online)*.
- **Schmollack, M.**, Siebert, D & Blombach, B. (2022). Engineering *Corynebacterium glutamicum* for the Production of Itaconic Acid from Acetate. *Conference of Key Technologies in the Bioeconomy, Straubing, Germany*.

Posters:

- **Schmollack, M.**, Siebert, D & Blombach, B. (2022). Engineering *Corynebacterium glutamicum* for the Production of Itaconic Acid from Acetate. *VAAM Annual Conference, Düsseldorf, Germany (online)*.

Abstract

Biotechnology is an essential cornerstone of a holistic bioeconomy strategy based on renewable resources. Biotechnological processes are capable of producing high-value products and platform chemicals from a variety of organic and inorganic carbon sources and can provide the chemical industry with building blocks derived from biogenic rather than fossil resources. However, to date, most biotechnological processes rely on sugars and sugar-rich substrates and compete directly with human and animal food and feed production. Recently, much research has been devoted to alternative substrates to overcome these ethical concerns of biotechnology. One of these future substrates could be the aqueous side stream of fast pyrolysis, referred to as pyrolysis water in this work. Fast pyrolysis is a method of decomposing lignocellulosic biomass to produce an energy-rich bio-crude oil intended for fuel production and as a substitute for fossil oil. During this process, the residual moisture of the converted biomass is separately condensed, resulting in the production of pyrolysis water. The pyrolysis water, however, contains a significant amount of carbon and energy, mainly in the form of small hydrophilic molecules. The pyrolysis water used in this work consists mainly of acetol and acetate, the latter of which has been shown to be an attractive substrate for various microorganisms.

Corynebacterium glutamicum is a well-established industrial production host optimally suited for the valorization of acetate. However, information on its acetol metabolism is scarce. Therefore, in this work, we investigated the utilization of acetol as a (co-)substrate by *C. glutamicum* ATCC 13032. We found that *C. glutamicum* was not able to grow efficiently on 5 g acetol L⁻¹ as the sole carbon and energy source, but suitable growth could be achieved by supplementing 10 g glucose or 10 g acetate L⁻¹. Interestingly, we observed a fairly linear disappearance of acetol from the culture supernatant in all cultures. Altered biomass yields and substrate uptake rates indicated that *C. glutamicum* could utilize acetol as a carbon and energy source when glucose was provided as a co-substrate. This effect was not observed when glucose was substituted by acetate. Bioreactor cultivations pointed out that the acetol metabolism in *C. glutamicum* strongly depends on a sufficient oxygen supply. Subsequent transcriptome sequencing revealed that a putative NADPH-dependent quinone:oxidoreductase encoded by cg3290 is highly significantly up-regulated in the presence of acetol during growth on glucose. Deletion of cg3290 increased the resistance of *C. glutamicum* towards acetol during growth on glucose, but decreased its intrinsic growth rate on acetate. In addition, we tested the

overexpression of several enzymes reported to catalyze different reactions for converting acetol to pyruvate. However, neither single nor simultaneous overexpression from synthetic operons resulted in increased acetol uptake. Overall, these results provide important information for further studies on the acetol metabolism in *C. glutamicum* and other microorganisms.

In parallel, we engineered *C. glutamicum* to convert acetate into the valuable platform chemical itaconic acid. Itaconic acid is an unsaturated dicarboxylic acid that can be used for various medical and chemical purposes, and its unique structure makes it particularly interesting for the polymer industry. In this work, we performed metabolic engineering to implement the production of itaconic acid from acetate in *C. glutamicum* and optimized the production regarding titers and yields. Therefore, we used plasmid-based expression of an engineered *cis*-aconitate decarboxylase from *Aspergillus terreus* published by other authors prior to this work. We showed that altered carbon flux to gluconeogenesis, overexpression of *ramA*, *gltA*, and *noxE*, and deletion of *acnR* are negligible for increased itaconic acid production by *C. glutamicum*. Neither the expression of itaconic acid transporters nor the genomic integration of the gene encoding the optimized *cis*-aconitate decarboxylase construct nor the application of phosphate limitation showed a reasonable increase in the desired product. In contrast, the reduction of isocitrate dehydrogenase activity, reduction of glyoxylate shunt enzymes by deletion of *ramB*, and disruption of nitrogen signaling and assimilation strongly increased the production of itaconic acid in the engineered strains. In addition, nitrogen limitation, increased substrate concentrations, and reduced cultivation temperatures during the production further promoted the final levels of itaconic acid. Finally, we identified *C. glutamicum* $\Delta ramB \Delta gdh$ IDH^{R453C} (pEKEx2-*malEcad*_{opt}), in this work referred to as *C. glutamicum* ITA24_{ATG}, as the best-producing strain obtaining a final titer of 5.01 ± 0.67 g itaconic acid L⁻¹ with a yield of 116 ± 15 mmol mol⁻¹ during shaking flask fermentation from 20 g acetate L⁻¹ under nitrogen limitation at 25 °C after 72 h. This yield represents 35% of the theoretical maximum and is the highest yield of itaconic acid produced from acetate reported to date. Ultimately, we demonstrated that our engineered strain was able to grow on pretreated pyrolysis water and efficiently valorize the contained low-value carbon into the bulk chemical itaconic acid.

Zusammenfassung

Die Biotechnologie ist ein wichtiger Eckpfeiler einer ganzheitlichen Bioökonomie-strategie. Biotechnologische Verfahren ermöglichen die Versorgung der chemischen Industrie mit Bausteinen aus biogenen Ressourcen und können so den Einsatz fossiler Rohstoffe verringern. Bisher basieren die meisten biotechnologischen Prozesse jedoch auf der Umwandlung von Zucker und zuckerhaltigen Substraten und stehen daher in direkter Konkurrenz zur Nahrungs- und Futtermittelproduktion. Um dieses ethische Problem zu überwinden, wird intensiv an der Verwendung von alternativen Substraten geforscht. Eines dieser zukünftigen Substrate könnte das wässrige Nebenprodukt der Schnellpyrolyse sein. Die Schnellpyrolyse ist ein Verfahren zur Umwandlung von Biomasse in ein energiereiches Bio-Rohöl. Dabei wird die Restfeuchtigkeit der eingesetzten Biomasse gesondert als Schwelwasser kondensiert. Letzteres enthält jedoch weiterhin hohe Mengen an Kohlenstoff und Energie, gespeichert in Form kleiner hydrophiler Moleküle. Das in dieser Arbeit verwendete Schwelwasser stammt aus dem Bioliq® Prozess und enthält hauptsächlich Acetol und Acetat, wobei sich Acetat bereits als attraktives Substrat für verschiedene Mikroorganismen erwiesen hat.

Corynebacterium glutamicum ist ein etablierter industrieller Produktionswirt, der sich hervorragend für die Verwertung von Acetat eignet. Über seinen Acetolstoffwechsel ist jedoch wenig bekannt. In dieser Arbeit haben wir deshalb die Assimilation von Acetol in *C. glutamicum* ATCC 13032 genauer untersucht. *C. glutamicum* war nicht in der Lage effektiv auf 5 g Acetol L⁻¹ als alleinige Kohlenstoff- und Energiequelle zu wachsen. Das Wachstum konnte jedoch durch die Zugabe von 10 g Glucose oder 10 g Acetat L⁻¹ stimuliert werden. Interessanterweise wurde bei allen Kulturen eine lineare Abnahme von Acetol aus dem Medium beobachtet. Veränderte Biomasseerträge und Substrataufnahmeraten in Anwesenheit von Glucose, nicht aber von Acetat, deuten darauf hin, dass *C. glutamicum* in der Lage ist, Acetol unter bestimmten Bedingungen als Kohlenstoff- und Energiequelle zu nutzen. Vergleiche zwischen Kultivierungen im Schüttelkolben und im Bioreaktor lassen vermuten, dass die Nutzung von Acetol stark von der Sauerstoffversorgung abhängt. Eine Sequenzierung des Transkriptoms ergab, dass eine putative NADPH-abhängige Chinon:Oxidoreduktase, kodiert von cg3290, während des Wachstums auf Glucose in Gegenwart von Acetol signifikant hochreguliert wurde. Die Deletion von cg3290 erhöhte die Toleranz von *C. glutamicum* gegenüber Acetol während des Wachstums mit Glucose im Schüttelkolben, reduzierte jedoch seine

intrinsische Wachstumsrate auf Acetat. Zusätzlich testeten wir die Überexpression verschiedener Enzyme, um einen synthetischen Abbauweg von Acetol zu Pyruvat zu implementieren. Insgesamt liefern die erhaltenen Ergebnisse wichtige Informationen für zukünftige Untersuchungen des Acetolstoffwechsels in *C. glutamicum* und anderen Mikroorganismen.

Parallel dazu haben wir *C. glutamicum* metabolisch so verändert, dass es in der Lage ist Acetat in die Plattformchemikalie Itaconsäure umzuwandeln. Itaconsäure ist eine ungesättigte Dicarbonsäure, die in einer Vielzahl von medizinischen und chemischen Anwendung eingesetzt werden kann. Aufgrund ihrer chemischen Struktur ist sie vor allem für die Polymerindustrie von besonderem Interesse. In dieser Arbeit haben wir die Produktion von Itaconsäure hinsichtlich Titer und Ausbeuten optimiert. Dabei wurde die initiale Itaconsäure-Produktion durch eine Plasmid basierte Expression einer optimierten *cis*-Aconitat Decarboxylase aus *Aspergillus terreus*, die bereits von anderen Autoren publiziert wurde, erreicht. Wir konnten zeigen, dass ein veränderter Kohlenstofffluss in die Gluconeogenese, die Überexpression von *ramA*, *gltA* und *noxE*, sowie die Deletion von *acnR*, für eine Erhöhung der Itaconsäure Produktion in *C. glutamicum* unerheblich ist. Außerdem führten weder die Expression von Itaconsäure Transportern, noch die genomische Integration des Gens für die optimierte *cis*-Aconitat Decarboxylase, noch eine Phosphatlimitierung zu einer zufriedenstellenden Ausbeute des gewünschten Produktes. Im Gegensatz dazu führten die Reduktion der Aktivität der Isocitrat-Dehydrogenase, die Reduktion der Enzymaktivität im Glyoxylat-Shunt durch eine Deletion von *ramB* und die Störung der Stickstoffsignalisierung und -assimilation zu einem starken Anstieg der Itaconsäure-Produktion in den entsprechend mutierten Stämmen. Zusätzlich förderten die Limitierung von Stickstoff, eine erhöhte Substratkonzentration und eine reduzierte Kultivierungstemperatur während der Produktion die finalen Ausbeuten an Itaconsäure. Schließlich identifizierten wir *C. glutamicum* $\Delta ramB \Delta gdh$ IDH^{R453C} transformiert mit pEKEx2-*malE*cad_{opt} (*C. glutamicum* ITA24_{ATG}), als den besten Stamm mit einer Ausbeute von $116 \pm 15 \text{ mmol mol}^{-1}$ und einem Endtiter von $5,01 \pm 0,67 \text{ g Itaconsäure L}^{-1}$ bei der Kultivierung im Schüttelkolben mit $20 \text{ g Acetat L}^{-1}$ unter Stickstofflimitierung, bei 25 °C für 72 h. Die erreichte Ausbeute entspricht 35 % des theoretischen Maximums und ist die höchste bisher erreichte Ausbeute an Itaconsäure aus Acetat. Zuletzt konnten wir zeigen, dass der von uns entwickelte Stamm in der Lage ist, auf vorbehandeltem Schwelwasser zu wachsen und den darin enthaltenen niederwertigen Kohlenstoff effizient in Itaconsäure umzusetzen.

Table of Content

Motivation.....	I
Acknowledgments	II
Associates and Students Involved in this Work	III
List of Publications.....	IV
Abstract.....	VI
Zusammenfassung.....	VIII
Table of Content.....	X
List of Figures.....	XII
List of Tables	XIII
List of Abbreviations	XIV
1 Introduction	17
1.1 Biotechnology at a Glance	17
1.2 Alternative Substrates in Biotechnology	19
1.2.1 Acetate and Acetol Generated by Fast Pyrolysis	21
1.3 Industrial Host: <i>Corynebacterium glutamicum</i>	23
1.3.1 Metabolization of Acetol.....	24
1.3.2 Acetate Metabolization and its Regulation	26
1.3.3 Nitrogen Assimilation and its Regulation	32
1.4 Itaconic Acid.....	34
1.4.1 Native and Artificial Producers of Itaconic Acid.....	35
1.5 Aims of this Work.....	38
2 Material and Methods.....	41
2.1 Cloning Procedures.....	41
2.1.1 Recombinant DNA Work.....	41
2.1.2 Bacterial Transformation.....	42
2.2 Cultivation and Growth Condition	43

2.2.1	Media and General Cultivation Conditions.....	43
2.2.2	Growth Experiments	45
2.3	Intracellular Analysis	46
2.3.1	Determination of Itaconic Acid Concentrations.....	46
2.3.2	Determination of <i>cis</i> -Aconitate Decarboxylase activity	47
2.4	Analytics	48
2.4.1	HPLC Measurements	48
2.4.2	Total Carbon Measurement.....	48
2.4.3	Determination of Nitrogen Concentrations	49
2.4.4	Calculations and Statistics.....	49
2.5	Next Generation Sequencing	50
2.6	Processing of Pyrolysis Water	51
3	Results.....	53
3.1	Studies on Acetol Metabolization.....	53
3.1.1	Investigation of Culture Conditions for Growth on Acetol.....	54
3.1.2	Growth on Acetol as co-Substrate with Glucose and Acetate.....	56
3.1.3	Whole Transcriptome Analysis	59
3.1.4	Implementing Synthetic Operons for Acetol Degradation.....	63
3.1.5	Adaptive Laboratory Evolution.....	65
3.2	Production of Itaconic Acid	65
3.2.1	Inhibition of Isocitrate Lyase by Itaconic Acid.....	66
3.2.2	Enabling Itaconic Acid Production from Acetate	67
3.2.3	Metabolic Engineering to Improve Production of Itaconic Acid	69
3.2.4	Spontaneously Evolved Strains	80
3.2.5	Optimization of Cultivation Conditions	81
3.3	Itaconic Acid Production from Pyrolysis Water and other Substrates	87
4	Discussion	91
4.1	Metabolization of Acetol by <i>C. glutamicum</i>	92
4.2	Acetate-Based Production of Itaconic Acid.....	99
4.3	Conclusion and Outlook	113
	List of References	CXV
	Appendix.....	CXXXIV

List of Figures

Figure 1-1: Illustration of the Different Colors of Biotechnology.....	18
Figure 1-2: Scheme of the Fast Pyrolysis Process.	22
Figure 1-3: Predicted Pathways for the Metabolization of Acetol.....	26
Figure 1-4: Overview of the Acetate Metabolism in <i>C. glutamicum</i>	28
Figure 1-5: Nitrogen Metabolism and Signaling in <i>C. glutamicum</i>	33
Figure 3-1: Growth and Uptake of Acetol by <i>C. glutamicum</i>	54
Figure 3-2: Cultivation of <i>C. glutamicum</i> ATCC 13032 on Glucose, Acetate and Acetol.	58
Figure 3-3: Growth Inhibition of <i>C. glutamicum</i> by Itaconate.	67
Figure 3-4: Comparison of Nitrogen and Phosphate Limitations during IA Production.....	68
Figure 3-5: Growth of <i>C. glutamicum</i> with Attenuated IDH Activities.	72
Figure 3-6: Nitrogen Assimilation by <i>C. glutamicum</i> ITA15 and ITA19.	75
Figure 3-7: Shaking Flask Cultivation of the Final <i>C. glutamicum</i> ITA24 Strains.	79
Figure 3-8: Shaking Flask Cultivation with NaHCO ₃ and PCA.....	82
Figure 3-9: Growth and Itaconic Acid Production at Different Cultivation Temperatures.....	84
Figure 3-10: Intracellular Itaconic Acid Concentrations and <i>cis</i> -Aconitate Decarboxylase Activities.	86
Figure 3-11: Itaconic Acid Production from Alternative Substrates.	88
Figure 4-1: Genealogical Tree of Engineered <i>C. glutamicum</i> ITA Strains.	101
Figure A1: Principal Component Analysis Plot of Transcriptome Sequencing. .	CXLVIII
Figure A2: MA Plot of Acetate vs Glucose.	CXLVIII
Figure A3: MA Plot of Acetate vs Acetate plus Acetol.....	CXLIX
Figure A4: MA Plot of Glucose vs Glucose plus Acetol.....	CXLIX

List of Tables

Table 1-1: Overview of IA Production from Second Generation Substrates.....	36
Table 2-1: Media Compositions.....	44
Table 3-1: Promising Genes Selected by Means of Transcriptome Sequencing.	61
Table 3-2: Growth Rates and Uptake of Acetol by RNAseq Derived Knockout Strains.....	62
Table 3-3: Growth Rates and Uptake of Acetol by Various <i>C. glutamicum</i> Overexpressing Strains.....	64
Table 3-4: Yields and Titers of Engineered <i>C. glutamicum</i> Strains during Cultivation at 1 mL Scale.....	70
Table 4-1: Final Conditions for IA Production in this Work.	113
Table A1: GC-Report on the Compound Analysis of PW.....	CXXXIV
Table A2: Consumables Used in this Study.....	CXXXVI
Table A3: Devices Used in this Study.	CXXXVII
Table A4: Chemicals Used in this Study.	CXXXVIII
Table A5: Strains Used and Generated in this Study.....	CXL
Table A6: Plasmids Used and Generated in this Study.....	CXLI
Table A7: Primers and Oligonucleotides Used in this Study.....	CXLIV

List of Abbreviations

ACN	Aconitase
AcnR	Transcriptional repressors of aconitase
ACS	Acetyl-CoA synthetase
ADH	Alcohol dehydrogenase
AK	Acetate kinase
ALDH	Acetaldehyde dehydrogenase
ALE	Adoptive laboratory evolution
BS	Back scatter
CAD	<i>cis</i> -aconitate decarboxylase
CCR	Carbon catabolite repression
CDW	Cell dry weight
CgLP	<i>C. glutamicum</i> landing pads
CoA	Coenzyme A
CS	Citrate synthase
DAD	Diode array detector
Fum	Fumarase
GDH	Glutamate dehydrogenase
GlxR	Repressor of the glyoxylate shunt
GOGAT	Glutamine oxoglutarate aminotransferase
GRAS	Generally recognized as safe
GS	Glutamine synthase
GSH	Reduced glutathion
IC	Inorganic carbon
ICL	Isocitrate lyase
IDH	Isocitrate dehydrogenase
IPTG	Isopropyl- β -D-thiogalactopyranosid

KIT	Karlsruhe Institute of Technology
MctC.....	Monocarboxylic acid transporter
MQO	Malate:quinone oxidoreductase
MS.....	Malate synthase
OdhI	Oxoglutarate dehydrogenase inhibitor
OGDHC	Oxoglutarate dehydrogenase complex
PCA.....	Protocatechuic acid
PCR.....	Polymerase chain reaction
PEP.....	Phosphoenolpyruvate
PEPck.....	PEP carboxykinase
PknG.....	Protein kinase G
PTA.....	Phosphotransacetylase
PW.....	Pyrolysis water
RamA/B	Regulator of acetate metabolism A and B
RID.....	Refractive index detector
RT.....	Room temperature
SCS.....	Succinyl-CoA synthetase
SNP	Single nucleotide polymorphisms
SQO.....	Succinate:menaquinone oxidoreductase
SugR.....	Repressor of sugar metabolism
TAD	trans-aconitate decarboxylase
TC.....	Total carbon
TOC.....	Total organic carbon

1 Introduction

1.1 Biotechnology at a Glance

The history of biotechnology probably began when humans started to settle and to domesticate animals and plants. The selective crossing of individuals to improve certain phenotypes, such as growth or yield in subsequent generations, were the ancient beginnings of genetic engineering [105, 295]. Later, humans developed the first “bioreactors” by mixing substrates such as stale bread, grains or fruits with water in closed vessels to produce alcohol and vinegar [7, 63]. But it was only in the last century that a fundamental knowledge of microorganisms, metabolic processes and genetic engineering enabled the development of modern biotechnology. In the last few decades high-precision tools such as the CRISPR/Cas9 system have become available for genetic modification of microorganisms [139]. Next-generation sequencing has enabled cost-effective sequencing of genomes and transcriptomes [8]. Mass spectroscopy and modern computers can now be used to study the metabolism and simulate carbon, nitrogen, and other fluxes within cells [300]. On the side of process engineering, new methods combining small sensors with on-line computerized process monitoring allow tightly controlled and efficient bioprocesses [208]. The emergence of these and other new technologies has led to a revolution in biotechnology allowing precise planning, evaluation and optimization, and ultimately upscaling for industrial applications of bioprocesses.

As indicated above, biotechnology itself is an interdisciplinary science from a wide variety of fields from engineering and natural sciences and, depending on the area of application, is assigned to different colors (Figure 1-1). Today, dark, purple/violet, brown, grey, gold, yellow, white, blue, red, and green are the 10 defined colors of biotechnology. Thereby, the most prominent areas of biotechnology are probably represented by the latter colors green, red, blue, and white, which refer to biotechnology in the context of plants and agriculture, pharmaceuticals and medicine, marine and aquatic systems, and industry and biorefinery, respectively. The work presented in this thesis can be categorized in the field of white/industrial biotechnology. Detailed information on all fields and colors can be found elsewhere in the literature [18, 19, 82, 122].

Introduction

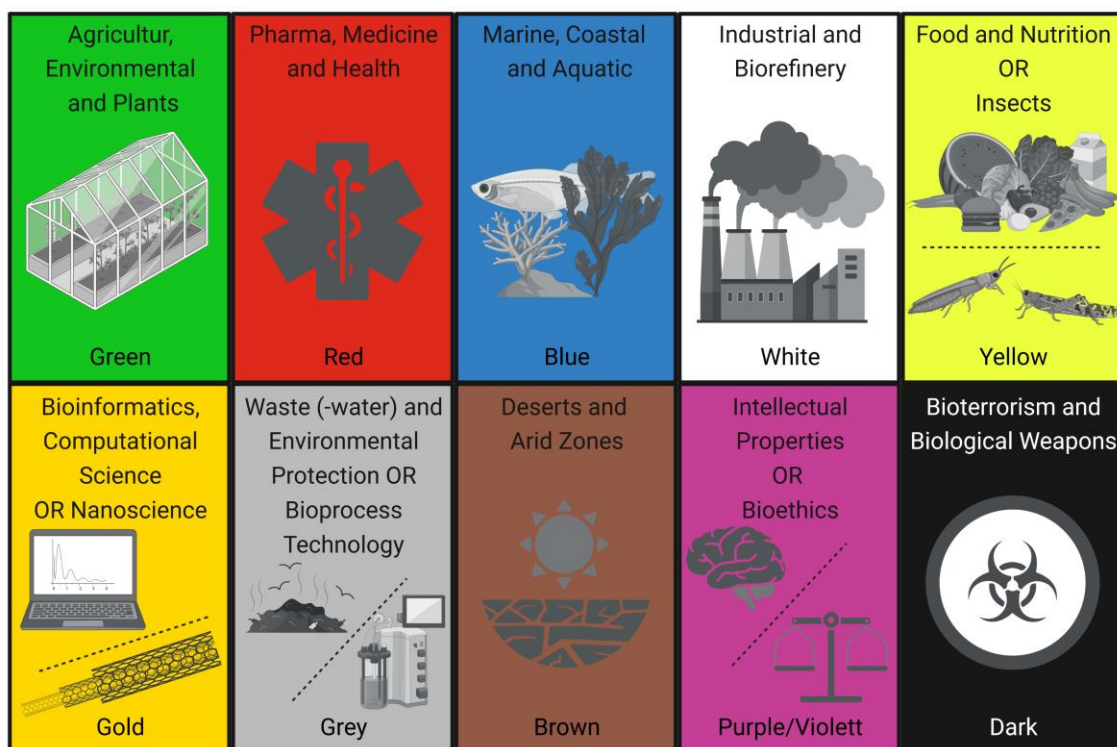


Figure 1-1: Illustration of the Different Colors of Biotechnology.

The figure shows the defined areas of biotechnology and the corresponding colors assigned that are used to categorize the different fields of application. Some colors are associated with multiple fields.

Today, the field of industrial biotechnology is considered as a key technology and an important cornerstone in mitigating climate change. Since the turn of the millennium, the debate on climate change and the need to reduce the use of fossil resources has become an increasingly important social and political issue. However, it is important to remember that the energy sector is not the only field that is heavily dependent on fossil fuels [2]. Almost the entire chemical industry, which works with organic compounds, relies on crude oil and natural gas as starting materials for various syntheses [6, 72, 160]. Industrial biotechnology has the potential to replace petroleum-derived fuels and platform chemicals used in chemical synthesis with biologically produced building blocks. Since biotechnological engineering aims at harnessing, optimizing and modifying natural processes for the production of a desired compound, it is also considered to be cleaner, safer and more environmentally friendly compared to classical chemical synthesis [91]. In future, biotechnology will contribute to a techno-economic paradigm shift within a holistic bioeconomy strategy [73, 275].

1.2 Alternative Substrates in Biotechnology

As outlined above, biotechnology plays a particularly important role in the bioeconomy. However, industrial biotechnology has also been criticized for contributing to the strained situation of global food distribution by converting sugars, oils, and other food-related substrates into chemicals and biofuels. This ethical dilemma also known as the 'food vs. fuel' problem, gained notoriety during the food price crisis of 2007/2008. At that time, sharp rise in food prices were attributed in part to the increased use of corn and sugar cane for biofuel production [125, 189, 216, 231]. Although the food price crisis at that time may have had other causes [116, 177, 269], the 'food vs. fuel' problem (or rather, 'industry vs. food' today) remains a serious obstacle for biotechnology and the entire bioeconomy. Indeed, processes that rely on the cultivation of high-energy crops compete directly with basic agricultural resources such as land, water, fertilizer, and labor that are needed to produce crops for human consumption [128, 235]. This is a major drawback in the face of land and water depletion due to human population growth, land sealing, pollution, and ongoing climate change associated with droughts and desertification. To overcome this substrate related shortcoming of bioeconomic production processes, a large scientific community is working on the introduction of so-called 2nd generation feedstocks. These substrates do not require the exclusive cultivation of energy crops and are mainly obtained by processing of agricultural by-products or sidestreams of food production, e.g. wheat straw [147, 179, 193, 268], corn stover [313], sugar cane bagasse [190, 209], coffee husks [151, 245], wood residues [156, 173, 202] and others [32, 190, 236]. Most of these future substrates can be classified as plant residues, consisting mainly of lignocellulose, a biopolymer of cross-linked cellulose, hemicellulose and lignin, which can make up about 30-40%, 20-30%, and 10-30%, respectively, of the total dry matter, depending on the origin [57, 204]. Due to the complex and stable chemical structure of lignocellulose, its individual components must first be separated to enable efficient and rapid valorization of the different fractions. The most commonly cited method for separating lignocellulose is the Kraft process, which is used in large-scale pulp production in the paper industry. However, this process was optimized to extract cellulose from wood for subsequent papermaking and results in the degradation of hemicelluloses and the production of poor-quality lignin [92, 95, 100]. A gentler method that results in more efficient purification of the three biopolymers of lignocellulose is the organosolv process, in which the lignocellulose is heated in a

Introduction

mixture of water and solvents such as methanol, ethanol, and acetone. However, the various process parameters depend on the specific application and the desired purity of the final products [51, 119, 176, 228]. If necessary, the biopolymers obtained can be further degraded into monomeric building blocks by enzymatic [97, 312] or acid hydrolysis [224], producing mainly derivatives of phenylpropanoid from lignin, glucose from cellulose, and pentoses such as xylose and arabinose from hemicellulose [57]. While hydrolysis of biomass aims at the extraction of intact biomolecules like fermentable sugars [30], other processes focus on the extraction of the energy stored in the biomass. For example, biomass combustion results in the direct release of energy and is mainly used for heating purposes, but also for electricity generation. In contrast, the process of fast pyrolysis aims to conserve and compact the energy in order to store it for later applications. This is achieved by decomposing the lignocellulosic biomass at high temperatures in the absence of oxygen, resulting in a bio-crude oil, syngas, ash and char, and an aqueous phase [48, 193] (see Chapter 1.2.1, Figure 1-2). Similar to fast pyrolysis, gasification involves high-temperature decomposition of biomass in the absence of oxygen to produce char, hydrocarbons, and syngas [179, 184]. However, whereas fast pyrolysis involves heating to approximately 500 °C in a matter of seconds, gasification involves a stepwise increase in temperature over a longer period of time. The syngas fractions resulting from the decomposition of biomass in the latter processes are mainly burned to generate heat for a self-fueling process, but also to generate electricity. In principle, however, the syngas fraction could also be further converted to small molecules such as methanol, acetate and ethanol, either by using metal catalysis [179, 186] or by syngas fermentation using acetogenic bacteria [106, 167]. In this context, it is worth mentioning that the conversion to small molecules can also be applied to synthetic syngas produced from industrial off gases and green hydrogen [185, 239].

All of the biomass degradation processes discussed in this chapter result in the production of small molecules such as sugars, alcohols, and organic acids. The latter, unlike primary biomass, are readily accessible to microbial hosts for conversion to biofuels and other bio-based chemicals and products. However, depending on the substrate used and the intended product, the microbial host must be carefully selected to ensure a stable and effective bioprocess. [38].

1.2.1 Acetate and Acetol Generated by Fast Pyrolysis

Fast pyrolysis is a process for decomposing lignocellulosic biomass to produce an energy-rich bio-oil/liquid that can be used as a fuel oil or as a feedstock for biofuel and chemical production [69, 84, 201]. The actual process of heating the biomass to about 500 °C in the absence of oxygen only takes a few seconds at most. In this short time, the chemical bonds within the large biopolymers of cellulose, hemicellulose, and lignin break down, forming a variety of different compounds that evaporate immediately. Subsequent condensation of the pyrolysis vapor results in the production of four different phases: (i) a solid phase consisting of ash and char, (ii) a non-condensable (syn-)gas phase, (iii) the intended hydrophobic bio-oil, and (iv) an aqueous phase rich in short-chain hydrophilic carbon compounds (Figure 1-2). The latter has been studied as an intended substrate for biotechnological conversion to itaconic acid (IA) (see Chapter 1.4) and is referred to as pyrolysis water (PW) [48, 214] in this work.

The biomass-to-liquid process, or bioliq[®] for short, is a concept developed at the Karlsruhe Institute of Technology (KIT) that combines decentralized decomposition of lignocellulosic biomass by fast pyrolysis followed by centralized valorization of the bio-oil fraction obtained. [71, 193]. To ensure the stability and quality of the produced bio-oil during transportation and processing, the aqueous phase must be thoroughly separated from the desired product [70, 214]. Within the bioliq[®] fast pyrolysis plant, the separation of the different condensable fractions is achieved by two discrete condensers in which the pyrolysis vapor is fractionated. In the first condenser, the hydrophobic bio-oil fraction condenses at temperatures around 80 °C. In the second condenser, the aqueous phase condenses at temperatures between 22 °C and 33 °C. Additional recycling, heating, cooling and quenching steps of the organic and aqueous condensates allow an efficient separation of the two phases [193, 214]. The bio-oil obtained consists of more than 50% (w/w) carbon with an energy density of 23 MJ kg⁻¹ and a residual water content of about 15%. The PW has a water content of over 80%, a pH of 2.5 to 3, and it contains about 90 g to 100 g of organic carbon L⁻¹ with a higher heating value¹ of 4 MJ kg⁻¹ [193]. The main carbon compounds in the PW produced by the bioliq[®] process

¹ Higher heating value: *“Defined as the amount of heat released by a specified quantity (initially at 25 °C) once it is combusted and the products have returned to a temperature of 25 °C. The higher heating value takes into account the latent heat of vaporization of water in the combustion products, and is useful in calculating heating values for fuels where condensation of the reaction products is practical”* (www.chemeuropa.com/en/encyclopedia/Higher_heating_value; 29.04.2023)

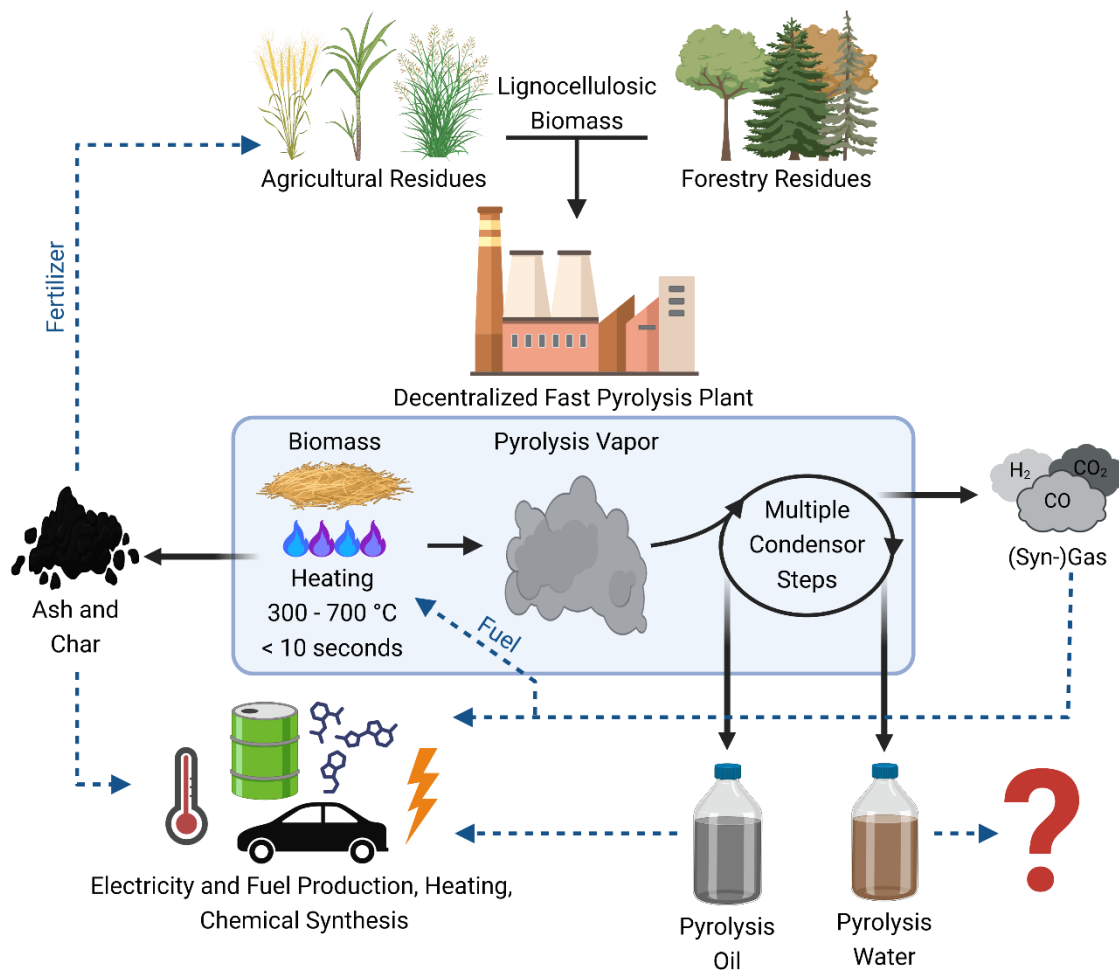


Figure 1-2: Scheme of the Fast Pyrolysis Process.

The figure provides an overview of the fast pyrolysis process (blue box), which uses lignocellulosic biomass as a feedstock to produce an energy-rich bio-oil. Dashed lines indicate possible applications of the resulting pyrolysis products.

and used for valorization in this work are acetol and acetic acid with 5.5% (w/w) and 3.7% (w/w), respectively, followed by propionic acid with 1.3% (w/w) and ethylene glycol with 1% (w/w). The remaining carbon is distributed among a variety of aldehydes, ketones, and heterocyclic compounds, which individually account for less than 1% (w/w) (Table A1). Thus, the composition of the PW generated by the bioliq[®] process is similar to the aqueous condensates of other fast pyrolysis approaches [33, 253, 310]. However, the high water content of PW makes its chemical upgrading cumbersome and unprofitable [162, 253, 305]. Therefore, biotechnological upgrading of PW [148, 154, 164] and, to some extent, of the bio-oil [12, 20, 115] has gained attention in recent years. In 2012, Lian and co-workers [164] started to use PW as a substrate for microbial conversion. The authors used oleaginous yeasts to produce 2.2 g lipids L⁻¹ from processed PW containing 20 g acetate L⁻¹, but observed negative effects of acetol on

lipid production [164]. Other authors discuss the anaerobic conversion of PW by mixed community fermentation with bacteria and archaea [226, 270, 314]. However, all studies on microbial valorization of pyrolysis oil and/or PW reported toxicity using crude pyrolysis fractions as substrate during cultivation. The observed toxicity effects were mainly attributed to aldehydes, phenols, and heterocyclic compounds, which are present in low amounts in PW but have strong antimicrobial properties [74, 137, 234]. Consequently, processing of PW is an essential step to increase its biocompatibility and allow its microbial upgrading. Most pre-treatment strategies involve neutralization, overliming, heat treatment, centrifugation, and filtration [11, 147, 155]. Other studies additionally suggest ion exchange [58] or osmosis [261] to specifically purify fermentable compounds from the crude PW. Novel approaches include co-fermentation of microbial communities for simultaneous *in situ* detoxification and production [226]. Recently, Kubisch and Ochsenreither [147] published a pre-treatment strategy for PW derived from the bioliq[®] process that allowed *Aspergillus oryzae* to grow on 100% processed PW [147]. The reported strategy involved a combination of rotary evaporation followed by overliming, heat treatment and active carbon extractions. In this work, we used the latter method to increase the biocompatibility of PW for the cultivation of *C. glutamicum* and investigated its use as a substrate for the production of IA (see Chapter 3.3).

1.3 Industrial Host: *Corynebacterium glutamicum*

Similar to chemical synthesis, biotechnological processes rely on the conversion of one or more defined substrates to a desired product under certain conditions by an appropriate catalyst. Catalysts in biotechnology can be natural or engineered enzymes, or microorganisms capable of carrying out the required reactions. In the late 1950s, Kinoshita et al. [133] discovered a bacterium that naturally overproduced glutamate, today known as *Corynebacterium glutamicum* [1]. *C. glutamicum* is a biotin-auxotrophic Gram-positive actinobacterium [165] with a genome size of approximately 3.3 million base pairs and an average GC content of 53.8% [123]. Today, the complete genome sequence of *C. glutamicum* is available and a large number of genes and proteins have been annotated and experimentally characterized [123]. In addition, a huge toolbox of different techniques and strategies allows precise genetic and metabolic engineering of this natural glutamate producer as well as profiling of the resulting strains [192].

Introduction

Furthermore, *C. glutamicum* is a very robust organism that is well suited for cultivation in large-scale bioreactors. It is a facultative anaerobic bacterium [181], metabolically active over a wide pH range with an optimum at pH 6 to 9 [89], and shows non-diauxic growth and simultaneous consumption on different substrate mixtures [61, 292]. *C. glutamicum* is generally recognized as safe (GRAS) organism and an established workhorse for the large-scale production of several amino acids on a multi-million ton scale per year [159, 290]. Its importance to the white biotechnology is evidenced by more than 2,700 research articles and over 1,700 patents published on *C. glutamicum* [159]. In the past, *C. glutamicum* has been intensively optimized for the industrial production of amino acids such as L-glutamate and L-lysine [132, 299], but intensive research has also been conducted to exploit this bacterium for the production of organic acids, proteins and biofuels [24, 37, 90, 297]. However, similar to most other biotechnological hosts, glucose and other sugar-derived compounds are the substrates of choice for cultivation of *C. glutamicum*, especially on an industrial scale [290], thus contributing to the ‘food vs. industry’ dilemma as outlined before (see Chapter 1.2). At the same time, *C. glutamicum* is of particular interest, with respect to the valorization of 2nd generation substrates on an industrial scale. In particular, the high tolerance of *C. glutamicum* towards acetate [13, 301] and the ability to take up acetol [155] make this organism an attractive host for microbial upgrading of PW.

1.3.1 Metabolization of Acetol

As described above, acetol and acetate are the major carbon compounds found in PW and together account for about 50% of its dry matter (see Chapter 1.2.1, Table A1). Therefore, an effective metabolization of these two compounds is a prerequisite to establish PW as a suitable substrate for biotechnological conversion. The acetate metabolism is well studied in most prominent production hosts, including *C. glutamicum* (see Chapter 1.3.2), thus acetate is generally considered to be an interesting future feedstock for biotechnological upgrading [128, 153, 200]. However, to our best knowledge, only two studies have focused on the application of acetol as a substrate for microbial valorization, using the hosts *A. oryzae* and *C. glutamicum* [148, 155]. Acetol was discovered as a direct precursor in the microbial metabolism of 1,2-propanediol [112]. Thus, Lange et al. [155] used an engineered *C. glutamicum* strain expressing the glycerol dehydrogenase of *E. coli* for the reduction of acetol to 1,2-propanediol by whole-cell catalysis. Therefore, the authors cultured the production strain in a two-stage bioreactor

process using pretreated PW obtained from the bioliq[®] process as substrate. In the first phase, the cells were cultured aerobically to accumulate biomass, mainly from the available acetate. In the second phase, oxygen saturation was slowly reduced and the remaining acetol was converted to 1,2-propanediol until the oxygen was completely depleted from the culture medium and the cells became metabolically inactive. In this way, the authors achieved a final yield of 96% (mol/mol) of 1,2-propanediol produced from acetol. It is noteworthy that the authors observed a simultaneous decrease in acetol and 1,2-propanediol concentrations after acetate was depleted from the culture supernatant during aerobic cultivation in shaking flasks. This suggests an unknown mechanism of acetol degradation in *C. glutamicum*. However, it should also be noted that the cultures were additionally supplemented with 5 g yeast extract L⁻¹ and its effect on the acetol metabolism remained unclear [155]. In other studies on malic acid production from PW, Kubisch and Ochsenreither [148] showed that *A. oryzae* is able to utilize acetol for biomass production. However, similar to the study on lipid production from PW by oleaginous yeasts mentioned earlier [164] (see Chapter 1.2.1), the authors reported that the yield of malic acid produced from acetate decreased with increasing acetol concentration [148]. Although the studies outlined above deal with the valorization of acetol by microbial hosts, only little information is available on the intracellular pathways involved in the degradation of acetol *in vivo*. In literature, acetol appears to be mentioned mostly as an intermediate in the detoxification of methylglyoxal [117, 138] or, as described before, in the production of the biofuel 1,2-propanediol. In this regard, some authors have suggested several enzymes that may be involved in the formation and degradation of acetol in different organisms (Figure 1-3) [154, 237, 250]. In summary, the intracellular degradation of acetol could follow two main pathways: (i) an aerobic conversion via methylglyoxal and lactate to pyruvate, which is degraded in the tricarboxylic acid (TCA) cycle, or (ii) a conversion to 1,2-propanediol, which can be oxidized to propionate, entering the central metabolism through the methylcitrate cycle. In this work, we analyzed the capacity of *C. glutamicum* to utilize acetol as a carbon and energy source. Therefore, we expressed several enzymes capable of catalyzing the predicted pathways via methylglyoxal and lactate, and tested their ability to facilitate an efficient acetol metabolism in *C. glutamicum*. In addition, we used transcriptome sequencing of cells cultured on acetol to screen for native enzymes that may be involved in the degradation of acetol in *C. glutamicum* (see Chapter 3.1).

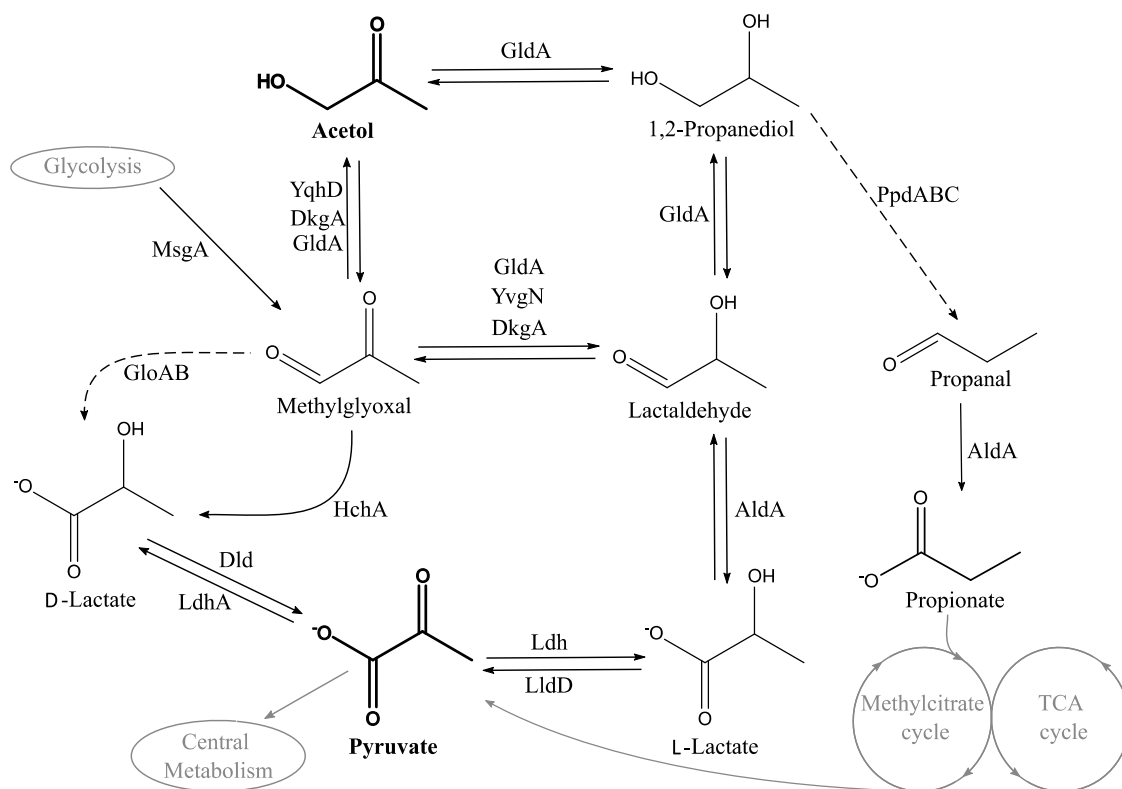


Figure 1-3: Predicted Pathways for the Metabolization of Acetol.

The figure shows different pathways that were predicted to be involved in the metabolization of acetol in different organisms [154, 237, 250]. Grey lines represent metabolic pathways including multiple reactions. Dashed lines indicate requirements for special co-factor or cultivation conditions. **AldA**: Aldehyde dehydrogenase; **DkgA**: 2,5-diketo-D-gluconic acid reductase; **Dld**: D-Lactate dehydrogenase; **GldA**: Glycerol dehydrogenase; **GloAB**: Glyoxylase I + II; **HchA**: Hsp31, a chaperon with glyoxylase III activity; **Ldh**: Fermentative L-lactate dehydrogenase; **LdhA**: Fermentative D-Lactate dehydrogenase; **LldD**: L-Lactate dehydrogenase; **Msg**: Methylglyoxal synthase; **PpdABC**: Diol dehydratase; **YqhD**: Primary alcohol dehydrogenase; **YvgN**: Glyoxal reductase.

1.3.2 Acetate Metabolization and its Regulation

In contrast to the metabolization of acetol, the acetate metabolism and its regulation is well studied in *C. glutamicum* and it appears to be optimally suited for the valorization of this alternative substrate. *C. glutamicum* shows no growth retardation when grown at concentrations of 200 mM acetate as the sole carbon and energy source [301] and has been shown to even tolerate concentrations up to 500 mM [13]. The growth rate (μ) and the carbon uptake rate (q_s) of *C. glutamicum* during growth on acetate are similar to those observed on glucose [292]. In 1980, Pelechová et al. [212] showed that sucrose could be partially substituted by ethanol or acetate during lysine production with mutant strains of *C. glutamicum* [212]. To date, several studies have reported engineered *C. glutamicum*

strains for the production of L-valine [40], L-lysine [41], ketoisovalerate [142], isobutanol [39] and 1,2-propanediol [155], using acetate as a co-substrate for biomass formation. Other authors reported the utilization of acetate as co-substrate to increase product yields [55, 163, 207]. However, studies of effective compound production from acetate as the sole carbon and energy source are rare. Recently, Kiefer *et al.* [127] developed a pH-coupled fed-batch process for high cell density cultivation of *C. glutamicum* using acetate as the sole carbon and energy source [127]. More recently, the same authors have shown that this process can be used for the high-level production of recombinant proteins [129]. In addition, the process was optimized for the production of IA by a *C. glutamicum* strain developed as part of this work. By cultivating *C. glutamicum* IDH^{R453C} (pEKEEx2-*malEcad*_{opt}) (referred to as *C. glutamicum* ITA4 in this work), 29.2 g IA L⁻¹ could be obtained with a yield of 73 mmol mol⁻¹ using acetate as the sole carbon and energy source [180].

As mentioned above, the acetate metabolism and its regulation have been extensively studied in *C. glutamicum*, providing essential information for efficient metabolic engineering of this organism (Figure 1-4). Acetate is taken up by *C. glutamicum* through active transport mediated by the monocarboxylic acid transporter MctC, gated by the electrochemical proton potential. However passive diffusion of acetic acid across the membrane at neutral pH has been shown to be sufficient to support growth [77, 120]. Inside the cell, acetate first becomes phosphorylated by the acetate kinase (AK) and is subsequently converted to acetyl-CoA by the action of the phosphotransacetylase (PTA) [222]. In this context, it should be mentioned that an alternative pathway, catalyzed by a CoA-transferase and independent of AK and PTA, has been described for the intracellular activation of acetate during growth with glucose as co-substrate [282]. The acetyl-CoA produced is channeled into the TCA cycle by the activity of the citrate synthase (CS). Therefore, CS transfers the acetyl-moiety of acetyl-CoA to oxaloacetate to form citrate [81]. The latter is structurally isomerized to isocitrate by the activity of aconitase (ACN) [21], which first catalyzes a dehydration of citrate to produce *cis*-aconitate. The latter is released from the active site of ACN and rebinds in the opposite orientation, followed by its rehydration leading to the formation of isocitrate [21, 170]. The activity of ACN is crucial for the production of IA, as the intermediate *cis*-aconitate is the direct precursor of IA (Figure 1-4, see Chapter 1.4.1). Isocitrate, on the other hand, can be channeled into the oxidative branch of the TCA cycle to provide the cell with energy and precursors for cell growth. Therefore, isocitrate is oxidized to 2-oxoglutarate

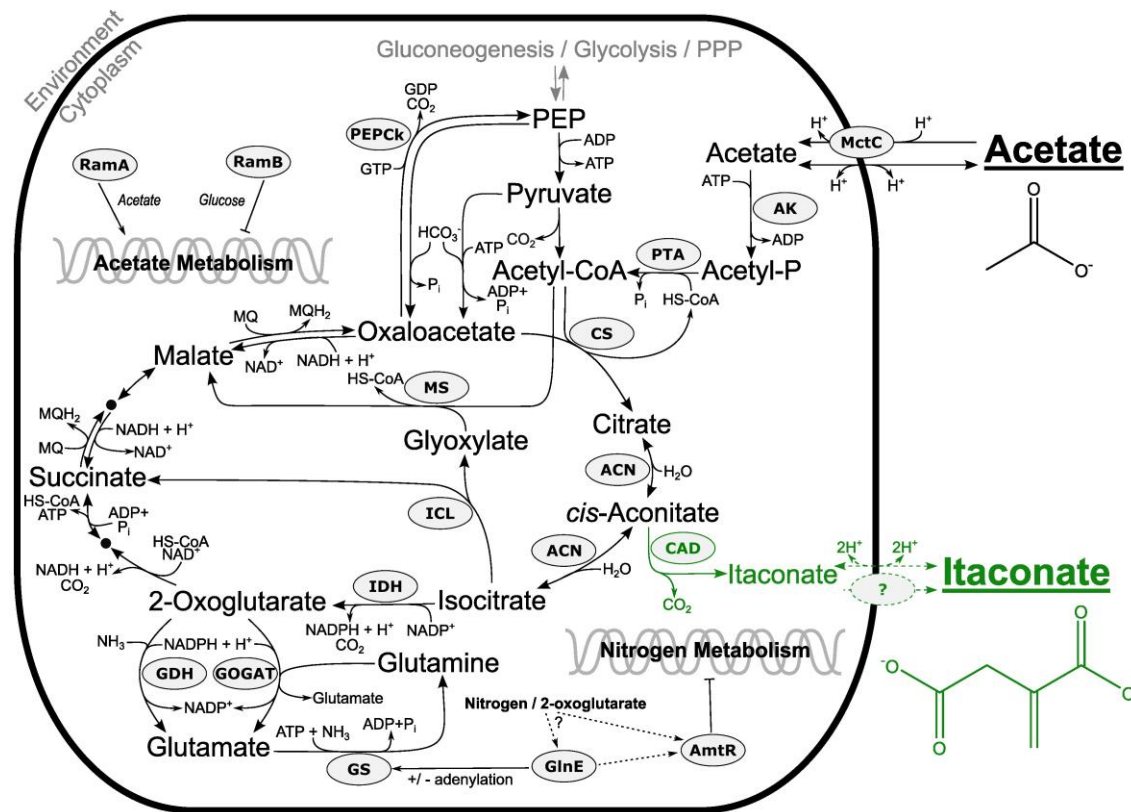


Figure 1-4: Overview of the Acetate Metabolism in *C. glutamicum*.

The figure shows the central metabolic pathways in *C. glutamicum* involved in the metabolism of acetate, relevant in this work. In addition, the heterologously expressed *cis*-aconitate decarboxylase (CAD) used to implement IA production in this work is shown in green. For indicated crosstalk with nitrogen assimilation pathways and signaling, see Figure 1-5. Dashed lines indicate indirect or unknown interactions. **ACN**: Aconitase; **AK**: Acetate kinase; **AmtR**: Master regulator of nitrogen metabolism; **CAD**: *cis*-Aconitate decarboxylase; **CS**: Citrate synthase; **GDH**: Glutamate dehydrogenase; **GlnE**: Adenylyl transferase involved in nitrogen signaling; **GOGAT**: Glutamine oxoglutarate aminotransferase; **GS**: Glutamine synthetase; **ICL**: Isocitrate lyase; **IDH**: Isocitrate dehydrogenase; **MctC**: Monocarboxylic acid transporter; **MS**: Malate synthase; **PEPck**: Phosphoenolpyruvate carboxykinase; **PTA**: Phosphotransacetylase; **RamA/B**: Regulator of acetate metabolism A/B. (Figure adopted from Schmollack et al. [240]).

through a NADP^+ -dependent isocitrate dehydrogenase (IDH) [80]. 2-Oxoglutarate can either serve as a substrate during nitrogen assimilation (see Chapter 1.3.3) or be further oxidized by the oxoglutarate dehydrogenase complex (ODGHC) to yield $\text{NADH} + \text{H}^+$ and succinyl-CoA [78]. The first two steps of the oxidative branch of the TCA cycle, catalyzed by IDH and ODGHC, are irreversible, as the initial C6 compound isocitrate is decarboxylated to the C4 compound succinyl-CoA (Figure 1-4). The latter is subsequently converted to succinate by succinyl-CoA synthetase (SCS) with the concomitant formation of ATP [78]. To complete the TCA cycle, succinate is successively oxidized to fumarate, malate, and oxaloacetate, catalyzed by the activities of succinate:menaquinone oxidoreductase (SQQ), fumarase (Fum), and malate:quinone oxidoreductase (MQO),

respectively [78, 183]. The reduction equivalents of FADH_2 and $\text{NADH} + \text{H}^+$ produced during the complete oxidation of one mole of acetate in the TCA cycle are sufficient to generate 7.3 mol ATP via oxidative respiration [45]. Finally, the regenerated oxaloacetate can again serve as a substrate for the reaction catalyzed by CS and re-enter the TCA cycle as described above.

In addition, oxaloacetate forms the branch point of the methylcitrate cycle, which is responsible for metabolization of propionate [60]. The uptake and intracellular activation of propionate follows the same metabolic pathways as acetate (see above) [77, 222, 282], followed by the condensation with oxaloacetate catalyzed by 2-methylcitrate synthase to produce 2-methylcitrate [60]. The latter is converted to 2-methylisocitrate, which is further cleaved to pyruvate and succinate [217]. Besides forming the acceptor molecule for the TCA and methylcitrate cycle, oxaloacetate also serves as a substrate for the gluconeogenic pathway essential for growth on non-glycolytic substrates such as ethanol and acetate (Figure 1-4). During growth on acetate as the sole carbon and energy source, approximately 13% of the total carbon taken up by *C. glutamicum* is channeled into the gluconeogenesis [292]. The first step of gluconeogenesis is catalyzed by the phosphoenolpyruvate (PEP) carboxykinase (PEPCK), which catalyzes the decarboxylation and GTP-dependent phosphorylation of oxaloacetate to PEP [223]. It should be noted that *C. glutamicum* harbors a variety of pathways involved in the PEP/pyruvate – malate/oxaloacetate node for glycolytic, anaplerotic, and gluconeogenetic reactions [78]. However, only PEPCK was found to be essential during growth on non-glycolytic substrates [223]. The anaplerotic reaction during growth on non-glycolytic substrates is carried out by the enzymes of the glyoxylate shunt. The first step of the glyoxylate shunt is catalyzed by the isocitrate lyase (ICL), which cleaves isocitrate to succinate and glyoxylate [220]. The latter is further converted to malate by the consumption of acetyl-CoA, catalyzed by malate synthase (MS) [221]. Thus, the reactions of the glyoxylate shunt bypass the decarboxylation steps within the oxidative branch of the TCA cycle catalyzed by ICL and OGDHC (see above).

As mentioned before, *C. glutamicum* shows similar rates of total carbon uptake during growth on glucose, acetate and a mixture of both. However, during growth on acetate as the sole carbon and energy source, the carbon flux into the TCA cycle is more than three times higher compared to growth on glucose. Furthermore, the carbon flux through the oxidative branch is about three times higher than the flux through the glyoxylate shunt [292]. Since glucose is metabolized first within the glycolysis, acetyl-CoA is only

Introduction

partially channeled into the TCA cycle. In contrast, acetate is first activated to acetyl-CoA and enters the central metabolism exclusively via the TCA cycle. It is noteworthy that *C. glutamicum* copes with the increased carbon flux through the TCA cycle almost entirely by transcriptional regulation of gene expression. The expression of the respective genes is primarily controlled by the transcriptional regulators of acetate metabolism A and B (RamA and RamB) (Figure 1-4). RamA was reported to be essential for the growth of *C. glutamicum* on acetate as the sole carbon source, and deletion of *ramA* impaired the expression of the genes encoding AK, PTA, ICL, and MS [65]. Thus, the authors suggested that RamA is a positive regulator of genes related to the acetate metabolism. In contrast to RamA, RamB was reported to function as a negative regulator of AK, PTA, ICL and MS during the growth of *C. glutamicum* on glucose [93]. In fact, RamA and RamB form a complex transcriptional regulatory system by regulating each other, themselves, and a variety of other genes such as *gltA*, *acn*, *sdhCAB*, or *pck*, which encode CS, ACN, SQO, and PEPCK, respectively [10, 14, 278]. However, the effector molecules that regulate the activity of RamA and RamB have not yet been identified [244]. It should be noted, that RamA and RamB have also been implicated in the transcriptional regulation of genes related to sugar uptake and glycolysis [14]. In addition to RamA and RamB, the repressor of the glyoxylate shunt (GlxR) is involved in the transcriptional regulation of the acetate metabolism in *C. glutamicum* [10]. Kim *et al.* [130] showed that GlxR binds to the promoters of *aceA* and *aceB*, which encode ICL and MS, respectively, in a cAMP-dependent manner. Furthermore, the authors showed that intracellular cAMP levels in *C. glutamicum* are four times lower during growth on acetate compared to growth on glucose. Overexpression of GlxR strongly reduced the enzymatic activities of ICL and MS during growth on acetate, but had no effect on the glucose metabolism. Therefore, the authors proposed GlxR as a negative regulator of the glyoxylate bypass during growth on glucose [130]. However, deletion of *gltA* caused strong growth defects in *C. glutamicum* knockout strains independent of the available carbon source [210]. Thus, the exact function of GlxR has not yet been identified, but it is thought to be involved in the rare cases of carbon catabolite repression (CCR) [271] observed in *C. glutamicum* during growth on substrate mixtures of e.g. glucose/ethanol or acetate/ethanol [9]. Another transcription factor indirectly involved in the regulation of acetate metabolism is the repressor of sugar metabolism (SugR). Among other targets involved in the glycolysis, SugR represses several phosphotransferase systems responsible for sugar uptake in *C. glutamicum* during

growth on gluconeogenic substrates such as acetate. Thus, the rate of sugar uptake is reduced during growth on mixtures of glycolytic and gluconeogenic carbon sources to ensure a balanced substrate and carbon uptake rate [87, 111].

Besides the global regulation mediated by the above-mentioned transcription factors, several enzymes of *C. glutamicum* related to the TCA cycle undergo additional regulation. The expression of ACN was found to be controlled by the transcriptional repressors of aconitase (AcnR) [143] and RipA [293], the latter repressing the transcription of *acn* during iron limitation. It has been reported that *acn* expression is also reduced in response to low external pH [89]. The large variety of regulators and the fact that deletion of *acn* leads to increased secondary mutations in *C. glutamicum* [22] highlight the importance of ACN in the central metabolism of this bacterium. In contrast to ACN, the expression of IDH was found to be independent of the substrate provided, but the enzyme itself was inhibited by oxaloacetate plus glyoxylate [80]. In addition, phosphoproteomic data show that IDH is subject to post-translational phosphorylation of unknown function [29]. Since ICL is inhibited by succinate and glyoxylate [220], the carbon flux at the branch point between ICL and IDH [292] (Figure 1-4) is most likely controlled by the affinities of the enzymes towards isocitrate (K_M of 280 μM and 12 μM , respectively) [80, 220] and fine-tuned by the concentration of the different TCA cycle intermediates. The OGDHC is of particular interest in terms of regulation because it shares the substrate 2-oxoglutarate with the pathways for nitrogen assimilation and is subject to nitrogen signaling itself (see Chapter 1.3.3). The activity of OGDHC is inhibited by the oxoglutarate dehydrogenase inhibitor (OdhI). OdhI, in turn, is a substrate of the protein kinase G (PknG) and is released from the OGDHC in its phosphorylated state [194]. Recently, PknG and OdhI were found to form a signaling cascade with the membrane proteins GlnX and GlnH, which are able to sense periplasmic levels of glutamate and aspartate [258]. Thus, it is suggested that the OGDHC-OdhI interplay may serve as a mediator between nitrogen-signaling and the carbon metabolism (Figure 1-5). In the context of acetate metabolism, it is important to note that ethanol follows the same metabolic pathways during its degradation. First, ethanol is taken up by the cell and successively oxidized to acetate by alcohol dehydrogenase (ADH) and acetaldehyde dehydrogenase (ALDH) [9] and is further metabolized as described above. The oxidation of ethanol to acetate results in the generation of additional reduction equivalents, thus ethanol may be the preferred substrate for the generation of more reduced products such as biofuels. However, the regulation of the ethanol metabolism is slightly different from

the regulation of the acetate metabolism. As described above, *C. glutamicum* exhibits diauxic growth on mixtures of ethanol with glucose or acetate [9], indicating an additional level of regulation during growth on ethanol, but not on acetate. Thus, the transcription factor GlxR could be a possible candidate for fulfilling the function of a catabolite repression system in *C. glutamicum* [10, 271].

1.3.3 Nitrogen Assimilation and its Regulation

Nitrogen is the third most abundant element in *C. glutamicum* with about 8 to 10%, after carbon and oxygen with about 40% and 38%, respectively [165]. Since *C. glutamicum* is used for the production of various amino acids on an industrial scale [290], its nitrogen metabolism was an early subject of many studies. *C. glutamicum* is capable of growing on different nitrogen sources such as ammonium, creatinine, glutamate, and urea as sole nitrogen source, as well as on some amino acids and peptides [102]. However, it is not able to grow on nitrate or nitrite as sole nitrogen source [195]. The following chapter will focus on the assimilation of nitrogen from ammonium (sulfate) and urea, as these compounds are commonly used to grow *C. glutamicum* in minimal media and were also used as nitrogen source in this work (Figure 1-5).

Similar to acetate (see Chapter 1.3.2), ammonia can enter the cell by passive diffusion, which was found to be sufficient to support growth at high ammonium concentrations present in standard CGXII minimal medium ($> 5 \text{ g L}^{-1}$) [102]. At lower concentrations, ammonium uptake in *C. glutamicum* is facilitated by the two ammonium transport systems AmtA and AmtB. While AmtA has been identified as a high-affinity transport system driven by the membrane potential [252], AmtB is thought to function in a low-affinity channel-like uptake of ammonium [178]. Similar to ammonium, urea can enter the cell by passive diffusion or active transport [25, 251]. Inside the cell, urea is cleaved by the urease complex producing two molecules of NH_4^+ and one molecule of CO_2 [197]. Inorganic ammonium can be assimilated by *C. glutamicum* via two different pathways. At high intracellular concentrations of $> 5 \text{ mM}$, most ammonium is assimilated by the glutamate dehydrogenase (GDH). The GDH catalyzes the reductive amination of 2-oxoglutarate to L-glutamate by consuming NH_4^+ and $\text{NADPH} + \text{H}^+$ in equimolar amounts [247, 263, 264]. At low intracellular concentrations of ammonium $< 5 \text{ mM}$, ammonium is mainly assimilated by the essential glutamine synthase (GS), which catalyzes the amination of glutamate to glutamine by the consumption of ATP. Subsequently, the produced glutamine serves as a nitrogen donor during the reductive

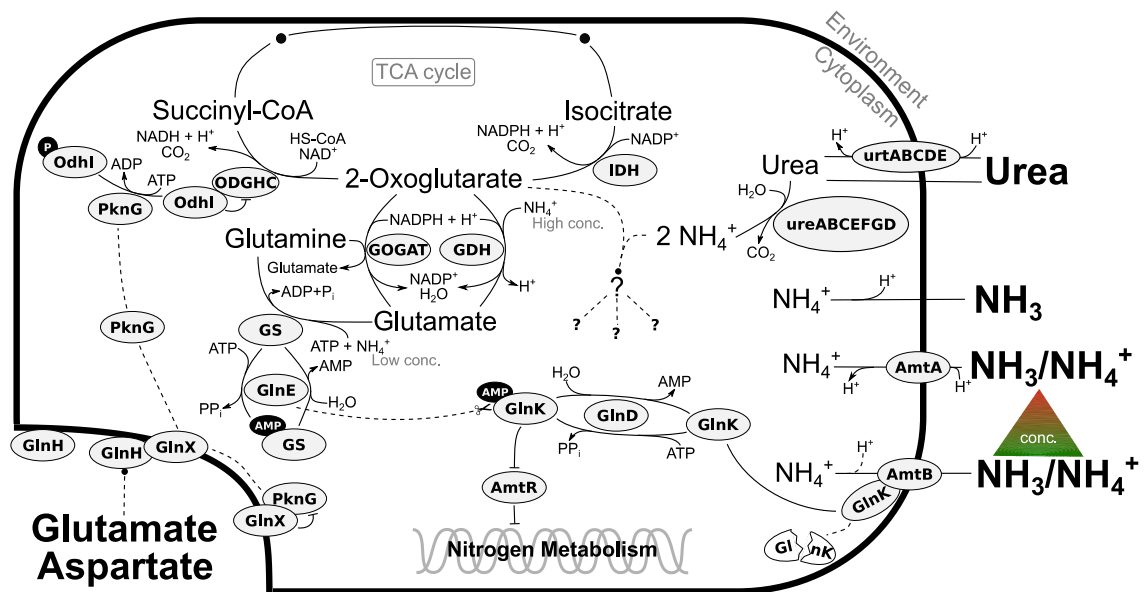


Figure 1-5: Nitrogen Metabolism and Signaling in *C. glutamicum*.

The figure shows the reactions involved in the nitrogen metabolism and its regulation in *C. glutamicum*. For an overview of the carbon metabolism in the TCA cycle, see Figure 1-4. Dashed lines indicate indirect or unknown interactions: GlnE shows an unknown control mechanism for the adenylation of GlnK. Glutamate and aspartate bind to GlnH. PknG is released from GlnX by binding of GlnH. GlnK is degraded by an unknown mechanism after binding to AmtB. 2-oxoglutarate has been suggested to function as an intracellular signaling molecule of the cellular nitrogen status.

AmtA: High-affinity ammonium importer; **AmtB:** Low-affinity ammonium permease; **AmtR:** Transcriptional repressor of nitrogen metabolism; **GDH:** Glutamate dehydrogenase; **GlnD:** Adenylyl transferase regulating GlnK; **GlnE:** Adenylyl transferase regulating GS; **GlnH:** Periplasmic binding protein involved in nitrogen sensing; **GlnK:** Signal transduction protein involved in nitrogen signaling; **GlnX:** Transmembrane protein involved in nitrogen sensing; **GOGAT:** Glutamine oxoglutarate aminotransferase; **GS:** Glutamine synthetase; **IDH:** Isocitrate dehydrogenase; **ODHGHC:** 2-Oxoglutarate dehydrogenase complex; **Odhl:** Oxoglutarate dehydrogenase inhibitor; **PknG:** Protein kinase G; **ureABCEFGD:** Urease complex; **urtABCDE:** Urea transporter complex.

transamination of 2-oxoglutarate by the NADPH + H⁺-dependent glutamine oxoglutarate aminotransferase (GOGAT). Thus, compared to the ammonium assimilation by GDH, assimilation via the GS/GOGAT pathway requires an additional mol of ATP per mol of ammonium assimilated [26, 264]. It is noteworthy, that the GS/GOGAT system can completely compensate for nitrogen assimilation in *gdh*-deficient strains of *C. glutamicum* [126, 188, 264]. The glutamate and glutamine produced by the described pathways are subsequently used as major nitrogen donors in other intracellular transamination reactions [56, 102].

In *C. glutamicum*, nitrogen assimilation is regulated at the transcriptional level by AmtR (Figure 1-4, Figure 1-5) [113]. During nitrogen excess, AmtR functions as a transcriptional repressor of its target genes. However, when the cell senses nitrogen deprivation, AmtR is sequestered from its target DNA by interacting with the adenylylated

Introduction

version of GlnK [27]. In contrast, during nitrogen excess, non-adenylated GlnK is sequestered at the cell membrane by interaction with AmtB, followed by degradation of GlnK [255]. The actual status of GlnK is controlled by GlnD, which catalyzes the adenylation and deadenylation of GlnK depending on the nitrogen status of the cell [27, 255]. Similar to GlnK, the activity of GS is regulated by post-transcriptional adenylation in a nitrogen-dependent manner, which is catalyzed by GlnE (Figure 1-4, Figure 1-5) [198]. It is noteworthy, that deletion of *glnE* leads to adenylation of GlnK and nitrogen limitation responses at the transcriptional level even under nitrogen excess [219]. In contrast, knockout strains of *glnD* or *glnK* were unable to induce nitrogen starvation responses [255]. A defined molecule used by the cell to sense its nitrogen status is still not identified. However, several studies suggest 2-oxoglutarate as a suitable candidate [102, 188]. As mentioned above, 2-oxoglutarate forms the junction between carbon metabolism and nitrogen assimilation, and serves as a substrate for OGDHC and GDH/GOGAT, respectively. In turn, carbon flux through the OGDHC is controlled by the GlnH-GlnX-PknG-OdhI signaling cascade (see Chapter 1.3.2), which senses periplasmic levels of glutamate and aspartate, indicating tightly regulated cross-talk between nitrogen and carbon metabolism in *C. glutamicum* [258].

1.4 Itaconic Acid

Itaconic acid (IA) (C₅H₆O₄) is an unsaturated dicarboxylic acid with pK_a values of 3.5 and 5.1 [110]. Its unique structure of two carboxyl groups and one vinylidene group allows a huge variety of possible chemical reactions, making IA a highly attractive bio-based platform chemical especially for the polymer industry [150, 175, 227]. In 2004, IA was identified as one of twelve platform chemicals with particular potential for biotechnological production in a study commissioned by the U.S. Department of Energy [294]. However, after a re-evaluation in 2010, IA was removed from this list due to declining attention in the scientific literature [46]. Since then IA has regained popularity, as evidenced by a steadily increasing number of publications and patents [68, 262]. Among others, IA can be used for the production of paints, resins, coatings, surfactants, fibers, and plastics [3, 4, 44, 150, 172, 227, 232, 274]. Current research is being conducted on the incorporation of IA into smart hydrogels that respond to specific pH, temperature, or ion concentrations and can be applied for drug delivery and water treatment [191, 265].

In addition, IA can serve as an environmentally friendly and sustainable substitute for (meth-)acrylic acid in the production of plastics [83, 287, 298]. As an immunomodulatory compound produced by human macrophages and due to its antimicrobial activity, IA has also gained interest in clinical research [64, 315]. Today, the global market volume for IA is estimated to be approximately 100 million USD [98]. At a cost of 1.5 to 2 USD per kg [306], this corresponds to an annual production of 50,000 to 67,000 t, compared to a global production capacity of about 80,000 t per year [203, 287]. To compete with petroleum-based platform chemicals, the market price of IA must fall below 0.55 USD per kg [294, 306]. Thus, the improvement of IA production, including the development of novel large-scale processes and the implementation of new production hosts and alternative substrates, is of high interest.

1.4.1 Native and Artificial Producers of Itaconic Acid

IA can be produced by various chemical syntheses, but due to its reactive nature the respective syntheses are tedious and accompanied by low yields [149, 298]. Today, IA is produced on an industrial scale exclusively by biotechnological fermentation. However, native overproducers of itaconic acid are presumably found exclusively in the fungal kingdom [15, 149, 311]. The most prominent representatives of the group of native IA producers are *Aspergillus terreus* and *Ustilago maydis*, which have been shown to be capable of reaching titers of 160 g and 220 g IA L⁻¹ from glucose, respectively [107, 145]. The metabolic pathways and key enzymes in IA production of both organisms are well studied and have been reviewed in detail by Wierckx *et al.* [296]. In summary, both fungi possess mitochondrial transporters that channel *cis*-aconitate formed by ACN from the mitochondria to the cytosol. In the cytosol of *A. terreus*, *cis*-aconitate is decarboxylated to itaconate by the activity of *cis*-aconitate decarboxylase (CAD). In contrast to *A. terreus*, *U. maydis* expresses an aconitate isomerase that first converts *cis*-aconitate to *trans*-aconitate, subsequently followed by decarboxylation of the latter catalyzed by the *trans*-aconitate decarboxylase (TAD). Finally, both organisms possess transporters for the cellular export of the produced IA [296]. It has been shown that heterologous expression of *cad* in non-producing organisms, such as yeast and bacteria, is sufficient to enable IA production in these organisms [34, 85, 103, 205]. The most promising approach to date for engineering bacterial IA producers was published by Harder *et al.* [103], who reported titers of 46.9 g IA L⁻¹ from glucose in a fed-batch process with a tailored *E. coli* strain [103]. In addition, an engineered *C. glutamicum* strain produced 7.9 g IA L⁻¹ from

Introduction

glucose in shaking flask cultivation [205]. However, IA production from glucose is ethically problematic (see Chapter 1.2), so IA production from alternative substrates has been investigated in several studies. Many approaches that focus on native IA producers like *A. terreus* as the intended production host use hydrolysates of various lignocellulosic materials as substrates, which occur as by-products of food, forestry, or agricultural industries. The respective hydrolysates are rich in fermentable sugars and different studies reported final titers between 27 g and 50 g IA L⁻¹ [144, 302] (Table 1-1). In this context, it should be noted that IA production from a corn stover hydrolysate by

Table 1-1: Overview of IA Production from Second Generation Substrates.

The table shows the key process indicators of IA production performed with different organisms on non-food derived substrates.

Organism	Substrate	Process duration in h	Titer in g L ⁻¹	Y _{P/S} in g g ⁻¹	q _P in g L ⁻¹ h ⁻¹	Ref.
<i>A. terreus</i>	Wheat Chaff Hydrolysate	163	27.7	0.41 ^a	0.19 (overall)	[144]
<i>A. terreus</i>	Wheat Bran Hydrolysate	120	49.7	0.50 ^a	0.41 (overall)	[302]
<i>A. terreus</i>	Corn Stover Hydrolysate	120	33.6	0.56 ^b	0.28 (overall)	[169]
<i>A. terreus</i>	Bamboo Residue Hydrolysate	240	41.5	-	0.25 (max)	[307]
<i>Synechocystis sp.</i>	CO ₂	400	0.015	-	36 × 10 ⁻⁶ (overall)	[59]
<i>Yarrowia lipolytica</i>	Waste Cooking Oil	120	54.6	0.3 ^c	0.6 (max)	[230]
<i>Pichia pastoris</i>	Methanol and CO ₂	192	2	-	0.01 (overall).	[23]
<i>Pseudomonas putida</i>	Lignin	48	1.4	0.79 ^d	0.03 (overall)	[85]
<i>E. coli</i>	Acetate and Yeast Extract	88	3.6	0.09 ^e	0.07 (max)	[196]
<i>C. glutamicum</i>	Acetate	46	29.2	0.16 ^e	1.01 (max)	[180] This work
<i>C. glutamicum</i>	Acetate	72	5.0	0.26 ^e	0.07 (overall)	[240] This work
<i>C. glutamicum</i>	Pyrolysis Water	72	3.4	0.23 ^e	0.05 (overall)	[240] This work

^a calculated based on the mass of sugar.

^b calculated based on the mass of glucose.

^c calculated based on the mass of oil.

^d calculated based on the mass of aromatic compounds.

^e calculated based on the mass of acetate.

A. terreus was strongly inhibited by acetate at concentrations of 0.85 g L^{-1} [169]. In addition to the use of sugar-rich substrates, several authors have focused on the production of IA from sugar-free substrates by engineering artificial IA producers (Table 1-1). Chin *et al.* [59] demonstrated photoautotrophic IA production from CO_2 by an engineered cyanobacterium that produced 15 mg IA L^{-1} within 400 h of cultivation [59]. In turn, Baumschabl *et al.* [23] reported the production of 2 g IA L^{-1} from CO_2 and methanol applied as carbon and energy sources, respectively, by an engineered *Pichia pastoris* strain [23]. Rong *et al.* [230] used waste cooking oil as substrate to produce IA by an engineered *Yarrowia lipolytica* strain. The authors optimized the provision of acetyl-CoA, reduced the ICL activity, and directed heterologous CAD expression into the peroxisomes. Thus, the tailored strain reached a final titer of 55 g L^{-1} with a maximum productivity of $0.6 \text{ g L}^{-1} \text{ h}^{-1}$ and a yield of 0.3 g IA per consumed gram of oil [230]. Elmore *et al.* [85] showed the production of 1.4 g IA L^{-1} from lignin under nitrogen-limited conditions by an engineered *Pseudomonas putida* strain. Therefore, the authors blocked the carbon flux to the storage polymer polyhydroxyalkanoate, reduced the expression of IDH, and expressed the *trans*-aconitate pathway of *U. maydis* [85]. Noh *et al.* [196] used acetate as substrate for the production of IA by an engineered *E. coli* strain. Therefore, the authors overexpressed the acetyl-CoA synthetase, CS, and CAD. In addition, the carbon flux within the TCA cycle and the glyoxylate shunt were modified to increase the final titer. Eventually, the engineered strain consumed $38.7 \text{ g acetate L}^{-1}$ and produced 3.57 g IA L^{-1} , in a fed-batch cultivation of 88 h, which corresponds to 13% of the theoretical maximum yield. However, the reported strain required the addition of yeast extract to the production medium to ensure cell vitality during the process [196]. Recently, we have shown that an engineered strain of *C. glutamicum* generated in this work (here referred to as *C. glutamicum* ITA4) can be used for the efficient production of IA from acetate as the sole carbon and energy source in an automated fed-batch process [180] (Table 1-1). By expressing an optimized version of the CAD enzyme and reducing the activity of IDH, the utilized strain was only marginally engineered. Nevertheless, cultivation under nitrogen limitation in a pH and DO-coupled fed-batch process allowed the production of 29.2 g IA L^{-1} with a maximum volumetric productivity of $1 \text{ g L}^{-1} \text{ h}^{-1}$ at 22% of the theoretical yield [180]. The results obtained demonstrate the considerable potential of *C. glutamicum* as a host for the valorization of acetate, especially for the production of IA, the optimization of which was also part of this thesis (see Chapter 3.2).

Finally, regarding the discussion of alternative substrates for IA production, whole-cell catalysis of citrate to IA has been shown to be a promising strategy for sustainable IA production, as well. An *E. coli* strain expressing the CAD and the ACN of *A. terreus* and *C. glutamicum*, respectively, produced 67 g IA L⁻¹ from citrate in only 8 h [108]. However, it is apparent that this process requires a supply of citrate produced from 2nd generation feedstocks to be considered as an alternative to glucose-based processes.

1.5 Aims of this Work

Overall, this work aims to establish acetate and acetate-containing sidestreams independent of food production as future substrates for microbial conversion. Thus, reducing ethical concerns about sugar-based, large-scale bioprocesses and contributing to a holistic bioeconomy approach. We aimed to introduce PW as a potential substrate for *C. glutamicum* to ensure a complete utilization of the initial biomass transformed by fast pyrolysis, contributing to a zero-waste process. Therefore, on the one hand, we analyzed the intrinsic ability of this organism to metabolize acetol and investigated native enzymes possibly involved in acetol utilization. On the other hand, we tested the heterologous expression of enzymes that have been reported to be involved in the conversion of acetol towards pyruvate. The results obtained are expected to provide important information about the acetol metabolism in *C. glutamicum* and other organisms, and to help to develop strategies for efficient valorization of this compound in further studies.

In addition, based on the theoretical assumption that *C. glutamicum* is a suitable microorganism for the valorization of acetate, we aimed to provide evidence proof that this organism can be used as a production host in acetate-based processes of industrial relevance. We set out to identify promising metabolic modifications and cultivation conditions that would redirect intracellular carbon flow and optimize the production of a desired compound. IA was chosen as an example as we aimed to develop a new strategy for sugar-independent production of this promising future bulk chemical. In this way, the supply of bio-based platform chemicals to the chemical industry is helping to transform our petroleum-based industry into a sustainable bioeconomy.

2 Material and Methods

An overview of all consumables, devices, chemicals, strains, plasmids, genomic DNA and primers used in this work, along with their corresponding abbreviations, properties, intended use, respective manufacturers, sources and references is given in Table A2 to Table A7. In addition, the cloning strategies for the construction of the respective plasmids are given in Table A6.

2.1 Cloning Procedures

2.1.1 Recombinant DNA Work

E. coli DH5 α [101] was used for plasmid amplification and maintenance. Plasmids used for cloning and/or transformation were purified from a respective 2YT overnight culture (Table 2-1) using the NucleoSpin[®] Plasmid Kit according to the manufacturer's recommendations. Genomic DNA was extracted from a respective 2YT overnight culture (Table 2-1) using the NucleoSpin[®] Microbial DNA Kit as recommended by the manufacturer. Codon optimization and synthesis of the genes encoding the IA transporters (*mfsA* and *itp1*) were performed commercially. DNA were stored at 4 °C or -20 °C for short and long term storage, respectively. If necessary, DNA restriction by the respective enzymes was performed as recommended by the manufacturer. After the reaction, cut DNA molecules were purified using the NucleoSpin[®] Gel and PCR Clean-up Kit according to the manufacturer's instructions. Plasmids and genomic DNA were used as templates for the amplification of DNA fragments and genes by polymerase chain reaction (PCR). PCR was performed using Q5[®] High-Fidelity DNA Polymerase in a Biometra TOne Thermocycler under the recommended conditions. Desalted and lyophilized oligonucleotides used as PCR primers were dissolved in ddH₂O according to the manufacturer's specifications. The success of the PCRs was confirmed by agarose gel electrophoresis conducted in TAE buffer (50x stock: 242g TRIS base L⁻¹, 57.1 ml glacial acetic acid L⁻¹, 0.05 M EDTA). Therefore, 5 μ l of the PCR reaction was mixed with 1 μ l of 6x Purple Loading Dye and loaded to the gel. Additionally, 3 μ l of Ready-to-Use

Material and Methods

1kb DNA Ladder was loaded on the gel as a size standard. The DNA fragments were separated in a Sub-Cell GT Electrophoresis System at 150 V for variable time. DNA was visualized by interaction with GelGreen[®] Nucleic Acid Gel Stain, which was added to the gel before casting. After electrophoresis, the gel was illuminated with blue light using an E-Box CX5 TS Gel Documentation System. PCR samples of the correct size were purified using the NucleoSpin[®] Gel and PCR Clean-up Kit as described above. Single nucleotide exchanges on plasmids were introduced by whole plasmid PCR, as described above, followed by DpnI treatment of the purified PCR product, according to the manufacturer's specifications. For oligonucleotide complementation, a PCR reaction mix was prepared without template and the samples were incubated in a Biometra TOne Thermocycler cycler (see above); cycles were reduced to a total of five. The amplified DNA fragments and linearized plasmids were joined either by Gibson-Assembly [94] in a total volume of 20 μ l or by restriction and ligation of the PCR products using T4 DNA Ligase, as recommended by the manufacturer. The entire reaction mix was used to transform *E. coli* DH5 α (see Chapter 2.1.2) to replicate the assembled plasmids. Purified plasmids and PCR products were verified by Sanger sequencing, commercially performed by Microsynth Seqlab GmbH (Göttingen, Germany). Chromosomal modifications of *C. glutamicum* were introduced to the genome by double homologue cross-over events using the pK19*mobsacB* vector system [238] (see Chapter 2.1.2, Table A6). Heterologous protein expression in *C. glutamicum* was facilitated by the *E. coli*/*C. glutamicum* shuttle vector pEKEx2, which contains an IPTG-inducible P_{tac} promoter (Table A6). When necessary, DNA concentrations were measured using a NanoPhotometer[™] N60 Micro-Volume UV-VIS Spectrophotometer.

2.1.2 Bacterial Transformation

In vitro assembled plasmids (see above) were used for transformation of chemically competent *E. coli* DH5 α . For this purpose, competent *E. coli* DH5 α were first prepared using the CaCl₂/MgSO₄ method and then transformed by heat shock in a Biometra TSC ThermoShaker at 45 °C for 90 seconds [101, 174]. The transformed cells were regenerated in 2YT medium, followed by separation on 2YT plates containing kanamycin (Table 2-1) for subsequent selection. The colonies obtained were screened by colony PCR using Quick-Load[®] Taq 2X Master Mix in a total volume of 10 μ l, according to the manufacturer's protocol. Finally, plasmids from positive clones were extracted and subsequently sent for sequencing (see Chapter 2.1.1). Clones containing correctly

assembled plasmids were stored in 30% (v/v) glycerol (aq.) at -80 °C. Plasmids verified by PCR and sequencing were used to transform electrocompetent *C. glutamicum* [260, 277]. To prepare electrocompetent *C. glutamicum*, a 5 mL BHIS culture (Table 2-1) was inoculated with a colony from a freshly prepared agar plate grown for up to 3 days, and cultured for 6 h. The entire volume of the culture tube was transferred to a 50 mL BHIS culture and cultured for an additional 16 h. 5 mL of the latter preculture was used to inoculate a 250 mL BHIS main culture, which was grown to an optical density (OD) of 1.75. When the culture reached its final OD, the cells were harvested by centrifugation in 50 mL centrifuge tubes in a 5910 Ri Refrigerated Centrifuge equipped with an S-4x Universal Rotor at 4,000 rcf and 4 °C. The cells were washed three times with 10 mL of 10% (v/v) sterile and ice cold glycerol (aq.). After the last centrifugation, the cells were resuspended in a total volume of 1 mL of 10% glycerol and divided into 100 µl aliquots, which were stored at -80 °C until further use. For transformation, the competent cells were thawed on ice and mixed with purified plasmid DNA in electroporation cuvettes with 2 mm gap wide and shocked with a pulse of 2.5 kV applied by a Gene Pulser Xcell Electroporator. Immediately, the cells were transferred to a culture tube containing 5 mL BHIS medium preheated to 46 °C and incubated at the same temperature for 6 min. Transformed cells were regenerated in BHIS medium for > 1 h and separated on BHIS plates containing kanamycin (Table 2-1) for subsequent selection. Colonies of cells transformed with pK19*mobsacB* [238] to introduce chromosomal mutations were then cultured in 2YT medium supplemented with kanamycin for 6 h, followed by incubation on 2YT plates supplemented with 10% (w/v) sucrose. The resulting colonies were counter-selected on 2YT and 2YT + kanamycin plates for loss of kanamycin resistance. Clones obtained after the transformation procedures were verified by colony PCR as described above. When necessary, PCRs were additionally verified by sequencing (see Chapter 2.1.1). Positive clones were stored at -80 °C as described above.

2.2 Cultivation and Growth Condition

2.2.1 Media and General Cultivation Conditions

An overview of the composition of the culture media used in this work, as well as stock solutions and other media additives, is given in Table 2-1. In general, *E. coli* was cultured

Material and Methods

in 2YT medium for 16 to 24 h at 37 °C. Unless otherwise stated, *C. glutamicum* cultures were incubated at 30 °C and respective plates were incubated for 2 to 3 days. All liquid cultures were incubated in a HT Multitron Incubator Shaker with an amplitude of 25 mm at 180 rpm. Solid cultures were incubated in a BD 260 Incubator. 5 mL cultures were prepared in culture tubes closed with a suitable metal cap. Cultivation in culture tubes was performed during cloning procedures (see Chapter 2.1) and for the preparation of precultures (see below). 50 mL cultures were prepared in 500 mL shaking flasks with

Table 2-1: Media Compositions.

The following table lists the composition of the culture media and stock solutions used in this work. All solutions were prepared with deionized water. Medium was prepared freshly and stored at room temperature for a maximum of 14 days. Plates were stored at 4 °C also for longer periods. Media were sterilized by autoclaving. Stock solutions were sterile filtered through a 0.2 µm cellulose-acetate syringe filter, aliquoted in 1.5 mL tubes, and stored at -20 °C.

Media, solutions	Composition
2YT [99]	16 g Bacto™ Tryptone L ⁻¹ , 10 g BBL™ Yeast Extract L ⁻¹ , 5 g NaCl L ⁻¹ .
Acetol 95% (w/v)	Used as supplied.
Agar Agar (for plates)	18 g L ⁻¹ added before autoclaving.
BHIS	37 g BD Bacto™ Brain Heart Infusion L ⁻¹ , 91 g Sorbitol L ⁻¹ . Each prepared two times concentrated and mixed 1:1 after autoclaving.
Biotin 1000x	200 mg D-Biotin L ⁻¹ .
CaCl₂ 1000x	10 g CaCl ₂ L ⁻¹ .
CGXII medium [79]	5 g (NH ₄) ₂ SO ₄ L ⁻¹ (omitted for nitrogen limitation), 5 g urea L ⁻¹ (reduced for nitrogen limitation, omitted for bioreactor cultures), 21 g MOPS L ⁻¹ (omitted for bioreactor cultures), 1 g K ₂ HPO ₄ L ⁻¹ , 1 g KH ₂ PO ₄ L ⁻¹ ; pH adjusted with KOH (pH of 6.5 or 7.4 for cultures supplemented with acetate or glucose as feedstock, respectively). Before inoculation, appropriate volumes of the following stock solutions were added: CaCl ₂ , MgSO ₄ , Biotin, Trace elements. Other supplements and feedstocks were added as required.
Ethanol 38.4% (v/v)	384 ml absolute Ethanol L ⁻¹ .
Glucose 50% (w/v)	550 g D-Glucose x H ₂ O L ⁻¹ .
Glutathione 100 mM	30.7 g reduced Glutathione L ⁻¹ .
IPTG 1000x	238.3 g IPTG L ⁻¹ .
Itaconate 2.5 M	325 g Itaconic acid L ⁻¹ , neutralized with KOH.
Kanamycin sulfate 1000x	50 g Kanamycin sulfate L ⁻¹ .
KCl 2.5 M	223.7 g KCl L ⁻¹ .
MgSO₄ 1000x	250 g MgSO ₄ x 7 H ₂ O L ⁻¹ .
NaHCO₃ 10x	42 g NaHCO ₃ L ⁻¹ .
PCA 195 mM	30 g Protocatechuic acid L ⁻¹ , neutralized with NaOH.
Potassium Acetate 81.7% (w/v)	817 g Potassium Acetate L ⁻¹ .
Trace elements 1000x	16.4 g FeSO ₄ x 7 H ₂ O L ⁻¹ , 0.1 g MnSO ₄ x H ₂ O L ⁻¹ , 0.313 g CuSO ₄ x 5 H ₂ O L ⁻¹ 1 g ZnSO ₄ x 7 H ₂ O L ⁻¹ , 0.02 g NiCl ₂ x 6 H ₂ O L ⁻¹ , pH adjusted to 1 with 37% (w/w) HCl.

four baffles closed with a cellulose plug. The respective cultures were used for the preparation of competent cells (see Chapter 2.1.2) and for pre- and main cultures during growth experiments (see Chapter 2.2.2). Media of 1 mL cultures used for screening experiments were prepared as 50 mL stocks, aliquoted onto an MTP-48-B Flower Plate, sealed with gas-permeable foil and incubated in a BioLector[®] I at 1000 rpm and 85% rel. humidity. When necessary, plates and liquid cultures were supplemented with 50 μ g kanamycin sulfate mL⁻¹. Gene expression from pEKEx2 plasmids was induced by addition of 1 mM IPTG (final concentration). The OD of the cultures was measured at an appropriate dilution with 0.9% (w/v) NaCl in a disposable Semi-Micro Polystyrene Cuvette using an Ultrospec[®] 10 Cell Density Meter at 600 nm. The linear range of the Cell Density Meter was determined to be 0.05 to 0.5 units. The correlation factor between OD₆₀₀ and cell dry weight (CDW) in g L⁻¹ was determined to be in the range of 0.23 to 0.27, depending on the respective instrument. The linear range and the correlation factor were determined experimentally as described by J. Lange [154] (data not shown). Liquid cultures were harvested by centrifugation. Volumes up to 2 mL were centrifuged in a 5425 Microcentrifuge equipped with an FA-24x2 Rotor. Larger volumes were centrifuged in a 5910 Ri Refrigerated Centrifuge equipped with an S-4xUniversal Rotor at room temperature (RT).

2.2.2 Growth Experiments

For growth experiments with *C. glutamicum*, a culture tube of 2YT medium (Table 2-1) was inoculated with a single colony from a freshly prepared agar plate. After 6 to 8 h, the entire volume was transferred to 50 mL 2YT and incubated for another 14 to 20 h. The latter culture was used to inoculate CGXII main cultures or additional precultures. Therefore, the OD of the respective preculture was measured and an appropriate volume was harvested by centrifugation at 4,000 rcf for 10 min at RT. The supernatant was discarded and the pellet was resuspended in 0.9% (w/v) NaCl (4% final volume of the new culture). If necessary, additional CGXII precultures were prepared in a final volume of 50 mL, inoculated to an OD of 1 and cultured as described in Chapter 2.2.1. CGXII precultures were supplemented with either 10 g acetate or 10 g glucose L⁻¹, depending on the feedstock provided in the subsequent main cultures. In general, main cultures of *C. glutamicum* were grown in CGXII minimal medium (Table 2-1) with pH adjusted to 6.5 when acetate or pyrolysis water were provided as substrate or with pH adjusted to 7.4 when ethanol or glucose were provided as substrate. The pH was adjusted

Material and Methods

with 5 M KOH prior to autoclaving. Shaking flasks were inoculated to an OD of 1, except for cultures containing *C. glutamicum* ITA strains, which were inoculated to an OD of 2. For screening experiments at 1 mL scale, cultures were prepared in a total volume of 2 mL and inoculated to an OD of 1. 1 mL was harvested before incubation and the remaining volume was incubated in a BioLector[®] (see Chapter 2.2.1). At the end of the cultivation, the temperature was shifted and held at 10 °C until the remaining volume was harvested. Biomass concentrations of each well were automatically recorded via backscatter (BS) signals at 620 nm with a gain set to 20. Because we observed inconsistent linearity between BS₆₂₀ signals and biomass concentrations (data not shown), relative BS signals were not converted to absolute biomass concentrations. To apply nitrogen limitation, the C:N ratio was increased to 40:1 by reducing the amount of urea to 0.5 g Urea L⁻¹ for 20 g acetate L⁻¹ (1 g urea L⁻¹ for 40 g glucose L⁻¹) and omitting (NH₄)₂SO₄ during media preparation. Bioreactor cultivation was performed in a DASGIP[®] Bioreactor System in a total volume of 1 L. The pH was set to 7.4 (independent of the supplied substrate) and automatically adjusted by the addition of 25% (w/v) aqueous ammonia or 10% (w/v) *o*-phosphoric acid. DO was adjusted to 35% (relative to air saturation) by a constant gas flow of 0.25 vvm and variable stirrer speed. Samples (generally 1 mL) of the various cultures described in this section were harvested at the indicated time points. Appropriate volumes were used for OD measurements, the remaining sample volume was centrifuged at 21,300 rcf for 10 min at RT, and the clear supernatant was stored at -20 °C until further analysis (see Chapter 2.4).

2.3 Intracellular Analysis

2.3.1 Determination of Itaconic Acid Concentrations

To measure intracellular concentrations of IA, cells were lysed by silicon oil centrifugation [76, 136]. For this purpose, 200 µl of the respective culture sample was added to a layer of 300 µl Silicon Oil PN200 floating on 100 µl of 35% perchloric acid. The samples were immediately centrifuged at 21,300 rcf for 10 min at RT. Afterwards, the remaining culture supernatant and the oil phase were carefully removed and discarded. The cell pellet was resuspended in the remaining acidic fraction and neutralized by the addition of 100 µl of 5.8 M KOH containing 1 M KH₂PO₄. Samples were vortexed

briefly and stored on ice for 30 min, followed by centrifugation at 15,000 rcf at 4 °C for 30 min using a CS-15R Refrigerated Centrifuge. Finally, the sample supernatant was filtered through a 0.45 µm cellulose-acetate syringe filter and stored at -20 °C until further analysis by HPLC (see Chapter 2.4.1). For the calculation of intracellular IA concentrations, a cytoplasmic volume of 1.7 µl per mg of cell dry weight was presumed [205] (see Chapter 2.4.4).

2.3.2 Determination of *cis*-Aconitate Decarboxylase activity

To determine CAD activity in the engineered *C. glutamicum* strains, a 50 mL culture was harvested by centrifugation at 4,000 rcf for 20 min at 4 °C. The supernatant was discarded and the pellet was resuspended in 25 mL of ice-cold 0.2 M potassium phosphate buffer, pH 6.5. The procedure was repeated and the pellet was finally resuspended in 1 mL of the same buffer. The suspension was transferred to a pre-cooled reaction tube containing 250 µl glass beads of 0.1 mm diameter. Cells were lysed using a Precellys® 24 Cell Disrupter in cycles of 6 x 30 s separated by 2 min cooling on ice. Glass beads were sedimented by short centrifugation. To remove cell debris, the supernatant was separated from the glass beads and centrifuged in a CS-15R Refrigerated Centrifuge at 15,000 rcf at 4 °C for 30 min. CAD activity was determined by an enzyme assay as previously described by Otten *et al.* [205]. Briefly, 100 µl of the prepared crude cell extract was added to 900 µl of 0.2 M potassium phosphate buffer containing 8 mM *cis*-aconitic acid (final pH of 6.2) on ice. Samples were vortexed briefly and incubated for 10 min at 37 °C and 300 rpm in a Biometra TSC ThermoShaker. To stop the reaction, 38 µl of 32% HCl was added to the samples while shaking. In addition, blank samples were prepared in a similar manner, but HCl was added prior to incubation. The samples were then centrifuged at 21,300 rcf for 10 min at RT. Finally, the sample supernatant was filtered through a 0.45 µm cellulose-acetate syringe filter and stored at -20 °C until further analysis by HPLC (see Chapter 2.4.1). In parallel, enzyme concentrations in the crude cell extracts were determined according to Bradford [47] using the Quick Start™ Bradford Protein Assay according to the manufacturer's specifications. The absorbance of three technical replicates was measured at 595 nm using a TECAN Spark Plate Reader. 1 unit of CAD activity was defined as 1 µmol of IA produced in 1 minute per mg of protein in the crude cell extract [205] (see Chapter 2.4.4).

2.4 Analytics

2.4.1 HPLC Measurements

The determination of organic acid and carbohydrate concentrations in the culture supernatants (see Chapter 2.2.2) was performed by isocratic HPLC, as previously described by Siebert *et al.* [249], using a 1260 Infinity II HPLC System equipped with a Hi-Plex H Column (7.7 x 300 mm, 8 μm) protected by a Hi-Plex H Guard Cartridge (3 x 5 mm, 8 μm). In general, the system was heated to 50 °C, except when samples with PW were analyzed, in which case the temperature was lowered to 30 °C during the analysis. 5 mM aqueous sulfuric acid was used as the mobile phase at a flow rate of 0.4 mL min⁻¹. Signals were acquired by a refractive index detector (RID) for 35 or 60 min at 50 and 30 °C, respectively. Received relative units obtained from the RID were calculated to a concentration in mM by measuring standardized concentrations between 1 mM and 250 mM of the respective analyte dissolved in deionized water. Samples for intracellular analysis of IA concentrations and CAD activities (see Chapter 2.3) were determined as described above, but signals were acquired using a diode array detector (DAD) at 215 nm. The relative units received by the DAD were calculated to a concentration in μM by measurements of standardized concentrations between 10 μM and 5 mM of itaconate.

2.4.2 Total Carbon Measurement

Total carbon measurements were performed with supernatants of cultures containing PW as substrate. Carbon fractions were determined according to Buchholz *et al.* [54] using a Multi N/C 2100S TOC/TNb Analyzer. Therefore, 100 μl of a properly diluted sample were used to measure total carbon (TC) by combustion at 800 °C or inorganic carbon (IC) by acidification with 10% (w/v) *o*-phosphoric acid in 3 to 4 technical replicates. CO₂ formed during TC and IC measurements was detected by a non-dispersive infrared sensor. The received relative units for CO₂ were calculated to a concentration in g L⁻¹ by measuring standardized concentrations in the range of 100 mg L⁻¹ to 1.5 g L⁻¹ of Na₂CO₃ for IC and 400 mg L⁻¹ to 3 g L⁻¹ of potassium hydrogen phthalate for TC. Total organic carbon (TOC) was calculated as the difference between TC and IC. The organic carbon fractions of the samples supplemented with potassium acetate as feedstock were calculated according to the concentrations obtained during the HPLC measurements and were not measured with the TOC/TNb Analyzer.

2.4.3 Determination of Nitrogen Concentrations

Nitrogen concentrations in the culture medium were determined by UV spectroscopy using a commercially available Ammonia/Urea UV-Method Kit (Table A2). Measurements were performed according to the manufacturer's recommendations in a total volume of 750 μ l. The respective absorbance of two technical replicates were measured in PMMA Semi-Micro Cuvettes at 340 nm, using a Specord[®] 50 plus UV/VIS Photometer. Calculations of nitrogen concentrations were performed as indicated in the manual, using the adjusted sample volume.

2.4.4 Calculations and Statistics

Growth rates (μ) were determined by r^2 maximization of an exponential regression fit of the biomass concentrations (c_X) versus time. For nitrogen-limited cultures incubated in the BioLector[®], exponential growth was assumed between a BS_{620} of 30 and 90. Biomass yield per substrate ($Y_{X/S}$) was determined by the absolute value of a linear regression fit of biomass concentrations plotted against substrate concentrations. Substrate uptake rate (q_S) was calculated by multiplying the reciprocal of $Y_{X/S}$ by μ . During cultivations with acetol, $Y_{X/S}$ and q_S were calculated according to the concentration of the main substrate glucose or acetate. Analogously, both values were calculated with the concentration of total carbon when acetol was included. The uptake of acetol appeared to be linear, so the substrate uptake rate for acetol (q_S') was calculated by the absolute value of a linear regression fit of the acetol concentration versus time. The intracellular concentration of IA was calculated by multiplying the concentration obtained during the HPLC analyses by the final samples volume of 200 μ l. The result obtained was divided by the product of the biomass concentration, the volume of the harvested culture (200 μ l), and the intracellular volume of *C. glutamicum*. The latter is 1.7 μ l per mg of cell dry weight [205]. For the calculation of CAD activity, the IA concentrations obtained from the HPLC measurements of the assay samples were corrected for that of the corresponding blanks. The final IA concentrations were multiplied by the final assay volume of 1.038 mL. The latter product was divided by the protein concentrations in the crude extract and time. Unless otherwise stated, all data presented in this work show the mean and standard deviation of at least three biological replicates. A biological replicate is defined as the independent cultivation of a single colony picked from a freshly prepared culture plate, in separately prepared media. Whenever possible, three positive clones from

independent transformation events were isolated and used for the respective replicates. A technical replicate is defined as an independent preparation and measurement of a specific sample from the same biological replicate. Error propagation of the technical replicates was not taken into account in the determination of standard deviations. Significance was determined in Microsoft Office Excel Professional Plus 2016 using a two sample t-test, assuming equal variance.

2.5 Next Generation Sequencing

Next generation sequencing of genomes and transcriptomes was commercially performed by Genewiz Germany GmbH (Leipzig, Germany), by ordering the Value Package of Illumina NovaSeq Sequencing of 2 x 150 base-pair reads for a total of 10 million read pairs. For genome sequencing of mutant *C. glutamicum* ITA strains, genomic and plasmid DNA of the respective strains were extracted using the NucleoSpin[®] Microbial DNA Kit according to the instructions. Library preparation, sequencing and processing of raw data were performed by Genewiz. Raw data processing included mapping of the reads to the available genome of *C. glutamicum* ATCC13032 (Refseq: NC_003450) and the plasmid pEKEx2-*malE*_{cad_{opt}} (unpublished), followed by variant analysis. We compared the variants obtained for the mutant strains with the variants obtained for the control *C. glutamicum* ITA1 in order to identify variants unique to the strains of interest. Samples for whole transcriptome analysis were generated during bioreactor cultivation. Therefore, 1 mL of culture was harvested at mid-exponential phase, prior to the first addition of antifoam agent, and immediately centrifuged at 15,000 rcf at 4 °C for 1 min using a CS-15 Refrigerated Centrifuge. Immediately after centrifugation, the supernatant was removed and the pellet was shock-frozen in liquid nitrogen. The pellets were sent to Genewiz for RNA extraction, library preparation including rRNA depletion, and sequencing. Normalization, mapping and further processing of the raw data between acetol-treated samples and the untreated controls was kindly performed by Dr. Richa Bharti and Prof. Dr. Dominik Grim from the TUM Campus Straubing for Biotechnology and Sustainability (Straubing, Germany). We further analyzed the processed data for the absolute value and the significance of transcriptional changes between the untreated controls supplemented with 10 g glucose or 10 g acetate L⁻¹, and the corresponding samples additionally supplemented with 5 g acetol L⁻¹.

2.6 Processing of Pyrolysis Water

The PW used in this study refers to the aqueous condensate that was formed during the bioliq[®] process and was kindly provided by Dr. Axel Funke and Prof. Dr. Nicolaus Dahmen of the IKFT at the KIT (Eggenstein-Leopoldshafen, Germany). For the evolutionary experiments with acetol and PW, crude PW was used to supplement the respective cultures. The PW used as substrate for IA production was pretreated according to Kubisch and Ochsenreither [147], prior to the cultivation. Therefore, the pH of 500 mL crude PW was adjusted to about 7 by adding solid KOH. The neutralized PW was then divided equally into 50 mL centrifugation tubes and centrifuged using a 5910 Ri Refrigerated Centrifuge equipped with an S-4x Universal Rotor at 4,000 rcf for 30 min. The supernatant obtained was filtered with a funnel filter equipped with two filter papers. The filtered PW was vacuum concentrated with a Hei-VAP Core Rotary Evaporator at 80 °C. The pressure was successively reduced from 400 mbar to 200 mbar within the first hour and kept at 200 mbar for 4 h. The remaining solid was resuspended in 500 mL deionized water and incubated in a Sonorex Super RK 510 H Ultrasonic Bath for 30 min. The pH of the dissolved PW salts was further increased to 13 by adding solid KOH, followed by boiling the PW in a closed bottle at 100 °C for 2 h while stirring. After cooling to RT, the processed PW was filtered as before and neutralized by adding 96% (w/v) H₂SO₄. The filtration was repeated and the neutralized PW was mixed with 10% (w/v) activated carbon. After stirring at room temperature for 10 min, the activated carbon was separated from the PW by centrifugation, followed by filtration as described above. Finally, the PW was sterile vacuum filtered with a 0.2 µm Polyethersulfone Membrane Filtration Cup. The processed PW was stored at 4 °C until further use.

3 Results

A holistic bioeconomy strategy aims to replace all fossil resources with renewable substitutes. This also includes the provision of basic building blocks for the chemical industry. Industrial biotechnology has made great strides in producing high and low-value chemicals from biomass. However, these processes suffer from ethical concerns, such as the ‘food vs. industry’ dilemma due to the high consumption of food-derived substrates, or the occupation of fertile land for the cultivation of the required high-energy crops used as substrates on an industrial scale. Therefore, novel processes are needed that can convert side and “waste” streams and do not interfere with human food production. In doing so, novel processes do not only address ethical concerns, but also contribute to a circular and zero waste economy strategy. With this work, we will contribute to the establishment of sustainable biotechnological processes by introducing PW, a sidestream of the thermal conversion of non-food biomass, as a substrate for the production of IA, a bio-based platform chemical with high potential for chemical and medical applications. To achieve this goal, we first performed growth experiments and transcriptome sequencing to analyze the metabolic capacity of *C. glutamicum* to utilize acetol as a substrate for biomass formation. Furthermore we tested different ways to enhance the metabolization of acetol by heterologous expression of different pathways and performed adoptive laboratory evolution (ALE) of *C. glutamicum* on PW. In parallel, we used acetate as a model substrate to engineer IA production strains optimized for yield and titer and to screen for optimal production conditions.

3.1 Studies on Acetol Metabolization

The crude PW used in this study was produced by the bioliq[®] process and consists of almost equal amounts of acetate (625 mM) and acetol (740 mM) (see Chapter 1.2.1). While acetate has been proposed as a potential substrate for biotechnological conversion and is a native substrate for several biotechnological production hosts, in particular *C. glutamicum* (see Chapter 1.3.2), little is known about acetol and its use as a substrate. However, acetol remains of special interest as a substrate for valorization, because, due

Results

to its high concentration, most of the carbon and energy in PW is stored in this molecule. Finding metabolic pathways to efficiently metabolize acetol in microbial hosts may help to establish PW as a novel sustainable feedstock for future processes at an industrial scale. Thus, in this work we aimed to characterize and optimize the acetol metabolization by *C. glutamicum* in order to subsequently improve the valorization of PW.

3.1.1 Investigation of Culture Conditions for Growth on Acetol

Previously, in his Ph.D. thesis, J. Lange [154] showed that *C. glutamicum* is unable to grow on acetol as the sole carbon and energy source, but bi-phasic growth could be enabled if the cells were supported with yeast extract or glucose [154]. We first tested that *C. glutamicum* is unable to grow on acetol as the sole carbon and energy source. Therefore, *C. glutamicum* ATCC13032 was cultured in shaking flasks containing CGXII medium supplemented with 5 g acetol L⁻¹ and inoculated to an OD of 1 at 30 °C (Figure 3-1 A). After 10 h, biomass concentrations increased slightly from 0.24 ± 0.02 g to 0.36 ± 0.03 g L⁻¹, and at the same time, acetol concentrations decreased from 3.16 ± 0.09 g to 1.70 ± 0.07 g L⁻¹. Since acetol decreased in a fairly linear manner, we determined a biomass-independent, time-dependent substrate uptake rate, referred to as q_s' in this work (see Chapter 2.4.4). The determined q_s' was 0.14 ± 0.01 g acetol h⁻¹, which corresponds to an uptake of 0.07 ± 0.01 g carbon (g_C) h⁻¹. The $Y_{X/S}$ amounted to 0.08 ± 0.01 g_X g_{Acetol}⁻¹. The pH of the culture increased from 7.51 ± 0.02 to

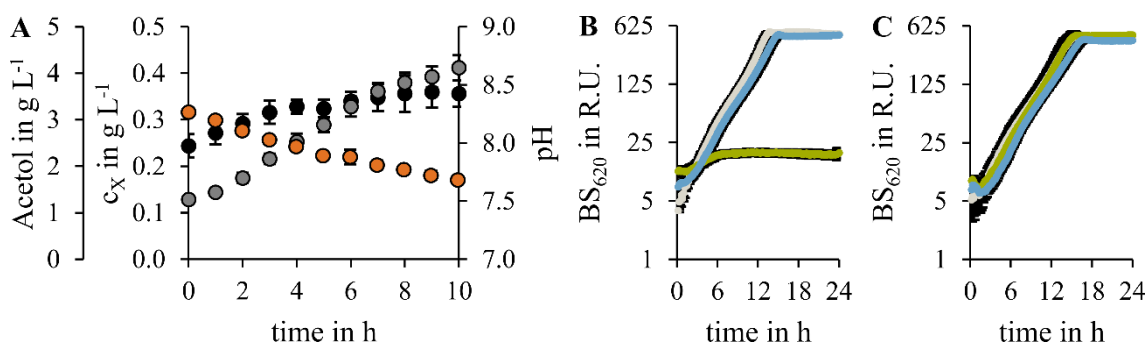


Figure 3-1: Growth and Uptake of Acetol by *C. glutamicum*.

A: Shaking flask cultivation of *C. glutamicum* on 5 g acetol L⁻¹ as sole carbon and energy source. The graph shows biomass concentrations (black), pH (grey) and acetol concentrations (orange). Error bars show standard deviation of three biological replicates. **B, C:** Cultivation of *C. glutamicum* in CGXII medium supplemented with 20 g glucose L⁻¹ and 5 g acetol L⁻¹ at 1 mL scale. Cultures were inoculated either from a 2YT preculture according to our standard seed-train conditions, showing variable growth phenotypes (**B**); or from a CGXII preculture according to the alternative seed-train procedure, showing uniform growth phenotypes (**C**). The three different colors in **B** and **C**, blue, grey and green indicate individual biological replicates. The respective error bars show standard deviation of three technical replicates.

8.65 ± 0.11 within the 10 h of cultivation, probably due to the degradation of urea. These results indicate that acetol can be used as the sole carbon and energy source by *C. glutamicum*, but its assimilation is severely impaired compared to other carbon sources.

Next, we analyzed the growth and substrate uptake of *C. glutamicum* when acetol was supplied as a co-substrate along with glucose. Therefore, cells were grown in CGXII medium supplemented with 10 g glucose L⁻¹ and various concentrations between 0 g and 20 g acetol L⁻¹. Control cultures without acetol showed a μ of 0.39 ± 0.01 h⁻¹, while cultures supplemented with 20 g acetol L⁻¹ showed no growth within 24 h of cultivation. For all other concentrations tested in this experiment, no clear growth phenotype could be observed, as the cells showed exponential growth until glucose was depleted in some cultures and severely inhibited growth in others. However, it should be noted that growth of the latter was observed when the cultivation time was extended up to 7 days. Furthermore, growth on 20 g acetol L⁻¹ was obtained when the culture was directly inoculated with cells previously successfully pre-cultured on lower concentrations of acetol (data not shown). Taken together, these initial observations led to the suggestion that acetol causes an unknown source of stress to the cells, to which *C. glutamicum* has the ability to adapt. We hypothesized that the adaptation of the cells to the CGXII minimal medium prior to the addition of acetol might benefit the overall growth of *C. glutamicum* under the conditions tested. Therefore, we modified our standard seed-train and introduced a second preculture in CGXII medium, following the first preculture in 2YT medium. The second preculture was supplemented with 10 g glucose L⁻¹ (or later with 10 g acetate L⁻¹, see below) and incubated for 24 h before an appropriate amount of biomass was used to inoculate the respective main cultures. The latter were supplemented with 20 g glucose L⁻¹ and different concentrations of acetol, between 0 g and 10 g L⁻¹, and screened at 1 mL scale. Indeed, a uniform growth phenotype was observed for all samples additionally pre-cultured in CGXII medium, but not for cultures inoculated from a 2YT preculture (exemplified for 5 g acetol L⁻¹ in Figure 3-1 B, C). It is noteworthy that samples without acetol showed a significantly reduced μ of 0.35 ± 0.01 h⁻¹ compared to 0.47 ± 0.02 h⁻¹ when cells were pre-cultured in CGXII medium or 2YT medium, respectively. In addition, the μ 's of the cultures containing acetol decreased progressively with increasing concentrations of acetol. Cells pre-cultured in CGXII medium and supplemented with 1 g, 5 g, or 10 g acetol L⁻¹ showed μ 's of 0.32 ± 0.01 , 0.30 ± 0.01 and 0.23 ± 0.01 h⁻¹, respectively. Since the cells exhibited a uniform growth phenotype when

Results

pre-cultured in CGXII medium and growth rates in the main cultures was only slightly reduced by the addition of 5 g acetol L⁻¹, we chose these conditions for further experiments.

Lange et al. [155] reported positive effects of reduced glutathione (GSH) on the growth of *C. glutamicum* on PW. In addition, protocatechuic acid (PCA) has been shown to generally support the growth of *C. glutamicum* in CGXII medium [166, 266]. Therefore, we tested the effect of GSH and PCA on *C. glutamicum* during growth on acetol at 1 mL scale. For this purpose, CGXII precultures were supplemented with either 30 mg PCA L⁻¹ or 1 mM GSH. In addition, CGXII main cultures were prepared with 20 g glucose L⁻¹ and 5 g acetol L⁻¹ and further supplemented with different concentrations of PCA (0 to 60 mg L⁻¹) or GSH (0 to 2 mM). In a single determination we observed that the addition of PCA to the preculture had no effect on the growth of *C. glutamicum* in the main culture. However, the addition of PCA to the main culture successively increased μ from 0.28 h⁻¹ without PCA to a maximum of 0.38 h⁻¹ at a PCA concentration of 30 mg L⁻¹; the positive effect was attenuated at higher PCA concentrations up to 60 mg L⁻¹. Similar effects were observed for GSH, as the μ gradually increased from 0.25 h⁻¹ without GSH to 0.37 h⁻¹ at concentrations of 1.5 mM GSH. Higher GSH concentrations in the main cultures had no further effect on cell growth. However, when GSH was added already to the precultures, μ was 0.33 h⁻¹ without GSH and further increased to 0.40 h⁻¹. Although we observed positive effects of PCA and GSH on cell growth, we did not observe any remarkable differences in the absolute consumption of acetol at the end of the cultivations. Therefore, we decided not to further consider PCA and GSH as culture supplements with respect to the acetol metabolism.

3.1.2 Growth on Acetol as co-Substrate with Glucose and Acetate

Above, we have shown that acetol as sole carbon source appears to be an unsuitable feedstock for the cultivation of *C. glutamicum* and does not support sufficient growth of this bacterium, but the wild-type strain was able to grow on mixtures of acetol and glucose when inoculated from a CGXII preculture. However, when using PW as a substrate, it is important to note that PW does not contain glucose, but acetate in high concentrations. Therefore, we included acetate in addition to glucose in further studies to characterize the growth and substrate uptake of *C. glutamicum* during cultivation on acetol as a co-substrate. It should be noted that the cells were pre-cultured according to the newly

established seed train (see above), but the CGXII preculture was supplemented with either 10 g glucose or 10 g acetate L⁻¹, depending on the substrate provided in the main culture.

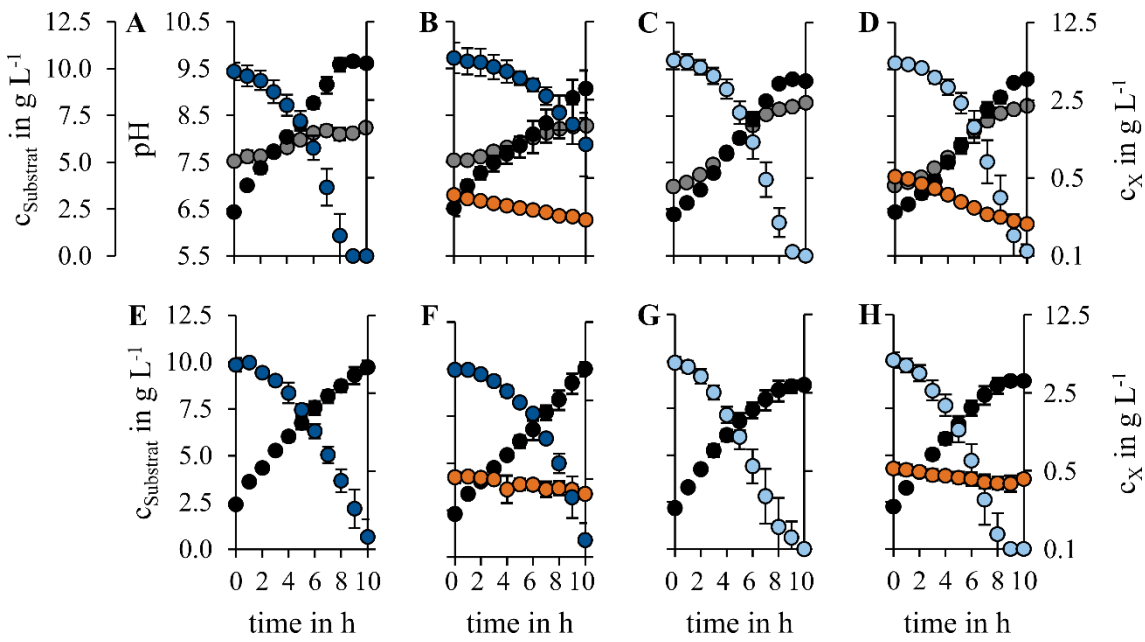
3.1.2.1 Characterizations during Shaking Flask Cultivation

To obtain more information on the metabolization of acetol by *C. glutamicum*, we studied growth and substrate uptake during shaking flask cultivation in more detail. Therefore, we prepared different main cultures of CGXII medium supplemented with either 10 g glucose or 10 g acetate L⁻¹, each with and without 5 g acetol L⁻¹ (Figure 3-2 A-D). *C. glutamicum* showed the same μ during growth on glucose and acetate, which was $0.35 \pm 0.01 \text{ h}^{-1}$ and $0.36 \pm 0.01 \text{ h}^{-1}$, respectively. However, during growth on glucose, μ was significantly reduced to $0.20 \pm 0.06 \text{ h}^{-1}$ when 5 g acetol L⁻¹ was added to the culture. Due to the reduced growth rates, the q_s of glucose decreased by 50% from 0.67 ± 0.04 to $0.33 \pm 0.01 \text{ g}_{\text{Glc}} \text{ g}_X \text{ h}^{-1}$, preventing a direct comparison of q_s in these samples. In contrast, during growth on acetate μ of *C. glutamicum* was not affected by acetol and, furthermore, q_s and $Y_{X/S}$ remained at about $1 \text{ g}_{\text{Ac}} \text{ g}_X^{-1} \text{ h}^{-1}$ and $0.36 \text{ g}_X \text{ g}_{\text{Ac}}^{-1}$, respectively, when acetol was added. As before, acetol decreased rather linearly with time and q_s' was 0.12 ± 0.01 and $0.14 \pm 0.02 \text{ g h}^{-1}$, for cultures supplemented with glucose and acetate, respectively. We also observed an increase in pH in all cultures. The pH increased from about 7.5 to 8.25 in cultures containing glucose and from about 7 to 8.75 in cultures containing acetate, but the increase in pH was not markedly affected by the presence or absence of acetol. However, it is noteworthy that the addition of acetol resulted in a significant increase in $Y_{X/S}$, which rose from $0.53 \pm 0.01 \text{ g}_X \text{ g}_{\text{Glc}}^{-1}$ without acetol to $0.61 \pm 0.03 \text{ g}_X \text{ g}_{\text{Glc}}^{-1}$ with acetol, during growth on glucose. On the other hand, $Y_{X/S}$ by total carbon decreased from $1.32 \pm 0.04 \text{ g}_X \text{ g}_C^{-1}$ without acetol to $1.08 \pm 0.15 \text{ g}_X \text{ g}_C^{-1}$ with acetol, in the same cultures.

3.1.2.2 Characterization during Bioreactor Cultivations

To exclude any side effects by cultivation in shaking flasks, such as changes in pH or oxygen deprivation on the acetol metabolism of *C. glutamicum*, we repeated the cultivations from above in a table-top bioreactor that allows tight control of aeration and pH (Figure 3-2 E-H). Growth rates of *C. glutamicum* during bioreactor cultivation on

Results



	Substrate	μ in h^{-1}	$Y_{X/S}$ in $\text{g}_X \text{g}_C^{-1}$	$Y_{X/S}$ in $\text{g}_X \text{g}_S^{-1}$	q_s in $\text{g}_C \text{g}_X^{-1} \text{h}^{-1}$	q_s in $\text{g}_S \text{g}_X^{-1} \text{h}^{-1}$	q_s' in $\text{g}_{\text{Acetol}} \text{h}^{-1}$
Shaking Flasks	Glucose 10 g L^{-1}	0.35 ± 0.01	1.32 ± 0.04	0.53 ± 0.01	0.27 ± 0.02	0.67 ± 0.04	-
	Glucose 10 g L^{-1} + Acetol 5 g L^{-1}	0.20 ± 0.06	1.08 ± 0.15	0.61 ± 0.03	0.18 ± 0.03	0.33 ± 0.01	0.12 ± 0.01
	Acetate 10 g L^{-1}	0.36 ± 0.01	0.86 ± 0.04	0.36 ± 0.02	0.42 ± 0.03	1.01 ± 0.10	-
	Acetate 10 g L^{-1} + Acetol 5 g L^{-1}	0.35 ± 0.02	0.64 ± 0.02	0.36 ± 0.02	0.55 ± 0.05	0.98 ± 0.10	0.14 ± 0.02
Bioreactor	Glucose 10 g L^{-1}	0.29 ± 0.02	1.04 ± 0.03	0.41 ± 0.02	0.27 ± 0.01	0.70 ± 0.01	-
	Glucose 10 g L^{-1} + Acetol 5 g L^{-1}	0.29 ± 0.02	1.10 ± 0.03	0.48 ± 0.03	0.26 ± 0.01	0.60 ± 0.02	0.09 ± 0.00
	Acetate 10 g L^{-1}	0.31 ± 0.04	0.66 ± 0.04	0.26 ± 0.01	0.47 ± 0.03	1.17 ± 0.10	-
	Acetate 10 g L^{-1} + Acetol 5 g L^{-1}	0.32 ± 0.03	0.60 ± 0.03	0.28 ± 0.02	0.54 ± 0.05	1.15 ± 0.04	0.07 ± 0.01

Figure 3-2: Cultivation of *C. glutamicum* ATCC 13032 on Glucose, Acetate and Acetol.

Graphs show concentrations of biomass (black), glucose (dark blue), acetate (light blue), and acetol (orange) during shaking flask cultivations (A-D) or bioreactor cultivations (E-H). The respective cultures were supplemented with $10 \text{ g glucose L}^{-1}$ (A, E); $10 \text{ g glucose L}^{-1}$ and $5 \text{ g acetol L}^{-1}$ (B, F); $10 \text{ g acetate L}^{-1}$ (C, G) or $10 \text{ g acetate L}^{-1}$ and $5 \text{ g acetol L}^{-1}$ (D, H). In addition, the pH during shaking flask cultivation is shown in grey. Furthermore, the growth rates (μ), biomass yields ($Y_{X/S}$), and substrate uptake rates (q_s) of the tested conditions are shown in the table below. The $Y_{X/S}$ and q_s values were calculated with respect to the uptake of total carbon (g_C) or the uptake of the main substrate glucose or acetate (g_S). As before, acetol uptake (q_s') was calculated independently of the biomass concentrations.

glucose or acetate were $0.29 \pm 0.02 \text{ h}^{-1}$ and $0.31 \pm 0.04 \text{ h}^{-1}$, respectively, and were markedly lower compared to cultivations in shaking flasks. Interestingly, similar to the μ on acetate, the μ on glucose was not attenuated after the addition of acetol, this time. In addition, acetol again decreased linearly with time during cultivation, but q_s ' was significantly reduced to 0.09 ± 0.00 and $0.07 \pm 0.01 \text{ g h}^{-1}$ on glucose and acetate, respectively, compared to cultivation in shaking flasks. On the other hand, q_s of acetate was slightly increased by 16% to about $1.17 \text{ g}_{\text{Ac}} \text{ g}_{\text{X}}^{-1} \text{ h}^{-1}$, but, $Y_{\text{X/S}}$ was decreased by 28% to about $0.26 \text{ g}_{\text{X}} \text{ g}_{\text{Ac}}^{-1}$, compared to shaking flask cultures. Again, these values were not significantly affected by the presence or absence of acetol. During cultivation on glucose, $Y_{\text{X/S}}$ was also reduced by 23% to about $0.41 \text{ g}_{\text{X}} \text{ g}_{\text{Glc}}^{-1}$, compared to shaking flask cultivation, but the q_s of glucose and total carbon did not show any significant differences between the two cultivation methods tested and were $0.70 \pm 0.01 \text{ g}_{\text{Glc}} \text{ g}_{\text{X}}^{-1} \text{ h}^{-1}$ and $0.27 \pm 0.01 \text{ g}_{\text{C}} \text{ g}_{\text{X}}^{-1} \text{ h}^{-1}$, respectively, during bioreactor cultivation without acetol. As mentioned above, μ was not affected by acetol during the bioreactor cultivation on glucose, allowing a comparison of the respective uptake rates and biomass yields with the cultures without acetol. After the addition of acetol, q_s of glucose was reduced by 14% to $0.60 \pm 0.02 \text{ g}_{\text{Glc}} \text{ g}_{\text{X}}^{-1} \text{ h}^{-1}$, while q_s of total carbon remained unaffected at $0.26 \pm 0.01 \text{ g}_{\text{C}} \text{ g}_{\text{X}} \text{ h}^{-1}$. Furthermore, $Y_{\text{X/S}}$ calculated for glucose or total carbon, significantly increased from 0.41 ± 0.02 to $0.48 \pm 0.03 \text{ g}_{\text{X}} \text{ g}_{\text{Glc}}^{-1}$ and from 1.04 ± 0.03 to $1.10 \pm 0.03 \text{ g}_{\text{X}} \text{ g}_{\text{C}}^{-1}$, respectively, in the presence of acetol.

In addition to the results described in this chapter, samples for transcriptome analysis were harvested and processed during the mid-exponential growth phase of all bioreactor cultivations. The results obtained are discussed in the following chapter.

3.1.3 Whole Transcriptome Analysis

Whole transcriptome analysis is a powerful tool for studying cellular responses to a given condition at the transcriptional level. Changes in the transcriptome can reveal up or downregulation of individual reactions, entire pathways, and shifts in regulatory clusters. Here, we performed a whole transcriptome analysis to identify promising genes encoding enzymes involved in the metabolization of acetol. Samples for RNA sequencing were collected during bioreactor cultivations of *C. glutamicum* on glucose or acetate with and without acetol supplementation (see Chapter 3.1.2). Samples were harvested at mid-exponential growth phase, at an OD between 3.5 and 6.5, between 4 and 7 h after inoculation, before the first addition of antifoam agents. RNA sequencing was performed

Results

by Genewiz GmbH (Leipzig, Germany) and the received raw data were kindly processed by Dr. Richa Bharti (TUM Campus Straubing; Straubing, Germany), who performed mapping to the reference genome and normalization of the data. With an RNA integrity number of ≥ 9.5 and more than 11 million reads per sample, the quality of the raw data can be assumed to be of good quality and provide reliable information.

3.1.3.1 Identification of Promising Candidates

The processed raw data were used to compare gene expression between the two control treatments containing glucose or acetate but no acetol, and between the acetol-treated and untreated samples containing glucose or acetate, respectively. However, principal component analysis showed no clear correlation between the samples due to the addition of acetol (Figure A1). We filtered the corresponding tables using thresholds for log₂ fold-change of ± 1 and ≤ 0.05 for the adjusted p-value. Comparing the transcriptomic data of *C. glutamicum* during growth on acetate or glucose without acetol, we found 11 genes that were downregulated and 23 genes that were upregulated in response to acetate (Figure A2). Among the latter, we identified *sdhA*, *acn*, *pck* and *aceA*, which is in agreement with the results of Hayashi et al [104]. Interestingly, during growth on acetate, not a single gene could be identified that met our statistical requirements when compared to the corresponding acetol-treated samples (Figure A3). Even during growth on glucose and acetol, only the transcript level of cg3290 was of significant and relevant change (Figure A4, Table 3-1). The latter encodes a predicted oxidoreductase and its transcription was increased approximately 3.5-fold by the addition of acetol during growth on glucose. Since cg3290 was the only gene identified as being regulated by acetol in our statistical setup, we lowered the thresholds and searched for other promising candidates that we considered to be worthy of further investigation. By doing so, we identified cg3412, which encodes a predicted azaleucine exporter [28], and was the only gene that was found to be up-regulated by acetol regardless of the primary substrate provided (Table 3-1). In addition, we suggested cg0354 and cg1423 as worthy for further investigation in the context of acetol metabolism (Table 3-1). The latter encodes a putative L-glyceraldehyde-3-phosphate reductase, which is a promising candidate for catalyzing reactions involved in the degradation of acetol [138]. On the other hand, cg0354 encodes a predicted thioredoxin-related protein and might be involved in the detoxification of methylglyoxal, similar to the GloAB system of *E. coli* [109] as

Table 3-1: Promising Genes Selected by Means of Transcriptome Sequencing.

The table shows promising candidates that were selected from the transcriptome sequencing data along with their intended function and statistical properties. The statistics were performed by Dr. Richa Bharti and provided to us for further analysis.

Gene	Description	log2 (fold-change)	base mean	p-value	p _{adj} -value
cg3290	Predicted oxidoreductase; identified on glucose	1.8	570	7.27×10^{-6}	0.02
cg3412	Predicted azaleucine exporter, identified on glucose and acetate	1.1 / 0.7	18	0.01/0.10	0.999 / 0.999
cg0354	Predicted thioredoxin related protein, identified on acetate	-1.1	34	0.002	0.999
cg1423	Putative L-GAP reductase, identified on acetate	0.6	70	0.07	0.999

described in Chapter 1.3.1. In summary, cg3290, cg3412, cg1423, and cg0354 were selected for further studies on the acetol metabolism in *C. glutamicum* (see below). Since we observed that the growth of *C. glutamicum* was affected by acetol only during growth on glucose, but not on acetate, we also included cg2115 in our studies. The latter encodes SugR that, among others, represses genes involved in sugar uptake and glycolysis during growth on gluconeogenic substrates [86, 87] (see Chapter 1.3.2).

3.1.3.2 Altering the Expression of Identified Genes

To investigate the role of the genes identified by whole transcriptome analysis of cells treated with acetol, we generated corresponding *C. glutamicum* knockout strains. In addition, we included *C. glutamicum* Δ sugR [87] in our studies, because this repressor is responsible for the repression of genes associated with the sugar metabolism. The newly generated strains were cultured in shaking flasks in CGXII medium supplemented with either 10 g glucose or 10 g acetate L⁻¹ and treated with 5 g acetol L⁻¹. The wild-type strain of *C. glutamicum* was included as control. Above, we observed a significant effect of acetol on the uptake rates and biomass yields during growth on glucose and no effect during growth on acetate during cultivation in shaking flasks (see Chapter 3.1.2). Here, we primarily focused on the growth rates and uptake rates of acetol (q_s') by the generated mutant strains (Table 3-2). During growth on glucose as the sole carbon and energy source, all strains exhibited a μ of 0.33 h⁻¹. As observed in the previous cultivations, the

Results

Table 3-2: Growth Rates and Uptake of Acetol by RNAseq Derived Knockout Strains.

The table shows growth rates (μ) and uptake rates of acetol (q_s') of different *C. glutamicum* knockout strains during growth in 50 mL CGXII medium supplemented with 10 g glucose or acetate L⁻¹ with or without the addition of 5 g acetol L⁻¹ for 12 h.

Substrate	Glucose			Acetate		
	-	+	+	-	+	+
Strain	μ in h ⁻¹		q_s' in g h ⁻¹	μ in h ⁻¹		q_s' in g h ⁻¹
WT	0.33 ± 0.01	0.19 ± 0.03	0.16 ± 0.02	0.37 ± 0.01	0.36 ± 0.02	0.15 ± 0.01
Δ cg0354	0.33 ± 0.02	0.29 ± 0.01	0.16 ± 0.02	0.26 ± 0.07	0.26 ± 0.07	0.15 ± 0.01
Δ cg3290	0.33 ± 0.01	0.26 ± 0.00	0.12 ± 0.03	0.28 ± 0.02	0.28 ± 0.02	0.15 ± 0.01
Δ cg3412	0.33 ± 0.01	0.20 ± 0.03	0.15 ± 0.03	0.35 ± 0.02	0.34 ± 0.02	0.14 ± 0.01
Δ cg1423	0.33 ± 0.02	0.20 ± 0.03	0.15 ± 0.02	0.33 ± 0.02	0.33 ± 0.02	0.14 ± 0.01
Δ cg2115 (<i>sugR</i>)	0.31 ± 0.01	0.16 ± 0.03	0.15 ± 0.03	0.36 ± 0.00	0.35 ± 0.02	0.14 ± 0.01

μ of *C. glutamicum* wild-type, but also of most of the other strains, was reduced to about 0.20 h⁻¹ by the addition of 5 g acetol L⁻¹. Interestingly, the μ of *C. glutamicum* Δ cg0354 and *C. glutamicum* Δ cg3290 was less affected compared to the other strains, remaining at 0.29 ± 0.01 h⁻¹ and 0.26 ± 0.00 h⁻¹, respectively. However, no differences were observed for q_s' , which was about 0.15 g h⁻¹ for all strains. Only the q_s' of *C. glutamicum* Δ cg3290 seemed to be slightly attenuated compared to the other strains, although this effect did not reach statistical significance. In contrast to glucose, μ 's of the different strains were not affected by acetol during growth on acetate. However, the intrinsic μ of *C. glutamicum* Δ cg0354 and *C. glutamicum* Δ cg3290 was notably reduced to about 0.26 h⁻¹ and 0.28 h⁻¹, compared to a μ between 0.33 and 0.38 h⁻¹ of the other strains. Again, q_s' was not altered by any mutation and was about 0.15 g h⁻¹ for all strains. In addition to the experiments performed with knockout strains, we generated strains for the overexpression of the respective genes from a pEKEx2 vector backbone (*sugR* was not included). Thus, we generated the plasmids pEKEx2-cg0354, pEKEx2-cg3290, pEKEx2-cg3412, and pEKEx2-cg1423, which were subsequently used to transform *C. glutamicum*, including the empty vector as a control. A single cultivation of one positive clone was performed in shaking flasks as described above. The growth of the strains was not monitored, only the acetol concentrations were measured at the beginning and after 12 h of cultivation. However, no differences in the final acetol concentrations were observed for the overexpressing strains compared to the empty vector control. Regardless of the primary substrate acetate or glucose, 21 to 25 mM acetol was degraded

in the cultures. In conclusion, neither the deletion, nor the overexpression of the genes selected from the transcriptome data showed promising results regarding an optimized metabolization of acetol by *C. glutamicum*.

3.1.4 Implementing Synthetic Operons for Acetol Degradation

As described above, neither the deletion nor the overexpression of genes selected from the transcriptome data showed promising results for establishing acetol as a suitable substrate for cultivation of *C. glutamicum*. Although further in-depth studies such as carbon flux analysis could help to reveal the native pathways involved in the acetol metabolism in *C. glutamicum*, we focused next on implementing artificial pathways to allow effective utilization of acetol by this organism. Acetol has been reported to be formed during the detoxification of methylglyoxal in several organisms. Furthermore, acetol occurs as an intermediate in the production of 1,2-propanediol (see Chapter 1.3.1, Figure 1-3). To redirect the carbon flux from acetol to pyruvate we selectively overexpressed several enzymes from different organisms that have been reported to catalyze distinct reactions in the acetol-methylglyoxal-pyruvate node. Therefore, we first overexpressed the following genes from a pEKEx2 plasmid in *C. glutamicum* ATCC 13032: (i) *yqhD* from *E. coli*, which encodes a NADP⁺-dependent, unspecific primary alcohol dehydrogenase [257]; (ii) *dkgA* from *C. glutamicum*, which encodes a putative 2,5-diketo-D-gluconic acid reductase, an NADP⁺-dependent aldo-keto reductase possibly involved in the conversion of methylglyoxal [117]; (iii) *hchA* from *E. coli* encoding heat-shock protein 31, a chaperone with glyoxalase III activity that catalyzes the conversion of methylglyoxal to D-lactate without the need for additional cofactors [256]; (iv) *yvgN* from *Bacillus subtilis* encoding an NAD⁺-dependent glyoxal reductase [233]; (v) *aldA* from *E. coli* encoding an aldehyde dehydrogenase with a broad substrate range, such as L-lactaldehyde and methylglyoxal [16]; (vi) *dld* from *C. glutamicum*, encoding the quinone-dependent D-lactate dehydrogenase, which catalyzes the oxidation of D-lactate to pyruvate [124]; (vii) *ldhA* from *E. coli* encoding the NAD⁺-dependent, soluble L-lactate dehydrogenase [259]. The strains transformed with the respective expression vectors were screened in 1 mL cultures supplemented with 10 g glucose or acetate L⁻¹ and 5 g acetol L⁻¹ for 12 h. *C. glutamicum* pEKEx2 (empty vector) was included to the cultures as a control (Table 3-3). The strains cultivated on glucose showed μ 's in the range of 0.23 and 0.26 h⁻¹, which were reduced to about 0.17 h⁻¹, similar to shaking flask cultivations, when acetol was included as co-substrate. During cultivation on acetate, the μ 's

Results

Table 3-3: Growth Rates and Uptake of Acetol by Various *C. glutamicum* Overexpressing Strains.

The table shows growth rates (μ) and uptake rates of acetol (q_s') of different *C. glutamicum* strains overexpressing different genes predicted to be involved in the conversion of acetol to pyruvate. The strains were cultured for 12 h in CGXII medium supplemented with 10 g glucose or acetate L⁻¹ with or without the addition of 5 acetol L⁻¹.

Substrate	Glucose			Acetate		
Acetol	-	+	Acetol	-	+	Acetol
Strain	μ in h ⁻¹		q_s' in g h ⁻¹	μ in h ⁻¹		q_s' in g h ⁻¹
pEKEx2	0.24 ± 0.01	0.17 ± 0.01	0.13 ± 0.00	0.21 ± 0.02	0.20 ± 0.00	0.20 ± 0.00
pEKEx2-yqhD	0.25 ± 0.01	0.17 ± 0.01	0.13 ± 0.00	0.23 ± 0.02	0.20 ± 0.01	0.20 ± 0.00
pEKEx2-dkgA	0.26 ± 0.02	0.17 ± 0.01	0.13 ± 0.00	0.19 ± 0.02	0.19 ± 0.01	0.20 ± 0.01
pEKEx2-hchA	0.25 ± 0.01	0.16 ± 0.00	0.14 ± 0.00	0.22 ± 0.01	0.20 ± 0.00	0.20 ± 0.01
pEKEx2-yvgN	0.25 ± 0.01	0.18 ± 0.01	0.13 ± 0.00	0.22 ± 0.01	0.21 ± 0.01	0.20 ± 0.01
pEKEx2-aldA	0.23 ± 0.02	0.17 ± 0.01	0.13 ± 0.01	0.22 ± 0.01	0.19 ± 0.01	0.20 ± 0.00
pEKEx2-dld	0.24 ± 0.00	0.16 ± 0.01	0.14 ± 0.00	0.21 ± 0.01	0.20 ± 0.00	0.20 ± 0.00
pEKEx2-ldhA	0.23 ± 0.00	0.15 ± 0.03	0.14 ± 0.00	0.20 ± 0.01	0.20 ± 0.01	0.21 ± 0.00

of the different strains were between 0.19 and 0.21 h⁻¹, independent of the presence of acetol. None of the strains showed a considerably increase in acetol uptake during 12 h of cultivation, as the q_s' remained at 0.13 g h⁻¹ or 0.20 g h⁻¹ in cultures supplemented with glucose or acetate, respectively. As it became clear that the overexpression of single enzymes of the predicted pathways was not sufficient to improve the acetol uptake by the tested *C. glutamicum* strains, we next aimed to overexpress multiple genes in parallel. Therefore, we created synthetic operons combining the expression of several enzymes involved in one of the possible pathways of acetol degradation. In addition, we included *mshA* from *C. glutamicum*, which has been shown to be involved in the mycothiol biosynthesis [283] and thus could promote the conversion of methylglyoxal to lactate and pyruvate, as described for the GloAB system of *E. coli* using GSH as a co-factor (see Chapter 1.3.1). We also included the expression of *noxE* and *TPnox*, which encode a native NADH oxidase and an engineered NADPH oxidase from *Lactococcus lactis* [171] and *Lactobacillus rhamnosus* [161], respectively. The latter two water-forming oxidases were included to disrupt the redox balance within the cell and were thought to shift the reaction equilibria toward the more oxidized product, pyruvate. Finally, *C. glutamicum* ATCC 13032 was transformed with the plasmids harboring the synthetic operons as followed: (i) pEKEx2-*mshA-hchA*, (ii) pEKEx2-*noxE-TPnox*, (iii) pEKEx2-*dkgA-yqhD-TPnox*, and (iv) pEKEx2-*gldA-aldA-noxE*. The resulting strains were analyzed as a single

determination by cultivation at 1 ml scale, performed as described above. Again, no differences in growth or acetol uptake were observed compared to the empty vector control (data not shown).

3.1.5 Adaptive Laboratory Evolution

Adaptive laboratory evolution (ALE) can be a powerful tool for developing microbial strains that perform a desired function. In ALE, the respective organism is cultured under a specific selection pressure that favors the evolution of the desired function. For the bacterium *C. glutamicum*, ALE has been used to increase growth rates on glucose [213], enhance glutarate production [218], improve methanol utilization and tolerance [286], and to increase resistance to inhibitors in corn stover hydrolysate [285]. In this work, we performed ALE with *C. glutamicum* to increase its resistance to acetol and to introduce its use as sole carbon and energy source. We cultured *C. glutamicum* ATCC 13032 in CGXII medium supplemented with 5 g acetol L⁻¹ as sole carbon and energy source. The initial culture was inoculated to an OD of 4. Cells were transferred to fresh medium every 3 to 4 days. After inoculation of the new culture the OD was measured and whenever the OD was ≤ 1 , glucose was added to the culture to a final concentration of 2 g L⁻¹ in order to restore the biomass concentrations. Since no growth of *C. glutamicum* could be detected on acetol as the sole carbon and energy source after 338 days, ALE was not further considered as a suitable method in the context of this project.

3.2 Production of Itaconic Acid

Next to acetol, acetate is the second most abundant carbon compound in PW. While acetol is not yet suitable to be used for high-level compound production with *C. glutamicum*, this organism has been shown to be optimally suited for the valorization of acetate (see Chapter 1.3.2). Therefore, we used the latter compound as a model substrate to engineer a *C. glutamicum* strain tailored for the efficient conversion of acetate to IA. IA is a bulk chemical of growing interest to industry and medicine. Its unique structure and its special potential for large-scale production by biotechnological fermentation make IA a sustainable building block for “green” chemistry (see Chapter 1.4). In nature, IA is found as a secondary metabolite of several organisms, such as various fungi or macrophages,

Results

but *C. glutamicum* is not on the list of native IA producers. However, Otten et al. [205] engineered *C. glutamicum* for heterologous expression of the ‘cis-pathway’ and reported IA production by *C. glutamicum* from glucose. For this purpose, the authors expressed a codon-optimized version of *cad* derived from the industrial IA production host *A. terreus*. The *cad* gene was further fused to the coding sequence of the maltose binding protein, encoded by *malE*, derived from *E. coli* to increase the stability of the enzyme. The entire construct was expressed under the control of an IPTG-inducible *tac*-promoter from the pEKEx2 vector backbone [205]. The corresponding pEKEx2-*malEcad*_{opt} plasmid was generously provided by the working group of Prof. Dr. Michael Bott at the Research Center Jülich (Jülich, Germany). In this study, we used the pEKEX2-*malEcad*_{opt} plasmid to enable IA production by *C. glutamicum*, and further engineered the respective strain for optimized IA production in terms of yield and titer from acetate.

3.2.1 Inhibition of Isocitrate Lyase by Itaconic Acid

C. glutamicum has been reported to tolerate concentrations of up to 75 g IA L⁻¹ during growth on glucose [280]. However, IA is also known to strongly inhibit the ICL of *C. glutamicum* in a linear uncompetitive manner with a K_i of 5.05 μ M *in vitro* [220], but the reaction catalyzed by the ICL is essential during growth on acetate as the sole carbon and energy source [220] (see Chapter 1.3.2). Thus, we first tested the ability of *C. glutamicum* to grow on acetate at elevated IA concentrations in shaking flasks. Therefore, we cultured *C. glutamicum* ATCC 13032 in CGXII medium supplemented with 10 g acetate L⁻¹ and 50 mM or 250 mM potassium itaconate. As controls, we included cultures supplemented with 10 g glucose L⁻¹ instead of acetate, and cultures containing 100 mM or 500 mM KCl instead of itaconate (Figure 3-3). Cells growing on glucose showed a μ of 0.32 ± 0.01 h⁻¹ and were not affected by the addition of 50 mM itaconate or 100 mM KCl. However, μ was reduced to 0.25 ± 0.00 h⁻¹ and 0.22 ± 0.01 h⁻¹ by the addition of 250 mM itaconate and 500 mM KCl, respectively. This was in agreement with the results published by Otten et al. [205] who showed that μ of *C. glutamicum* was slightly affected by the addition of 500 mM NaCl during growth on glucose. Similar to these observations, μ of cells growing on acetate was 0.31 ± 0.01 h⁻¹ and was not affected by the addition of 100 mM KCl, but was reduced to 0.20 ± 0.00 h⁻¹ by the addition of 500 mM KCl. However, the addition of 50 mM itaconate reduced μ to 0.26 ± 0.01 h⁻¹ and 250 mM IA completely suppressed growth. These results indicate that IA is able to inhibit growth of *C. glutamicum* on acetate, but rather high extracellular concentrations were

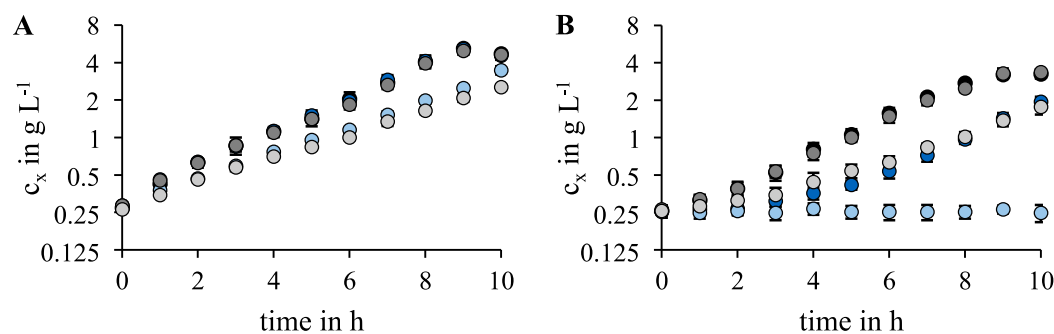


Figure 3-3: Growth Inhibition of *C. glutamicum* by Itaconate.

The figure shows the growth of *C. glutamicum* ATCC 13032 on 10 g glucose L⁻¹ (A) or 10 g acetate L⁻¹ (B). Cultures were supplemented with 50 mM (dark blue) or 250 mM (light blue) potassium itaconate, or with 100 mM (dark grey) or 500 mM (light grey) KCl. Corresponding controls without further supplements are shown in black.

required for a complete growth inhibition. Nevertheless, increasing the resistance of ICL to IA will remain an important issue in subsequent studies to enable the production of high titers of industrial relevance.

3.2.2 Enabling Itaconic Acid Production from Acetate

To enable IA production by *C. glutamicum* ATCC13032, we first introduced the plasmid pEKEx2-*malEcad*_{opt}, which encodes the codon optimized and stabilized *cad* gene, generated by Otten et al. [205]. The functional capability of the resulted *C. glutamicum* pEKEx2-*malEcad*_{opt} (*C. glutamicum* ITA1) strain was confirmed according to the studies published by the respective authors. Therefore, we cultured *C. glutamicum* ITA1 in CGXII medium under nitrogen-limited conditions (1 g urea L⁻¹) supplemented with 40 g glucose L⁻¹ in shaking flasks. After 72 h, the IA titer in the culture supernatant was only 9 ± 2 mM IA (Figure 3-4 A), whereas Otten et al. [205] detected 29 mM IA after 72 h cultivation of the same strain under similar conditions. Regardless of the reduced titers compared to the original study, we were able to confirm the functionality of *C. glutamicum* transformed with pEKEx2-*malEcad*_{opt} to produce IA from glucose. Next, we aimed at the production of IA from acetate by *C. glutamicum* ITA1. Therefore, we cultured *C. glutamicum* ITA1 in CGXII minimal medium (without limitations) supplemented with 20 g acetate L⁻¹ in shaking flasks. We also prepared a culture supplemented with a mixture of 10 g glucose and 10 g acetate L⁻¹ and included a culture supplemented with 20 g glucose L⁻¹ as a control. In a single determination, the growth rates amounted to 0.31, 0.28, and 0.28 h⁻¹, respectively, but no IA could be detected in any culture after

Results

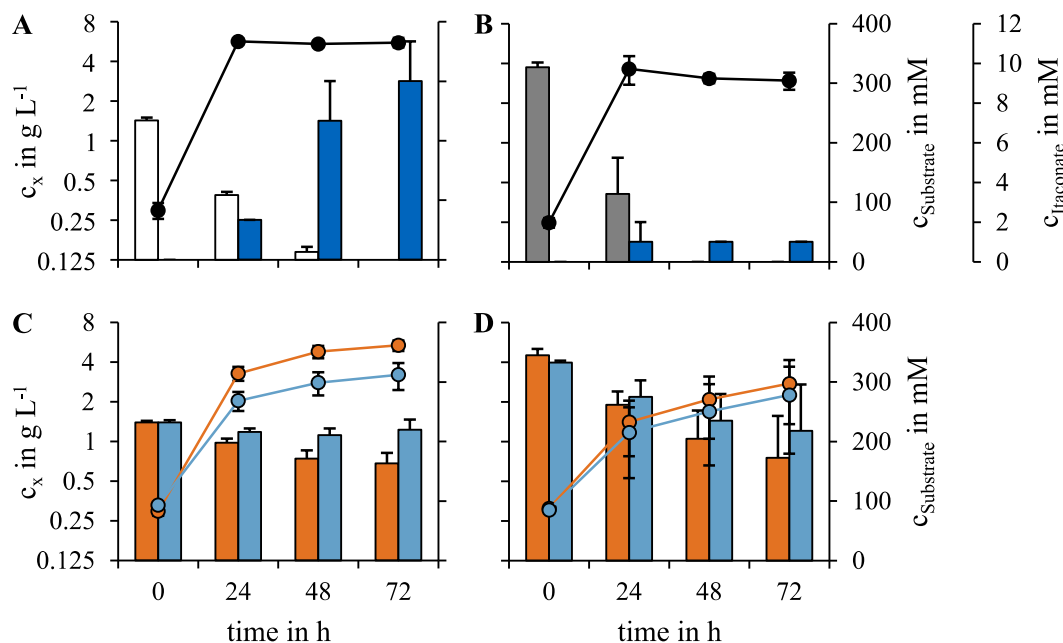


Figure 3-4: Comparison of Nitrogen and Phosphate Limitations during IA Production.

The figure shows IA production from glucose (A, C) and acetate (B, D) by *C. glutamicum* ITA1 cultured in shaking flasks under nitrogen limitation (A, B) and phosphate limitation or starvation (C, D). A, B: Glucose is indicated by white bars, acetate by grey bars, IA by blue bars, biomass concentration by black circles. C, D: Bars indicate glucose (C) and acetate (D) concentrations, respectively. Biomass concentrations are indicated by circles. Phosphate limitation (0.1 mM and 0.05 mM for glucose and acetate, respectively) is shown in orange, phosphate starvation (without addition of phosphate in the main culture) is shown in blue. No IA was produced under the latter conditions.

72 h. In contrast to the work published by Otten et al. [205], the production medium used in our study was free of PCA. PCA supports iron assimilation in *C. glutamicum* and has been shown to promote its growth on various substrates in CGXII minimal medium [166, 187, 266]. Iron itself is an important cofactor for several enzymes such as ACN, which is an important key enzyme in IA production (see Chapter 1.4). Therefore, the lack of PCA could be a reason for the reduced final titers produced by *C. glutamicum* ITA1 compared to the original work. To analyze the effect of iron assimilation by *C. glutamicum* on IA production, we repeated the cultivations without nitrogen limitation as described above and added 30 mg PCA L^{-1} to the respective main cultures. The growth rates of the different cultures amounted to 0.31, 0.31, and 0.27 h^{-1} , respectively, but again no IA could be detected in the culture broth after 72 h. Thus, PCA was excluded as supplement in the subsequent cultivations. As confirmed above, Otten et al. [205] successfully applied nitrogen limitation to increase IA production by *C. glutamicum* from glucose. The authors reported 8-fold higher titers after reducing the nitrogen concentrations to a C:N ratio of 40:1 (1 g urea L^{-1} and 40 g glucose L^{-1}). We adopted the nitrogen limitation

in our experiments on IA production from acetate by reducing the urea concentration and completely omitting ammonium sulfate in the production medium (0.5 g urea L⁻¹ and 20 g acetate L⁻¹) to set the C:N ratio to 40:1 (Figure 3-4 B), as described for the validation of the pEKEx2-*malEcad*_{opt} plasmid (see above). In parallel, we investigated the effect of phosphate limitation and starvation during IA production with *C. glutamicum* ITA1 from 40 g glucose or 20 g acetate L⁻¹. Therefore, we prepared cultures with reduced phosphate concentrations of 0.1 mM and 0.05 mM, respectively, and cultures without additional phosphate sources (Figure 3-4 C, D) [289]. However, regardless of the substrate, phosphate limitation and starvation failed to stimulate IA production and severely impaired growth and substrate uptake by *C. glutamicum* ITA1. In contrast, during cultivation under nitrogen limitation, acetate was completely consumed and 1 mM IA could be detected in the supernatant after 72 h. Thus, we included nitrogen limitation as a standard condition in the following cultivations with respect to IA production.

3.2.3 Metabolic Engineering to Improve Production of Itaconic Acid

3.2.3.1 Reduction of Isocitrate Dehydrogenase Activity

Natural IA producers belong to the domain of eukaryotes (see Chapter 1.4.1) in which TCA cycle reactions take place in the mitochondria, whereas CAD is located in the cytosol. Thus, the transport of aconitate from the mitochondria to the cytosol is a prerequisite for IA production in these hosts. Furthermore, increased translocation of aconitate due to overexpression of appropriate transporters is sufficient to enhance IA production in *A. terreus* and *U. maydis* [296]. In engineered prokaryotic hosts such as *C. glutamicum*, both the TCA cycle and the CAD enzyme are located in the cytosol and compete for the same substrate, *cis*-aconitate (Figure 1-4). However, due to the rather low affinity of CAD for its substrate *cis*-aconitate (K_M of 2.45 mM vs. 18.5 μ M of ACN) [75], the majority of the assimilated carbon is likely to be channeled into the oxidative branch of the TCA cycle. Thus, a common strategy to reduce carbon flux into the TCA cycle and increase IA production in prokaryotic hosts is to reduce IDH activity [85, 196, 205]. In this study, the native *icd* gene in *C. glutamicum* ITA1 encoding IDH was replaced by one of three versions that encode IDH^{A94D}, IDH^{G407S}, and IDH^{R453C}, which remain 10%, 55%, and 29% of the wild-type IDH activity, respectively [242]. The resulting strains *C. glutamicum* IDH^{A94D}, *C. glutamicum* IDH^{G407S}, and *C. glutamicum* IDH^{R453C}, each also harboring the pEKEx2-*malEcad*_{opt} plasmid and designated *C. glutamicum* ITA2,

Results

ITA3, and ITA4, respectively, were analyzed for the yield and titer of IA produced from acetate (Table 3-4). Screening of the engineered strains was performed in 1 mL of nitrogen-limited CGXII medium supplemented with 20 g acetate L⁻¹. After 72 h, the strains *C. glutamicum* ITA2 and *C. glutamicum* ITA3 reached titers of 0.35 ± 0.06 g L⁻¹ and 0.49 ± 0.18 g L⁻¹ with yields of 9 ± 2 mmol mol⁻¹ and 13 ± 6 mmol mol⁻¹, respectively. These values were only slightly increased compared to the titer and yield of 0.32 ± 0.09 g L⁻¹ and 8 ± 2 mmol mol⁻¹ obtained by *C. glutamicum* ITA1. The highest titer of 20 ± 5 mmol mol⁻¹ with a yield of 0.75 ± 0.18 g L⁻¹, among the strains tested was produced with *C. glutamicum* ITA4 expressing IDH^{R453C}. Recently, we showed that this strain was able to reach titers of 29.2 g IA L⁻¹ produced from acetate in an optimized fed-batch process [180]. It is noteworthy, however, that the best performance for IA

Table 3-4: Yields and Titers of Engineered *C. glutamicum* Strains during Cultivation at 1 mL Scale.

The table shows yields and titers of the respective *C. glutamicum* strains obtained during cultivation in nitrogen-limited CGXII medium supplemented with 20 g acetate L⁻¹, cultured at 1 mL scale for 72 h. Unless otherwise noted, all strains were transformed with pEKEx2-*malEcad*_{opt}.

<i>C. glutamicum</i>	Genotype	Y _{P/S} in mmol mol ⁻¹	Titer in g L ⁻¹
ITA1	-	8 ± 2	0.32 ± 0.09
ITA2	IDH ^{A94D}	9 ± 2	0.35 ± 0.06
ITA3	IDH ^{G407S}	13 ± 6	0.49 ± 0.18
ITA4	IDH ^{R453C}	20 ± 5	0.75 ± 0.18
ITA5	IDH ^{A94D} _{ATG::GTG}	29 ± 8	1.00 ± 0.29
ITA6	IDH ^{A94D} _{ATG::TTG}	30 ± 2	1.04 ± 0.00
ITA7	IDH ^{G407S} _{ATG::GTG}	25 ± 1	0.82 ± 0.06
ITA8	IDH ^{G407S} _{ATG::TTG}	39 ± 4	1.26 ± 0.16
ITA9	IDH ^{R453C} _{ATG::GTG}	31 ± 4	1.00 ± 0.06
ITA10	IDH ^{R453C} _{ATG::TTG}	52 ± 4	1.86 ± 0.14
ITA11	IDH ^{R453C} ΔP _{pck} ::P _{dapA} -A8	10 ± 1	0.39 ± 0.00
ITA12	IDH ^{R453C} ΔP _{pck} ::P _{dapA} -A16	19 ± 4	0.73 ± 0.13
ITA13	IDH ^{R453C} ΔP _{pck} ::P _{dapA} -C5	no growth	
ITA14	IDH ^{R453C} ΔP _{pck} ::P _{dapA} -C7	12 ± 1	0.39 ± 0.00
ITA15	ΔramB	36 ± 4	1.54 ± 0.18
ITA16	ΔramB (pEKEx2- <i>malEcad</i> _{opt} -ramA)	39 ± 6	1.35 ± 0.23
ITA17	ΔramB ΔP _{pck} ::P _{dapA} -A16 (pEKEx2- <i>malEcad</i> _{opt} -ramA)	29 ± 2	0.81 ± 0.06
ITA18	ΔramB ΔglnE	18 ± 4	0.60 ± 0.21
ITA19	ΔramB Δgdh	62 ± 12	2.36 ± 0.75
ITA20	ΔramB ΔglnE Δgdh	15 ± 1	0.46 ± 0.07
ITA21	IDH ^{R453C} (pEKEx2- <i>malEcad</i> _{opt} -gltA)	7 ± 0	0.26 ± 0.00
ITA22	ΔramB ΔacnR	43 ± 11	1.58 ± 0.40
ITA23	ΔramB (pEKEx2- <i>malEcad</i> _{opt} -noxE)	23 ± 3	1.04 ± 0.11
ITA24 _{ATG}	ΔramB Δgdh IDH ^{R453C}	81 ± 9	3.43 ± 0.59

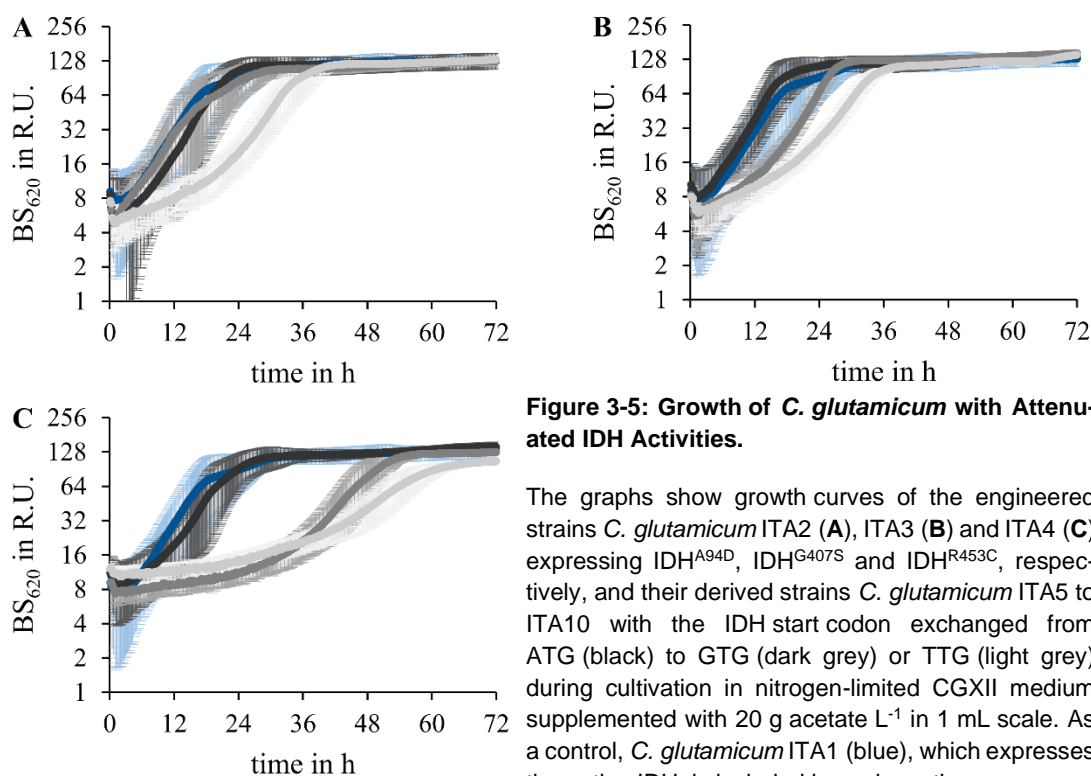
production in our screening experiments was obtained with moderate attenuation of IDH activity, while stronger and weaker attenuation of its activity had a negative impact on IA production from acetate. In contrast, a residual IDH activity of only 3% proved to be the most suitable for IA production from glucose [205]. The observed discrepancy between studies performed on glucose and acetate could be caused either by different carbon flux distributions induced by the substrates [292] or by the respective mode of IDH attenuation. While in this work, we reduced the intrinsic activity of the IDH by point mutations with probably no or only little effect on the absolute enzyme concentration, Otten *et al.* [205] specifically reduced the expression of IDH by replacing the start codon from ATG to TTG. Hence, we further reduced the IDH activity in the engineered *C. glutamicum* strains ITA2, ITA3, and ITA4 by exchanging the start codon of the mutated *icd* genes to GTG and TTG. The resulting strains were screened for their respective yields and titers of IA produced from acetate, as described above (Table 3-4). Interestingly, both strains derived from *C. glutamicum* ITA2, namely *C. glutamicum* expressing $\text{IDH}^{\text{A94D}}_{\text{ATG::GTG}}$ or $\text{IDH}^{\text{A94D}}_{\text{ATG::TTG}}$, harboring the pEKEx2-*malEcad*_{opt} and designated *C. glutamicum* ITA5 and ITA6, respectively, showed increased yields of about 30 mmol mol⁻¹ and final titers of about 1 g L⁻¹. The yield and final titer achieved by *C. glutamicum* $\text{IDH}^{\text{G407S}}_{\text{ATG::GTG}}$ (pEKEx2-*malEcad*_{opt}) (*C. glutamicum* ITA7) were increased to 25 ± 1 mmol mol⁻¹ and 0.82 ± 0.06 g L⁻¹. In contrast to *C. glutamicum* ITA5 and ITA6, the exchange of the start codon to TTG in the $\text{IDH}^{\text{G407S}}$ mutant (*C. glutamicum* $\text{IDH}^{\text{G407S}}_{\text{ATG::TTG}}$ (pEKEx2-*malEcad*_{opt}), ITA8) further increased yield and titer to 39 ± 4 mmol mol⁻¹ and 1.26 ± 0.16 g L⁻¹, respectively. The yield and final titer of *C. glutamicum* $\text{IDH}^{\text{R453C}}_{\text{ATG::GTG}}$ (pEKEx2-*malEcad*_{opt}) (*C. glutamicum* ITA9) amounted to 1.00 ± 0.06 g L⁻¹ and 31 ± 4 mmol mol⁻¹, respectively, after 72 h. It is noteworthy that *C. glutamicum* $\text{IDH}^{\text{R453C}}_{\text{ATG::TTG}}$ (pEKEx2-*malEcad*_{opt}) (*C. glutamicum* ITA10) showed strong variations in growth and production phenotypes during the individual cultivations. We assumed that the rather strong reduction of IDH activity caused severe evolutionary pressure in the latter strain. However, we were able to isolate three different individual clones of *C. glutamicum* ITA10 that showed suitable growth and production phenotypes. The yields and titers of these clones were 52 ± 4 mmol mol⁻¹ and 1.86 ± 0.14 g L⁻¹ during cultivation in 1 mL scale. *C. glutamicum* ITA10 showed the highest yields and titers of all strains with reduced IDH activity in our experimental setup. In order to identify possible mutations that arose in *C. glutamicum* ITA10, the genomes of the three isolated clones were sent for re-sequencing (see Chapter 3.2.4). It should be noted, however, that

Results

the exchange of the start codons did not only increase the yields and titers obtained by the respective strains, but also the lag-phases were successively extended by the GTG and TTG start codons compared to the respective versions harboring the native start codon ATG (Figure 3-5). This effect was most pronounced for *C. glutamicum* ITA9 and ITA10. However, since the strains expressing the IDH^{R453C} version showed the highest yields and titers among the strains tested with respect to the different start codons, we used *C. glutamicum* ITA4 for further genetic modifications and re-evaluated the exchange of IDH start codons in later steps of this work (see Chapter 3.2.3.8).

3.2.3.2 Promotor Exchange of Phosphoenolpyruvate Carboxykinase

In *C. glutamicum* PEPCk is encoded by the gene *pck* and catalyzes the first step of gluconeogenesis. Therefore, PEPCk converts oxaloacetate to PEP by decarboxylation and transphosphorylation [223] (see Chapter 1.3.2). In doing so, the enzyme removes carbon from the TCA cycle and thus potentially competes with IA production for available precursors. In turn, we hypothesized that reduced flux *via* PEPCk could increase the pools of TCA cycle intermediates and consequently increase the yields and titers of IA produced from acetate. First, we analyzed a *pck* knockout strain of *C. glutamicum* [36] that we transformed with the pEKEx2-*malEcad*_{opt}. The resulting strain was cultured in



shaking flasks in 50 mL of nitrogen-limited CGXII medium, inoculated to an OD of 10. As expected, the cells showed no growth on acetate as the sole substrate. Notably, the resting cells were metabolically inactive, neither consuming acetate nor producing any IA. Next, we replaced the native promoter of *pck* in *C. glutamicum* ITA4 with four different variants of a *dapA*-promoter library [281]. The resulting strains *C. glutamicum* ITA11-14, carrying the promoter versions $\Delta P_{pck}::P_{dapA}$ -A8, -A16, -C5 and -C7, respectively, were screened in 1 mL cultures as described above (Table 3-4). However, all strains showed similar or even reduced product yields and IA titers compared to the parental strain *C. glutamicum* ITA4. Furthermore, *C. glutamicum* ITA13 carrying the P_{dapA} -C5 promoter, which is considered to have the lowest intrinsic activity among the constructs tested [279, 281], showed no growth at all, during 72 h of cultivation. Thus, we assumed that carbon flux *via* PEPCk does not form a bottleneck in the production of IA by *C. glutamicum* from acetate.

3.2.3.3 Interfering the Regulation of the Glyoxylate Shunt

During growth on non-glycolytic substrates such as acetate, the glyoxylate shunt is active to perform the essential anaplerotic reactions (see Chapter 1.3.2). The first step of the glyoxylate shunt is catalyzed by the *aceA*-encoded ICL, which converts isocitrate to succinate and glyoxylate [220] (Figure 1-4). In doing so, ICL competes with IDH for isocitrate as substrate. Similar to the reduction of IDH activity, a reduced activity of ICL could lead to a backlog of isocitrate, which in turn would increase the pools of *cis*-aconitate and consequently increase the production of IA. Gerstmeir *et al.* [93] showed, that the global regulator of acetate metabolism RamB is involved in the transcriptional activation of *aceA* and *aceB* during growth of *C. glutamicum* on acetate. The authors observed reduced ICL and MS activities in a *ramB* knockout strain compared to the wild-type strain. In this work, we took advantage of this particular aspect and excised the *ramB* gene from the genome of *C. glutamicum* ITA1 to reduce the activity of the glyoxylate shunt in the resulting strain *C. glutamicum* $\Delta ramB$ (pEKEx2-*malE*_{cad}_{opt}), designated *C. glutamicum* ITA15. The growth rate of *C. glutamicum* ITA15 was reduced from 0.16 ± 0.06 to 0.12 ± 0.01 , compared to *C. glutamicum* ITA1. However, the yield and titer increased to 36 ± 4 mmol mol⁻¹ and 1.54 ± 0.18 g L⁻¹ during cultivation in 1 mL scale (Table 3-4). It is noteworthy that the yields obtained with *C. glutamicum* ITA15 were increased by 80% compared to *C. glutamicum* ITA4 expressing the attenuated

Results

IDH^{R453C}, although the carbon flux via IDH is three times higher than via ICL during growth on acetate [292]. Even so, it cannot be excluded that the deletion of the global regulator RamB has other side effects that are beneficial for IA production. Furthermore, it has been shown that overexpression of *ramA* in *C. glutamicum* during cultivation on mixtures of sugars and acetate resulted in increased IA production [121]. Therefore, we next overexpressed *ramA* together with the optimized *cad*-construct by transforming *C. glutamicum* $\Delta ramB$ with pEKEx2-*malEcad*_{opt}-*ramA*. The resulting strain was named *C. glutamicum* ITA16, but the yield obtained by this strain remained unchanged and the final titer was even slightly reduced to $1.35 \pm 0.23 \text{ g L}^{-1}$, compared to the precursor strain *C. glutamicum* ITA15 (Table 3-4). Both, RamA and RamB are also involved in the transcriptional regulation of *pck*, and as speculated above, altered expression of PEPCK could affect IA production from acetate. Therefore, we replaced the native promoter of *pck* in *C. glutamicum* ITA16 with the P_{dapA}-A16 version, which had no effect on IA production in the strains tested before (see Chapter 3.2.3.2), but lost the binding regions of *ramA* and *ramB*. However, the yield and final titer of the obtained strain *C. glutamicum* ITA17 (*C. glutamicum* $\Delta ramB \Delta P_{pck}::P_{dapA}$ -A16 (pEKEx2-*malEcad*_{opt}-*ramA*)) were reduced by 25% and 40%, respectively, compared to *C. glutamicum* ITA16.

3.2.3.4 Engineering Nitrogen Assimilation

Above, we showed that cultivation under nitrogen limitation was crucial to facilitate IA production from acetate by the engineered *C. glutamicum* strains (see Chapter 3.2.2). To further improve IA production, we next focused on manipulating nitrogen signaling and assimilation in *C. glutamicum* to mimic nitrogen limitation at the intracellular level. First, we deleted *glnE* from the genome of *C. glutamicum* ITA15 to generate *C. glutamicum* $\Delta ramB \Delta glnE$ (pEKEx2-*malEcad*_{opt}), which was designated *C. glutamicum* ITA18. *GlnE* encodes an adenylyltransferase that has been shown to be involved in nitrogen signaling, and when deleted, causes a nitrogen limitation response at the transcriptional level [219] (see Chapter 1.3.3). However, during cultivation in nitrogen-limited medium in 1 mL scale, the yield and titer of *C. glutamicum* ITA18 were $18 \pm 4 \text{ mmol mol}^{-1}$ and $0.60 \pm 0.21 \text{ g L}^{-1}$, respectively (Table 3-4), which represents a reduction of more than 50% compared to the precursor strain *C. glutamicum* ITA15. The results obtained suggested that an altered transcriptome might not be responsible for the beneficial effects on IA production observed during nitrogen limitation. Thus, we next knocked out *gdh* to generate *C. glutamicum* $\Delta ramB \Delta gdh$ (pEKEx2-*malEcad*_{opt}), which we named

C. glutamicum ITA19. GDH catalyzes the primary nitrogen assimilation pathway in *C. glutamicum* during nitrogen excess, but its function can be completely compensated by the essential GS in *gdh* knockout strains [126, 264] (see Chapter 1.3.3). Yield and titer obtained with *C. glutamicum* ITA19 were $62 \pm 12 \text{ mmol mol}^{-1}$ and $2.36 \pm 0.75 \text{ g L}^{-1}$, respectively (Table 3-4), which represents an increase of more than 70% compared to *C. glutamicum* ITA15. It is worth mentioning that the yield and titer in the *ramB*, *glnE*, *gdh* triple knockout strain *C. glutamicum* ITA20, were similar to those of the *ramB*, *glnE* double knockout strain *C. glutamicum* ITA18 (Table 3-4). Furthermore none of the three generated strains *C. glutamicum* ITA18 - ITA20 showed IA production when cultured under nitrogen excess. To investigate the cause of the positive effect of *gdh* deletion on IA production in *C. glutamicum* ITA19, we cultured the strain in 50 mL nitrogen-limited CGXII medium supplemented with $20 \text{ g acetate L}^{-1}$, inoculated to an OD of 2. Biomass, itaconate, acetate, and nitrogen (ammonia and urea) concentrations were measured over 48 h. In addition, *C. glutamicum* ITA15 was cultured under the same conditions as control (Figure 3-6). Within the first 24 h of cultivation, no notable differences in growth, substrate uptake, or IA production were observed between the two strains *C. glutamicum* ITA15 and *C. glutamicum* ITA19. However, after 28 h, the *ramB gdh* double knock out strain entered a short plateau-phase of 2 h with almost no growth. At the same time, the uptake of nitrogen, but not of acetate, was reduced compared to *ramB* knock out strain, which showed a steady growth until reaching stationary phase after 32 h when nitrogen was depleted. Nitrogen was depleted in the culture of *C. glutamicum* ITA19 and the strain entered stationary phase 4 h later, after 36 h. During this time, IA concentrations produced by *C. glutamicum* ITA19 exceeded those produced by

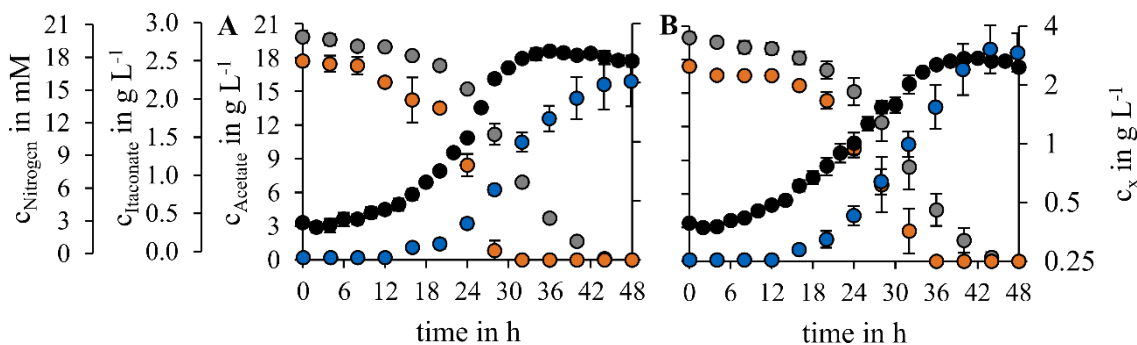


Figure 3-6: Nitrogen Assimilation by *C. glutamicum* ITA15 and ITA19.

The graphs show concentrations of biomass (black), acetate (grey), itaconate (blue), and nitrogen (orange) during shaking flask cultivation of *C. glutamicum* ITA15 (A) and ITA19 (B) under nitrogen-limited conditions.

C. glutamicum ITA15. After 48 h, the final IA titer and yield achieved by *C. glutamicum* ITA15 were $2.25 \pm 0.32 \text{ g L}^{-1}$ and $51 \pm 6 \text{ mmol mol}^{-1}$, respectively and amounted to $2.64 \pm 0.25 \text{ g L}^{-1}$ and $60 \pm 7 \text{ mmol mol}^{-1}$ for *C. glutamicum* ITA19. It should be noted that the differences in IA production between the two strains were less pronounced in shaking flask cultivation compared to 1 mL cultivation. Furthermore, the increased production by *C. glutamicum* ITA19 was independent of urease activity, as urea was completely converted to ammonium by both strains after 12 h (data not shown). Our data suggest that a prolonged growth phase caused by *gdh* deletion increases the final titer of IA and that the bi-phasic growth of *C. glutamicum* ITA19 is probably related to impaired nitrogen assimilation. However, the molecular mechanisms responsible for the specific growth and production phenotype of *C. glutamicum* ITA19, and the variation observed between cultivation methods remain to be elucidated.

3.2.3.5 Further Modifications of the Central Metabolism

It has been reported that overexpression of CS increases IA production from acetate by *E. coli* [196], thus we tested the same strategy for IA production by *C. glutamicum*. Therefore, we generated a synthetic operon of *malEcad_{opt}-gltA* expressed from the pEKEx2 vector backbone, which was used to transform *C. glutamicum* IDH^{R453C}. The resulting strain *C. glutamicum* IDH^{R453C} (pEKEx2-*malEcad_{opt}-gltA*), which we named *C. glutamicum* ITA21, was cultured in 1 mL scale as before. However, compared to *C. glutamicum* ITA4, the yield and titer of *C. glutamicum* ITA21 were reduced by 65% (Table 3-4). Next, we generated *C. glutamicum* ITA22 by deleting *acnR* in the *ramB* deficient *C. glutamicum* ITA15. We reasoned that deletion of *acnR*, which has been shown to increase the expression of *acn* [143], would in turn lead to higher levels of *cis*-aconitate and thus improve IA production. However, no significant differences were observed between *C. glutamicum* ITA15 and ITA22 with respect to the yield and final IA titer (Table 3-4). In addition, we overexpressed *noxE*, which encodes a NADH oxidase from *Lactococcus lactis* [171], in *C. glutamicum* $\Delta ramB$. We hypothesized that the expression of *noxE* could lead to an imbalanced redox state and thus increase uptake and metabolization of acetate by the cell to restore its native NADH + H⁺ levels. However, compared to *C. glutamicum* ITA15, the final IA titer and yield reached by *C. glutamicum* $\Delta ramB$ (pEKEx2-*malEcad_{opt}-noxE*) (*C. glutamicum* ITA23) were reduced by about one third to $1.04 \pm 0.11 \text{ g L}^{-1}$ and $23 \pm 3 \text{ mmol mol}^{-1}$, respectively (Table 3-4).

3.2.3.6 Genomic Integration of the *cis*-Aconitate Decarboxylase Gene

In this work, we used plasmid-based expression of the key enzyme CAD to enable IA production by *C. glutamicum*. However, the use of plasmids requires mechanisms to ensure plasmid stability in the respective host during long-term cultivation. The most popular method to ensure plasmid stability is the expression of an antibiotic resistance from the vector backbone while cultivating the cells in medium supplemented with the respective antibiotic. In this work, we used the pEKEx2 vector for heterologous gene expression that contains a gene encoding an aminoglycoside phosphotransferase that induces kanamycin resistance. In addition, gene expression from the pEKEx2 vector relies on an IPTG-inducible P_{tac} promoter [81]. Both features (selection marker and inducibility) are advantageous for ease of cultivation and tight control of gene expression during laboratory-scale cultivation. However, pEKEx2-based expression may be particularly disadvantageous for large-scale industrial cultivation, since the addition of large amounts of additives increases the cost of the respective process and adversely affects downstream processing. To overcome these drawbacks, we decided to integrate the codon-optimized *malEcad_{opt}* construct, under the control of the native and constitutive P_{tuf} promoter into the genome of *C. glutamicum* following the strategy published by Lange *et al.* [156], thus eliminating the need for the addition of IPTG and kanamycin during cultivation and IA production. For this purpose, the P_{tuf} -*malEcad_{opt}* construct was integrated into two different expression *loci* of *C. glutamicum*, which were previously identified and characterized for heterologous gene expression, and designated as “landing pads” (CgLP) [156]. The resulting strains *C. glutamicum* CgLP4:: P_{tuf} -*malEcad_{opt}* and *C. glutamicum* CgLP12:: P_{tuf} -*malEcad_{opt}* were cultured in nitrogen-limited CGXII medium supplemented with 20 g acetate L⁻¹ in shaking flasks. However, after 72 h, the IA produced remained below the quantification limit of 1 mM. Since the final titer obtained with the plasmid harboring strain *C. glutamicum* ITA1 was only marginally higher (1 ± 1 mM) (see Chapter 3.2.2) we further integrated the CgLP4:: P_{tuf} -*malEcad_{opt}* construct into the plasmid free precursor strain of *C. glutamicum* ITA4. The resulting strain *C. glutamicum* IDH^{R453C} CgLP4:: P_{tuf} -*malEcad_{opt}* was cultured as described above, but final IA titers remained below 1 mM (data not shown). Due to the rather low affinity of CAD for its substrate *cis*-aconitate (see Chapter 1.4), we suspected that expression levels of the genome-integrated construct might be too low compared to the gene expression using the high copy number plasmid pEKEx2. To obtain higher expression

Results

levels of the CAD enzyme, we cloned the *malEcad*_{opt} construct under the control of the *P*_{tacM} promoter, which showed 5-fold higher activity compared to the *P*_{tuf} promoter in *C. glutamicum* [246]. The construct was integrated into CgLP4 in the parental strain of *C. glutamicum* ITA19 to generate *C. glutamicum* Δ *ramB* Δ *gdh* CgLP4::*P*_{tacM}-*malEcad*_{opt}. The novel strain was cultured as described above, but the final IA titer did not exceed 1 mM, after 72 h. Due to the low titers achieved in our cultivations, genomic integration of the *cad* gene was not further considered in this study.

3.2.3.7 Expression of Itaconic Acid Transporters

During studies on IA production from glucose, Otten *et al.* [205] observed intracellular IA concentrations that were nearly twice as high as the extracellular concentrations measured in the culture supernatant after 72 h [205]. As outlined below, we made similar observations during IA production from acetate with *C. glutamicum* ITA24_{ATG} (see Chapter 3.2.5.2, Figure 3-10 A). These observations suggest that *C. glutamicum* lacks sufficient machinery for proper IA export. To support IA export, we expressed the IA transporters MfsA (GeneBank: AGV15467.1) and Itp1 (GeneBank: ALS30797.1), derived from the native IA producers *A. terreus* and *U. maydis*, respectively [296] (see Chapter 1.4.1), in *C. glutamicum* ITA8. Therefore, we used codon-optimized versions of *mfsA* and *itp1* to generate a synthetic operon with *malEcad*_{opt} on the pEKEx2 plasmid. The resulting plasmids pEKEx2-*malEcad*_{opt}-*mfsA* and pEKEx2-*malEcad*_{opt}-*itp1* were used to transform *C. glutamicum* IDH^{G407S}_{ATG::TTG}. The two resulting strains were cultured in shaking flasks under nitrogen limitation. After 72 h, the control strain *C. glutamicum* ITA8 showed a final titer of 0.74 ± 0.06 g IA L⁻¹, which was reduced by almost 50% compared to 1 mL scale cultivation. As described earlier in this work, similar discrepancies between the different cultivation methods were also observed for other *C. glutamicum* ITA strains (see Chapter 3.2.3.4 and Chapter 3.2.5). However, the final titers of the two strains additionally expressing *mfsA* or *itp1* were further reduced by 53% and 41%, respectively, compared to *C. glutamicum* ITA8 (data not shown). These observations suggest that the expressed transporters were not functional in *C. glutamicum*. Furthermore, the reduced IA titers compared to the control strain led to the conclusion that the strains might suffer from an additional protein load or some kind of unfolded protein response due to the overexpression of the respective transporters. Other export strategies were not tested in this work, but improving IA export remains an interesting target for future studies.

3.2.3.8 Combination of Beneficial Mutations

Above, we presented different strategies for metabolic engineering of *C. glutamicum* to enable and improve IA production from acetate. During screening in 1 mL scale, the highest yield ($62 \pm 12 \text{ mmol mol}^{-1}$) and titer ($2.36 \pm 0.75 \text{ g L}^{-1}$) were achieved by *C. glutamicum* ITA19 after deletion of *ramB* and *gdh*. In addition, attenuation of the IDH activity showed promising results in terms of IA production. Among the latter, the IDH versions IDH^{R453C}, IDH^{R453C}_{ATG::GTG} and IDH^{R453C}_{ATG::TTG}, expressed in the strains *C. glutamicum* ITA4, ITA9 and ITA10, respectively, showed the highest yields and titers compared to the strains harboring the corresponding start codons ATG, GTG, and TTG for IDH^{A94D} and IDH^{G407S}. Therefore, we combined the genetic modifications of *C. glutamicum* ITA19 with those of *C. glutamicum* ITA4, ITA9, and ITA10, resulting in *C. glutamicum* $\Delta ramB \Delta gdh$ IDH^{R453C} / IDH^{R453C}_{ATG::GTG} / IDH^{R453C}_{ATG::TTG}, which were transformed with the pEKE_{x2-malEcad_{opt}} plasmid and named *C. glutamicum* ITA24_{ATG}, ITA24_{GTG}, and ITA24_{TTG}, respectively. The strains were analyzed during cultivation in shaking flasks in 50 mL nitrogen-limited CGXII medium, inoculated to an OD of 2, as a single determination (Figure 3-7). *C. glutamicum* ITA24_{ATG} showed a lag-phase of 8 h followed by a rather exponential growth phase and reached a final biomass concentration of 2.76 g L^{-1} after 30 h. The lag-phase of *C. glutamicum* ITA24_{GTG} was increased to 12 h followed by a non-exponential growth phase and a biomass concentration of 2.34 g L^{-1} after 72 h. The latter strain produced 4.03 g IA L^{-1} with a yield of 95 mmol mol^{-1} , which was more than 60% higher compared to *C. glutamicum* ITA24_{ATG}, which reached a final titer of 2.47 g IA L^{-1} with a yield of 57 mmol mol^{-1} . In contrast to these strains, *C. glutamicum* ITA24_{TTG} showed no growth within 72 h, thus it was excluded from further studies.

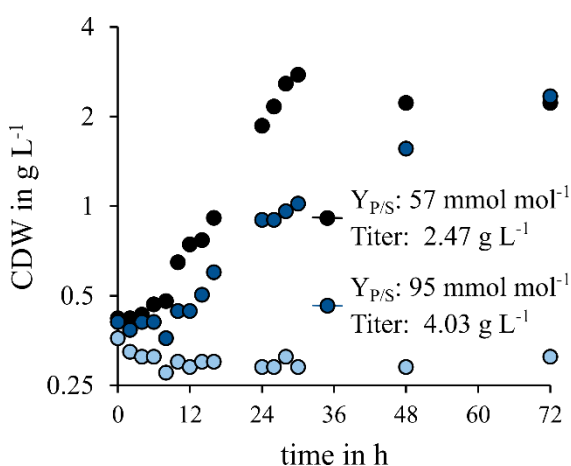


Figure 3-7: Shaking Flask Cultivation of the Final *C. glutamicum* ITA24 Strains.

The graph shows the growth of the strains *C. glutamicum* ITA24_{ATG} in black (also included in Figure 3-8), *C. glutamicum* ITA24_{GTG} in dark blue, and *C. glutamicum* ITA24_{TTG} in light blue during cultivation in 50 mL of nitrogen-limited CGXII medium supplemented with 20 g acetate L⁻¹ (n = 1). The titer and yield of IA produced by *C. glutamicum* ITA24_{ATG} and ITA24_{GTG} after 72 h are indicated in the graph. (Data of this cultivation was not included in Figure 3-9).

3.2.4 Spontaneously Evolved Strains

During our studies on the attenuation of IDH activity, we observed that all three clones of *C. glutamicum* ITA10 that were isolated after transformation, exhibited different phenotypes with respect to growth and IA production when screened in 1 mL scale (see Chapter 3.2.3.1). In addition, we identified other putatively evolved clones of the engineered strains *C. glutamicum* ITA3 and *C. glutamicum* ITA12 during BioLector[®] cultivation, which we named *C. glutamicum* ITA3evo and *C. glutamicum* ITA12evo. The yields and titers achieved by the latter two strains exceeded those of their parental strains by 220% and 250%, respectively. These observations suggested that these strains must have evolved spontaneously during the cloning procedure. Apparently, the different strains were under evolutionary pressure, which could be caused by increased citrate levels as a result of IDH attenuation [22]. This assumption is supported by the increased concentration of IA produced by the spontaneously mutated strains, as a more efficient conversion of aconitate to itaconate could reduce citrate pools and thus reduce the deleterious effects of citrate on the cell. However, it should be noted that the revealed strains *C. glutamicum* ITA10, ITA3evo and ITA12evo apparently evolved during the cloning procedure in which CAD expression was not induced. To identify the mutations that enhanced IA production from acetate in the different strains, we extracted the genomic DNA from *C. glutamicum* ITA3evo and *C. glutamicum* ITA12evo, as well as from the three clones of *C. glutamicum* ITA10 isolated in Chapter 3.2.3.1. The extracted DNA was sent to Genewiz (Leipzig, Germany) for re-sequencing. The identified single nucleotide polymorphisms (SNPs) were compared with those detected in *C. glutamicum* ITA1. In all strains, SNPs of the engineered IDH occurred with a frequency of almost 100%. It is noteworthy that the artificial mutations of the P_{dapA}-A16 promoter used for *pck* expression in *C. glutamicum* ITA12evo were detected with a frequency of only 14% to 20%, which could be due to interference with the wild-type *dapA* promoter during sequence alignments. On the other hand, the missing 370 base pairs of the *pck* promoter could not be identified by the sequencing method used (see Chapter 2.5). In addition to the intended mutations introduced by targeted engineering, two SNPs were detected with a frequency of 100% in the uncharacterized *psp1* gene in one clone of *C. glutamicum* ITA10. Another SNP was found with a frequency of 100% in the *ansA* gene, encoding an asparaginase, in the genome of *C. glutamicum* ITA3evo. However, no common mutations in similar genes or related pathways could be detected between the

re-sequenced strains, compared to the control *C. glutamicum* ITA1. Thus, the molecular reasons for the increased yields and titers of IA produced from acetate in the screening experiments of the apparently mutated strains remain to be elucidated. As a result, the evolved strains were not further pursued as production strains in this study, but a more detailed analysis of these strains remains to be an interesting topic for further studies.

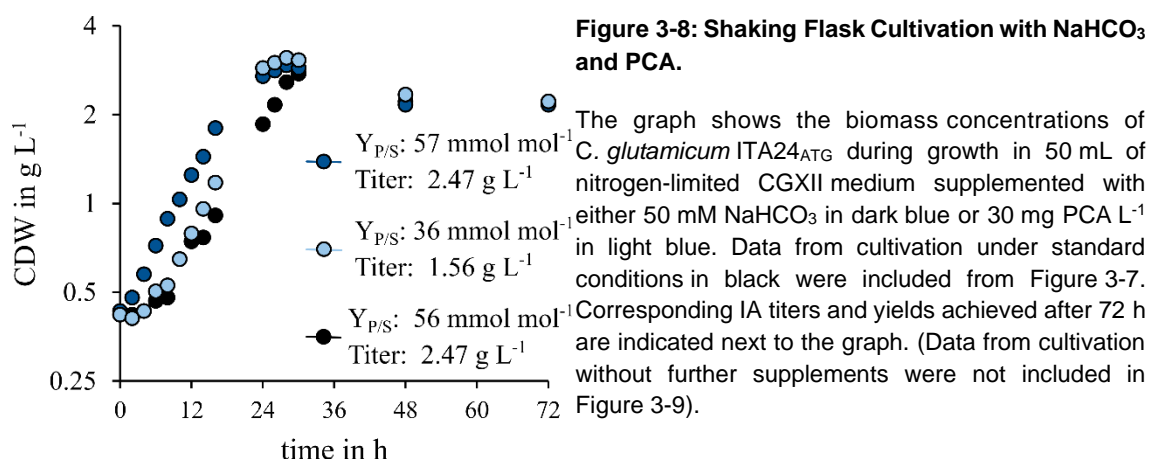
3.2.5 Optimization of Cultivation Conditions

Above, we have successfully applied genetic engineering to improve IA production with *C. glutamicum* from acetate. However, besides of the genetic equipment of the production host, biotechnological processes are strongly influenced by a variety of different process parameters and cultivation conditions. Kim et al. [131] reported different effects of pH, temperature, oxygen availability, and other parameters on IA production during whole cell bioconversion of citrate by *E. coli*. In addition, we have previously shown in this work the effect of preculture conditions on the resistance of *C. glutamicum* to acetol (see Chapter 3.1.1). Thus, we further analyzed the effects of different culture supplements and different cultivation temperatures on the IA production with the *C. glutamicum* ITA strains generated in this work.

3.2.5.1 Testing Preculture Conditions and Culture Supplements

First we investigated the effect of different preculture conditions on IA production from acetate with *C. glutamicum* ITA24_{ATG} in shaking flasks. Precultures were prepared as 50 mL cultures of 2YT, 2YT + 5 g acetate L⁻¹, and full CGXII medium (no nitrogen limitation) supplemented with 10 g acetate L⁻¹ to grow the inoculum of the main cultures. Main cultures were prepared in shaking flasks using nitrogen-limited CGXII medium supplemented with 20 g acetate L⁻¹ according to our standard production procedure. In a single determination cells pre-cultured in CGXII medium showed no IA production after 72 h. Cells pre-cultured in 2YT medium and additionally primed with 5 g acetate L⁻¹ showed a severely impaired growth phenotype compared to cells that were pre-cultured in 2YT medium without further supplements. Consequently, the preculture conditions were not varied in subsequent cultivations. Next, we analyzed the effect of different culture supplements during IA production with *C. glutamicum* ITA24_{ATG}. For this purpose, we prepared 50 mL cultures of nitrogen-limited CGXII medium supplemented with either 50 mM NaHCO₃, 30 mg PCA L⁻¹, or both NaHCO₃ and PCA (Figure 3-8), as both

Results



compounds have been reported to support the growth of *C. glutamicum* and improve its iron assimilation [36, 187]. Although we had initially shown that PCA had no positive effect on the production of IA by *C. glutamicum* ITA1 (see Chapter 3.2.2), we decided to re-evaluate the effect of PCA on the highly engineered strain *C. glutamicum* ITA24_{ATG}. In a single determination, the addition of 50 mM NaHCO₃ completely abolished the lag-phase without affecting the yield and titer of IA produced compared to the control without addition of NaHCO₃ or PCA. In both cultures, a final IA concentration of 2.47 g L⁻¹ was measured after 72 h, corresponding to yields of 56 and 57 mmol mol⁻¹, respectively. Contrary to the experiments initially performed with *C. glutamicum* ITA1 (see Chapter 3.2.2), the addition of PCA stabilized the growth of *C. glutamicum* ITA24_{ATG}. Although the effect was less pronounced compared to NaHCO₃, the culture reached the maximum biomass concentrations 4 h before the control. However, IA yield and titer were strongly reduced to 36 mmol mol⁻¹ and 1.56 g L⁻¹ when PCA was added to the main culture (Figure 3-8). When PCA was supplemented together with NaHCO₃, the negative effect of PCA was abolished and the strain behaved similarly to the culture supplemented with NaHCO₃ alone (data not shown). Since none of the evaluated conditions resulted in improved IA production, the tested supplements were not included in the following cultivations, but NaHCO₃ remains a promising substitute to improve the growth of *C. glutamicum*, particularly in the early stages of fed-batch cultivations. In this work, we used acetate as feedstock, which is known to exhibit antimicrobial activity, especially at elevated concentrations (see Chapter 1.3.2). To exclude possible negative effects of high acetate concentrations on *C. glutamicum* ITA24_{ATG} during IA production, we analyzed IA formation at lower acetate concentrations. Therefore, *C. glutamicum* ITA24_{ATG} was cultured in 50 mL of nitrogen-limited CGXII medium containing 10 g acetate L⁻¹. To remain a C:N ratio of 40:1, the amounts of urea were further reduced to 0.25 g L⁻¹. As

expected, the maximum biomass concentration was reduced by about 50% compared to the culture grown with 20 g acetate and 0.5 g urea L⁻¹. Interestingly, the yield of IA production was also reduced by 42% to 33 mmol mol⁻¹. Thus, the final titer of IA produced from 10 g acetate L⁻¹ was reduced by 68% and amounted to only 0.78 g IA L⁻¹ (data not shown). Based on these results, we continued with concentrations of 20 g acetate L⁻¹ in subsequent cultivations.

3.2.5.2 Adjusting the Cultivation Temperature

Previously, Vuoristo *et al.* [284] showed that reduced cultivation temperatures had a positive effect on the expression of *cad* and IA titers in *E. coli*. At 37 °C, the authors found that most CAD were located in inclusion bodies accompanied with rather low enzymatic activities, whereas during cultivation at 30 °C, CAD activities were increased more than 12-fold and final titers were increased more than 24-fold [284]. In contrast to that, Joo *et al.* [121] reported, that elevated cultivation temperatures of 35 °C slightly increased IA production in engineered *C. glutamicum* from rice wine residues. Therefore, we tested the effect of elevated and reduced cultivation temperatures on IA production from acetate with *C. glutamicum* ITA24_{ATG}. First, we performed a single shaking flask cultivation according to our standard conditions in nitrogen-limited CGXII medium incubated at 25 °C, 30 °C and 37 °C. When cultured at 37 °C, *C. glutamicum* ITA24_{ATG} showed a severely attenuated growth and produced only marginal amounts of IA (data not shown). In contrast, growth at 25 °C was only slightly affected compared to 30 °C, but the final IA titer and yield were significantly increased. Based on these observations, we performed additional shaking flask cultivations with *C. glutamicum* ITA1, ITA15, ITA19, ITA24_{ATG} and ITA24_{GTG} and compared their specific IA production from acetate at 25 and 30 °C (Figure 3-9). Interestingly, the growth of *C. glutamicum* ITA1, ITA15, and ITA19 appeared to be only slightly affected by the cultivation temperature and the effects on yield and titer were not statistically significant. Under both conditions, *C. glutamicum* ITA1 reached maximum biomass concentrations of 2.60 ± 0.12 and 2.90 ± 0.07 g L⁻¹ after 24 h, respectively, and in both cases produced about 0.15 g IA L⁻¹ within 72 h of cultivation. Deletion of *ramB* in *C. glutamicum* ITA15 and ITA19 strongly prolonged the lag-phase compared to *C. glutamicum* ITA1. This effect was even more pronounced at the lower cultivation temperature of 25 °C. However, similar to the latter strain, the final IA titers of *C. glutamicum* ITA15 and ITA19 were only slightly affected

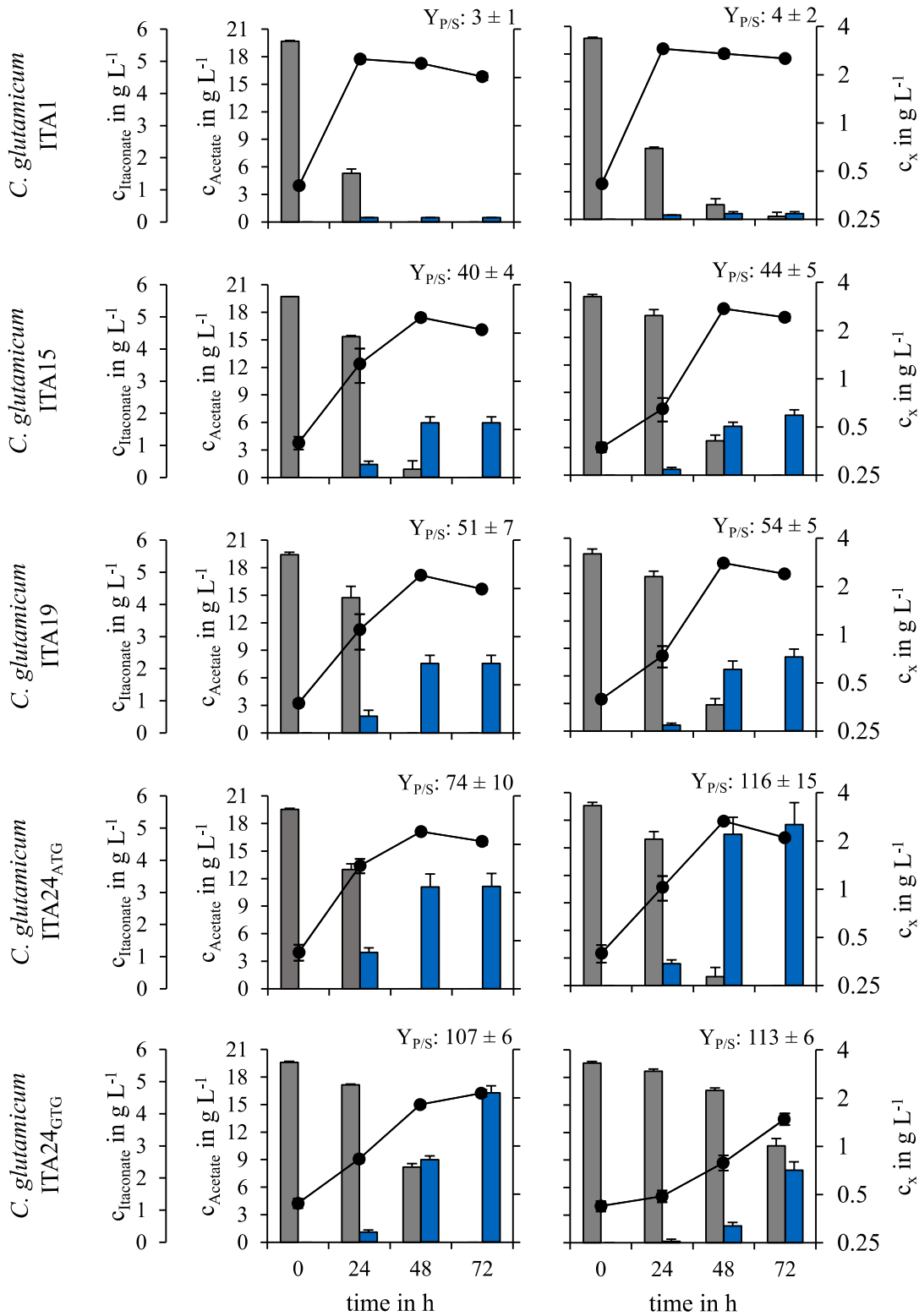


Figure 3-9: Growth and Itaconic Acid Production at Different Cultivation Temperatures.

The graphs show the concentrations of biomass (black circles), acetate (grey bars), and itaconate (blue bars) of *C. glutamicum* ITA1, ITA15, ITA19, ITA24_{ATG}, and ITA24_{GTG} cultured in 50 mL of nitrogen-limited CGXII medium at 30 °C (left panel) or 25 °C (right panel). Each graph shows the calculated yield ($Y_{P/S}$) in mmol IA produced per mol acetate consumed after 72 h.

by the cultivation temperature. Cultures of the respective strains reached maximum biomass concentration after 48 h, which was by approximately 10% to 15% higher at 25 °C compared to cultures incubated at 30 °C. Final IA titers produced by the strains *C. glutamicum* ITA15 and ITA19 were $1.69 \pm 0.18 \text{ g L}^{-1}$ and $2.17 \pm 0.25 \text{ g L}^{-1}$ after 72 h of cultivation at 30 °C, respectively. The titers increased slightly to $1.86 \pm 0.16 \text{ g IA L}^{-1}$ and $2.30 \pm 0.25 \text{ g IA L}^{-1}$ during cultivation at 25 °C. Interestingly, additional attenuation of the IDH activity in *C. glutamicum* ITA24_{ATG} counteracted the prolonged lag-phase observed for *C. glutamicum* ITA15 and ITA19 during cultivation at 30 °C, but even more evident at 25 °C, as indicated by a 39% increase in biomass concentration after 24 h at this temperature. However, μ of *C. glutamicum* ITA1, which reached maximum biomass within 24 h could not be restored. Furthermore, the strain *C. glutamicum* ITA24_{ATG} produced $3.19 \pm 0.40 \text{ g IA L}^{-1}$ with a yield of $74 \pm 10 \text{ mmol mol}^{-1}$ after 72 h of cultivation at 30 °C. When the cultivation temperature was lowered to 25 °C, the final titer and yield increased significantly to $5.01 \pm 0.67 \text{ g IA L}^{-1}$ and $116 \pm 15 \text{ mmol mol}^{-1}$, respectively. The latter represents a 57% increase in the final titer compared to cultivation at 30 °C, and corresponds to 35% of the theoretical maximum yield of $333 \text{ mmol mol}^{-1}$ [196]. In contrast to *C. glutamicum* ITA24_{ATG}, growth of *C. glutamicum* ITA24_{GTG} was further attenuated compared to *C. glutamicum* ITA15 and ITA19 expressing the wild-type IDH, as maximum biomass concentrations were not reached within the first 48 h of cultivation at 30 °C. Nevertheless, during cultivation at 30 °C, the yield and final titer were further increased by 45% to $107 \pm 6 \text{ mmol mol}^{-1}$ and $4.64 \pm 0.22 \text{ g L}^{-1}$, respectively, compared to *C. glutamicum* ITA24_{ATG}. However, cultivation at 25 °C severely inhibited the growth of *C. glutamicum* ITA24_{GTG}, such that the final biomass of this strain was reduced to $1.48 \pm 0.12 \text{ g L}^{-1}$ after 72 h and 53% of the initial acetate remained in the culture supernatant. As a result, final titers of IA were reduced to $2.25 \pm 0.27 \text{ g L}^{-1}$, although the yield remained high at $113 \pm 6 \text{ mmol mol}^{-1}$. Next, we further investigated the cause of the increased IA production at lower cultivation temperature in *C. glutamicum* ITA24_{ATG}. Ozcan et al. [206] reported changes in the membrane composition of *C. glutamicum* cultured at different temperatures. An altered lipid composition could influence the membrane integrity and favor IA export, which in turn would reduce possible negative effects caused by elevated intracellular IA levels (see Chapter 3.2.1). To test this hypothesis, we determined the intracellular IA concentration of *C. glutamicum* ITA24_{ATG} cultured at 25 and 30 °C (Figure 3-10 A). After 24 h, the intracellular IA concentrations were $16 \pm 4 \text{ mM}$ and $33 \pm 11 \text{ mM}$, respectively, probably due to the higher IA levels

Results

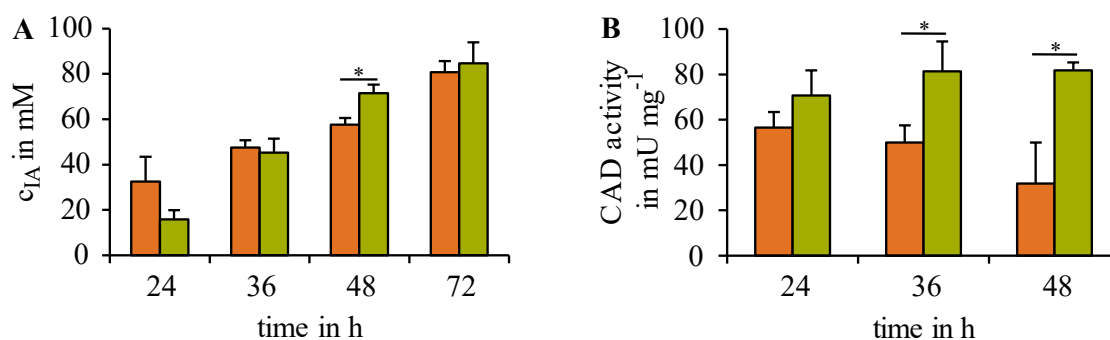


Figure 3-10: Intracellular Itaconic Acid Concentrations and *cis*-Aconitate Decarboxylase Activities.

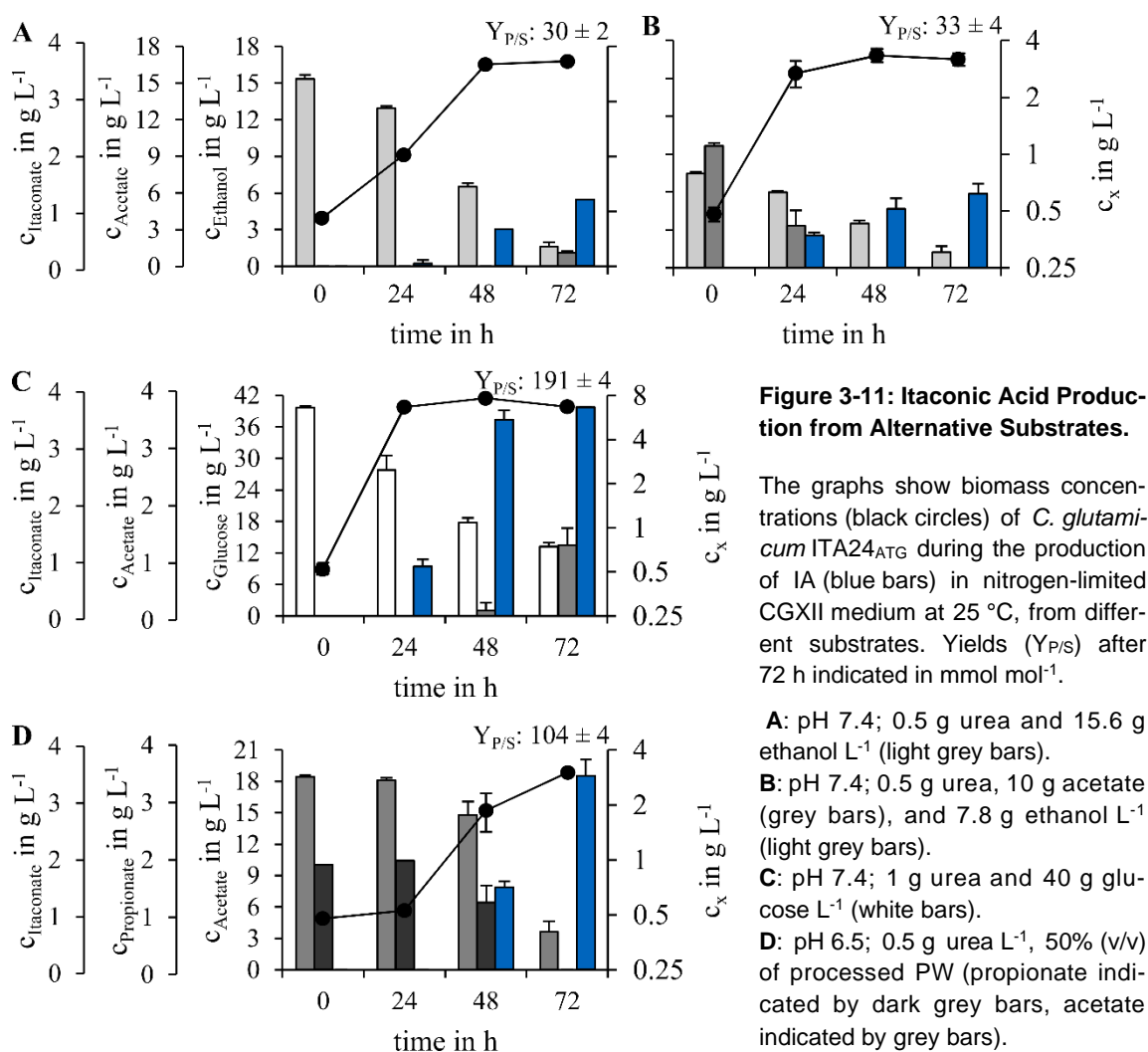
The graphs show the intracellular concentrations of IA (A) and the intracellular enzyme activity of the *cis*-aconitate decarboxylase (B) measured in the crude cell extract of *C. glutamicum* ITA24_{ATG} cultured at 30 °C (orange) or 25 °C (green). Asterisks indicate significance ($p < 0.05$) according to two-sample t-test, assuming equal variance.

produced at 30 °C at that time. After 72 h, however, the intracellular concentrations of *C. glutamicum* ITA24_{ATG} increased to > 80 mM, independent of the temperature. Based on this result, we hypothesized that improved IA export may not contribute to improved IA production at lower cultivation temperatures. However, as mentioned above, an increase in CAD activity due to reduced cultivation temperatures has been reported during IA production with engineered *E. coli* [284]. Therefore, we compared the CAD activity of *C. glutamicum* ITA24_{ATG} cultured at 25 and 30 °C (Figure 3-10 B). During cultivation at 30 °C, the measured CAD activity was 57 ± 7 mU mg^{-1} after 24 h and decreased continuously to 32 ± 18 mU mg^{-1} after 48 h. In contrast, the CAD activity of cells cultured at 25 °C was 71 ± 11 mU mg^{-1} after 24 h and increased further to 81 ± 13 and 82 ± 3 mU mg^{-1} after 36 and 48 h of cultivation, respectively. These results suggest that the improved IA titers were caused by higher CAD activities during cultivation at 25 °C. Based on the results described in here, we selected *C. glutamicum* ITA24_{ATG} as the best IA-producing strain generated in this study and reduced the cultivation temperatures to 25 °C for further cultivations conducted regarding IA production. In addition, for a better comparison between the final strain *C. glutamicum* ITA24_{ATG} and the other engineered strains, we also performed a cultivation in 1 mL scale at 30 °C. Under the latter conditions the strain produced 3.43 ± 0.59 g IA L^{-1} with a yield of 81 ± 9 mmol mol^{-1} , the results of which are included in Table 3-4. Again, these values were increased compared to the cultivation in shaking flask, but the differences were smaller compared to the other strains. It is noteworthy that we also included *C. glutamicum* ITA24_{GTG} in the same cultivation, but this strain did not show any growth within 72 h, so it is not listed in the corresponding table.

3.3 Itaconic Acid Production from Pyrolysis Water and other Substrates

Above, we have described the engineering of *C. glutamicum* ITA24_{ATG} for efficient IA production from acetate under optimized culture conditions. Acetate itself is a very promising candidate for future biotechnological processes. However, similar to acetate, ethanol is an interesting candidate as an alternative non-food derived feedstock for biotechnological conversion. In principle, ethanol is a reduced derivative of acetate, and syngas fermentations and electro-(bio-)chemical conversion of biomass often lead to the production of a mixture of ethanol and acetate (see Chapter 1.2). Since the metabolism of ethanol mainly follows the same pathways as acetate, we considered that ethanol could be another promising substrate for IA production with *C. glutamicum* ITA24_{ATG}. To investigate the ability of *C. glutamicum* ITA24_{ATG} to produce IA from ethanol and mixtures of ethanol and acetate, we cultured the strain in 50 mL of nitrogen-limited CGXII medium at pH 7.4 at 25 °C. The culture was supplemented with either 15.6 g ethanol L⁻¹ or with 10 g acetate L⁻¹ and 7.8 g ethanol L⁻¹, each equivalent to C-moles of 20 g acetate L⁻¹ (Figure 3-11 A, B). Similar to growth on acetate, stationary phase was reached after 48 h during growth on ethanol as the sole carbon and energy source, but the maximum biomass concentration was increased by 25% to 3.33 ± 0.03 g L⁻¹. However, only 1.17 ± 0.00 g IA L⁻¹ with a yield of 30 ± 2 mmol mol⁻¹ was produced after 72 h. It is noteworthy that 1.59 ± 0.36 g ethanol L⁻¹ remained in the culture supernatant at the end of the cultivation, and an additional 1.10 ± 0.15 g acetate L⁻¹ was produced after the strain entered the stationary phase. Similar results were obtained during cultivation on a mixture of equimolar amounts of ethanol and acetate. Although acetate was completely consumed after 48 h, 1.23 ± 0.49 g ethanol L⁻¹ remained in the culture broth, after 72 h. Finally, 1.30 ± 0.18 g IA L⁻¹ was produced, corresponding to a yield of 33 ± 4 mmol of IA produced per mol of substrate consumed. However, growth of *C. glutamicum* ITA24_{ATG} on the acetate/ethanol mixture was markedly improved compared to cultures containing pure ethanol or pure acetate, as the stationary phase was already reached about 24 h after inoculation. Next, we tested the ability of *C. glutamicum* ITA24_{ATG} to produce IA from glucose, since glucose is still the most preferred substrate used in biotechnological processes. Therefore, we cultured *C. glutamicum* ITA24_{ATG} in 50 mL of nitrogen-limited CGXII medium (pH 7.4) at 25 °C, and increased urea and glucose concentrations to

Results



1 g L^{-1} and 40 g L^{-1} , respectively (Figure 3-11 C). Cells entered the stationary phase approximately 24 h after inoculation, and reached a maximum biomass concentration of 6.71 ± 0.34 g L^{-1} . Glucose was consumed throughout the whole cultivation, but 16.62 ± 1.54 g L^{-1} remained in the culture supernatant after 72 h, representing 42% of the initial glucose concentration. In addition, 1.24 ± 0.29 g acetate L^{-1} was detected in the culture broth, after 72 h. *C. glutamicum* ITA24_{ATG} produced 3.64 ± 0.00 g IA L^{-1} with a yield of 191 ± 4 mmol mol^{-1} , which is only 19% of the theoretical maximum. Finally, we aimed at the production of IA from PW, which is a sidestream generated during fast pyrolysis. PW has a water content of about 80% and contains, among other compounds, up to 40 g acetate L^{-1} (see Chapter 1.2.1 and Table A1). Thus, PW is an interesting substrate for valorization by our engineered strains. However, crude PW was found to inhibit the growth of *C. glutamicum* at concentrations below 2% (v/v) in CGXII medium. To increase its biocompatibility, the crude PW was treated by over-liming, vacuum evaporation, heat, and activated carbon treatment as previously described by Kubisch

and Ochsenreither [147]. While all acetate remained in the PW during this process, acetol was completely lost. The resulting processed PW was used as a substrate for IA production by *C. glutamicum* ITA24_{ATG} cultured in 50 mL nitrogen-limited CGXII medium (pH 6.5) at 25 °C. A initial concentration of 50% PW was used in order to reach a starting concentration of 18.41 ± 0.17 g acetate L⁻¹ at the beginning of the cultivation and to prevent adverse effects caused by higher acetate concentrations (Figure 3-11 D). Under these conditions, *C. glutamicum* ITA24_{ATG} showed a lag-phase of more than 24 h, but reached a final biomass concentration of 3.32 ± 0.11 g L⁻¹ after 72 h. However, 3.64 ± 1.02 g acetate L⁻¹ remained in the culture supernatant at the end of the cultivation. Nevertheless, 3.38 ± 0.28 g IA L⁻¹ was produced by *C. glutamicum* ITA24_{ATG} with a yield of 104 ± 4 mmol IA produced per mole of acetate consumed. It is noteworthy that at the beginning of the cultivation an additional 1.83 ± 0.00 g propionate L⁻¹ was detected in the supernatant by HPLC analysis, which after 72 h was completely consumed by *C. glutamicum* ITA24_{ATG}. Since we cannot exclude that propionate or other carbon compounds of the PW were also converted to IA, the actual yield is probably lower than the calculated yield. For a better comparison between the feedstocks PW and pure acetate, TC measurements were performed on the cultures grown on PW. At the beginning of the cultivation, 18.25 ± 0.17 g TOC L⁻¹ were detected in the culture supernatant. A major fraction of 8.22 ± 0.09 g TOC L⁻¹ originated from the MOPS buffer in the CGXII medium. The remaining 10.02 ± 0.18 g TOC L⁻¹ came from the PW and consisted, according to HPLC analysis, of acetate with 7.49 ± 0.07 g carbon L⁻¹, propionate with 0.90 ± 0.00 g carbon L⁻¹, and 1.64 ± 0.11 g carbon L⁻¹ of unknown origin. After 72 h, 4.68 ± 0.29 g carbon L⁻¹ was measured in the culture supernatant. The remaining acetate accounted for 1.48 ± 0.41 g carbon L⁻¹ and 1.56 ± 0.13 g carbon L⁻¹ originated from the formed IA. Still 1.64 ± 0.27 g carbon L⁻¹ was of unknown origin, indicating that this small fraction could not function as a substrate for *C. glutamicum*. Assuming that the biomass of *C. glutamicum* consists of 41.1% carbon when grown on minimal medium [165], 1.04 ± 0.04 g carbon L⁻¹ was incorporated into cells. Based on these data, 4.30 ± 0.16 g carbon L⁻¹ was lost during the cultivation, probably due to CO₂ formation. However, off-gas analyses need to be performed to confirm this assumption. Overall 15% of the initial TOC in PW was converted to IA by *C. glutamicum* ITA24_{ATG} within 72 h, which can be explained by the prolonged lag-phase and incomplete conversion of acetate. Thus, an extended cultivation time could further increase the final IA titers produced from PW.

4 Discussion

As outlined at the beginning of this thesis, biotechnology is considered to be an important cornerstone of a successful bioeconomy strategy. Biotechnological processes are capable of replacing petroleum-based chemical synthesis, which often require harsh reaction conditions, with biological pathways and reactions that generally take place under more moderate settings. In principle, bio-based catalysts such as enzymes and cells can facilitate the conversion of organic residues, by-products and waste streams into desired products and chemical building blocks. However, to date, most biotechnological processes are based on food-derived substrates, such as glucose, contributing to the ‘food vs. industry’ dilemma. Consequently, novel substrates that do not compete with the production of food and feed must be introduced as a matter of urgency. Acetate and acetate-containing sidestreams, obtained from the processing of biomass or biological fixation of C1 gases, are considered as promising feedstocks for future processes. [96, 128, 153, 200], but until today acetate has rarely been used as the sole carbon and energy source for the development of novel biotechnological processes (see Chapter 1.2). In this work, we focused on the practical introduction of acetate and the acetate-containing PW obtained from the bioliq[®] process as a substrate for microbial conversion to IA, a bio-based building block for the chemical industry. For this purpose, we choose the bacterium *C. glutamicum* as the intended production host. *C. glutamicum* is a well-established host for research and industrial purposes, but especially its properties regarding to its metabolism of acetate and complex substrate mixtures make it a highly interesting candidate for our studies (see Chapter 1.3). A major drawback addressed in this study is the inefficient utilization of acetol as a substrate by *C. glutamicum*. Acetol is found in varying concentrations in the aqueous sidestreams of different fast pyrolysis processes, but is the main component in the PW formed in the bioliq[®] process, accounting for over 50 g L⁻¹ (see Chapter 1.2.1) (Table A1). In order to ensure a resource-friendly and holistic upgrading of the main carbon fraction in PW, we analyzed the metabolization of acetol by *C. glutamicum* and tested the expression of different possible key enzymes regarding an increased assimilation of acetol (see Chapter 3.1). In parallel, we have engineered *C. glutamicum* to produce the versatile platform chemical IA from acetate, which is used for various chemical and medical purposes (see chapter 1.4). In doing so,

we aimed for an efficient IA production and optimized *C. glutamicum* for the production of high titers of IA at high yields, and tested the effect of different supplements and culture conditions (see Chapter 3.2). Finally, we transferred our results to cultures using processed PW as the sole carbon and energy source and demonstrated the effective valorization of this industrial sidestreams through biotechnological conversion.

4.1 Metabolization of Acetol by *C. glutamicum*

Considering the huge carbon and energy fractions stored as acetol in PW, its conversion into valuable products is of high interest to ensure a resource-friendly utilization of renewable resources. In this study, the acetol was completely removed from the PW used as feedstock for IA production during the pretreatment procedure (see Chapter 3.3). This was in contrast to the original study published by Kubisch and Ochsenreither [147], where acetol remained to a small fraction of about 3.5 g L^{-1} after processing. Loss of acetol during pretreatment of PW has also been reported by other authors [155]. In future, however, an optimized condensation of the different pyrolysis fractions during the bioliq[®] process [211] and/or utilization of more resistant production hosts [38] might allow for less harsh pretreatment procedures, thus leaving more acetol for microbial conversion. Therefore, we focused on the investigation and the optimization of the acetol metabolism in *C. glutamicum*, in this work.

Only limited information can be found in the literature dealing with the catabolization of acetol as a substrate. Most studies focus on acetol as an intermediate of single reactions, either during detoxification of methylglyoxal [138] or in the biotechnological production of 1,2-propanediol [237], in different organisms. A common strategy for 1,2-propanediol production from glucose is the conversion of the glycolytic intermediate dihydroxyacetone phosphate to methylglyoxal, which is first reduced to acetol and finally to 1,2-propanediol [237]. The latter reaction can be catalyzed by the glycerol dehydrogenase GldA. Lange et al. [155] expressed *gldA* from *E. coli* in *C. glutamicum* and showed that the resulting strain is able to directly convert acetol to 1,2-propanediol under anaerobic conditions with a yield of almost 100% [155]. Thus, it can be assumed that acetol can easily translocate into the cytosol of *C. glutamicum*, and since it is a small uncharged molecule, it is likely to do so simply by diffusion. In the referenced study, the authors used PW as a substrate for microbial valorization, similar to this work. However, a

different pretreatment strategy was used, which resulted in more acetol remaining, but also in higher toxicity to the engineered strain. To counteract the growth inhibition caused by the applied PW, the authors added yeast extract to their cultures. In his PhD thesis, J. Lange [154] investigated the growth of *C. glutamicum* on acetol as sole carbon and energy source, as well as co-cultivation on acetol and glucose in more detail. In contrast to our study, the author reported a biphasic growth phenotype on acetol, but also on acetol and glucose [154]. In our study, marginal growth was observed when acetol was provided as the sole carbon and energy source, and different growth phenotypes were observed if glucose was included as an additional substrate (Figure 3-1). The exact reason for the latter remains unclear, but is most likely related to a disturbed adaptation to the minimal medium caused by acetol or toxic intermediates, such as methylglyoxal, which could be formed during the degradation of acetol (Figure 1-3). This assumption is further supported, by the fact that a uniform growth phenotype could be adjusted by introducing an additional CGXII preculture to allow the cells to adapt to the new medium before adding acetol during the main culture. Furthermore, we observed that cultures initially considered as non-growing within the first 24 h adapted to the CGXII medium after a long lag-phase and reached final biomass concentrations similar to those of immediately growing cultures, after several days of cultivation. Moreover, strains that grew in CGXII medium supplemented with glucose and 5 g acetol L⁻¹ continued to grow when transferred into fresh medium with increased concentrations of 20 g acetol L⁻¹. J. Lange [154] also reported a positive effect of GSH on cultures supplemented with acetol. In this work, we proved that supplementation with GSH, but also with PCA, was beneficial for the growth of *C. glutamicum* on cultures containing acetol. However, since no effect on the uptake of acetol itself was observed, both supplements were not further considered to be directly involved in the acetol metabolism.

We further analyzed the growth of *C. glutamicum* on mixtures of 10 g glucose and 5 g acetol L⁻¹. It is noteworthy that the μ of the cultures was reduced from $0.35 \pm 0.01 \text{ h}^{-1}$ to $0.20 \pm 0.06 \text{ h}^{-1}$ during shaking flask cultivation, when acetol was present. Interestingly, μ was only slightly reduced from $0.32 \pm 0.01 \text{ h}^{-1}$ to 0.30 ± 0.01 during cultivation at 1 mL scale in the BioLector[®] device, and during bioreactor cultivation μ amounted to $0.29 \pm 0.02 \text{ h}^{-1}$ and was not affected by the presence of acetol. The reason for the observed discrepancy in μ between the different cultivation methods was not further investigated, but might indicate important principles of the acetol metabolism in *C. glutamicum*. We hypothesized that insufficient oxygen supply during shaking flask cultivation could lead

Discussion

to the accumulation of toxic intermediates that severely inhibit cell growth. Although, we did not measure oxygen transfer in either 1 mL, or 50 mL cultures, in the latter we observed the formation of lactate by *C. glutamicum* ATCC 13032 on 20 g glucose L⁻¹. Lactate is a fermentation product that is naturally produced by *C. glutamicum* under oxygen deprivation [181]. Consequently, it can be assumed, that oxygen limitation occurs at least during the later stages of shaking flask cultivations. This, in turn, could lead to the inhibition of membrane-associated oxidases, which channel their electrons directly into the menaquinone pool under aerobic conditions, but are inhibited in their function under oxygen limitation. *C. glutamicum* possesses at least 8 of such oxidases, such as the catabolic lactate dehydrogenases, pyruvate:quinone oxidoreductase, and the malate:quinone oxidoreductase [45]. In particular, lactate- and pyruvate oxidoreductases could be directly involved in the metabolization of acetol (Figure 1-3), but we could not exclude the involvement of other (unknown) oxidoreductases (see below). Due to the differences in μ obtained between shaking flask cultivation on glucose and glucose plus acetol, the substrate uptake rates differed greatly between the two conditions. However, $Y_{X/S}$ from glucose was significantly increased from $0.53 \pm 0.01 \text{ g}_X \text{ g}_{\text{Glc}}^{-1}$ to $0.61 \pm 0.03 \text{ g}_X \text{ g}_{\text{Glc}}^{-1}$ after the addition of acetol. In contrast $Y_{X/S}$ per gram of consumed carbon decreased from $1.32 \pm 0.04 \text{ g}_X \text{ g}_C^{-1}$ to $1.08 \pm 0.15 \text{ g}_X \text{ g}_C^{-1}$. It might be that extra reduction equivalents generated by the oxidation of acetol would reduce the amount of glucose that must be oxidized to produce the equivalent amount of energy, thus making more carbon of glucose available for biomass production. However, due to the oxygen limitations as described above, the carbon from acetol cannot be efficiently channeled into the central metabolism and thus cannot be fully oxidized nor incorporated into biomass, resulting in a lower biomass yield for the total carbon supplied. These observations lead to the conclusion that acetol could be used as an energy source, but not or only partially as a carbon source during shaking flask cultivations. This assumption is further supported by the results obtained during bioreactor cultivations performed at a DO set to 35% (relative to air). As mentioned above, the μ of *C. glutamicum* was not affected by the addition of acetol in this cultivation system, allowing a direct comparison of substrate uptake rates between the two cultures. Furthermore, carbon uptake by *C. glutamicum* in both cultures was 0.26 and 0.27 $\text{g}_C \text{ g}_X^{-1} \text{ h}^{-1}$, which was similar to that in shaking flask cultivations on glucose alone. However, uptake of glucose was significantly reduced from 0.70 ± 0.01 to $0.60 \pm 0.02 \text{ g g}^{-1} \text{ h}^{-1}$ by the addition of acetol during bioreactor cultivation. A steady carbon uptake rate, but adjusted uptake rates of the individual compounds during growth

on substrate mixtures is a special feature of *C. glutamicum* [292]. In addition, we observed an increase in $Y_{X/S}$ calculated for glucose and for total carbon by the addition of acetol. In contrast to the results obtained during shaking flask cultivations, these values indicate that acetol can be channeled into the central metabolism and can be used by the cell to fuel catabolic and anabolic pathways. Overall, our results indicate that *C. glutamicum* can natively utilize acetol as a carbon and energy source along with glucose under strictly aerobic conditions. Interestingly, none of the analyzed performance indicators described above were affected by the addition of acetol during any cultivation when acetate was provided as the primary substrate instead of glucose. In contrast to *C. glutamicum*, *A. oryzae* has been reported to grow on acetol as the sole carbon and energy source, as well as on mixtures of acetate and acetol. Similar to our studies, the growth rate, substrate uptake, and maximum biomass concentrations of the fungus were reduced with increasing acetol concentrations. Interestingly, *A. oryzae* tolerated up to 40 g acetol L⁻¹ without acetate, but its tolerance was reduced to 20 g acetol L⁻¹ when 40 g acetate L⁻¹ was added to the cultures [148]. Taken together, these results show that the acetol metabolism in *C. glutamicum* and other organisms is influenced not only by the culture method, but also by the co-substrate provided. In addition, the metabolization of acetol appears to be associated with growth inhibition in several organisms, again suggesting the formation of toxic intermediates and cell stress. Further cultivations with e.g. fructose or glycerol, and glutamate or citrate as different examples of glycolytic or non-glycolytic substrates, respectively, could help to clarify the question, why and how the provided substrate influences the assimilation of acetol by *C. glutamicum*. Contrary to our hypothesis are the observation that uptake of acetol did not follow a typical substrate uptake curve. Instead, acetol was removed from the culture supernatant in a more linear fashion, similar to the increase in pH (Figure 3-2). It is noteworthy that in shaking flask cultivation, the q_s ' of acetol was in the same range of 0.12 to 0.14 g h⁻¹ independent of the co-substrate and was 0.14 ± 0.01 g h⁻¹ even when no other substrate was provided and the cells showed only marginal growth (Figure 3-1). On the other hand, the acetol concentration did not change if acetol was incubated in CGXII medium supplemented with acetate and glucose but without cells. It should also be noted that all cultures were prepared with 5 g acetol L⁻¹, which corresponds to a concentration of 67.5 mM. However, only 43 ± 2 , 44 ± 4 , and 57 ± 3 mM acetol were measured directly after inoculation of cultures containing acetol alone, glucose and acetol, and acetate and acetol, respectively. A similar effect was also reported regarding the studies on *A. oryzae*,

Discussion

where the initial acetol concentrations were reduced by up to 9%, which the authors attributed to Maillard reactions occurring during the thermal sterilization process of the medium [148]. In contrast to the results described before, these observations suggest that acetol is chemically converted, maybe in a pH-dependent manner, which is further indicated by a yellowish discoloration of CGXII medium containing acetol, after several days of incubation. However, further studies are necessary to clarify the behavior of acetol in this regard.

To reveal possible native pathways that could be involved in the metabolization of acetol in *C. glutamicum*, we performed transcriptome analysis of samples generated during bioreactor cultivation on acetol together with glucose or acetate. Interestingly, only the gene expression of cg3290 was significantly upregulated 3.6-fold by the presence of acetol during growth on glucose, but not on acetate. This gene is annotated as a predicted NADPH:quinone-dependent oxidoreductase (WP_011015533.1). Thus, considering our hypothesis on the oxygen transfer in the different cultivation systems (see above), cg3290 is of high interest regarding the acetol metabolism in *C. glutamicum*. Indeed, we found that the deletion of this gene increased the resistance of *C. glutamicum* towards acetol during shaking flask cultivation on glucose, as indicated by a higher μ compared to the wild-type strain. Thus, it is possible that this oxidoreductase catalyzes the formation of toxic intermediates, most likely methylglyoxal, whose concentration would be reduced in the respective knock out strain. Since we hypothesized, that this reaction is inhibited due to oxygen deprivation at late stages of the cultivation leading to insufficient assimilation of acetol, the enzyme might be highly active at early stages of the cultivation, when oxygen is not limited leading to the accumulation of toxic intermediates. This in turn would suggest that the bottleneck of acetol assimilation must be located downstream of this reaction, so most likely due to insufficient conversion of methylglyoxal. However, our assumptions are contradicted by the fact that a corresponding strain overexpressing cg3290, did not show an increased uptake of acetol during shaking flask cultivation. Furthermore, we found that cg3290 was upregulated 2.6-fold during growth on acetate compared to growth on glucose, which could explain the fact that this gene was not found to be further upregulated by acetol during growth on acetate. This could also explain the reduced μ of the corresponding knockout strain when cultured on acetate compared to the wild-type strain. The question remains, however, why the growth of *C. glutamicum* is only inhibited by acetol during growth on glucose, but not on acetate. To get a clear picture of the function of cg3290, it might be helpful to perform additional bioreactor

cultivations with the corresponding knockout and overexpressing strains. In addition to cg3290, cg0354 was selected as interesting candidates regarding the acetol metabolism in *C. glutamicum*. Cg0354 (WP_011013540.1) is predicted to encode a thioredoxin related protein that might be involved in the maintenance of mycothiol. Mycothiol is the thiol analog of GSH in actinobacteria, which the latter was found to be involved in the detoxification of methylglyoxal by the glyoxalase I + II system [267] and also to increase the resistance of *C. glutamicum* to acetol [155]. The glyoxylase I + II system and the GSH biosynthesis pathway were also found to be significantly upregulated in *A. oryzae* during growth on pyrolysis water compared to growth on acetate as substrate [146]. Similar to the deletion of cg3290, the deletion of cg0354 resulted in an increased resistance to acetol during cultivation on glucose. This observation is again in contrast to the expected function of the protein, as impaired detoxification of methylglyoxal or other reactive aldehydes caused by deletion of this gene should rather decrease resistance to acetol. As observed for cg3290, the knockout of cg0354 decreased the μ of the respective strain on acetate, compared to the wild-type strain. But unlike cg3290, the expression of cg0354 was not upregulated the presence of acetate compared to glucose alone. Again, no differences in acetol uptake were observed by deletion or overexpression of cg0354. As mentioned above, bioreactor cultivations performed with the respective strains might help to reveal the function of this protein regarding the acetol metabolism in *C. glutamicum*. It is noteworthy that, similar to the wild-type strain, the addition of acetol to the cultures had no further effect on the discussed knockout strains when cultivated on acetate. However, since the intrinsic μ of both strains was generally reduced during growth on acetate, the enzymes appear to have an important function during growth on acetate. Taken together, these results show that cg3290 and cg0354 are interesting candidates with respect to the acetol metabolism, but also for the overall carbon metabolism in *C. glutamicum*. In addition, we investigated the function of cg3412 (WP_011015618.1) and cg1423 (WP_011014239.1), which encode a subunit of a predicted azaleucine exporter and an L-glyceraldehyde 3-phosphate reductase, respectively. However, neither deletion nor overexpression of the two genes affected the uptake of acetol or the growth of the corresponding strains during shaking flask cultivations on glucose or acetate. Since we observed the effects of acetol solely during growth on glucose, but not on acetate, we further included *sugR* (cg2115) in our studies, which encodes a global transcriptional repressor of the sugar metabolism in *C. glutamicum*. SugR represses the transcription of several genes involved in the uptake and metabolization of sugars and glycolysis-related

Discussion

genes in the absence of sugars [10, 86, 87]. Thus, we hypothesized that SugR might be involved in the transcriptional regulation of genes responsible for metabolization of acetol, which are inactivated during growth on acetate and activated during growth on glucose. However, deletion of *sugR* did not result in any remarkable differences in growth or acetol uptake in our cultivations, neither on glucose nor on acetate.

Although, the studies performed on promising candidates obtained by transcriptome sequencing revealed two interesting genes that were somehow involved in the viability of *C. glutamicum* during growth on acetol, deletion or overexpression of the respective genes did not lead to increased degradation of acetol. Hence, we additionally tested the implementation of reactions and pathways within the acetol-methylglyoxal-pyruvate node to improve the metabolization of acetol. Therefore, we analyzed the effect of overexpression of several enzymes alone, but also the parallel expression of different enzymes from synthetic operons. Our studies included overexpression of the *hchA* derived from *E. coli*, encoding chaperon with glyoxalase III activity, catalyzing a GSH independent reaction from methylglyoxal to pyruvate [256]. In addition, we tested the overexpression of *yqhD* derived from *E. coli* and the native *dkgA* from *C. glutamicum*, as both enzymes have been reported to be involved in the conversion of methylglyoxal to acetol [114, 117, 158], and we hypothesized that they would catalyze the reverse reaction at an altered reaction equilibrium (see below). While the enzymes described above primarily catalyze the conversion between methylglyoxal and acetol, we further tested enzymes that might be involved in the conversion of methylglyoxal to lactaldehyde and lactate towards pyruvate (Figure 1-3). Therefore, we overexpressed, *yvgN* from *B. subtilis*, *aldA* and *ldhA* from *E. coli*, and the native *dld* from *C. glutamicum*, which are capable of catalyzing different reactions within the predicted acetol metabolism. Another approach to shift the reaction equilibrium from the reduced compound acetol to the less reduced pyruvate, was followed by overexpressing water-forming NADH and NADPH dehydrogenases to disturb the redox balance of the cell and stimulate the oxidation of acetol. Finally, we tested the overexpression of *mshA*, which encodes a mycothiol glycosyltransferase that catalyzes the first step of the mycothiol biosynthesis. As mentioned above, mycothiol is the thiol equivalent of GSH and Liu et al. [168] showed that overexpression of *mshA* increased the resistance of *C. glutamicum* towards methylglyoxal. However, none of the overexpressed genes, neither alone nor in combination, resulted in an increased acetol uptake by *C. glutamicum*. Recently, Iacometti et al. [109] showed that only GloA and GloB with glyoxylase I and glyoxylase II activity, respectively, were able to catalyze

the conversion of methylglyoxal to pyruvate in a glycolysis-deficient *E. coli* mutant *in vivo* [109]. These findings may explain, why the pathways tested in this study showed no activity with respect to acetol metabolization. However, functional expression of the *E. coli*-derived GloAB system has not yet been possible in *C. glutamicum* [154]. An alternative route for channeling acetol into the central metabolism in *C. glutamicum* could be the conversion of acetol to 1,2-propanediol, which has been shown to be possible under anaerobic conditions with yields approaching 100% [155]. Subsequently, the formed 1,2-propanediol could be converted to 1-propanol [250], which can then be oxidized to propionate [140] and fed into the central metabolism via the methylcitrate cycle [60]. However, the enzymes that catalyze the reaction of 1,2-propanediol to 1-propanol either require strictly anaerobic conditions or the expensive cofactor cobalamin [155, 250]. In turn, anaerobic conditions could inhibit the (methyl-)citrate cycles if NAD⁺ is not restored e.g. by the production of highly reduced products. Thus, this pathway seems rather unsuitable to implement acetol as a substrate for IA production in this study. While it does not seem trivial to introduce metabolization of acetol into *C. glutamicum*, other authors suggest the purification of acetate as the preferred carbon source from PW [261]. Although this approach could solve the problems of toxicity of PW as described elsewhere in this work, it would not solve the huge loss of carbon and energy stored in acetol and other compounds. A much more promising approach was published by Xiao *et al.* [304] who showed that acetol can be isomerized to lactic acid by Cu-Sn based metal catalysis with a C-mol yield of 91.8%. The resulting lactic acid could then easily be used as a substrate for biotechnological conversion by *C. glutamicum* and other microorganisms [31, 118, 309].

4.2 Acetate-Based Production of Itaconic Acid

C. glutamicum does not have the ability to naturally produce or degrade IA [205], but IA production can be achieved by heterologous expression of one of two biological pathways that have been identified in native IA producers. The first is the direct decarboxylation of *cis*-aconitate, catalyzed by CAD (*'cis-pathway'*), and the second is the isomerization of *cis*-aconitate to *trans*-aconitate followed by decarboxylation of the latter catalyzed by the aconitate-delta-isomerase 1 and TAD, respectively [296]. It is important to note that Elmore *et al.* [85] reported a 12.5% higher yield in the production of IA from lignin

Discussion

with engineered *P. putida* strains when expressing the *trans*-pathway compared to the *cis*-pathway. The authors linked this observation to the higher thermodynamic stability of *trans*-aconitate and the inhibition of ACN by this compound [85]. Notwithstanding the results published by these authors, in this work IA production in *C. glutamicum* ITA1 was enabled by plasmid-based expression of the *cad* gene derived from *A. terreus*, as this construct had previously been optimized for studies on IA production with *C. glutamicum* from glucose by Otten et al. [205]. However, in contrast to the results published by the authors, the exclusive overexpression of the engineered *cad* gene in *C. glutamicum* ITA1 did not lead to IA production in our experiments, neither from glucose, nor from acetate, nor from a mixture of both. Furthermore, the final titers obtained in control cultivations, performed with glucose under nitrogen limitation were only one-third of the originally published titers, obtained under similar conditions. The reasons for this discrepancy remain unclear, but limitations in iron availability can be ruled out, as IA production was not increased by the addition of PCA. Independent of the results obtained regarding IA production from glucose, the application of nitrogen limitation during shaking flask cultivations resulted in the production of trace amounts of IA by *C. glutamicum* ITA1 from acetate as the sole carbon and energy source. Nitrogen limitation has also been successfully applied to enhance IA production in natural hosts such as *U. maydis* [135], but not necessarily in *A. terreus* [134]. For the latter organism, phosphate limitation has been reported to improve IA production from glucose [288] due to uncoupling of the glycolysis and the respiratory chain, thereby increasing carbon flux towards IA [134]. However, in contrast to nitrogen limitation, phosphate limitation or even starvation was unfavorable for IA production in *C. glutamicum* ITA1, as indicated by poor substrate uptake, reduced final biomass and heavily reduced IA titers during cultivation on acetate or glucose (Figure 3-4). The specific phosphate starvation response of *C. glutamicum* is characterized by the downregulation of genes involved in RNA translation and DNA replication [112, 289], which in turn is probably accompanied by reduced metabolic activity and insufficient CAD expression. The moderate cell growth observed even in the complete absence of phosphate in the medium can be attributed to the polyphosphate used as internal phosphate storage by *C. glutamicum*, which is sufficient to support the growth of approximately 4 to 6 generations [291]. Next, we performed metabolic engineering to rewire the carbon flux of *C. glutamicum* and create an optimal genetic foundation to obtain a viable production host with maximized yields and titers of IA produced from acetate (Figure 4-1).

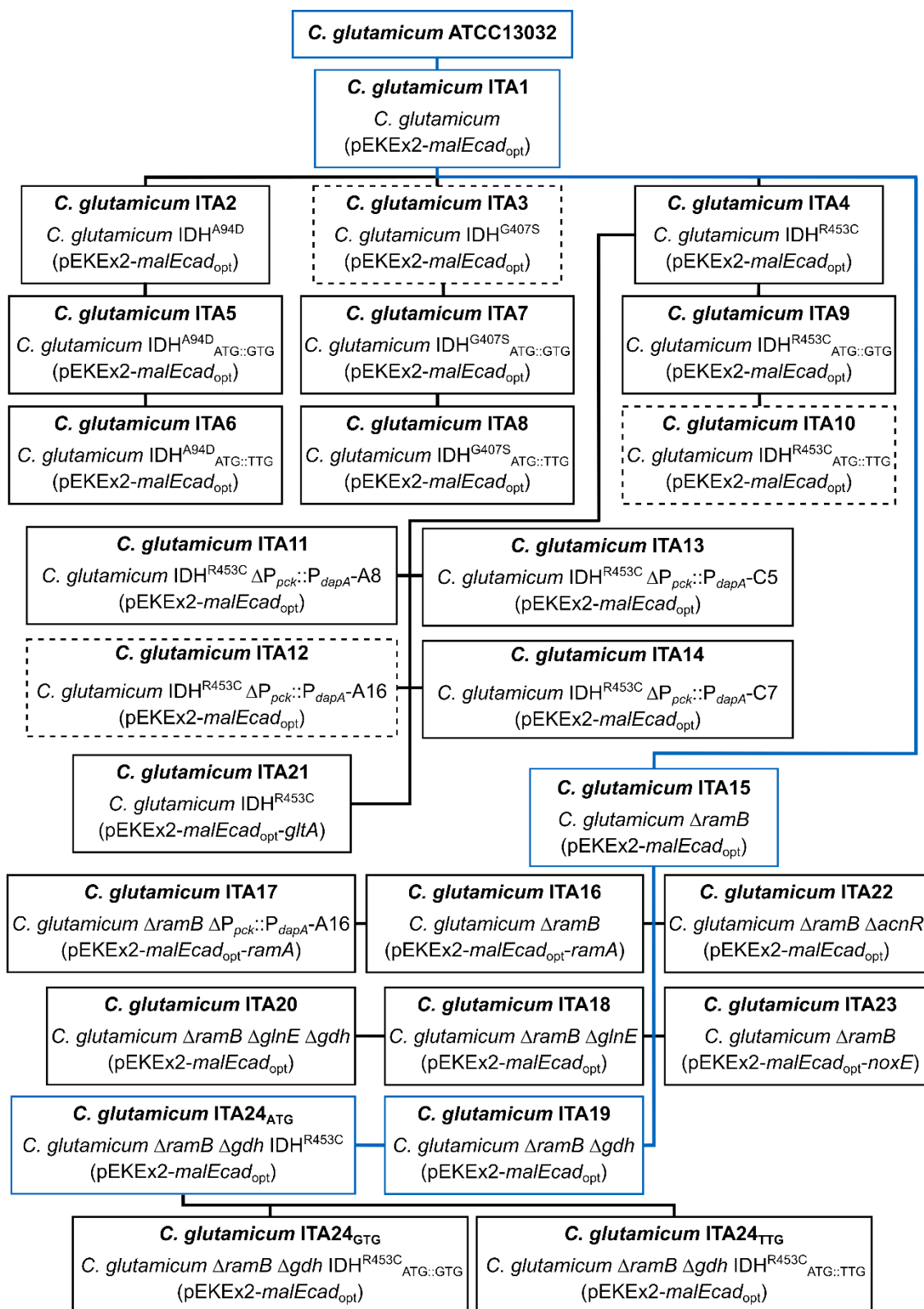


Figure 4-1: Genealogical Tree of Engineered *C. glutamicum* ITA Strains.

Genealogy of *C. glutamicum* strains engineered to maximize titer and yield of IA produced from acetate in this work. The blue line marks the path of the most beneficial mutations tested for increased IA production of each strain relative to its corresponding parental strain. Dashed boxes indicate strains with spontaneously mutated derivatives with increased yields and titers that were further analyzed by genomic re-sequencing.

Discussion

In *A. terreus*, CAD, which catalyzes the decarboxylation of *cis*-aconitate to IA, is located in the cytosol, whereas the reaction of ACN, which produces *cis*-aconitate, takes place in the mitochondrion. The spatial separation of the two distinct reactions prevents the direct competition between the ACN, ICL and IDH, enzymes of the TCA cycle, and CAD, which has a K_M of 2.45 mM for *cis*-aconitate and thus a rather low affinity for its substrate [75]. Therefore, efficient export of *cis*-aconitate from the mitochondria into the cytosol is required to induce high IA production. In native IA producers, this is ensured by specific mitochondrial *cis*-aconitate exporters [296]. Bacterial hosts, however, do not possess mitochondria or similar organelles that could maintain a spatial separation similar to that of native IA producers, and thus the enzymes of the enzymes ACN and CAD are both localized in the same sphere of the cytosol and compete directly for *cis*-aconitate. In *C. glutamicum*, the ACN possesses K_M values of 480 μM , 18.5 μM , and 552 μM for its three substrates citrate, *cis*-aconitate, and isocitrate, respectively [21]. The subsequent TCA cycle enzymes IDH and ICL have affinities for isocitrate of 12 μM [80] and 280 μM [220], respectively. Thus, these three enzymes form an efficient carbon sink within the TCA cycle and outcompete the CAD enzyme during IA production, which has an over 100-fold lower affinity for *cis*-aconitate compared to ACN. This circumstance is also similar in other bacterial hosts, hence reducing carbon flux within the TCA by attenuating IDH activity is a common strategy to increase IA production [85, 196]. In this work, we replaced the native IDH of *C. glutamicum* ITA1 by three mutated versions that show different residual activities. To allow easy and parallel screening for final IA titers and yields, the engineered strains were screened in a 48-well flower plate in a total volume of 1 mL. The highest yield and titer in IA were observed for *C. glutamicum* ITA4 expressing IDH^{R453C} with 29% residual activity compared to the wild-type version [242]. The versions IDH^{A94D} and IDH^{G407S} with 10% and 55% residual activity [242] only slightly improved IA production from acetate compared to *C. glutamicum* ITA1. Beyond the scope of this work, *C. glutamicum* ITA4 was successfully used to develop an optimized pH and DO coupled fed-batch process for IA production from acetate. Thereby the strain produced 29.2 g IA L⁻¹ with a maximal productivity of 1 g L⁻¹ h⁻¹ within 44 h [180]. The results obtained demonstrate that IA production from acetate by the marginally engineered strain *C. glutamicum* ITA4 is in the same range as IA production with *E. coli* from glucose [103] or by *A. terreus* from sugar-rich biomass hydrolysates (Table 1-1). Regardless of the results obtained in fed-batch fermentations, it should be noted that, in contrast to our observations with acetate, a residual IDH activity of only 3% was

found to be most suitable for IA production in *C. glutamicum* from glucose [205]. This discrepancy could be explained by the differences in carbon flux distribution observed for the provided substrates [292]. Due to the 3-fold lower carbon flux via IDH during growth on glucose, a greater reduction of IDH activity might be required to sufficiently improve *cis*-aconitate availability for IA production. However, we could not exclude that lower expression levels of IDH, as in the case of the studies on glucose [205], might have different effects on IA production than the reduction of the enzyme activity itself tested in this work, especially since phospho-proteome studies indicate post-transcriptional modifications of IDH in *C. glutamicum* [29]. Thus, we further reduced IDH activity by exchanging the native start codon 'ATG' to 'GTG' or 'TTG' in *C. glutamicum* ITA2, ITA3, and ITA4, which additionally lead to lower translation of the respective *icd* genes. Interestingly, successive reductions in *icd* expression levels resulted in successively higher yields and titers of IA produced compared to the respective parental strains. It is noteworthy that the strains expressing the IDH^{R453C} always showed the highest yields and titers along the three different start codons, tested. Although IDH activity was not measured in this work, Otten et al. [205] reported 20% and 3% of residual IDH activity in *C. glutamicum* by exchanging the native 'ATG' start codon of *icd* to 'GTG' or 'TTG', respectively, if the cells were cultured under nitrogen limitation on glucose. Thus, it can be assumed that due to the additional point mutations the remaining IDH activities in *C. glutamicum* ITA5 - ITA10 were below these reported values. However, the increased IA production of these strains is not consistent with the results obtained with the parental strains *C. glutamicum* ITA2 - ITA4, which showed that 10% residual IDH resulted in a reduction in final titers of over 50% compared to a residual IDH activity of 29%. The reason for the additive effect observed for reduced IDH activity and reduced translation remains to be elucidated. It could either be related to altered protein levels in the cells, or it could support the theory of a functional post-translational modification of the IDH in *C. glutamicum* [29]. We also observed that a successive reduction of the IDH activity gradually prolonged the lag-phases and slightly reduced the μ 's of the respectively engineered strains (Figure 3-5).

During growth on acetate, gluconeogenesis is an essential pathway, but it removes carbon from the TCA cycle and thus may limit IA production. The first step of the gluconeogenesis in *C. glutamicum* is performed by the PEPCk, which catalyzes the decarboxylation and phosphorylation of oxaloacetate to PEP. We hypothesized that a reduction of PEPCk activity could help to sequester carbon within the TCA cycle and subsequently increase

Discussion

IA production from acetate. Therefore, we replaced the native promoter of PEPCK in *C. glutamicum* ITA4 with different versions of a *dapA* promoter library [281]. However, the yield and titer of the respective strains *C. glutamicum* ITA11 - ITA14 could not be increased compared to the control strain *C. glutamicum* ITA4. It is noteworthy that the promoter version P_{dapA}-A16, which originally showed the highest activity among the tested versions [279, 281], resulted in yields and titers similar to those obtained with the strain carrying the native promoter. In contrast, the promoter version P_{dapA}-C5, which originally showed the lowest activity among the tested constructs [279, 281], completely abolished the growth of *C. glutamicum* ITA13 under our experimental conditions. Most likely, the supply of intermediates of the gluconeogenesis was insufficient to support the growth of the latter strain. Overall, these results suggest that gluconeogenesis is not a significant carbon sink during overproduction of TCA cycle derived intermediates from acetate. Rather, the reduced flux via PEPCK is detrimental to growth and production on acetate and perhaps other non-glycolytic substrates. However, overexpression of PEPCK might be of interest for overproduction of gluconeogenic products from acetate.

Another essential pathway active during growth on acetate is the glyoxylate shunt, which forms the anaplerotic pathway within the TCA cycle during growth on non-glycolytic substrates. The first reaction of the glyoxylate shunt is catalyzed by ICL, which directly competes with IDH for their common substrate isocitrate, thereby removing carbon from the reaction catalyzed by CAD. To reduce the carbon flux via the glyoxylate shunt and thus further improve *cis*-aconitate availability, we deleted *ramB*, encoding the transcriptional regulator RamB, which is required for proper transcriptional activation of *aceA* and *aceB*, encoding ICL and MS, respectively [220, 221]. Interestingly, IA titers achieved by *C. glutamicum* ITA15 with inactivated RamB doubled compared to those of *C. glutamicum* ITA4 with reduced IDH activity, and this despite the carbon flux over IDH being 3-times higher compared to the flux over ICL in the *C. glutamicum* wild-type strain during growth on acetate [292]. This unexpectedly high improvement in the yield and titer achieved by the deletion of *ramB* indicates that in *C. glutamicum* ITA2 - ITA10 the carbon flux through the glyoxylate shunt has most likely increased due to attenuation of the IDH activities. This assumption is further supported by the fact that the glyoxylate shunt in *C. glutamicum* can be activated solely by reducing IDH activity during growth on glucose [242], and may also explain why reducing IDH activity to 3% performed best during IA production from glucose [205] (see above). However, it is important to note that RamB is a global regulator of the carbon metabolism in *C. glutamicum* and the role

of RamB during growth on acetate as the sole substrate has not yet been fully investigated. Therefore, additional regulatory effects other than the reduced activity of the glyoxylate shunt could positively influence IA production in *C. glutamicum* ITA15. In contrast to the deletion of *ramB*, overexpression of *ramA* had no appreciable effect on IA production from acetate in *C. glutamicum*. We also did not observe strong growth defects as it was previously reported for overexpression of *ramA* [272]. The complex network of the global transcriptional regulators in *C. glutamicum* is not yet fully understood. Several authors showed, that the respective regulators in *C. glutamicum*, such as RamA, RamB, GlxR and SugR, form complex feed-forward loops for the joint regulation of target genes [50, 271]. The complex interaction of RamA and RamB motivated us to re-examine the flux into gluconeogenesis in *C. glutamicum* ITA16, as both regulators are found to be involved in regulating the expression of PEPCK. In addition to the deletion of *ramB* and overexpression of *ramA*, the native promoter of PEPCK was exchanged with the P_{dapA}-A16 variant. However, in this strain background the promoter exchange resulted in a significantly lower yield and titer. These results again highlight the complexity of fine-tuning PEPCK activity (see above).

Other authors have shown that overexpression of CS and ACN improves IA production from acetate by engineered *E. coli* [196], thus we tested whether similar results could be obtained in *C. glutamicum*. Overexpression of *glcA* severely impaired IA production from acetate in *C. glutamicum*. The reason for this remains unclear, but Baumgart et al. [22] reported a strong occurrence of secondary mutations in *C. glutamicum*, probably caused by elevated citrate levels, after deletion of ACN or IDH [22]. Further, we deleted *ancR*, which has been shown to increase the activity of ACN by over 80% during growth on acetate compared to the wild-type [143]. However, deletion of *ancR* also did not increase final titers and yields. This was surprising because ACN from *C. glutamicum* has been used to increase the *cis*-aconitate supply for IA production in *E. coli* due to its high substrate affinities [88, 131]. This suggests that higher expression of ACN probably might not automatically lead to higher pools of *cis*-aconitate in *C. glutamicum*. In contrast to the results obtained for *glcA* overexpression, these results indicate that citrate supply, and thus general carbon uptake, could be rate limiting during IA production from acetate in *C. glutamicum*. We hypothesized that carbon uptake could be increased by decoupling the TCA cycle from respiratory chain. Since this could not be achieved by applying phosphate limitation as described above, we assumed that disturbing the redox balance might have similar effects. Therefore, we expressed the water generating NADH oxidase

Discussion

derived from *L. lactis* in *C. glutamicum* ITA15. However, expression of *noxE* had no effect on the growth pattern of this strain, but the final titer and yield were reduced by one third. Overall, our results regarding engineering of the carbon metabolism again emphasize that *C. glutamicum* is well suited for the valorization of acetate. Expected bottlenecks in protein expression and carbon flux distributions that might impede the utilization of acetate, as observed in IA production from acetate by *E. coli* [284], did not appear to be present in *C. glutamicum*. On the contrary, acetate was so efficiently assimilated and used for biomass production that the carbon flux had to be restricted at certain points in order to channel adequate amounts of carbon to the desired product. However, it is remarkable that only a little fine-tuning of one or more of a few enzymes in *C. glutamicum* can be sufficient to achieve a reasonable production of an desired compound from acetate, as shown by fed-batch fermentations with the IDH^{R453C} mutant strain *C. glutamicum* ITA4 [180] (see above). However, it remains questionable whether carbon uptake and metabolization by *C. glutamicum* could be further increased beyond its natural capacity. The import of acetate is unlikely to be rate limiting during acetate assimilation, as passive diffusion has been shown to be sufficient to support growth [222]. Nevertheless, assimilation of acetate might be enhanced by accelerating its intracellular activation. AK of *C. glutamicum*, which is responsible for the initial activation of acetate to acetyl-phosphate, showed rather low affinities for its substrate ($K_M = 7.9$ mM) [222]. In contrast, acetyl-CoA synthetase (ACS) expressed by *E. coli*, which catalyzes the direct conversion of acetate to acetyl-CoA by the consumption of two ATP equivalents, showed much higher affinities toward acetate ($K_M = 0.2$ mM) [52]. In turn, an increase in ATP consumption could generally accelerate the turnover rates of the TCA cycle. Therefore, additional heterologous overexpression of *acs* in *C. glutamicum* could be an interesting subject for further studies on valorization of acetate. A common drawback reported about the use of acetate as a carbon source is its toxicity towards the microbial hosts, caused by its membrane uncoupling potential [128]. Previously, *C. glutamicum* has been shown to tolerate acetate concentrations up to 12 g L⁻¹ without any effects on growth [301]. In this study, we demonstrated that *C. glutamicum* still showed reasonable growth at elevated concentrations up to 20 g L⁻¹. During shaking flask cultivations of the wild-type strain, we observed lag-phases of up to 4 h and a μ of about 0.29 h⁻¹ during cultivation in CGXII minimal medium containing 20 g acetate L⁻¹ (unpublished results). Other authors have shown that *C. glutamicum* can even grow at concentrations as high as 30 g acetate L⁻¹ under certain conditions [13]. Interestingly, we observed a doubling of the yield of IA

produced by doubling the initial substrate concentration from 10 g to 20 g acetate L⁻¹. So far, the cause of this phenomenon remains to be elucidated. On the one hand, it could be related to the rather high intracellular nitrogen concentration of *C. glutamicum*, which was reported to be more than 200 mM, stored as glutamate and glutamine [141, 199], during cultivation in nitrogen-rich CGXII medium. When growing on less substrate, the amount of intracellular nitrogen storage would have a greater effect on the C:N ratio than when growing on higher substrate concentrations. On the other hand, it is more likely that increased concentrations in the culture supernatant enhance the passive diffusion of acetate into the cell. Contrary to above, this suggests that the uptake of acetate, rather than its intracellular activation, is the rate-limiting step during IA production with engineered *C. glutamicum*. Therefore, it can be suggested that the application of even higher acetate concentrations could further positively affect the yields and final IA titers. However, to ensure stable processes at elevated acetate concentrations, it would be necessary to stabilize the intrinsic membrane potential of *C. glutamicum*. In this context, the global regulator GlxR might be a promising candidate for overexpression in *C. glutamicum*. It has been shown that functional GlxR signaling is required to maintain the membrane potential and thus is essential for growth of *C. glutamicum* on acetate [301]. Therefore, overexpression of GlxR might positively affect the membrane potential and counteract the weak acid cycle, possibly allowing stable growth of *C. glutamicum* at elevated acetate concentrations above 20 g L⁻¹. Furthermore, Kim *et al.* [130] have reported that overexpression of GlxR in *C. glutamicum* inhibited the expression of ICL and MS [130]. Thus, similar to *ramB* deletion, overexpression of GlxR might have additional beneficial effects on IA production from acetate.

Cultivation under nitrogen limitation was found to enhance IA production in native and non-native IA producers (see above). However, in our experiments limiting the access to nitrogen was a prerequisite for enabling IA production by the engineered *C. glutamicum* strains. Therefore, we hypothesized that IA production could be enhanced by exploiting the native cellular response to nitrogen shortage. To mimic nitrogen limitation at the intracellular level, we first deleted the adenylytransferase GlnE, resulting in a nitrogen limitation phenotype at the transcriptional level [219]. However, the respective strain showed strongly reduced yield and titers of IA if cultured under nitrogen limitation. Thus, IA production is probably not related to transcriptional changes in response to low nitrogen concentrations. The effector molecule that is used by *C. glutamicum* to sense the nitrogen status of the cell has not yet been identified, but Müller *et al.* [188] suggested

Discussion

2-oxoglutarate as a promising candidate for this purpose [188]. Interestingly, deletion of *glnE*, which showed partial activation of the nitrogen starvation response was found to reduce the intracellular pools of 2-oxoglutarate by 50% compared to the wild-type strain [219]. In contrast, it has been shown that a deletion of *gdh*, which is part of the major nitrogen assimilation pathway in *C. glutamicum*, resulted in a 4-fold increase levels in 2-oxoglutarate [188]. Consequently, we inactivated the GDH in *C. glutamicum* ITA15, and observed that yield and titer of the resulting strain *C. glutamicum* ITA19 increased by more than 70% if cultivated under nitrogen limitation, compared to the parental strain. It is noteworthy that neither deletion of *glnE*, nor deletion of *gdh*, nor a simultaneous deletion of both enabled IA production during shaking flask cultivation under nitrogen surplus. Furthermore, deletion of *glnE* completely abolished the beneficial effects of *gdh* deletion on IA production in the *glnE gdh* double knockout strain. These results suggest that an altered carbon flux caused by nitrogen limitation and *gdh* knockout is responsible for the positive effects during IA production in *C. glutamicum* from acetate. Among others, high levels of 2-oxoglutarate inhibit the IDH of *C. glutamicum* with a K_i of 12 mM [80], which is in the same range as the intracellular concentrations measured in *gdh* knock out strains [188]. This additional level of IDH attenuation might explain, at least in part, the increased production of IA caused by *gdh* deletion. It might be possible to further increase the intracellular levels of 2-oxoglutarate, and thus IA production, by deleting the ODHC- specific E1 subunit encoded by *odhA* or by deleting PknG, which is responsible for the phosphorylation of OdhI [194]. Both approaches would prevent the conversion of 2-oxoglutarate to succinyl-CoA, thus increasing the intracellular pool of 2-oxoglutarate. This strategy has also been used to improve precursor availability during overproduction of glutamate [241]. During IA production, however, the flux towards glutamate would be prevented due to insufficient nitrogen supply, thus allowing more carbon to be channeled to IA.

After evaluating different strategies to alter the central metabolism for IA production from acetate in *C. glutamicum*, we tested a combination of the respective mutations that were found to be beneficial for this purpose. Therefore, we used the *ramB gdh* double knockout strain *C. glutamicum* ITA19 and incorporated the IDH^{R453C}_{ATG}, IDH^{R453C}_{GTG}, and IDH^{R453C}_{TTG}, respectively. While *C. glutamicum* ITA24_{ATG} and ITA24_{GTG} showed reasonable growth and IA production, *C. glutamicum* ITA24_{TTG} appeared to be unable to grow under the applied production conditions within 72 h of cultivation in shaking flasks. However, it remains unknown whether the growth inhibition was due to the combination

of the different mutations or to spontaneous mutations caused by the IDH^{R453C}_{TTG} as observed in *C. glutamicum* ITA10. In any case, we considered this strain unsuitable for future biotechnological processes. In addition, we evaluated the effect of different cultivation temperatures on IA production and found that growth and IA production of *C. glutamicum* ITA24_{ATG} was severely reduced at 37 °C, which we therefore did not test further for *C. glutamicum* ITA24_{GTG}. However, after lowering the temperature to 25 °C, the yield and titer produced by the same strain increased more than 50% compared to growth at 30 °C (Figure 3-9). Finally, during cultivation of *C. glutamicum* ITA24_{ATG} in nitrogen-limited CGXII medium supplemented with 20 g acetate L⁻¹ at 25 °C, the $Y_{P/S}$ was 116 ± 15 mmol mol⁻¹, which corresponds to 35% of the theoretical maximum and is the highest yield of IA produced from acetate as the sole carbon and energy source that has been reported to date. It is noteworthy that comparable yields of 107 ± 6 mmol mol⁻¹ and 113 ± 6 mmol mol⁻¹ were achieved by *C. glutamicum* ITA24_{GTG} during cultivation at 30 °C and 25 °C, respectively. However, especially when cultured at 25 °C, the growth of this strain was strongly impaired. Although we have shown that the addition of NaHCO₃ can positively affect the growth without affecting yield and titer, we did not further consider *C. glutamicum* ITA24_{GTG} to be suitable for future biotechnological processes, due to the severely impaired growth. In addition, it should be noted that the effect of lowered cultivation temperature on IA production was insignificant for the other strains tested, namely *C. glutamicum* ITA1, ITA15 and ITA19. Considering the results obtained for the CAD activity (see below), it can be assumed that in the latter strains the supply of *cis*-aconitate might limit the production of IA, whereas in *C. glutamicum* ITA24_{ATG}, which showed a strong temperature-dependent effect, the CAD activity is rate limiting. We found that during cultivation of *C. glutamicum* ITA24_{ATG} at 30 °C, CAD activity was highest at 57 ± 7 mU after 24 h and slightly decreased during the following cultivation. In contrast, when cultured at 25 °C, CAD activity was 71 ± 11 mU after 24 h and further increased to 82 ± 3 mU after 48 h of cultivation. Similar observations have been reported by Vuoristo et al. [284], who found 12-fold higher CAD activity in IA producing *E. coli* cultured at 30 °C, compared to cells cultured at 37 °C. Consistent with our results, several studies have shown that maintaining high CAD expression is a key element for adequate IA production [43, 131], which may be one reason why we found that IA production was almost abolished after the genomic integration of the *malEcad_{opt}* construct. Nevertheless, global analysis of transcriptome, metabolome and carbon flux needs to be performed in order to fully understand the positive effect of

Discussion

lowering the cultivation temperature during IA production with *C. glutamicum* from acetate. In addition, we observed that over 80 mM IA accumulated within *C. glutamicum* ITA24_{ATG} during IA production. These results are consistent with the concentrations of intracellular IA that have been measured during IA production from glucose [205]. However, it has to be considered that IA is a potent inhibitor of ICL in different species and also inhibits the purified ICL of *C. glutamicum* in a linear uncompetitive manner with a K_i of 5.05 μM [80]. Indeed, we observed that non-induced cultures had higher μ 's compared to cultures with induced IA production. Furthermore, we observed that μ of the wild-type strain was reduced to $0.26 \pm 0.01 \text{ h}^{-1}$ by the addition of 50 mM IA, and completely abolished by the addition of 250 mM IA, compared to $0.31 \pm 0.01 \text{ h}^{-1}$ without IA, during cultivation on acetate at 30 °C. During growth on glucose, μ was not affected by the addition of IA, although slightly reduced growth was observed after the addition of 250 mM, which could be attributed to the elevated potassium concentrations in these cultures. In fact, the wild-type strain *C. glutamicum* ATCC13032 has been shown to tolerate over 500 mM IA if cultured in minimal medium supplemented with glucose [280]. Nevertheless, our results suggest that the inhibitory effect of IA on ICL *in vivo* seemed to be less pronounced compared to the *in vitro* studies. In turn, inhibition of ICL by high intracellular IA concentrations may even promote IA production from acetate, similar to reduced ICL expression caused by deletion of *ramB*. On the other hand, elevated IA concentrations combined with reduced ICL expression could also prevent high IA titers by complete inhibition of ICL. This assumption is supported by the fact that the maximum titers achieved by *C. glutamicum* ITA24_{ATG} in preliminary fed-batch cultivations were reduced compared to the titers achieved with *C. glutamicum* ITA4 (unpublished results). Thus, optimizing the IA export might be a promising target to enable the production of higher titers, especially from non-glycolytic substrates. However, we showed that IA export could not be increased by the heterologous expression of the codon optimized IA exporters MfsA and Itp1 derived from *A. terreus* and *U. maydis*, respectively [296]. It has to be considered that IA has pK_s values of 3.84 and 5.55 [298], and should therefore be present in its dissociated form at an intracellular pH of 7.4 [89]. However, charged molecules can only cross the lipophilic membrane barrier with great difficulty if there is no suitable channel or transporter present to facilitate the export of the respective compound. The fact that IA can still be detected in the culture supernatant suggests that *C. glutamicum* might possess a transporter that can naturally export IA from the cell. The high intracellular IA concentrations, however, indicate that the respective

carrier is either poorly expressed or has only a low affinity for IA. The latter would imply that IA might be an off-target of the respective exporter. Based on the structural similarity to IA, to native dicarboxylic acids like succinate or 2-oxoglutarate, the transporters of these compounds are interesting candidates regarding this issue. Therefore, screening and targeted optimization of native transporters for IA export is a promising approach to ensure high IA export. In addition, it might be useful to screen for ICL variants that are insensitive to inhibition by IA. Both strategies could help to prevent adverse effects of IA in the cells and possibly increase the maximum titer of IA that can be achieved with *C. glutamicum* from acetate.

Eventually, we investigated the ability of *C. glutamicum* ITA24_{ATG} to produce IA from other potential carbon sources. First, we cultured the strain in CGXII medium containing 1 g urea and 40 g glucose L⁻¹, since glucose is still the substrate of choice in industrial IA production (see Chapter 1.4). After 72 h, 58% of the initial glucose was converted to 3.64 ± 0.00 g IA L⁻¹ with a yield of 191 ± 4 mmol mol⁻¹, which compared to *C. glutamicum* ITA1, represent an increase in titer and yield of 200% and 380%, respectively. Although, Otten *et al.* [205] reported a final titer of 7.8 g L⁻¹, a yield of 400 mmol mol⁻¹ and 67% of glucose converted by *C. glutamicum* (pEKEx2-*malEcad*_{opt}) strain with attenuated IDH activity, titer and yield only increased by 100% and 196% compared to *C. glutamicum* (pEKEx2-*malEcad*_{opt}) expressing the native *icd*. Thus, we conclude that the mutations introduced in *C. glutamicum* for optimized IA production from acetate in this work, can also be considered as highly beneficial for IA production from glucose. Next, we investigated ethanol as a potential substrate for IA production. Ethanol is another promising non-food derived feedstock that, similar to acetate, can be produced from biomass and C1 gases (see Chapter 1.2). In principle, ethanol follows the same metabolic pathways as acetate during its intracellular degradation. However, the regulation of the ethanol metabolism is somewhat different from the regulation of the acetate metabolism, as indicated by the catabolite repression that is observed during growth on different substrate mixtures containing ethanol [10]. In addition, the initial oxidation of ethanol to acetate generates an additional 2 mol of NADH + H⁺ per mol of ethanol converted [10]. In this study, yield and titer of IA produced from ethanol were strongly diminished compared to the production from acetate. Y_{P/S} was reduced to only 9% of the theoretical yield and the final titer was reduced to 1.1 ± 0.00 g IA L⁻¹. Furthermore, 10% of the initial ethanol remained in the culture supernatant after 72 h. Similar results were obtained for cultivations on substrate mixtures of 50% (mol/mol) of acetate

Discussion

and ethanol. The reason for the negative effect of ethanol on IA production remains unknown. On the one hand, additional redox equivalents generated by the oxidation of ethanol may overload the intracellular redox balance of the cell, leading to an inhibition of several enzymes in the TCA cycle [78]. On the other hand, the reduced IA production could be related to the distinct regulation of the ethanol and acetate metabolism as mentioned above, which could even be intensified by deletion of *ramB*. Again, these results highlight the complex interplay of the global network of transcription regulators in *C. glutamicum* [49, 50].

Finally, we evaluated IA production with *C. glutamicum* ITA24_{ATG} from PW. PW is a sidestream of fast pyrolysis that varies in its composition depending on the process flow of fast pyrolysis and the utilized biomass. Several of the formed carbon compounds, mainly furan- and phenol derivatives, have been found to strongly inhibit the growth of various microorganisms. In this study, we observed that the crude PW from the bioliq[®] process was toxic to *C. glutamicum* at concentrations of 2% in CGXII medium, which is consistent with other studies [147, 154]. Thus, we performed pretreatment of the PW to increase its biocompatibility during batch cultivations, according to the protocol that has been previously published by Kubisch and Ochsenreither [147], who reported growth of *A. oryzae* on 100% PW after the appropriate pretreatment. Since no acetate was lost during the preparation procedure, we reduced the initial PW concentration to 50% to obtain a starting concentration of approximately 20 g acetate L⁻¹. Additionally, we identified 1.83 ± 0.00 g propionate L⁻¹ in the culture that was completely metabolized by *C. glutamicum* throughout the cultivation. Interestingly, in contrast to acetate-grown cells, the lag-phase on PW was extended to over 24 h and 3.64 ± 1.02 g acetate L⁻¹ remained in the culture supernatant, but the final biomass concentration was still 25% higher at the end of the cultivation. The strain produced 3.38 ± 0.28 g IA L⁻¹ with an Y_{PS} of 104 ± 4 mmol mol⁻¹, corresponding to a theoretical yield of 31% calculated on the basis of the acetate consumed. On the other hand, only 15% of the total TOC in PW could be converted to IA within 72 h. This discrepancy is due to a large fraction of acetate and other unknown carbon compounds remaining in PW after the cultivation. The incomplete conversion of the TOC in the PW, especially acetate, may be related to the observed prolonged lag-phase and could possibly be overcome by longer cultivation times, higher biomass concentrations, or reduction of the lag-phase. The latter could be achieved by the addition of 50 mM NaHCO₃, as mentioned above. NaHCO₃ has been shown to support growth of *C. glutamicum* by increasing iron uptake and assimilation, and the same effect

has been reported for PCA [187]. The addition of PCA, however, resulted in lower yields and titers of IA caused by an unknown reason. In conclusion, we have shown that *C. glutamicum* ITA24_{ATG} produces the highest yields of IA from acetate as the sole carbon and energy source, reported to date. Furthermore, the strain is also capable of producing IA from acetate-containing sidestreams obtained during fast pyrolysis with similar yields as from pure acetate (Table 4-1).

4.3 Conclusion and Outlook

In this study, we tailored *C. glutamicum* for the efficient production of IA from the non-food carbon source acetate by rewiring the central carbon and nitrogen metabolism and optimizing the culture conditions. The maximum product yield that was achieved by *C. glutamicum* $\Delta ramB \Delta gdh$ IDH^{R453C} (pEKEx2-*malE*_{cad_{opt}}) (ITA24_{ATG}) was 35% of the theoretical maximum and is the highest IA yield reported to date, produced from acetate as sole carbon and energy source. The results demonstrate that *C. glutamicum* is a suitable host for the effective valorization of acetate, and that only minor engineering is required to redirect carbon flow within the cell. In addition, our findings provide evidence for an increased carbon flux through the glyoxylate shunt in IDH knockdown strains, and thus it represents a serious carbon sink within the TCA cycle alongside IDH. In contrast, reducing the flux into glycolysis and generally overexpressing of enzymes within the

Table 4-1: Final Conditions for IA Production in this Work.

The table shows the process conditions and production parameters of the final shaking flask cultivations with maximized yield and titer of IA produced from acetate and PW performed in this work.

Strain	<i>C. glutamicum</i> $\Delta ramB \Delta gdh$ IDH ^{R453C} (pEKEx2- <i>malE</i> _{cad_{opt}}) (<i>C. glutamicum</i> ITA24 _{ATG})	
Preculture medium	2YT (5 mL and 50 mL)	
Production medium	CGXII (50 mL)	
Cultivation temperature	25 °C	
Cultivation time	72 h	
Nitrogen concentration	0.5 g urea L ⁻¹ (C:N 40:1)	
Substrate concentration	20 g acetate L ⁻¹	50% processed pyrolysis water
Maximum biomass concentration	2.66 ± 0.10 g L ⁻¹	3.32 ± 0.11 g L ⁻¹
Final IA Titer	5.01 ± 0.67 g L ⁻¹	3.38 ± 0.28 g L ⁻¹
Yield	116 ± 15 mmol mol ⁻¹	104 ± 4 mmol mol ⁻¹
% of maximal yield	35%	31% (calculated for acetate)

Discussion

TCA cycle is not required to improve IA production. Our work also contributes to a better understanding of the effect of nitrogen limitation during compound production, which is likely based on increased 2-oxoglutarate levels and is not due to an altered transcriptome. These insights can be used for future metabolic engineering studies with *C. glutamicum*, but also with other microorganisms, for overproduction of desired compounds from acetate and other non-glycolytic substrates. It was not possible to achieve a suitable metabolization of acetol by *C. glutamicum* within the scope of this work. However, we have shown that the ability to utilize acetol as a substrate is strongly dependent on the co-substrate provided and the cultivation method. Furthermore, our results suggest that the predicted oxidoreductase encoded by cg3290 may have a key function in the acetol metabolism in *C. glutamicum*. Despite this, deletion or overexpression of individual enzymes or entire (predicted) pathways was not sufficient to achieve an increased acetol uptake. These findings provide valuable insights into the acetol metabolism and can help to achieve its effective metabolization by *C. glutamicum* in future studies. Finally, we demonstrated that our engineered production strain is capable of converting various carbon sources of processed PW into reasonable amounts of IA during batch fermentation. Therefore, our work is highly interesting from a bioeconomic point of view, as our results contribute to a resource-friendly conversion of biomass into valuable compounds for a bio-based chemical industry. Future studies will focus on further genetic optimization of the IA production by *C. glutamicum* strains and other possible hosts, by increasing their resistance towards acetate and increasing the carbon flux to the desired product, as suggested in the discussion section. The resulting strains will be used for the implementation and optimization of pathways allowing to the efficient production of other compounds from acetate. On the other hand, an optimized fed-batch process tailored for the large-scale production of valuable products from acetate by *C. glutamicum* and other microorganisms will be established. Engineered strains and tailored bio-processes will allow high volumetric production rates, improved yields, and increased final titers, to obtain biotechnological compound production of industrial relevance.

List of References

1. **Abe S., Takayama K.-I., and Kinoshita S. (1967)**, Taxonomical studies on glutamic acid-producing bacteria. *The Journal of General and Applied Microbiology*.
2. **Administration U. S. E. I. (2020)**, U.S. petroleum products consumption by source and sector. *Monthly Energy Review*.
3. **Ali M. A. and Kaneko T. (2022)**, High-performance BioNylons from itaconic and amino acids with pepsin degradability. *Advanced Sustainable Systems*.
4. **Ali M. A., Nag A., and Singh M. (2021)**, Microbial-derived polymers and their degradability behavior for future prospects. *Environmental and Agricultural Microbiology: Applications for Sustainability*.
5. **European Commission (2012)**, Innovating for sustainable growth: A bioeconomy for Europe. *Publication Office Directorate-General for Research Innovation*.
6. **German Energy Agency (2019)**, Feedstocks for the chemical industry. *Global Alliance Powerfuels*.
7. **Aouizerat T., Gutman I., Paz Y., Maeir A. M., Gadot Y., Gelman D., Szitenberg A., Drori E., Pinkus A., and Schoemann M. (2019)**, Isolation and characterization of live yeast cells from ancient vessels as a tool in bio-archaeology. *Mbio*.
8. **Ari Ş. and Arikan M. (2016)**, Next-generation sequencing: Advantages, disadvantages, and future. *Plant omics: Trends and applications, 1st ed. Springer*.
9. **Arndt A., Auchter M., Ishige T., Wendisch V., and Eikmanns B. (2008)**, Ethanol catabolism in *Corynebacterium glutamicum*. *Microbial Physiology*.
10. **Arndt A. and Eikmanns B. (2008)**, Regulation of carbon metabolism in *Corynebacterium glutamicum*. *Handbook of Corynebacterium, 1st ed. Caister Academic Press*.
11. **Arnold S., Moss K., Dahmen N., Henkel M., and Hausmann R. (2019)**, Pretreatment strategies for microbial valorization of bio-oil fractions produced by fast pyrolysis of ash-rich lignocellulosic biomass. *GCB Bioenergy*.
12. **Arnold S., Moss K., Henkel M., and Hausmann R. (2017)**, Biotechnological perspectives of pyrolysis oil for a bio-based economy. *Trends in Biotechnology*.
13. **Arnold S., Tews T., Kiefer M., Henkel M., and Hausmann R. (2019)**, Evaluation of small organic acids present in fast pyrolysis bio-oil from lignocellulose as feedstocks for bacterial bioconversion. *GCB Bioenergy*.
14. **Auchter M., Cramer A., Hüser A., Rückert C., Emer D., Schwarz P., Arndt A., Lange C., Kalinowski J., and Wendisch V. F. (2011)**, RamA and RamB are global transcriptional regulators in *Corynebacterium glutamicum* and control genes for enzymes of the central metabolism. *Journal of Biotechnology*.
15. **Bafana R. and Pandey R. A. (2018)**, New approaches for itaconic acid production: Bottlenecks and possible remedies. *Critical Reviews in Biotechnology*.
16. **Baldoma L. and Aguilar J. (1987)**, Involvement of lactaldehyde dehydrogenase in several metabolic pathways of *Escherichia coli* K12. *Journal of Biological Chemistry*.
17. **Balsari S., Dresser C., and Leaning J. (2020)**, Climate change, migration, and civil strife. *Current Environmental Health Reports*.

List of References

18. **Barabadi H. (2017)**, Nanobiotechnology: A promising scope of gold biotechnology. *Cellular and Molecular Biology*.
19. **Barcelos M. C., Lupki F. B., Campolina G. A., Nelson D. L., and Molina G. (2018)**, The colors of biotechnology: General overview and developments of white, green and blue areas. *FEMS Microbiology Letters*.
20. **Basaglia M., Favaro L., Torri C., and Casella S. (2021)**, Is pyrolysis bio-oil prone to microbial conversion into added-value products? *Renewable Energy*.
21. **Baumgart M. and Bott M. (2011)**, Biochemical characterisation of aconitase from *Corynebacterium glutamicum*. *Journal of Biotechnology*.
22. **Baumgart M., Mustafi N., Krug A., and Bott M. (2011)**, Deletion of the aconitase gene in *Corynebacterium glutamicum* causes strong selection pressure for secondary mutations inactivating citrate synthase. *Journal of Bacteriology*.
23. **Baumschabl M., Ata Ö., Mitic B. M., Lutz L., Gassler T., Troyer C., Hann S., and Mattanovich D. (2022)**, Conversion of CO₂ into organic acids by engineered autotrophic yeast. *Proceedings of the National Academy of Sciences*.
24. **Becker J. and Wittmann C. (2012)**, Bio-based production of chemicals, materials and fuels – *Corynebacterium glutamicum* as versatile cell factory. *Current Opinion in Biotechnology*.
25. **Beckers G., Bendt A. K., Krämer R., and Burkovski A. (2004)**, Molecular identification of the urea uptake system and transcriptional analysis of urea transporter- and urease-encoding genes in *Corynebacterium glutamicum*. *Journal of Bacteriology*.
26. **Beckers G., Nolden L., and Burkovski A. (2001)**, Glutamate synthase of *Corynebacterium glutamicum* is not essential for glutamate synthesis and is regulated by the nitrogen status. *Microbiology*.
27. **Beckers G., Strösser J., Hildebrandt U., Kalinowski J., Farwick M., Krämer R., and Burkovski A. (2005)**, Regulation of AmtR-controlled gene expression in *Corynebacterium glutamicum*: Mechanism and characterization of the AmtR regulon. *Molecular Microbiology*.
28. **Belitsky B. R., Gustafsson M., Sonenshein A. L., and Von Wachenfeldt C. (1997)**, An *lrp*-like gene of *Bacillus subtilis* involved in branched-chain amino acid transport. *Journal of Bacteriology*.
29. **Bendt A. K., Burkovski A., Schaffer S., Bott M., Farwick M., and Hermann T. (2003)**, Towards a phosphoproteome map of *Corynebacterium glutamicum*. *Proteomics: International Edition*.
30. **Binder J. B. and Raines R. T. (2010)**, Fermentable sugars by chemical hydrolysis of biomass. *Proceedings of the National Academy of Sciences*.
31. **Biryukova E., Arinbasarova A. Y., and Medentsev A. (2022)**, L-Lactate oxidase systems of microorganisms. *Microbiology*.
32. **Biswas B., Pandey N., Bisht Y., Singh R., Kumar J., and Bhaskar T. (2017)**, Pyrolysis of agricultural biomass residues: Comparative study of corn cob, wheat straw, rice straw and rice husk. *Bioresource Technology*.
33. **Black B. A., Michener W. E., Ramirez K. J., Bidy M. J., Knott B. C., Jarvis M. W., Olstad J., Mante O. D., Dayton D. C., and Beckham G. T. (2016)**, Aqueous stream characterization from biomass fast pyrolysis and catalytic fast pyrolysis. *ACS Sustainable Chemistry & Engineering*.
34. **Blazeck J., Miller J., Pan A., Gengler J., Holden C., Jamoussi M., and Alper H. S. (2014)**, Metabolic engineering of *Saccharomyces cerevisiae* for itaconic acid production. *Applied Microbiology and Biotechnology*.

35. **Blombach B., Arndt A., Auchter M., and Eikmanns B. J. (2009)**, L-Valine production during growth of pyruvate dehydrogenase complex-deficient *Corynebacterium glutamicum* in the presence of ethanol or by inactivation of the transcriptional regulator SugR. *Applied and Environmental Microbiology*.
36. **Blombach B., Buchholz J., Busche T., Kalinowski J., and Takors R. (2013)**, Impact of different CO₂/HCO₃⁻ levels on metabolism and regulation in *Corynebacterium glutamicum*. *Journal of Biotechnology*.
37. **Blombach B. and Eikmanns B. J. (2011)**, Current knowledge on isobutanol production with *Escherichia coli*, *Bacillus subtilis* and *Corynebacterium glutamicum*. *Bioengineered Bugs*.
38. **Blombach B., Grünberger A., Centler F., Wierckx N., and Schmid J. (2021)**, Exploiting unconventional prokaryotic hosts for industrial biotechnology. *Trends in Biotechnology*.
39. **Blombach B., Riester T., Wieschalka S., Ziert C., Youn J.-W., Wendisch V. F., and Eikmanns B. J. (2011)**, *Corynebacterium glutamicum* tailored for efficient isobutanol production. *Applied and Environmental Microbiology*.
40. **Blombach B., Schreiner M. E., Holátko J. i., Bartek T., Oldiges M., and Eikmanns B. J. (2007)**, L-Valine production with pyruvate dehydrogenase complex-deficient *Corynebacterium glutamicum*. *Applied and Environmental Microbiology*.
41. **Blombach B., Schreiner M. E., Moch M., Oldiges M., and Eikmanns B. J. (2007)**, Effect of pyruvate dehydrogenase complex deficiency on L-lysine production with *Corynebacterium glutamicum*. *Applied Microbiology and Biotechnology*.
42. **Boldt C., Teitelbaum L., and Patermann C. (2020)**, Global bioeconomy policy report (IV). *Secretariat of the Global Bioeconomy Summit*.
43. **Bonnarme P., Gillet B., Sepulchre A., Role C., Beloeil J., and Ducrocq C. (1995)**, Itaconate biosynthesis in *Aspergillus terreus*. *Journal of Bacteriology*.
44. **Boondaeng A., Suwanruji P., Vaithanomsat P., Apiwatanapiwat W., Trakunjae C., Janchai P., Apipatpapha T., Chanka N., and Chollakup R. (2021)**, Bio-synthesis of itaconic acid as an anti-crease finish for cellulosic fiber fabric. *RSC Advances*.
45. **Bott M. and Niebisch A. (2005)**, Respiratory energy metabolism. *Handbook of Corynebacterium glutamicum, 1st ed. CRC Press*.
46. **Bozell J. J. and Petersen G. R. (2010)**, Technology development for the production of biobased products from biorefinery carbohydrates – The US Department of Energy’s “Top 10” revisited. *Green Chemistry*.
47. **Bradford M. M. (1976)**, A rapid and sensitive method for the quantitation of microgram quantities of protein utilizing the principle of protein-dye binding. *Analytical Biochemistry*.
48. **Bridgwater A. V., Meier D., and Radlein D. (1999)**, An overview of fast pyrolysis of biomass. *Organic Geochemistry*.
49. **Brinkrolf K., Brune I., and Tauch A. (2007)**, The transcriptional regulatory network of the amino acid producer *Corynebacterium glutamicum*. *Journal of Biotechnology*.
50. **Brinkrolf K., Schröder J., Pühler A., and Tauch A. (2010)**, The transcriptional regulatory repertoire of *Corynebacterium glutamicum*: Reconstruction of the network controlling pathways involved in lysine and glutamate production. *Journal of Biotechnology*.
51. **Brosse N., Hussin M. H., and Rahim A. A. (2017)**, Organosolv processes. *Biorefineries*.

List of References

52. **Brown T., Jones-Mortimer M., and Kornberg H. (1977)**, The enzymic interconversion of acetate and acetyl-coenzyme A in *Escherichia coli*. *Microbiology*.
53. **Bruhn T., Loose C., Lucht W., Niebert K., Paulini I., Pilardeaux B., Rosol C., Schulz A., Schwägerl C., Springer A.-S., and Zalasiewicz J. (2018)**, Anthropozän. *Bundeszentrale für politische Bildung*.
54. **Buchholz J., Graf M., Blombach B., and Takors R. (2014)**, Improving the carbon balance of fermentations by total carbon analyses. *Biochemical Engineering Journal*.
55. **Bückle-Vallant V., Krause F. S., Messerschmidt S., and Eikmanns B. J. (2014)**, Metabolic engineering of *Corynebacterium glutamicum* for 2-ketoisocaproate production. *Applied Microbiology and Biotechnology*.
56. **Burkovski A. (2005)**, Nitrogen metabolism and its regulation. *Corynebacterium glutamicum*, 1st ed. *Springer*.
57. **Chen H. (2014)**, Chemical composition and structure of natural lignocellulose. *Biotechnology of lignocellulose*. *Springer*.
58. **Chen K., Hao S., Lyu H., Luo G., Zhang S., and Chen J. (2017)**, Ion exchange separation for recovery of monosaccharides, organic acids and phenolic compounds from hydrolysates of lignocellulosic biomass. *Separation and Purification Technology*.
59. **Chin T., Sano M., Takahashi T., Ohara H., and Aso Y. (2015)**, Photosynthetic production of itaconic acid in *Synechocystis sp.* PCC6803. *Journal of Biotechnology*.
60. **Claes W. A., Pühler A., and Kalinowski J. r. (2002)**, Identification of two *prpDBC* gene clusters in *Corynebacterium glutamicum* and their involvement in propionate degradation via the 2-methylcitrate cycle. *Journal of Bacteriology*.
61. **Cocaign M., Monnet C., and Lindley N. D. (1993)**, Batch kinetics of *Corynebacterium glutamicum* during growth on various carbon substrates: Use of substrate mixtures to localise metabolic bottlenecks. *Applied Microbiology and Biotechnology*.
62. **Collier M. and Webb R. H. (2021)**, Floods, droughts, and climate change. *University of Arizona Press*.
63. **Cooney C. L. (1983)**, Bioreactors: Design and operation. *Science*.
64. **Cordes T., Michelucci A., and Hiller K. (2015)**, Itaconic acid: The surprising role of an industrial compound as a mammalian antimicrobial metabolite. *Annual Review of Nutrition*.
65. **Cramer A., Gerstmeir R., Schaffer S., Bott M., and Eikmanns B. J. (2006)**, Identification of RamA, a novel LuxR-type transcriptional regulator of genes involved in acetate metabolism of *Corynebacterium glutamicum*. *Journal of Bacteriology*.
66. **Crippa M., Guizzardi D., Muntean M., Schaaf E., Solazzo E., Monforti-Ferrario F., Olivier J., and Vignati E. (2020)**, Fossil CO₂ emissions of all world countries. *European Commission*.
67. **Crutzen P. J. (2002)**, Geology of mankind. *Nature*.
68. **Cunha da Cruz J., Machado de Castro A., and Camporese Sérvulo E. F. (2018)**, World market and biotechnological production of itaconic acid. *3 Biotech*.
69. **Dahmen N., Abeln J., Eberhard M., Kolb T., Leibold H., Sauer J., Stapf D., and Zimmerlin B. (2017)**, The bioliq process for producing synthetic transportation fuels. *Wiley Interdisciplinary Reviews: Energy and Environment*.

70. **Dahmen N., Dinjus E., Kolb T., Arnold U., Leibold H., and Stahl R. (2012)**, State of the art of the bioliq[®] process for synthetic biofuels production. *Environmental Progress & Sustainable Energy*.
71. **Dahmen N., Henrich E., Dinjus E., and Weirich F. (2012)**, The bioliq[®] bioslurry gasification process for the production of biosynfuels, organic chemicals, and energy. *Energy, Sustainability and Society*.
72. **Diercks R., Arndt J. D., Freyer S., Geier R., Machhammer O., Schwartz J., and Volland M. (2008)**, Raw material changes in the chemical industry. *Chemical Engineering & Technology: Industrial Chemistry-Plant Equipment-Process Engineering-Biotechnology*.
73. **Dietz T., Börner J., Förster J. J., and Von Braun J. (2018)**, Governance of the bioeconomy: A global comparative study of national bioeconomy strategies. *Sustainability*.
74. **Dörsam S., Kirchoff J., Bigalke M., Dahmen N., Syldatk C., and Ochsenreither K. (2016)**, Evaluation of pyrolysis oil as carbon source for fungal fermentation. *Frontiers in Microbiology*.
75. **Dwiarti L., Yamane K., Yamatani H., Kahar P., and Okabe M. (2002)**, Purification and characterization of *cis*-aconitic acid decarboxylase from *Aspergillus terreus* TN484-M1. *Journal of Bioscience and Bioengineering*.
76. **Ebbighausen H., Weil B., and Krämer R. (1989)**, Transport of branched-chain amino acids in *Corynebacterium glutamicum*. *Archives of Microbiology*.
77. **Ebbighausen H., Weil B., and Krämer R. (1991)**, Carrier-mediated acetate uptake in *Corynebacterium glutamicum*. *Archives of Microbiology*.
78. **Eikmanns B. (2004)**, Central metabolism: Tricarboxylic acid cycle and anaplerotic reactions. *Handbook of Corynebacterium glutamicum, 1st ed. CRC Press*.
79. **Eikmanns B. J., Metzger M., Reinscheid D., Kircher M., and Sahn H. (1991)**, Amplification of three threonine biosynthesis genes in *Corynebacterium glutamicum* and its influence on carbon flux in different strains. *Applied Microbiology and Biotechnology*.
80. **Eikmanns B. J., Rittmann D., and Sahn H. (1995)**, Cloning, sequence analysis, expression, and inactivation of the *Corynebacterium glutamicum* *icd* gene encoding isocitrate dehydrogenase and biochemical characterization of the enzyme. *Journal of Bacteriology*.
81. **Eikmanns B. J., Thum-Schmitz N., Eggeling L., Lüdtke K.-U., and Sahn H. (1994)**, Nucleotide sequence, expression and transcriptional analysis of the *Corynebacterium glutamicum* *gltA* gene encoding citrate synthase. *Microbiology*.
82. **Ejiofor A. O. (2016)**, Insect biotechnology. *Short Views on Insect Genomics and Proteomics, 1st ed. Springer*.
83. **El-Imam A. A. and Du C. (2014)**, Fermentative itaconic acid production. *Journal of Biodiversity, Bioprospecting and Development*.
84. **Elliott D. C., Hart T. R., Neuenschwander G. G., Rotness L. J., and Zacher A. H. (2009)**, Catalytic hydroprocessing of biomass fast pyrolysis bio-oil to produce hydrocarbon products. *Environmental Progress & Sustainable Energy*.
85. **Elmore J. R., Dexter G. N., Salvachúa D., Martinez-Baird J., Hatmaker E. A., Huenemann J. D., Klingeman D. M., Peabody G. L., Peterson D. J., and Singer C. (2021)**, Production of itaconic acid from alkali pretreated lignin by dynamic two stage bioconversion. *Nature Communications*.
86. **Engels V., Lindner S. N., and Wendisch V. F. (2008)**, The global repressor SugR controls expression of genes of glycolysis and of the L-lactate dehydrogenase LdhA in *Corynebacterium glutamicum*. *Journal of Bacteriology*.

List of References

87. **Engels V. and Wendisch V. F. (2007)**, The DeoR-type regulator SugR represses expression of *ptsG* in *Corynebacterium glutamicum*. *Journal of Bacteriology*.
88. **Feng J., Li C., He H., Xu S., Wang X., and Chen K. (2022)**, Construction of cell factory through combinatorial metabolic engineering for efficient production of itaconic acid. *Microbial Cell Factories*.
89. **Follmann M., Ochrombel I., Krämer R., Trötschel C., Poetsch A., Rückert C., Hüser A., Persicke M., Seiferling D., and Kalinowski J. (2009)**, Functional genomics of pH homeostasis in *Corynebacterium glutamicum* revealed novel links between pH response, oxidative stress, iron homeostasis and methionine synthesis. *BMC Genomics*.
90. **Freudl R. (2017)**, Beyond amino acids: Use of the *Corynebacterium glutamicum* cell factory for the secretion of heterologous proteins. *Journal of Biotechnology*.
91. **Gavrilescu M. and Chisti Y. (2005)**, Biotechnology – A sustainable alternative for chemical industry. *Biotechnology Advances*.
92. **Gellerstedt G. and Lindfors E.-L. (1984)**, Structural changes in lignin during kraft pulping. *Holzforschung*.
93. **Gerstmeir R., Cramer A., Dangel P., Schaffer S., and Eikmanns B. J. (2004)**, RamB, a novel transcriptional regulator of genes involved in acetate metabolism of *Corynebacterium glutamicum*. *Journal of Bacteriology*.
94. **Gibson D. G. (2011)**, Enzymatic assembly of overlapping DNA fragments. *Methods in Enzymology*.
95. **Gierer J. (1980)**, Chemical aspects of kraft pulping. *Wood Science and Technology*.
96. **Gong G., Wu B., Liu L., Li J., Zhu Q., He M., and Hu G. (2022)**, Metabolic engineering using acetate as a promising building block for the production of bio-based chemicals. *Engineering Microbiology*.
97. **Gong Z., Wang X., Yuan W., Wang Y., Zhou W., Wang G., and Liu Y. (2020)**, Fed-batch enzymatic hydrolysis of alkaline organosolv-pretreated corn stover facilitating high concentrations and yields of fermentable sugars for microbial lipid production. *Biotechnology for Biofuels*.
98. **Gopaliya D., Kumar V., and Khare S. K. (2021)**, Recent advances in itaconic acid production from microbial cell factories. *Biocatalysis and Agricultural Biotechnology*.
99. **Green M. R. and Sambrook J. (2012)**, Molecular cloning: A laboratory manual. 4th ed. Cold Spring Harbor Laboratory Press.
100. **Gustafson R. R., Sleicher C. A., McKean W. T., and Finlayson B. A. (1983)**, Theoretical model of the kraft pulping process. *Industrial & Engineering Chemistry Process Design and Development*.
101. **Hanahan D. (1983)**, Studies on transformation of *Escherichia coli* with plasmids. *Journal of Molecular Biology*.
102. **Hänbller E. and Burkovski A. (2008)**, Molecular mechanisms of nitrogen control in *corynebacteria*. 1st ed. Caister Academic Press.
103. **Harder B. J., Bettenbrock K., and Klamt S. (2018)**, Temperature-dependent dynamic control of the TCA cycle increases volumetric productivity of itaconic acid production by *Escherichia coli*. *Biotechnology and Bioengineering*.

104. **Hayashi M., Mizoguchi H., Shiraishi N., Obayashi M., Nakagawa S., Imai J.-i., Watanabe S., Ota T., and Ikeda M. (2002)**, Transcriptome analysis of acetate metabolism in *Corynebacterium glutamicum* using a newly developed metabolic array. *Bioscience, Biotechnology, and Biochemistry*.
105. **Hays S. M. and Mazzola V. (1991)**, Good breeding: From simple beginnings to genetic engineering. *Agricultural Research*.
106. **Heffernan J. K., Valgepea K., de Souza Pinto Lemgruber R., Casini I., Plan M., Tappel R., Simpson S. D., Köpke M., Nielsen L. K., and Marcellin E. (2020)**, Enhancing CO₂-valorization using *Clostridium autoethanogenum* for sustainable fuel and chemicals production. *Frontiers in Bioengineering and Biotechnology*.
107. **Hosseinpour Tehrani H., Becker J., Bator I., Saur K., Meyer S., Rodrigues Lóia A. C., Blank L. M., and Wierckx N. (2019)**, Integrated strain- and process design enable production of 220 g L⁻¹ itaconic acid with *Ustilago maydis*. *Biotechnology for Biofuels*.
108. **Hsiang C.-C., Diankristanti P. A., Tan S.-I., Ke Y.-C., Chen Y.-C., Effendi S. S. W., and Ng I.-S. (2022)**, Tailoring key enzymes for renewable and high-level itaconic acid production using genetic *Escherichia coli* via whole-cell bioconversion. *Enzyme and Microbial Technology*.
109. **Iacometti C., Marx K., Hönick M., Biletskaia V., Schulz-Mirbach H., Dronsella B., Satanowski A., Delmas V. A., Berger A., and Dubois I. (2022)**, Activating silent glycolysis bypasses in *Escherichia coli*. *BioDesign Research*.
110. **Ibarra-Montaña E. L., Rodríguez-Laguna N., Sánchez-Hernández A., and Rojas-Hernández A. (2015)**, Determination of pKa values for acrylic, methacrylic and itaconic acids by ¹H and ¹³C NMR in deuterated water. *Journal of Applied Solution Chemistry and Modeling*.
111. **Ikeda M. (2012)**, Sugar transport systems in *Corynebacterium glutamicum*: Features and applications to strain development. *Applied Microbiology and Biotechnology*.
112. **Ishige T., Krause M., Bott M., Wendisch V. F., and Sahn H. (2003)**, The phosphate starvation stimulon of *Corynebacterium glutamicum* determined by DNA microarray analyses. *Journal of Bacteriology*.
113. **Jakoby M., Nolden L., Meier-Wagner J., Krämer R., and Burkovski A. (2000)**, AmtR, a global repressor in the nitrogen regulation system of *Corynebacterium glutamicum*. *Molecular Microbiology*.
114. **Jarboe L. R. (2011)**, YqhD: A broad-substrate range aldehyde reductase with various applications in production of biorenewable fuels and chemicals. *Applied Microbiology and Biotechnology*.
115. **Jarboe L. R., Wen Z., Choi D., and Brown R. C. (2011)**, Hybrid thermochemical processing: Fermentation of pyrolysis-derived bio-oil. *Applied Microbiology and Biotechnology*.
116. **Jarosz L. (2009)**, Energy, climate change, meat, and markets: Mapping the coordinates of the current world food crisis. *Geography compass*.
117. **Jeudy S., Monchois V., Maza C., Claverie J. M., and Abergel C. (2006)**, Crystal structure of *Escherichia coli* DkgA, a broad-specificity aldo-keto reductase. *Proteins: Structure, Function, and Bioinformatics*.
118. **Jiang T., Gao C., Ma C., and Xu P. (2014)**, Microbial lactate utilization: Enzymes, pathogenesis, and regulation. *Trends in microbiology*.
119. **Jiménez L., De la Torre M., Maestre F., Ferrer J., and Pérez I. (1997)**, Organosolv pulping of wheat straw by use of phenol. *Bioresource Technology*.

List of References

120. **Jolkver E., Emer D., Ballan S., Krämer R., Eikmanns B. J., and Marin K. (2009)**, Identification and characterization of a bacterial transport system for the uptake of pyruvate, propionate, and acetate in *Corynebacterium glutamicum*. *Journal of Bacteriology*.
121. **Joo Y. C., You S. K., Shin S. K., Ko Y. J., Jung K. H., Sim S. A., and Han S. O. (2017)**, Bio-based production of dimethyl itaconate from rice wine waste-derived itaconic acid. *Biotechnology Journal*.
122. **Kafarski P. (2012)**, Rainbow code of biotechnology. *Chemik*.
123. **Kalinowski J. (2005)**, The genomes of amino acid-producing *Corynebacteria*. *Handbook of Corynebacterium glutamicum, 1st ed.* Taylor & Francis.
124. **Kato O., Youn J.-W., Stansen K. C., Matsui D., Oikawa T., and Wendisch V. F. (2010)**, Quinone-dependent D-lactate dehydrogenase Dld (Cg1027) is essential for growth of *Corynebacterium glutamicum* on D-lactate. *BMC microbiology*.
125. **Katz S. H. (2008)**, Food to fuel and the world food crisis. *Anthropology Today*.
126. **Kholy E. R. B.-E., Eikmanns B. J., Gutmann M., and Sahn H. (1993)**, Glutamate dehydrogenase is not essential for glutamate formation by *Corynebacterium glutamicum*. *Applied and Environmental Microbiology*.
127. **Kiefer D., Merkel M., Lilge L., Hausmann R., and Henkel M. (2021)**, High cell density cultivation of *Corynebacterium glutamicum* on bio-based lignocellulosic acetate using pH-coupled online feeding control. *Bioresource Technology*.
128. **Kiefer D., Merkel M., Lilge L., Henkel M., and Hausmann R. (2021)**, From acetate to bio-based products: Underexploited potential for industrial biotechnology. *Trends in Biotechnology*.
129. **Kiefer D., Tadele L. R., Lilge L., Henkel M., and Hausmann R. (2022)**, High-level recombinant protein production with *Corynebacterium glutamicum* using acetate as carbon source. *Microbial Biotechnology*.
130. **Kim H.-J., Kim T.-H., Kim Y., and Lee H.-S. (2004)**, Identification and characterization of *glxR*, a gene involved in regulation of glyoxylate bypass in *Corynebacterium glutamicum*. *Journal of Bacteriology*.
131. **Kim J., Seo H.-M., Bhatia S. K., Song H.-S., Kim J.-H., Jeon J.-M., Choi K.-Y., Kim W., Yoon J.-J., and Kim Y.-G. (2017)**, Production of itaconate by whole-cell bioconversion of citrate mediated by expression of multiple *cis*-aconitate decarboxylase (*cadA*) genes in *Escherichia coli*. *Scientific Reports*.
132. **Kimura E. (2003)**, Metabolic engineering of glutamate production. *Microbial Production of L-Amino Acids*.
133. **Kinoshita S., Udaka S., and Shimono M. (1957)**, Studies on the amino acid fermentation Part I. Production of L-glutamic acid by various microorganisms. *The Journal of General and Applied Microbiology*.
134. **Klement T. and Büchs J. (2013)**, Itaconic acid – A biotechnological process in change. *Bioresource Technology*.
135. **Klement T., Milker S., Jäger G., Grande P. M., Domínguez de María P., and Büchs J. (2012)**, Biomass pretreatment affects *Ustilago maydis* in producing itaconic acid. *Microbial Cell Factories*.
136. **Klingenberg M. and Pfaff E. (1967)**, Means of terminating reactions. *Methods in enzymology*.

137. **Klinke H. B., Thomsen A., and Ahring B. K. (2004)**, Inhibition of ethanol-producing yeast and bacteria by degradation products produced during pre-treatment of biomass. *Applied Microbiology and Biotechnology*.
138. **Ko J., Kim I., Yoo S., Min B., Kim K., and Park C. (2005)**, Conversion of methylglyoxal to acetol by *Escherichia coli* aldo-keto reductases. *Journal of Bacteriology*.
139. **Kormann M. (2016)**, Modern tools for genetic engineering. *1st ed. IntechOpen*.
140. **Kotrbova-Kozak A., Kotrba P., Inui M., Sajdok J., and Yukawa H. (2007)**, Transcriptionally regulated *adhA* gene encodes alcohol dehydrogenase required for ethanol and n-propanol utilization in *Corynebacterium glutamicum* R. *Applied Microbiology and Biotechnology*.
141. **Krämer R. and Lambert C. (1990)**, Uptake of glutamate in *Corynebacterium glutamicum*: 2. Evidence for a primary active transport system. *European Journal of Biochemistry*.
142. **Krause F. S., Blombach B., and Eikmanns B. J. (2010)**, Metabolic engineering of *Corynebacterium glutamicum* for 2-ketoisovalerate production. *Applied and Environmental Microbiology*.
143. **Krug A., Wendisch V. F., and Bott M. (2005)**, Identification of AcnR, a TetR-type repressor of the aconitase gene *acn* in *Corynebacterium glutamicum*. *Journal of Biological Chemistry*.
144. **Krull S., Eidt L., Hevekerl A., Kuenz A., and Prüße U. (2017)**, Itaconic acid production from wheat chaff by *Aspergillus terreus*. *Process Biochemistry*.
145. **Krull S., Hevekerl A., Kuenz A., and Prüße U. (2017)**, Process development of itaconic acid production by a natural wild type strain of *Aspergillus terreus* to reach industrially relevant final titers. *Applied Microbiology and Biotechnology*.
146. **Kubisch C., Kövilein A., Aliyu H., and Ochsenreither K. (2022)**, RNA-Seq based transcriptome analysis of *Aspergillus oryzae* DSM 1863 grown on glucose, acetate and an aqueous condensate from the fast pyrolysis of wheat straw. *Journal of Fungi*.
147. **Kubisch C. and Ochsenreither K. (2022)**, Detoxification of a pyrolytic aqueous condensate from wheat straw for utilization as substrate in *Aspergillus oryzae* DSM 1863 cultivations. *Biotechnology for Biofuels and Bioproducts*.
148. **Kubisch C. and Ochsenreither K. (2022)**, Valorization of a pyrolytic aqueous condensate and its main components for L-malic acid production with *Aspergillus oryzae* DSM 1863. *Fermentation*.
149. **Kuenz A. and Krull S. (2018)**, Biotechnological production of itaconic acid – Things you have to know. *Applied Microbiology and Biotechnology*.
150. **Kumar S., Krishnan S., Samal S. K., Mohanty S., and Nayak S. K. (2017)**, Itaconic acid used as a versatile building block for the synthesis of renewable resource-based resins and polyesters for future prospective: A review. *Polymer International*.
151. **Kumar S. S., Swapna T., and Sabu A. (2018)**, Coffee husk: A potential agro-industrial residue for bioprocess. *Waste to Wealth. Springer*.
152. **Kunst F., Ogasawara N., Moszer I., Albertini A., Alloni G., Azevedo V., Bertero M., Bessières P., Bolotin A., and Borchert S. (1997)**, The complete genome sequence of the Gram-positive bacterium *Bacillus subtilis*. *Nature*.
153. **Kutscha R. and Pflügl S. (2020)**, Microbial upgrading of acetate into value-added products – Examining microbial diversity, bioenergetic constraints and metabolic engineering approaches. *International Journal of Molecular Sciences*.

List of References

154. **Lange J. (2018)**, Valorization of biorefinery side streams and systemic analysis of the adaptation towards anaerobiosis-studies with *Corynebacterium glutamicum*. *Institute of Biochemical Engineering, University of Stuttgart*.
155. **Lange J., Müller F., Bernecker K., Dahmen N., Takors R., and Blombach B. (2017)**, Valorization of pyrolysis water: A biorefinery side stream, for 1,2-propanediol production with engineered *Corynebacterium glutamicum*. *Biotechnology for Biofuels*.
156. **Lange J., Müller F., Takors R., and Blombach B. (2018)**, Harnessing novel chromosomal integration loci to utilize an organosolv-derived hemicellulose fraction for isobutanol production with engineered *Corynebacterium glutamicum*. *Microbial Biotechnology*.
157. **Lashof D. A. and Ahuja D. R. (1990)**, Relative contributions of greenhouse gas emissions to global warming. *Nature*.
158. **Lee C., Kim I., Lee J., Lee K.-L., Min B., and Park C. (2010)**, Transcriptional activation of the aldehyde reductase YqhD by YqhC and its implication in glyoxal metabolism of *Escherichia coli* K-12. *Journal of Bacteriology*.
159. **Lee J.-Y., Na Y.-A., Kim E., Lee H.-S., and Kim P. (2016)**, The actinobacterium *Corynebacterium glutamicum*, an industrial workhorse. *Journal of Microbiology and Biotechnology*.
160. **Lee R. P. (2019)**, Alternative carbon feedstock for the chemical industry? – Assessing the challenges posed by the human dimension in the carbon transition. *Journal of Cleaner Production*.
161. **Li F.-L., Zhou Q., Wei W., Gao J., and Zhang Y.-W. (2019)**, Switching the substrate specificity from NADH to NADPH by a single mutation of NADH oxidase from *Lactobacillus rhamnosus*. *International Journal of Biological Macromolecules*.
162. **Li H., Xu Q., Xue H., and Yan Y. (2009)**, Catalytic reforming of the aqueous phase derived from fast-pyrolysis of biomass. *Renewable Energy*.
163. **Li N., Zeng W., Zhou J., and Xu S. (2022)**, O-Acetyl-L-homoserine production enhanced by pathway strengthening and acetate supplementation in *Corynebacterium glutamicum*. *Biotechnology for Biofuels and Bioproducts*.
164. **Lian J., Garcia-Perez M., Coates R., Wu H., and Chen S. (2012)**, Yeast fermentation of carboxylic acids obtained from pyrolytic aqueous phases for lipid production. *Bioresource Technology*.
165. **Liebl W. (2005)**, *Corynebacterium* taxonomy. *Handbook of Corynebacterium glutamicum*., 1st ed. *CRC Press*.
166. **Liebl W., Klammer R., and Schleifer K.-H. (1989)**, Requirement of chelating compounds for the growth of *Corynebacterium glutamicum* in synthetic media. *Applied Microbiology and Biotechnology*.
167. **Liew F. E., Nogle R., Abdalla T., Rasor B. J., Canter C., Jensen R. O., Wang L., Strutz J., Chirania P., and De Tissera S. (2022)**, Carbon-negative production of acetone and isopropanol by gas fermentation at industrial pilot scale. *Nature Biotechnology*.
168. **Liu Y.-B., Chen C., Chaudhry M. T., Si M.-R., Zhang L., Wang Y., and Shen X.-H. (2014)**, Enhancing *Corynebacterium glutamicum* robustness by over-expressing a gene, *mshA*, for mycothiol glycosyltransferase. *Biotechnology Letters*.
169. **Liu Y., Liu G., Zhang J., Balan V., and Bao J. (2020)**, Itaconic acid fermentation using activated charcoal-treated corn stover hydrolysate and process evaluation based on Aspen plus model. *Biomass Conversion and Biorefinery*.

170. **Lloyd S., Lauble H., Prasad G., and Stout C. (1999)**, The mechanism of aconitase: 1.8 Å resolution crystal structure of the S642A:citrate complex. *Protein Science*.
171. **Lopez de Felipe F. and Hugenholtz J. (2001)**, Purification and characterisation of the water forming NADH-oxidase from *Lactococcus lactis*. *International Dairy Journal*.
172. **Ma S., Liu X., Jiang Y., Tang Z., Zhang C., and Zhu J. (2013)**, Bio-based epoxy resin from itaconic acid and its thermosets cured with anhydride and comonomers. *Green Chemistry*.
173. **Mai C., Kües U., and Militz H. (2004)**, Biotechnology in the wood industry. *Applied Microbiology and Biotechnology*.
174. **Mandel M. and Higa A. (1970)**, Calcium-dependent bacteriophage DNA infection. *Journal of Molecular Biology*.
175. **Marvel C. and SHEPHERD T. H. (1959)**, Polymerization reactions of itaconic acid and some of its derivatives. *The Journal of Organic Chemistry*.
176. **McDonough T. J. (1992)**, The chemistry of organosolv delignification. *Technical Paper*.
177. **McMichael P. (2009)**, A food regime analysis of the ‘world food crisis’. *Agriculture and Human Values*.
178. **Meier-Wagner J., Nolden L., Jakoby M., Siewe R., Krämer R., and Burkovski A. (2001)**, Multiplicity of ammonium uptake systems in *Corynebacterium glutamicum*: Role of Amt and AmtB. *Microbiology*.
179. **Melin K., Nieminen H., Klüh D., Laari A., Koiranen T., and Gaderer M. (2022)**, Techno-economic evaluation of novel hybrid biomass and electricity-based ethanol fuel production. *Frontiers in Energy Research*.
180. **Merkel M., Kiefer D., Schmollack M., Blombach B., Lilge L., Henkel M., and Hausmann R. (2022)**, Acetate-based production of itaconic acid with *Corynebacterium glutamicum* using an integrated pH-coupled feeding control. *Bioresource Technology*.
181. **Michel A., Koch-Koerfges A., Krumbach K., Brocker M., and Bott M. (2015)**, Anaerobic growth of *Corynebacterium glutamicum* via mixed-acid fermentation. *Applied and Environmental Microbiology*.
182. **Misra A. K. (2014)**, Climate change and challenges of water and food security. *International Journal of Sustainable Built Environment*.
183. **Molenaar D., van der Rest M. E., and Petrović S. (1998)**, Biochemical and genetic characterization of the membrane-associated malate dehydrogenase (acceptor) from *Corynebacterium glutamicum*. *European Journal of Biochemistry*.
184. **Molino A., Chianese S., and Musmarra D. (2016)**, Biomass gasification technology: The state of the art overview. *Journal of Energy Chemistry*.
185. **Molitor B., Richter H., Martin M. E., Jensen R. O., Juminaga A., Mihalcea C., and Angenent L. T. (2016)**, Carbon recovery by fermentation of CO₂-rich off gases—turning steel mills into biorefineries. *Bioresource Technology*.
186. **Muffler K. and Ulber R. (2008)**, Use of renewable raw materials in the chemical industry – Beyond sugar and starch. *Chemical Engineering & Technology: Industrial Chemistry-Plant Equipment-Process Engineering-Biotechnology*.
187. **Müller F., Rapp J., Hacker A.-L., Feith A., Takors R., and Blombach B. (2020)**, CO₂/HCO₃⁻ accelerates iron reduction through phenolic compounds. *Mbio*.

List of References

188. **Müller T., Strösser J., Buchinger S., Nolden L., Wirtz A., Krämer R., and Burkovski A. (2006)**, Mutation-induced metabolite pool alterations in *Corynebacterium glutamicum*: Towards the identification of nitrogen control signals. *Journal of Biotechnology*.
189. **Muscat A., De Olde E., de Boer I. J., and Ripoll-Bosch R. (2020)**, The battle for biomass: A systematic review of food-feed-fuel competition. *Global Food Security*.
190. **Mustafa G., Arshad M., Bano I., and Abbas M. (2020)**, Biotechnological applications of sugarcane bagasse and sugar beet molasses. *Biomass Conversion and Biorefinery*.
191. **Narayanaswamy R. and Torchilin V. P. (2019)**, Hydrogels and their applications in targeted drug delivery. *Molecules*.
192. **Nešvera J. and Pátek M. (2011)**, Tools for genetic manipulations in *Corynebacterium glutamicum* and their applications. *Applied Microbiology and Biotechnology*.
193. **Niebel A., Funke A., Pfitzer C., Dahmen N., Weih N., Richter D., and Zimmerlin B. (2021)**, Fast pyrolysis of wheat straw – Improvements of operational stability in 10 years of bioliq pilot plant operation. *Energy & Fuels*.
194. **Niebisch A., Kabus A., Schultz C., Weil B., and Bott M. (2006)**, *Corynebacterial* protein kinase G controls 2-oxoglutarate dehydrogenase activity via the phosphorylation status of the OdhI protein. *Journal of Biological Chemistry*.
195. **Nishimura T., Vertès A. A., Shinoda Y., Inui M., and Yukawa H. (2007)**, Anaerobic growth of *Corynebacterium glutamicum* using nitrate as a terminal electron acceptor. *Applied Microbiology and Biotechnology*.
196. **Noh M. H., Lim H. G., Woo S. H., Song J., and Jung G. Y. (2018)**, Production of itaconic acid from acetate by engineering acid-tolerant *Escherichia coli* W. *Biotechnology and Bioengineering*.
197. **Nolden L., Beckers G., Möckel B., Pfefferle W., Nampoothiri K. M., Krämer R., and Burkovski A. (2000)**, Urease of *Corynebacterium glutamicum*: Organization of corresponding genes and investigation of activity. *FEMS Microbiology Letters*.
198. **Nolden L., Farwick M., Krämer R., and Burkovski A. (2001)**, Glutamine synthetases of *Corynebacterium glutamicum*: Transcriptional control and regulation of activity. *FEMS Microbiology Letters*.
199. **Nolden L., Ngouoto-Nkili C. E., Bendt A. K., Krämer R., and Burkovski A. (2001)**, Sensing nitrogen limitation in *Corynebacterium glutamicum*: The role of *glnK* and *glnD*. *Molecular Microbiology*.
200. **Novak K. and Pflügl S. (2018)**, Towards biobased industry: Acetate as a promising feedstock to enhance the potential of microbial cell factories. *FEMS Microbiology Letters*.
201. **Oasmaa A., Lehto J., Solantausta Y., and Kallio S. (2021)**, Historical review on VTT fast pyrolysis bio-oil production and upgrading. *Energy & Fuels*.
202. **Oasmaa A., Solantausta Y., Arpiainen V., Kuoppala E., and Sipila K. (2010)**, Fast pyrolysis bio-oils from wood and agricultural residues. *Energy & Fuels*.
203. **Okabe M., Lies D., Kanamasa S., and Park E. Y. (2009)**, Biotechnological production of itaconic acid and its biosynthesis in *Aspergillus terreus*. *Applied Microbiology and Biotechnology*.
204. **Okeke B. and Obi S. (1994)**, Lignocellulose and sugar compositions of some agro-waste materials. *Bioresource Technology*.
205. **Otten A., Brocker M., and Bott M. (2015)**, Metabolic engineering of *Corynebacterium glutamicum* for the production of itaconate. *Metabolic Engineering*.

206. **Ozcan N., Ejsing C. S., Shevchenko A., Lipski A., Morbach S., and Krämer R. (2007)**, Osmolality, temperature, and membrane lipid composition modulate the activity of betaine transporter BetP in *Corynebacterium glutamicum*. *Journal of Bacteriology*.
207. **Paegle L. and Ruklisha M. (2003)**, Lysine synthesis control in *Corynebacterium glutamicum* RC115 in mixed substrate (glucose-acetate) medium. *Journal of Biotechnology*.
208. **Pandey A., Sirohi R., Larroche C., and Taherzadeh M. (2022)**, Current developments in biotechnology and bioengineering: Advances in bioprocess engineering. *Elsevier*.
209. **Pandey A., Soccol C. R., Nigam P., and Soccol V. T. (2000)**, Biotechnological potential of agro-industrial residues. I: Sugarcane bagasse. *Bioresource Technology*.
210. **Park S.-Y., Moon M.-W., Subhadra B., and Lee J.-K. (2010)**, Functional characterization of the *glxR* deletion mutant of *Corynebacterium glutamicum* ATCC 13032: Involvement of GlxR in acetate metabolism and carbon catabolite repression. *FEMS Microbiology Letters*.
211. **Parku G. K., Krutof A., Funke A., Richter D., and Dahmen N. (2023)**, Using fractional condensation to optimize aqueous pyrolysis condensates for downstream microbial conversion. *Industrial & engineering chemistry research*.
212. **Pelechova J., Smekal F., Koura V., Plachý J., and Krumphanzl V. (1980)**, Biosynthesis of L-lysine in *Corynebacterium glutamicum* on sucrose, ethanol and acetic acid. *Folia Microbiologica*.
213. **Pfeifer E., Gätgens C., Polen T., and Frunzke J. (2017)**, Adaptive laboratory evolution of *Corynebacterium glutamicum* towards higher growth rates on glucose minimal medium. *Scientific Reports*.
214. **Pfitzer C., Dahmen N., Troger N., Weirich F., Sauer J., Gunther A., and Muller-Hagedorn M. (2016)**, Fast pyrolysis of wheat straw in the bioliq pilot plant. *Energy & Fuels*.
215. **Piguet E., Pécoud A., and De Guchteneire P. (2011)**, Migration and climate change: An overview. *Refugee Survey Quarterly*.
216. **Pimentel D., Marklein A., Toth M. A., Karpoff M. N., Paul G. S., McCormack R., Kyriazis J., and Krueger T. (2009)**, Food versus biofuels: Environmental and economic costs. *Human Ecology*.
217. **Plassmeier J., Barsch A., Persicke M., Niehaus K., and Kalinowski J. (2007)**, Investigation of central carbon metabolism and the 2-methylcitrate cycle in *Corynebacterium glutamicum* by metabolic profiling using gas chromatography-mass spectrometry. *Journal of Biotechnology*.
218. **Prell C., Busche T., Rückert C., Nolte L., Brandenbusch C., and Wendisch V. F. (2021)**, Adaptive laboratory evolution accelerated glutarate production by *Corynebacterium glutamicum*. *Microbial Cell Factories*.
219. **Rehm N., Buchinger S., Strösser J., Dotzauer A., Walter B., Hans S., Bathe B., Schomburg D., Krämer R., and Burkovski A. (2010)**, Impact of adenylyltransferase GlnE on nitrogen starvation response in *Corynebacterium glutamicum*. *Journal of Biotechnology*.
220. **Reinscheid D. J., Eikmanns B. J., and Sahn H. (1994)**, Characterization of the isocitrate lyase gene from *Corynebacterium glutamicum* and biochemical analysis of the enzyme. *Journal of Bacteriology*.
221. **Reinscheid D. J., Eikmanns B. J., and Sahn H. (1994)**, Malate synthase from *Corynebacterium glutamicum*: Sequence analysis of the gene and biochemical characterization of the enzyme. *Microbiology*.

List of References

222. **Reinscheid D. J., Schnicke S., Rittmann D., Zahn U., Sahn H., and Eikmanns B. J. (1999)**, Cloning, sequence analysis, expression and inactivation of the *Corynebacterium glutamicum* *pta-ack* operon encoding phosphotransacetylase and acetate kinase. *Microbiology*.
223. **Riedel C., Rittmann D., Dangel P., Möckel B., Petersen S., Sahn H., and Eikmanns B. J. (2001)**, Characterization of the phosphoenolpyruvate carboxykinase gene from *Corynebacterium glutamicum* and significance of the enzyme for growth and amino acid production. *Journal of Molecular Microbiology and Biotechnology*.
224. **Rinaldi R. and Schüth F. (2009)**, Acid hydrolysis of cellulose as the entry point into biorefinery schemes. *Chemistry & Sustainability Energy & Materials*.
225. **Ritchie H. and Roser M. (2019)**, CO₂ emissions. *Our World in Data*.
226. **Robazza A., Welter C., Kubisch C., Baleeiro F. C. F., Ochsenreither K., and Neumann A. (2022)**, Co-fermenting pyrolysis aqueous condensate and pyrolysis syngas with anaerobic microbial communities enables L-malate production in a secondary fermentative stage. *Fermentation*.
227. **Robert T. and Friebel S. (2016)**, Itaconic acid – A versatile building block for renewable polyesters with enhanced functionality. *Green Chemistry*.
228. **Rodríguez A., Serrano L., Moral A., and Jiménez L. (2008)**, Pulping of rice straw with high-boiling point organosolv solvents. *Biochemical Engineering Journal*.
229. **Román-Palacios C. and Wiens J. J. (2020)**, Recent responses to climate change reveal the drivers of species extinction and survival. *Proceedings of the National Academy of Sciences*.
230. **Rong L., Miao L., Wang S., Wang Y., Liu S., Lu Z., Zhao B., Zhang C., Xiao D., and Pushpanathan K. (2022)**, Engineering *Yarrowia lipolytica* to produce itaconic acid from waste cooking oil. *Frontiers in Bioengineering and Biotechnology*.
231. **Rosillo-Calle F. (2012)**, Food versus fuel: Toward a new paradigm – The need for a holistic approach. *International Scholarly Research Notices*.
232. **Saha B. C. (2017)**, Emerging biotechnologies for production of itaconic acid and its applications as a platform chemical. *Journal of Industrial Microbiology and Biotechnology*.
233. **Sakai A., Katayama K., Katsuragi T., and Tani Y. (2001)**, Glycolaldehyde-forming route in *Bacillus subtilis* in relation to vitamin B6 biosynthesis. *Journal of Bioscience and Bioengineering*.
234. **Sakai S., Tsuchida Y., Okino S., Ichihashi O., Kawaguchi H., Watanabe T., Inui M., and Yukawa H. (2007)**, Effect of lignocellulose-derived inhibitors on growth of and ethanol production by growth-arrested *Corynebacterium glutamicum* R. *Applied and Environmental Microbiology*.
235. **Salim I., Gonzalez-Garcia S., Feijoo G., and Moreira M. T. (2019)**, Assessing the environmental sustainability of glucose from wheat as a fermentation feedstock. *Journal of Environmental Management*.
236. **Sawangkeaw R. and Ngamprasertsith S. (2013)**, A review of lipid-based biomasses as feedstocks for biofuels production. *Renewable and Sustainable Energy Reviews*.
237. **Saxena R., Anand P., Saran S., Isar J., and Agarwal L. (2010)**, Microbial production and applications of 1,2-propanediol. *Indian Journal of Microbiology*.
238. **Schäfer A., Tauch A., Jäger W., Kalinowski J., Thierbach G., and Pühler A. (1994)**, Small mobilizable multi-purpose cloning vectors derived from the *Escherichia coli* plasmids pK18 and pK19: Selection of defined deletions in the chromosome of *Corynebacterium glutamicum*. *Gene*.

239. **Schievano A., Pant D., and Puig S. (2019)**, Microbial synthesis, gas-fermentation and bioelectroconversion of CO₂ and other gaseous streams. *Frontiers Media SA*.
240. **Schmollack M., Werner F., Huber J., Kiefer D., Merkel M., Hausmann R., Siebert D., and Blombach B. (2022)**, Metabolic engineering of *Corynebacterium glutamicum* for acetate-based itaconic acid production. *Biotechnology for Biofuels and Bioproducts*.
241. **Schultz C., Niebisch A., Gebel L., and Bott M. (2007)**, Glutamate production by *Corynebacterium glutamicum*: Dependence on the oxoglutarate dehydrogenase inhibitor protein OdhI and protein kinase PknG. *Applied Microbiology and Biotechnology*.
242. **Schwentner A., Feith A., Münch E., Busche T., Rückert C., Kalinowski J., Takors R., and Blombach B. (2018)**, Metabolic engineering to guide evolution – Creating a novel mode for L-valine production with *Corynebacterium glutamicum*. *Metabolic Engineering*.
243. **Shafiee S. and Topal E. (2008)**, An econometrics view of worldwide fossil fuel consumption and the role of US. *Energy policy*.
244. **Shah A., Blombach B., Gauttam R., and Eikmanns B. J. (2018)**, The RamA regulon: Complex regulatory interactions in relation to central metabolism in *Corynebacterium glutamicum*. *Applied Microbiology and Biotechnology*.
245. **Shankaranand V. and Lonsane B. (1994)**, Coffee husk: An inexpensive substrate for production of citric acid by *Aspergillus niger* in a solid-state fermentation system. *World Journal of Microbiology and Biotechnology*.
246. **Shi F., Luan M., and Li Y. (2018)**, Ribosomal binding site sequences and promoters for expressing glutamate decarboxylase and producing γ -aminobutyrate in *Corynebacterium glutamicum*. *AMB Express*.
247. **Shiio I. and OZAKI H. (1970)**, Regulation of nicotinamide adenine dinucleotide phosphate-specific glutamate dehydrogenase from *Brevibacterium flavum*, a glutamate-producing bacterium. *The Journal of Biochemistry*.
248. **Shope R. (1991)**, Global climate change and infectious diseases. *Environmental Health Perspectives*.
249. **Siebert D., Altenbuchner J., and Blombach B. (2021)**, A timed off-switch for dynamic control of gene expression in *Corynebacterium glutamicum*. *Frontiers in Bioengineering and Biotechnology*.
250. **Siebert D. and Wendisch V. F. (2015)**, Metabolic pathway engineering for production of 1,2-propanediol and 1-propanol by *Corynebacterium glutamicum*. *Biotechnology for Biofuels*.
251. **Siewe R. M., Weil B., Burkovski A., Eggeling L., Krämer R., and Jahns T. (1998)**, Urea uptake and urease activity in *Corynebacterium glutamicum*. *Archives of Microbiology*.
252. **Siewe R. M., Weil B., Burkovski A., Eikmanns B. J., Eikmanns M., and Krämer R. (1996)**, Functional and genetic characterization of the (methyl) ammonium uptake carrier of *Corynebacterium glutamicum* *Journal of Biological Chemistry*.
253. **Starace A. K., Black B. A., Lee D. D., Palmiotti E. C., Orton K. A., Michener W. E., ten Dam J., Watson M. J., Beckham G. T., and Magrini K. A. (2017)**, Characterization and catalytic upgrading of aqueous stream carbon from catalytic fast pyrolysis of biomass. *ACS Sustainable Chemistry & Engineering*.
254. **Steffen W., Broadgate W., Deutsch L., Gaffney O., and Ludwig C. (2015)**, The trajectory of the Anthropocene: The great acceleration. *The Anthropocene Review*.

List of References

255. **Strösser J., Lüdke A., Schaffer S., Krämer R., and Burkovski A. (2004)**, Regulation of GlnK activity: Modification, membrane sequestration and proteolysis as regulatory principles in the network of nitrogen control in *Corynebacterium glutamicum*. *Molecular Microbiology*.
256. **Subedi K. P., Choi D., Kim I., Min B., and Park C. (2011)**, Hsp31 of *Escherichia coli* K-12 is glyoxalase III. *Molecular Microbiology*.
257. **Sulzenbacher G., Alvarez K., Van Den Heuvel R. H., Versluis C., Spinelli S., Campanacci V., Valencia C., Cambillau C., Eklund H., and Tegoni M. (2004)**, Crystal structure of *E. coli* alcohol dehydrogenase YqhD: Evidence of a covalently modified NADP coenzyme. *Journal of Molecular Biology*.
258. **Sundermeyer L., Bosco G., Gujar S., Brocker M., Baumgart M., Willbold D., Weiergräber O. H., Bellinzoni M., and Bott M. (2022)**, Characteristics of the GlnH and GlnX signal transduction proteins controlling PknG-mediated phosphorylation of OdhI and 2-oxoglutarate dehydrogenase activity in *Corynebacterium glutamicum*. *Microbiology Spectrum*.
259. **Tarmy E. and Kaplan N. (1968)**, Chemical characterization of D-lactate dehydrogenase from *Escherichia coli* B. *Journal of Biological Chemistry*.
260. **Tauch A., Kirchner O., Löffler B., Götter S., Pühler A., and Kalinowski J. (2002)**, Efficient electrotransformation of *Corynebacterium diphtheriae* with a mini-replicon derived from the *Corynebacterium glutamicum* plasmid pGA1. *Current Microbiology*.
261. **Teella A., Huber G. W., and Ford D. M. (2011)**, Separation of acetic acid from the aqueous fraction of fast pyrolysis bio-oils using nanofiltration and reverse osmosis membranes. *Journal of Membrane Science*.
262. **Teleky B.-E. and Vodnar D. C. (2021)**, Recent advances in biotechnological itaconic acid production, and application for a sustainable approach. *Polymers*.
263. **Tesch M., De Graaf A., and Sahn H. (1999)**, In vivo fluxes in the ammonium-assimilatory pathways in *Corynebacterium glutamicum* studied by ¹⁵N nuclear magnetic resonance. *Applied and Environmental Microbiology*.
264. **Tesch M., Eikmanns B. J., de Graaf A. A., and Sahn H. (1998)**, Ammonia assimilation in *Corynebacterium glutamicum* and a glutamate dehydrogenase-deficient mutant. *Biotechnology Letters*.
265. **Thakur S., Chaudhary J., Thakur A., Gunduz O., Alsanie W. F., Makatsoris C., and Thakur V. K. (2022)**, Highly efficient poly (acrylic acid-co-aniline) grafted itaconic acid hydrogel: Application in water retention and adsorption of rhodamine B dye for a sustainable environment. *Chemosphere*.
266. **Thoma F., Appel C., Russ D., Huber J., Werner F., and Blombach B. (2023)**, Improving growth properties of *Corynebacterium glutamicum* by implementing an iron-responsive protocatechuate biosynthesis. *Microbial Biotechnology*.
267. **Thornalley P. (2003)**, Glyoxalase I – Structure, function and a critical role in the enzymatic defence against glycation. *Biochemical Society Transactions*.
268. **Tian S.-Q., Zhao R.-Y., and Chen Z.-C. (2018)**, Review of the pretreatment and bioconversion of lignocellulosic biomass from wheat straw materials. *Renewable and Sustainable Energy Reviews*.
269. **Timmer C. P. (2010)**, Reflections on food crises past. *Food policy*.
270. **Torri C. and Fabbri D. (2014)**, Biochar enables anaerobic digestion of aqueous phase from intermediate pyrolysis of biomass. *Bioresource Technology*.

271. **Toyoda K. and Inui M. (2016)**, Regulons of global transcription factors in *Corynebacterium glutamicum*. *Applied Microbiology and Biotechnology*.
272. **Toyoda K., Teramoto H., Gunji W., Inui M., and Yukawa H. (2013)**, Involvement of regulatory interactions among global regulators GlxR, SugR, and RamA in expression of *ramA* in *Corynebacterium glutamicum*. *Journal of Bacteriology*.
273. **Trenberth K. E. (2005)**, The impact of climate change and variability on heavy precipitation, floods, and droughts. *Encyclopedia of Hydrological Sciences*.
274. **Trotta J. T. (2019)**, Renewable polymers from itaconic acid. *Cornell University*.
275. **Tylecote A. (2019)**, Biotechnology as a new techno-economic paradigm that will help drive the world economy and mitigate climate change. *Research Policy*.
276. **Urban M. C. (2015)**, Accelerating extinction risk from climate change. *Science*.
277. **van der Rest M. E., Lange C., and Molenaar D. (1999)**, A heat shock following electroporation induces highly efficient transformation of *Corynebacterium glutamicum* with xenogeneic plasmid DNA. *Applied Microbiology and Biotechnology*.
278. **van Ooyen J., Emer D., Bussmann M., Bott M., Eikmanns B. J., and Eggeling L. (2011)**, Citrate synthase in *Corynebacterium glutamicum* is encoded by two *gltA* transcripts which are controlled by RamA, RamB, and GlxR. *Journal of Biotechnology*.
279. **van Ooyen J., Noack S., Bott M., Reth A., and Eggeling L. (2012)**, Improved L-lysine production with *Corynebacterium glutamicum* and systemic insight into citrate synthase flux and activity. *Biotechnology and Bioengineering*.
280. **Vasco-Cárdenas M. F., Baños S., Ramos A., Martín J. F., and Barreiro C. (2013)**, Proteome response of *Corynebacterium glutamicum* to high concentration of industrially relevant C4 and C5 dicarboxylic acids. *Journal of Proteomics*.
281. **Vašicová P., Pátek M., Nešvera J., Sahn H., and Eikmanns B. (1999)**, Analysis of the *Corynebacterium glutamicum* *dapA* promoter. *Journal of Bacteriology*.
282. **Veit A., Rittmann D., Georgi T., Youn J.-W., Eikmanns B. J., and Wendisch V. F. (2009)**, Pathway identification combining metabolic flux and functional genomics analyses: Acetate and propionate activation by *Corynebacterium glutamicum*. *Journal of Biotechnology*.
283. **Vetting M. W., Frantom P. A., and Blanchard J. S. (2008)**, Structural and enzymatic analysis of MshA from *Corynebacterium glutamicum*: Substrate-assisted catalysis. *Journal of Biological Chemistry*.
284. **Vuoristo K. S., Mars A. E., Sangra J. V., Springer J., Eggink G., Sanders J. P., and Weusthuis R. A. (2015)**, Metabolic engineering of itaconate production in *Escherichia coli*. *Applied Microbiology and Biotechnology*.
285. **Wang X., Khushk I., Xiao Y., Gao Q., and Bao J. (2018)**, Tolerance improvement of *Corynebacterium glutamicum* on lignocellulose derived inhibitors by adaptive evolution. *Applied Microbiology and Biotechnology*.
286. **Wang Y., Fan L., Tuyishime P., Liu J., Zhang K., Gao N., Zhang Z., Ni X., Feng J., and Yuan Q. (2020)**, Adaptive laboratory evolution enhances methanol tolerance and conversion in engineered *Corynebacterium glutamicum*. *Communications Biology*.
287. **Weastra S. (2016)**, Determination of market potential for selected platform chemicals – Itaconic acid, succinic acid, 2,5-furandicarboxylic acid. *Applied Microbiology and Biotechnology*.
288. **Welter K. (2000)**, Biotechnische Produktion von Itaconsäure aus nachwachsenden Rohstoffen mit immobilisierten Zellen. *Technischen Universität Braunschweig*.

List of References

289. **Wendisch V. and Bott M. (2005)**, Phosphorus Metabolism. *Handbook of Corynebacterium glutamicum*, 1st ed. Taylor & Francis.
290. **Wendisch V. F. (2020)**, Metabolic engineering advances and prospects for amino acid production. *Metabolic Engineering*.
291. **Wendisch V. F. and Bott M. (2008)**, Phosphorus metabolism and its regulation. *Corynebacteria: Genomics and Molecular Biology*, 1st ed. Caister Academic Press.
292. **Wendisch V. F., de Graaf A. A., Sahm H., and Eikmanns B. J. (2000)**, Quantitative determination of metabolic fluxes during coutilization of two carbon sources: Comparative analyses with *Corynebacterium glutamicum* during growth on acetate and/or glucose. *Journal of Bacteriology*.
293. **Wennerhold J., Krug A., and Bott M. (2005)**, The AraC-type regulator RipA represses aconitase and other iron proteins from *Corynebacterium* under iron limitation and is itself repressed by DtxR. *Journal of Biological Chemistry*.
294. **Werpy T. and Petersen G. (2004)**, Top value added chemicals from biomass: Volume I-results of screening for potential candidates from sugars and synthesis gas. *National Renewable Energy Lab*.
295. **Wieczorek A. and Wright M. (2012)**, History of agricultural biotechnology: How crop development has evolved. *Nature Education Knowledge*.
296. **Wierckx N., Agrimi G., Lübeck P. S., Steiger M. G., Mira N. P., and Punt P. J. (2020)**, Metabolic specialization in itaconic acid production: A tale of two fungi. *Current Opinion in Biotechnology*.
297. **Wieschalka S., Blombach B., Bott M., and Eikmanns B. J. (2013)**, Bio-based production of organic acids with *Corynebacterium glutamicum*. *Microbial Biotechnology*.
298. **Willke T. and Vorlop K.-D. (2001)**, Biotechnological production of itaconic acid. *Applied Microbiology and Biotechnology*.
299. **Wittmann C. and Becker J. (2007)**, The L-lysine story: From metabolic pathways to industrial production. *Amino Acid Biosynthesis, Pathways, Regulation and Metabolic Engineering*. Springer.
300. **Wittmann C. and Heinzle E. (1999)**, Mass spectrometry for metabolic flux analysis. *Biotechnology and Bioengineering*.
301. **Wolf N., Bussmann M., Koch-Koerfges A., Katcharava N., Schulte J., Polen T., Hartl J., Vorholt J. A., Baumgart M., and Bott M. (2020)**, Molecular basis of growth inhibition by acetate of an adenylate cyclase-deficient mutant of *Corynebacterium glutamicum*. *Frontiers in Microbiology*.
302. **Wu X., Liu Q., Deng Y., Li J., Chen X., Gu Y., Lv X., Zheng Z., Jiang S., and Li X. (2017)**, Production of itaconic acid by biotransformation of wheat bran hydrolysate with *Aspergillus terreus* CICC40205 mutant. *Bioresource Technology*.
303. **Wu X., Lu Y., Zhou S., Chen L., and Xu B. (2016)**, Impact of climate change on human infectious diseases: Empirical evidence and human adaptation. *Environment International*.
304. **Xiao Y., Chen S., Li J., Lu Z., and Hu C. (2022)**, Cooperative roles of Sn^{IV} and Cu^{II} for efficient transformation of biomass-derived acetol towards lactic acid production. *Science of The Total Environment*.

-
305. **Xing R., Dagle V. L., Flake M., Kovarik L., Albrecht K. O., Deshmane C., and Dagle R. A. (2016)**, Steam reforming of fast pyrolysis-derived aqueous phase oxygenates over Co, Ni, and Rh metals supported on MgAl₂O₄. *Catalysis Today*.
306. **Yang J., Xu H., Jiang J., Zhang N., Xie J., Wei M., and Zhao J. (2019)**, Production of itaconic acid through microbiological fermentation of inexpensive materials. *Journal of Bioresources and Bioproducts*.
307. **Yang J., Xu H., Jiang J., Zhang N., Xie J., Zhao J., Bu Q., and Wei M. (2020)**, Itaconic acid production from undetoxified enzymatic hydrolysate of bamboo residues using *Aspergillus terreus*. *Bioresource Technology*.
308. **Yoro K. O. and Daramola M. O. (2020)**, CO₂ emission sources, greenhouse gases, and the global warming effect. *Advances in carbon capture*. Elsevier.
309. **Zahoor A., Lindner S. N., and Wendisch V. F. (2012)**, Metabolic engineering of *Corynebacterium glutamicum* aimed at alternative carbon sources and new products. *Computational and Structural Biotechnology Journal*.
310. **Zhang S.-p., Li X.-j., Li Q.-y., Xu Q.-l., and Yan Y.-j. (2011)**, Hydrogen production from the aqueous phase derived from fast pyrolysis of biomass. *Journal of Analytical and Applied Pyrolysis*.
311. **Zhao M., Lu X., Zong H., Li J., and Zhuge B. (2018)**, Itaconic acid production in microorganisms. *Biotechnology Letters*.
312. **Zhao X., Cheng K., and Liu D. (2009)**, Organosolv pretreatment of lignocellulosic biomass for enzymatic hydrolysis. *Applied Microbiology and Biotechnology*.
313. **Zhao Y., Damgaard A., and Christensen T. H. (2018)**, Bioethanol from corn stover – A review and technical assessment of alternative biotechnologies. *Progress in Energy and Combustion Science*.
314. **Zhou H., Brown R. C., and Wen Z. (2019)**, Anaerobic digestion of aqueous phase from pyrolysis of biomass: Reducing toxicity and improving microbial tolerance. *Bioresource Technology*.
315. **Zhu X., Guo Y., Liu Z., Yang J., Tang H., and Wang Y. (2021)**, Itaconic acid exerts anti-inflammatory and antibacterial effects via promoting pentose phosphate pathway to produce ROS. *Scientific Reports*.

Appendix

Table A1: GC-Report on the Compound Analysis of PW

GC-report on the compositional analysis of crude PW performed by the Thünen-Institute of Wood Research in Braunschweig, Germany. The table shows mean and standard deviation of two technical replicates of the same batch of PW. The report was provided by Dr. Axel Funke of the IKFT at KIT (Eggenstein-Leopoldshafen, Germany). Non-identified compounds (< 0.000%) were excluded from the edition below. Major compounds discussed in this study are marked in red. c = calibrated compound, n.q. = not quantified, # = estimated response factor.

GC-Report (Thünen Institute of Wood Research)						
	Total chromatogram Area		2,47E+08			
	Area of identified peaks		2,08E+08	=	84,0%	
	Area of unknown peaks		3,95E+07	=	16,0%	
	Identified peaks		64			
	m (Oil) [mg] wet basis (as received)		50,00			
	Water Content [%]		81,30			
	m (Oil) [mg] dry basis- anhydrous mass		9,35			
CAS-No.	Compound		wt.% wet	SD	wt.% dry	SD
	NONAROMATIC COMPOUNDS					
	Acids		4,953	0,03	26,486	0,14
64-19-7	Acetic acid	c	3,667	0,023	19,610	0,125
79-09-4	Propionic acid	c	1,286	0,003	6,875	0,013
	Nonaromatic Esters		0,022	0,00	0,117	0,00
542-59-6	Acetic acid 2-hydroxyethyl ester	c	0,022	0,001	0,117	0,004
	Nonaromatic Alcohols		1,028	0,01	5,495	0,06
107-21-1	Ethylene glycol	c	0,988	0,011	5,284	0,058
	2-Propen-1-ol (NIST MQ 84)	#	0,040	0,000	0,212	0,001
	Nonaromatic Aldehydes		0,137	0,00	0,732	0,00
	Butandial (or Propanal) (NIST MQ 92)	#	0,026	0,000	0,140	0,002
4170-30-3	Crotonaldehyde, cis	#	0,059	0,000	0,316	0,001
123-73-9	Crotonaldehyde, trans	c	0,032	0,000	0,171	0,002
	2-Butenal, 2-methyl- (NIST MQ 92)	#	0,020	0,001	0,105	0,003
	Nonaromatic Ketones		8,164	0,03	43,657	0,16
116-09-6	Acetol (Hydroxypropanone)	c	5,472	0,007	29,264	0,038
110-13-4	Acetylacetone (Hexandione, 2,5-)	c	0,010	0,000	0,055	0,000
78-93-3	Butanone, 2-	c	0,190	0,005	1,017	0,027
5077-67-8	Butanone, 1-hydroxy-2-	c	0,756	0,014	4,045	0,073
431-03-8	Butandione, 2,3- (Diacyl)	c	0,233	0,000	1,245	0,001
513-86-0	Acetoin (Hydroxy-2-butanone, 3-)	c	0,130	0,002	0,695	0,010
592-20-1	Propan-2-one, 1-acetyloxy-	c	0,310	0,001	1,656	0,006
930-30-3	Cyclopenten-1-one, 2-	c	0,344	0,002	1,842	0,013
2758-18-1	Cyclopenten-1-one, 3-methyl-2-	c	0,083	0,000	0,446	0,001
568-26-99	Cyclopenten-1-one, 3-ethyl-2-	#	0,015	0,000	0,078	0,002
80-71-7	Cyclopenten-3-one, 2-hydroxy-1-methyl-1-	c	0,177	0,001	0,946	0,003

Table A1 continued.

<u>CAS-No.</u>	<u>Compound</u>		<u>wt.% wet</u>	<u>SD</u>	<u>wt.% dry</u>	<u>SD</u>
930-68-7	Cyclohexen-1-one, 2-	c	0,009	0,000	0,046	0,001
	Methyl vinyl ketone = 2-Butenone (NIST MQ 84)	#	0,010	0,000	0,051	0,000
	poss: 3-Buten-2-one, 3-methyl- (NIST MQ 82)	#	0,017	0,000	0,089	0,001
	2-Pentanone (NIST MQ 94)	#	0,043	0,000	0,229	0,001
	2,3-Pentanedione	#	0,066	0,000	0,355	0,002
	3-Penten-2-one (NIST MQ 84)	#	0,030	0,001	0,160	0,007
	Cyclopentanone, 2-methyl- (NIST MQ 87)	#	0,040	0,000	0,214	0,002
	Cyclopentanone, 3-methyl- (NIST MQ 92)	#	0,035	0,001	0,186	0,006
	Isomere of 2-Cyclopenten-1-one, 3-methyl-	#	0,030	0,000	0,159	0,001
	2-Butanone, 1-hydroxy-3-methyl- (NIST MQ 78)	#	0,033	0,000	0,175	0,001
	Isomere of 2-Cyclopenten-1-one, 3,4-dimethyl-	#	0,018	0,001	0,095	0,003
	Isomere of Cyclopenten-1-one, 2,3-dimethyl-2-	#	0,041	0,001	0,221	0,003
	2-Cyclopenten-1-one, 3,4-dimethyl- (NIST MQ 94)	#	0,021	0,001	0,113	0,003
	2-Cyclopenten-1-one, 2,3,4-trimethyl- (NIST MQ 88)	#	0,018	0,000	0,097	0,001
	poss: 2-Pentanone, 4-hydroxy- (NIST MQ 82)	#	0,020	0,000	0,110	0,001
	2-Cyclohexene-1,4-dione (NIST MQ 78)	#	0,013	0,000	0,068	0,002
	HETEROCYCLIC COMPOUNDS					
	Furans		0,668	0,01	3,573	0,04
497-23-4	Furanone, 2(5H)-	c	0,068	0,002	0,366	0,012
98-00-0	Furfuryl alcohol, 2-	c	0,019	0,001	0,099	0,005
98-01-1	Furaldehyde, 2-	c	0,339	0,002	1,810	0,012
498-60-2	Furaldehyde, 3-	c	0,022	0,001	0,115	0,005
620-02-0	Furaldehyde, 5-methyl-2-	c	0,020	0,000	0,105	0,001
1192-62-7	Ethanone, 1-(2-furanyl)-	c	0,041	0,000	0,221	0,002
22122-36-7	Furan-2-one, 3-methyl-, (5H)-	c	0,019	0,000	0,103	0,000
96-48-0	Butyrolactone, γ -	c	0,080	0,001	0,430	0,005
	Furan, tetrahydro-2-methoxy- (NIST MQ (/))	#	0,011	0,000	0,056	0,000
591-11-17	Furan-2-one, 5-methyl-, (5H)-	#	0,021	0,000	0,110	0,000
	Furan-2-one, 2,5-dihydro-3,5-dimethyl-	#	0,029	0,000	0,158	0,002
	AROMATIC COMPOUNDS					
	Benzenes		0,009	0,00	0,046	0,00
91-20-3	Naphthalene	c	0,004	0,000	0,019	0,000
	Benzene (NIST MQ 97)	#	0,005	0,000	0,027	0,002
	Catechols		0,000	0,00	0,000	0,00
	Aromatic Alcohols		0,000	0,00	0,000	0,00
	Aromatic Aldehydes		0,007	0,00	0,036	0,00
100-52-7	Benzaldehyde	c	0,007	0,000	0,036	0,002
	Aromatic Ketones		0,000	0,00	0,000	0,00
	Aromatic Esters		0,000	0,00	0,000	0,00
	Lignin derived Phenols		0,162	0,00	0,864	0,01
108-95-2	Phenol	c	0,070	0,000	0,377	0,002
95-48-7	Cresol, o-	c	0,037	0,001	0,197	0,003
106-44-5	Cresol, p-	c	0,016	0,000	0,084	0,001
108-39-4	Cresol, m-	c	0,019	0,001	0,103	0,004

Appendix

Table A1 continued.

<u>CAS-No.</u>	<u>Compound</u>		<u>wt.% wet</u>	<u>SD</u>	<u>wt.% dry</u>	<u>SD</u>
123-07-9	Phenol, 4-ethyl-	c	0,019	0,000	0,104	0,000
	Guaiacols (Methoxy phenols)		0,268	0,00	1,432	0,00
90-05-1	Guaiacol	c	0,196	0,000	1,050	0,002
93-51-6	Guaiacol, 4-methyl-	c	0,038	0,000	0,201	0,002
2785-89-9	Guaiacol, 4-ethyl-	c	0,034	0,000	0,181	0,000
	Syringols (Dimethoxy phenols)		0,000	0,00	0,000	0,00
	OTHER ORGANIC COMPOUNDS					
	Terpenes		0,018	0,00	0,096	0,00
	D-Limonene (NIST MQ 94)	#	0,011	0,000	0,059	0,000
	2-Acetyl-5-norbornene (NIST MQ 92)	#	0,007	0,000	0,037	0,001

Table A2: Consumables Used in this Study.

The table lists the consumables used in this study, their intended use, and their manufacturer. Standard laboratory supplies such as reaction tubes, pipette tips and others are not included in this list.

Abbreviation/ Designation	Description Intended use	Manufacturer/ Source/ Reference
0.2 µm PES Membrane Filtration Cup	Processing of Pyrolysis Water	VWR International GmbH; Darmstadt, Germany
0.2 µm Cellulose-Acetate Filter	Sterile Filtration of Stock Solutions	VWR International GmbH; Darmstadt, Germany
0.45 µm Cellulose-Acetate Filter	Filtration of HPLC Samples	Agilent Technologies; Waldbronn, Germany
6x Purple Loading Dye	Agarose Gel Electrophoresis	New England BioLabs GmbH; Frankfurt am Main, Germany
Ammonia/urea UV-method Kit	Determination of Nitrogen in the Culture Medium	R-Biopharm AG; Darmstadt, Germany
Electroporation Cuvettes with 2 mm Gap Width	Transformation of Electro Competent <i>C. glutamicum</i>	VWR International GmbH; Darmstadt, Germany
GelGreen®	Agarose Gel Stain	Biotium, Inc.; Fermtont, USA
Glass Beads (Diameter of 0.1 mm)	Mechanical Cell Lysis	Scientific industries Inc.; Bohemia, USA
NucleoSpin® Gel and PCR Clean-up Kit	Purification of PCR Fragments and Linearized Plasmids	Machery-Nagel GmbH & Co. KG; Düren, Germany
NucleoSpin® Microbial DNA Kit	Purification of Genomic DNA	Machery-Nagel GmbH & Co. KG; Düren, Germany
NucleoSpin® Plasmid Kit	Purification of Plasmids	Machery-Nagel GmbH & Co. KG; Düren, Germany
Oligonucleotides	PCR	Sigma-Aldrich Chemie GmbH; Taufkirchen, Germany
PMMA Semi-Micro Cuvettes	Determination of Nitrogen in the Culture Medium	VWR International GmbH; Darmstadt, Germany
PS Semi-Micro Cuvettes	Determination of OD ₆₀₀	VWR International GmbH; Darmstadt, Germany
Q5® High-Fidelity DNA Polymerase	Amplification of DNA (PCR)	New England BioLabs GmbH; Frankfurt am Main, Germany
Quick Start™ Bradford Protein Assay	Determining Protein Concentrations	Bio-Rad Laboratories GmbH; Puchheim, Germany
Quick-Load® Taq 2X Master Mix	Colony PCR	New England BioLabs GmbH; Frankfurt am Main, Germany
Ready-to-Use 1 kb DNA Ladder	Agarose Gel Electrophoresis	Biotium, Inc.; Fermtont, USA
Restriction Enzymes	Molecular Cloning	New England BioLabs GmbH; Frankfurt am Main, Germany
T4-DNA Ligase	Molecular Cloning	New England BioLabs GmbH; Frankfurt am Main, Germany

Table A3: Devices Used in this Study.

The table lists the devices used in this study, their intended use, and their manufacturer.

Abbreviation/ Designation	Description Intended use	Manufacturer/ Source/ Reference
1260 Infinity II HPLC equipped with a Hi-Plex H Column (7.7 x 300 mm, 8 µm) and Hi-Plex H Guard Cartridge (3 x 5 mm, 8 µm)	Determination of Sugars and Organic Acids (HPLC Measurements)	Agilent Technologies; Waldbronn, Germany
500 mL Shaking Flasks with appropriate Cellulose Plugs	Liquid Cultures	VWR International GmbH; Darmstadt, Germany
5425 Micro Centrifuge with FA-24x2 Rotor	Centrifugation of Samples up to Volumes of 2 mL at RT	Eppendorf SE; Hamburg, Germany
5910 Ri Refrigerated Centrifuge with S-4x Universal Rotor	Centrifugation of Samples > 2 mL Volume	Eppendorf SE; Hamburg, Germany
BD 260 Incubator	Incubation of Culture Plates	Binder GmbH; Tuttlingen, Germany
BioLector® I	Strain Screening Experiments	Beckman Coulter GmbH; Baesweiler, Germany
Biometra TSC ThermoShaker	Heating and Shaking of Samples in 1.5 – 2 mL Reaction Tubes	Analytik Jena GmbH; Jena, Germany
Biometra TOne Thermocycler	PCR	Analytik Jena GmbH; Jena, Germany
CS-15R Refrigerated Centrifuge	Centrifugation of Samples up to Volumes of 2 mL at 4 °C	Beckman Coulter GmbH; Krefeld, Germany
Culture Tubes with appropriate Metal Cups, Height 130 mm, Width 16 mm	Liquid Cultures	DWK life science GmbH; Wertheim/Main, Germany
DASGIP® Parallel Bioreactor System	Bioreactor Cultivations	Eppendorf SE; Hamburg, Germany
E-Box CX5 TS	Agarose Gel Documentation System	Vilber Lourmat Deutschland GmbH; Eberhardzell, Germany
FiveEasy F20 pH Meter	pH Measurements	Mettler-Toledo GmbH; Gießen, Germany
Gene pulser Xcell Electroporator	Transformation of Electro-Competent <i>C. glutamicum</i>	Bio-Rad Laboratories GmbH; Feldkirchen, Germany
Hei-VAP Core Rotary Evaporator	Processing of Pyrolysis Water	Heidolph instruments GmbH & Co. KG; Kehlheim, Germany
MTP-48-B Flower Plate with appropriate Sealing Foil	BioLector® Cultivation	Beckman Coulter GmbH; Baesweiler, Germany
Multi N/C 2100S TOC/TNb Analyzer	Total Carbon Measurements	Analytik Jena GmbH; Jena, Germany
Multitron Incubation Shaker	Incubation of Liquid Cultures	Infors AG, Bottmingen, Switzerland
NanoPhotometer™ N60 Micro-Volume	UV-VIS Spectrophotometer	Implen GmbH; München, Germany
Precellys® 24 Cell Disrupter	Mechanical Cell Lysis	Bertin instruments; Montigny-le-Bretonneux, France
Sonorex Super RK 510 H Ultrasonic Bath	Processing of Pyrolysis Water	Bandelin electronic GmbH & Co. KG; Berlin, Germany
Specord® 50 Plus UV/VIS Photometer	Determination of Nitrogen in the Culture Medium	Analytik Jena GmbH; Jena, Germany
Sub-Cell GT Electrophoresis System	Agarose Gel Electrophoresis	Bio-Rad Laboratories GmbH; Feldkirchen, Germany
TECAN Spark Plate Reader	Determination of Protein Concentrations	Tecan Trading AG; Männedorf, Switzerland
Ultrospec® 10 Cell Density Meter	Determination of Culture OD	Biochrom US; Holliston, USA

Appendix

Table A4: Chemicals Used in this Study.

The table lists the chemicals used in this study, their intended use, and their manufacturer.

Abbreviation/ Designation	Description/ Intended use	Manufacturer/ Source/ Reference
(NH ₄) ₂ SO ₄	CGXII Medium	VWR chemicals GmbH; Darmstadt, Germany
25% NH ₃ (aq.)	pH Control during Bioreactor Cultivations	VWR chemicals GmbH; Darmstadt, Germany
35% Perchloric Acid	Silicone Oil Centrifugation	Carl Roth GmbH & Co. KG; Karlsruhe, Germany
37% HCl	pH Adjustment, Termination of Enzyme Reactions	VWR chemicals GmbH; Darmstadt, Germany
40% o-Phosphoric Acid	pH Control during Bioreactor Cultivations, Total Carbon Measurements	Carl Roth GmbH & Co. KG; Karlsruhe, Germany
96% H ₂ SO ₄	pH Adjustment, HPLC mobile phase	Carl Roth GmbH + Co. KG; Karlsruhe, Germany
Absolute Ethanol	Feedstock Preparation, HPLC Calibrator	Sigma-Aldrich Chemie GmbH; Taufkirchen, Germany
Acetol (Hydroxyacetone)	Feedstock Preparation, HPLC Calibrator	Alfa Aesar; Kandel, Germany
Activated Carbon	Processing of Pyrolysis Water	Carl Roth GmbH + Co. KG; Karlsruhe, Germany
Agarose	Agarose Gel Electrophoresis	Serva Electrophoresis GmbH; Heidelberg, Germany
Bacto™ Tryptone	2YT Medium	Becton Dickinson GmbH; Heidelberg, Germany
BBL™ Yeast Extract	2YT Medium, CGXII Supplement	Becton Dickinson GmbH; Heidelberg, Germany
BD Bacto™ Brain Heart Infusion	BHIS Medium	Becton Dickinson GmbH; Heidelberg, Germany
CaCl ₂	Preparation of Competent <i>E. coli</i> ; CGXII Medium	VWR chemicals GmbH; Darmstadt, Germany
CuSO ₄ x 5 H ₂ O	Trace Elements Stock Solution	Carl Roth GmbH + Co. KG; Karlsruhe, Germany
D-Biotin	CGXII Medium	Sigma-Aldrich Chemie GmbH; Taufkirchen, Germany
EDTA	TEA Buffer	Carl Roth GmbH + Co. KG; Karlsruhe, Germany
FeSO ₄ x 7 H ₂ O	Trace Elements Stock Solution	Carl Roth GmbH + Co. KG; Karlsruhe, Germany
Glacial Acetic Acid	TAE Buffer	Carl Roth GmbH + Co. KG; Karlsruhe, Germany
Glucose x H ₂ O (Glc)	Feedstock Preparation, HPLC Calibrator	Carl Roth GmbH & Co. KG; Karlsruhe, Germany
Glutathione (GSH)	Media Supplement	Sigma-Aldrich Chemie GmbH; Taufkirchen, Germany
Glycerol (80%)	Glycerol Stocks, Competent Cells	Carl Roth GmbH + Co. KG; Karlsruhe, Germany
IPTG	Induction of Gene Expression from pEKEx2 Plasmids	Carl Roth GmbH + Co. KG; Karlsruhe, Germany
Itaconic Acid	HPLC Calibrator, Media Supplement	VWR chemicals GmbH; Darmstadt, Germany
K ₂ HPO ₄	CGXII Medium, Enzyme Buffer	Carl Roth GmbH + Co. KG; Karlsruhe, Germany
Kanamycin Sulfate	Media Supplement	Carl Roth GmbH + Co. KG; Karlsruhe, Germany
KCl	Media Supplement	Sigma-Aldrich Chemie GmbH; Taufkirchen, Germany
KH ₂ PO ₄	CGXII Medium, Enzyme Buffer	Carl Roth GmbH + Co. KG; Karlsruhe, Germany
MgSO ₄ x 7 H ₂ O	Preparation of Competent <i>E. coli</i> ; CGXII Medium	VWR chemicals GmbH; Darmstadt, Germany
MnSO ₄ x H ₂ O	Trace Elements Stock Solution	Carl Roth GmbH + Co. KG; Karlsruhe, Germany
MOPS	CGXII Medium	Sigma-Aldrich Chemie GmbH; Taufkirchen, Germany
Na ₂ CO ₃	TC Calibrator	Carl Roth GmbH + Co. KG; Karlsruhe, Germany
NaCl	0.9% (w/v) in ddH ₂ O for Sample Dilution and Preparation of Inoculums	Carl Roth GmbH + Co. KG; Karlsruhe, Germany
NaHCO ₃	Media Supplement	Carl Roth GmbH + Co. KG; Karlsruhe, Germany
NaOH	pH Adjustment	VWR chemicals GmbH; Darmstadt, Germany
NiCl ₂ x 6 H ₂ O	Trace Elements Stock Solution	Carl Roth GmbH + Co. KG; Karlsruhe, Germany

Table A4 continued.

Abbreviation/ Designation	Description/ Intended use	Manufacturer/ Source/ Reference
Potassium Acetate	Feedstock Preparation, HPLC Calibrator	Carl Roth GmbH + Co. KG; Karlsruhe, Germany
Potassium Hydrogen Phthalate	TC Calibrator	Carl Roth GmbH + Co. KG; Karlsruhe, Germany
Potassium Hydroxide (KOH)	pH Adjustment	VWR chemicals GmbH; Darmstadt, Germany
Protocatechuic Acid (PCA)	Media Supplement	Thermo Fischer (Kandel) GmbH; Kandel, Germany
Silicon Oil PN200	Silicone Oil Centrifugation	Carl Roth GmbH & Co. KG; Karlsruhe, Germany
Sorbitol	BHIS Medium	Carl Roth GmbH + Co. KG; Karlsruhe, Germany
Struktol J647	Anti-Foam Agent during Bioreactor Cultivations	Schill + Seilacher "Struktol" GmbH; Hamburg, Germany
Sucrose	2YT + 10% Sucrose Plates	VWR chemicals GmbH; Darmstadt, Germany
TRIS	TEA Buffer	Carl Roth GmbH + Co. KG; Karlsruhe, Germany
Urea	CGXII Medium	Carl Roth GmbH + Co. KG; Karlsruhe, Germany
ZnSO ₄ x 7 H ₂ O	Trace Elements Stock Solution	Carl Roth GmbH + Co. KG; Karlsruhe, Germany

Appendix

Table A5: Strains Used and Generated in this Study.

The table lists the strains used in this study, their genetic modifications, their intended use, and their references.

Strain	Genomic characteristics	Intended use	Source/ Ref.
<i>Bacillus subtilis</i>	168	Cloning	[152]
<i>Corynebacterium glutamicum</i>	ATCC13032	Wild-Type Strain, Cloning, Control Strain	[1, 133]
<i>Escherichia coli</i> DH5a	F ⁻ φ80/ <i>lacZ</i> ΔM15 Δ(<i>lacZ</i> YA- <i>argF</i>)U169 <i>recA1 endA1 hsdR17</i> (r _K ⁻ , m _K ⁺) <i>phoA supE44 λ⁻ thi-1 gyrA96 relA1</i>	Plasmid Amplification and Maintenance	[101]
<i>C. glutamicum</i>	Δcg0354	Genomic Deletion of cg0354 (Thioredoxin Related Protein)	This Work
<i>C. glutamicum</i>	Δcg3290	Genomic Deletion of cg3290 (Oxidoreductase)	This Work
<i>C. glutamicum</i>	Δcg3412	Genomic Deletion of cg3412 (<i>azlD</i>)	This Work
<i>C. glutamicum</i>	Δcg1423	Genomic Deletion of cg1423 (L-GAP reductase)	This Work
<i>C. glutamicum</i>	Δcg2115	Genomic Deletion of cg2115 (<i>sugR</i>)	This Work
<i>C. glutamicum</i>	IDH ^{A94D}	Exchange of Native IDH with IDH ^{A94D}	[240]
<i>C. glutamicum</i>	IDH ^{G407S}	Exchange of Native IDH with IDH ^{G407S}	[240]
<i>C. glutamicum</i>	IDH ^{R453C}	Exchange of Native IDH with IDH ^{R453C}	[180]
<i>C. glutamicum</i>	IDH ^{A94D} _{ATG::GTG}	Exchange of Native IDH with IDH ^{A94D} _{ATG::GTG}	This Work
<i>C. glutamicum</i>	IDH ^{A94D} _{ATG::TTG}	Exchange of Native IDH with IDH ^{A94D} _{ATG::TTG}	This Work
<i>C. glutamicum</i>	IDH ^{G407S} _{ATG::GTG}	Exchange of Native IDH with IDH ^{G407S} _{ATG::GTG}	This Work
<i>C. glutamicum</i>	IDH ^{G407S} _{ATG::TTG}	Exchange of Native IDH with IDH ^{G407S} _{ATG::TTG}	This Work
<i>C. glutamicum</i>	IDH ^{R453C} _{ATG::GTG}	Exchange of Native IDH with IDH ^{R453C} _{ATG::GTG}	This Work
<i>C. glutamicum</i>	IDH ^{R453C} _{ATG::TTG}	Exchange of Native IDH with IDH ^{R453C} _{ATG::TTG}	This Work
<i>C. glutamicum</i>	Δ <i>pck</i>	Genomic Deletion of <i>pck</i>	[36]
<i>C. glutamicum</i>	Δ <i>P</i> _{<i>pck</i>} :: <i>P</i> _{<i>dapA</i>-A8} IDH ^{R453C}	Exchange of the <i>pck</i> Promoter in <i>C. glutamicum</i> IDH ^{R453C} with the <i>dapA</i> Promoter Version A8	[240]
<i>C. glutamicum</i>	Δ <i>P</i> _{<i>pck</i>} :: <i>P</i> _{<i>dapA</i>-A16} IDH ^{R453C}	Exchange of the <i>pck</i> Promoter in <i>C. glutamicum</i> IDH ^{R453C} with the <i>dapA</i> Promoter Version A16	[240]
<i>C. glutamicum</i>	Δ <i>P</i> _{<i>pck</i>} :: <i>P</i> _{<i>dapA</i>-C5} IDH ^{R453C}	Exchange of the <i>pck</i> Promoter in <i>C. glutamicum</i> IDH ^{R453C} with the <i>dapA</i> Promoter Version C5	This Work
<i>C. glutamicum</i>	Δ <i>P</i> _{<i>pck</i>} :: <i>P</i> _{<i>dapA</i>-C7} IDH ^{R453C}	Exchange of the <i>pck</i> Promoter in <i>C. glutamicum</i> IDH ^{R453C} with the <i>dapA</i> Promoter Version C7	This Work
<i>C. glutamicum</i>	Δ <i>ramB</i>	Genomic Deletion of <i>ramB</i>	[36]
<i>C. glutamicum</i>	<i>CgLP4</i> :: <i>P</i> _{<i>tuf</i>} - <i>malEcad</i> _{opt}	Expression of the <i>malEcad</i> _{opt} Gene Integrated in Landing Pad 4 under Control of the Constitutive <i>tuf</i> Promoter	This Work
<i>C. glutamicum</i>	<i>CgLP12</i> :: <i>P</i> _{<i>tuf</i>} - <i>malEcad</i> _{opt}	Expression of the <i>malEcad</i> _{opt} Gene Integrated in Landing Pad 12 under Control of the Constitutive <i>tuf</i> Promoter	This Work
<i>C. glutamicum</i>	IDH ^{R453C} <i>CgLP12</i> :: <i>P</i> _{<i>tuf</i>} - <i>malEcad</i> _{opt}	Expression of the <i>malEcad</i> _{opt} Gene in <i>C. glutamicum</i> IDH ^{R453C} Integrated in Landing Pad 12 under Control of the Constitutive <i>tuf</i> Promoter	This Work
<i>C. glutamicum</i>	Δ <i>ramB</i> Δ <i>glnE</i>	<i>C. glutamicum</i> Δ <i>ramB</i> with Genomic Deletion of <i>glnE</i>	[240]
<i>C. glutamicum</i>	Δ <i>ramB</i> Δ <i>gdh</i>	<i>C. glutamicum</i> Δ <i>ramB</i> with Genomic Deletion of <i>gdh</i>	[240]
<i>C. glutamicum</i>	Δ <i>ramB</i> Δ <i>glnE</i> Δ <i>gdh</i>	<i>C. glutamicum</i> Δ <i>ramB</i> Δ <i>gdh</i> with Genomic Deletion of <i>glnE</i>	This Work
<i>C. glutamicum</i>	Δ <i>ramB</i> Δ <i>acnR</i>	<i>C. glutamicum</i> Δ <i>ramB</i> with Genomic Deletion of <i>acnR</i>	This Work
<i>C. glutamicum</i>	Δ <i>ramB</i> Δ <i>gdh</i> IDH ^{R453C}	<i>C. glutamicum</i> Δ <i>ramB</i> Δ <i>gdh</i> with Exchange of the Native IDH with IDH ^{R453C}	[240]
<i>C. glutamicum</i>	Δ <i>ramB</i> Δ <i>gdh</i> IDH ^{R453C} _{ATG::GTG}	<i>C. glutamicum</i> Δ <i>ramB</i> Δ <i>gdh</i> with Exchange of the Native IDH with IDH ^{R453C} _{ATG::GTG}	This Work
<i>C. glutamicum</i>	Δ <i>ramB</i> Δ <i>gdh</i> IDH ^{R453C} _{ATG::TTG}	<i>C. glutamicum</i> Δ <i>ramB</i> Δ <i>gdh</i> with exchange of the native IDH with IDH ^{R453C} _{ATG::TTG}	This Work
<i>C. glutamicum</i>	Δ <i>ramB</i> Δ <i>P</i> _{<i>pck</i>} :: <i>P</i> _{<i>dapA</i>-A16}	Exchange of <i>pck</i> Promoter in <i>C. glutamicum</i> Δ <i>ramB</i> with <i>dapA</i> Promoter Version A16	[240]
<i>C. glutamicum</i>	Δ <i>ramB</i> Δ <i>gdh</i> <i>CgLP4</i> :: <i>P</i> _{<i>tacM</i>} - <i>malEcad</i> _{opt}	<i>C. glutamicum</i> Δ <i>ramB</i> Δ <i>gdh</i> with Genomic Integration of <i>P</i> _{<i>tacM</i>} - <i>malEcad</i> _{opt} into Landing Pad 4	This Work

Table A6: Plasmids Used and Generated in this Study.

The table lists the plasmids used in this study, their intended use, and their reference. For plasmids generated in this study, the cloning procedure of the respective backbone and insert, which were ligated by Gibson assembly, is indicated.

Name	Backbone	Insert	Intended use	Source/Ref.
pEKEx2	<i>Kan^R</i> , <i>P_{tac}</i> , <i>lacI^f</i> , <i>oriV_{g.G.}</i> , <i>oriV_{E.c.}</i>	-	<i>E. coli</i> , <i>C. glutamicum</i> Shuttle Vector for IPTG Inducible Genexpression	[81]
pEKEx2-aldA	pEKEx2 cut with BamHI and Sall	Amplification of <i>yqhD</i> with Oligos 77 + 78 from gDNA of <i>E. coli</i> DH5a	Overexpression of <i>aldA</i>	This Work
pEKEx2-cg0354	pEKEx2 cut with BamHI and Sall	Amplification of cg0354 with Oligos 61 + 62 from gDNA of <i>C. glutamicum</i>	Overexpression of cg0354	This Work
pEKEx2-cg1423	pEKEx2 cut with BamHI and Sall	Amplification of cg0354 with Oligos 67 + 68 from gDNA of <i>C. glutamicum</i>	Overexpression of cg1423	This Work
pEKEx2-cg3290	pEKEx2 cut with BamHI and Sall	Amplification of cg0354 with Oligos 63 + 64 from gDNA of <i>C. glutamicum</i>	Overexpression of cg3290	This Work
pEKEx2-cg3412	pEKEx2 cut with BamHI and Sall	Amplification of cg0354 with Oligos 65 + 66 from gDNA of <i>C. glutamicum</i>	Overexpression of cg3412	This Work
pEKEx2-dkgA	pEKEx2 cut with BamHI and Sall	Amplification of <i>dkgA</i> with Oligos 71 + 72 from gDNA of <i>C. glutamicum</i>	Overexpression of <i>dkgA</i>	This Work
pEKEx2-dkgA-yqhD-TPnox	pEKEx2 cut with BamHI and Sall	Amplification of <i>dkgA</i> with Oligos 91 + 92 from pEKEx2- <i>dkgA</i> . Amplification of <i>yqhD</i> with Oligos 93 + 94 from pEKEx2- <i>yqhD</i> . Amplification of <i>TPnox</i> with Oligos 95 + 90 from pET24- <i>TPnox</i> .	Overexpression of <i>dkgA</i> , <i>yqhD</i> and <i>TPnox</i>	This Work
pEKEx2-dld	pEKEx2 cut with BamHI and Sall	Amplification of <i>dkgA</i> with oligos 79 + 80 from gDNA of <i>C. glutamicum</i>	Overexpression of <i>dld</i>	This Work
pEKEx2-gldA-aldA-noxE	pEKEx2 cut with BamHI and Sall	Amplification of <i>gldA</i> with Oligos 96 + 97 from gDNA of <i>C. glutamicum</i> . Amplification of <i>aldA</i> with Oligos 98 + 99 from pEKEx2- <i>aldA</i> . Amplification of <i>noxE</i> with Oligos 100 + 101 from pET28- <i>noxE</i> .	Overexpression of <i>gldA</i> , <i>aldA</i> and <i>noxE</i>	This Work
pEKEx2-hchA	pEKEx2 cut with BamHI and Sall	Amplification of <i>yqhD</i> with Oligos 73 + 74 from gDNA of <i>E. coli</i> DH5a	Overexpression of <i>hchA</i>	This Work
pEKEx2-ldhA	pEKEx2 cut with BamHI and Sall	Amplification of <i>yqhD</i> with Oligos 81 + 82 from gDNA of <i>E. coli</i> DH5a	Overexpression of <i>ldhA</i>	This Work
pEKEx2-malEcad _{opt}	-	-	Overexpression of Codon Optimized <i>cad</i> fused to <i>malE</i>	[205]
pEKEx2-malEcad _{opt} -gltA	pEKEx2- <i>malEcad_{opt}</i> cut with EcoRI	Amplification of <i>gltA</i> with Oligos 39 + 40 from gDNA of <i>C. glutamicum</i>	pEKEx2- <i>malEcad_{opt}</i> with additional Overexpression of <i>gltA</i>	This Work
pEKEx2-malEcad _{opt} -itp1	pEKEx2- <i>malEcad_{opt}</i> cut with EcoRI	Amplification of <i>itp1</i> from pMK- <i>itp1</i> with Oligos 3 + 4	pEKEx2- <i>malEcad_{opt}</i> with additional Overexpression of IA Transporter <i>itp1</i>	This Work
pEKEx2-malEcad _{opt} -mfsA	pEKEx2- <i>malEcad_{opt}</i> cut with EcoRI	Amplification of <i>mfsA</i> from pMK- <i>mfsA</i> with Oligos 5 + 6	pEKEx2- <i>malEcad_{opt}</i> with additional Overexpression of IA Transporter <i>mfsA</i>	This Work
pEKEx2-malEcad _{opt} -noxE	pEKEx2- <i>malEcad_{opt}</i> cut with EcoRI	Amplification of <i>noxE</i> from pET28- <i>noxE</i> with Oligos 13 + 14	pEKEx2- <i>malEcad_{opt}</i> with additional Overexpression of <i>noxE</i>	This Work
pEKEx2-malEcad _{opt} -ramA	pEKEx2- <i>malEcad_{opt}</i> cut with EcoRI	Amplification of <i>ramA</i> from gDNA of <i>C. glutamicum</i> with Oligos 1 + 2	pEKEx2- <i>malEcad_{opt}</i> with additional Overexpression of <i>ramA</i>	[240]
pEKEx2-mshA-hchA	pEKEx2 cut with BamHI and Sall	Amplification of <i>mshA</i> with Oligos 83 + 84 from gDNA of <i>C. glutamicum</i> . Amplification of <i>hchA</i> with Oligos 85 + 86 from pEKEx2- <i>hchA</i> .	Overexpression of <i>mshA</i> and <i>hchA</i>	This Work
pEKEx2-noxE-TPnox	pEKEx2 cut with BamHI and Sall	Amplification of <i>noxE</i> with Oligos 87 + 88 from pET28- <i>noxE</i> . Amplification of <i>TPnox</i> with Oligos 89 + 90 from pET24- <i>TPnox</i> .	Overexpression of <i>noxE</i> and <i>TPnox</i>	This Work
pEKEx2-yqhD	pEKEx2 cut with BamHI and Sall	Amplification of <i>yqhD</i> with Oligos 69 + 70 from gDNA of <i>E. coli</i> DH5a	Overexpression of <i>yqhD</i>	This Work
pEKEx2-yvgN	pEKEx2 cut with BamHI and Sall	Amplification of <i>yqhD</i> with Oligos 75 + 76 from gDNA of <i>B. subtilis</i>	Overexpression of <i>yvgN</i>	This Work
pET24-TPnox	-	-	Template for Amplification of <i>TPnox</i>	[161]
pET28-noxE	-	-	Template for Amplification of <i>noxE</i>	[171]
pK19mobsacB	<i>Kan^R</i> , <i>oriV</i> , <i>sacB</i> , <i>lacZ</i>	-	Genomic Modifications in <i>C. glutamicum</i>	[238]

Appendix

Table A6 continued.

Name	Backbone	Insert	Intended use	Source/Ref.
pK19mobsacB- Δ acnR	pK19mobsaB cut with EcoRI and BamHI	Flank1 Amplified with Oligos 19 + 20 from gDNA of <i>C. glutamicum</i> . Flank 2 Amplified with Oligos 21 + 22 from gDNA of <i>C. glutamicum</i>	Construction of <i>C. glutamicum</i> Δ ramB Δ acnR	This work
pK19mobsacB- Δ cg0354	pK19mobsaB cut with EcoRI and BamHI	Flank1 Amplified with Oligos 45 + 46 from gDNA of <i>C. glutamicum</i> . Flank 2 Amplified with Oligos 47 + 48 from gDNA of <i>C. glutamicum</i> .	Construction of <i>C. glutamicum</i> Δ cg0354	This work
pK19mobsacB- Δ cg1423	pK19mobsaB cut with EcoRI and BamHI	Flank1 Amplified with Oligos 57 + 58 from gDNA of <i>C. glutamicum</i> . Flank2 Amplified with Oligos 59 + 60 from gDNA of <i>C. glutamicum</i> .	Construction of <i>C. glutamicum</i> Δ cg1423	This work
pK19mobsacB- Δ cg2115	-	-	Construction of <i>C. glutamicum</i> Δ cg2115	[35]
pK19mobsacB- Δ cg3290	pK19mobsaB cut with EcoRI and BamHI	Flank1 Amplified with Oligos 49 + 50 from gDNA of <i>C. glutamicum</i> . Flank2 Amplified with Oligos 51 + 52 from gDNA of <i>C. glutamicum</i> .	Construction of <i>C. glutamicum</i> Δ cg3290	This work
pK19mobsacB- Δ cg3412	pK19mobsaB cut with EcoRI and BamHI	Flank1 Amplified with Oligos 53 + 54 from gDNA of <i>C. glutamicum</i> . Flank2 Amplified with Oligos 55 + 56 from gDNA of <i>C. glutamicum</i> .	Construction of <i>C. glutamicum</i> Δ cg3412	This work
pK19mobsacB- Δ gdh	-	-	Construction of <i>C. glutamicum</i> Δ ramB Δ gdh and <i>C. glutamicum</i> Δ ramB Δ glnE Δ gdh	[240]
pK19mobsacB- Δ glnE	pK19mobsaB cut with EcoRI and BamHI	Flank1 Amplified with Oligos 15 + 16 from gDNA of <i>C. glutamicum</i> . Flank 2 Amplified with Oligos 17 + 18 from gDNA of <i>C. glutamicum</i>	Construction of <i>C. glutamicum</i> Δ ramB Δ glnE	[240]
pK19mobsacB- Δ P _{gltA} ::P _{dapA} -A16	-	-	Template for amplification of P _{dapA} -A16	[279]
pK19mobsacB- Δ P _{gltA} ::P _{dapA} -A8	-	-	Template for amplification of P _{dapA} -A8	[279]
pK19mobsacB- Δ P _{gltA} ::P _{dapA} -C5	-	-	Template for amplification of P _{dapA} -C5	[279]
pK19mobsacB- Δ P _{gltA} ::P _{dapA} -C7	-	-	Template for amplification of P _{dapA} -C7	[279]
pK19mobsacB- Δ P _{pck} ::P _{dapA} -A16	pK19mobsaB cut with EcoRI and BamHI	Flank1 Amplified with Oligos 7 + 8 from gDNA of <i>C. glutamicum</i> . Flank2 Amplified with Oligos 9 + 10 from gDNA of <i>C. glutamicum</i> . Promoter Fragment Amplified with Oligos 11 + 12 from pK19mobsacB- Δ P _{gltA} ::P _{dapA} -A16	Construction of <i>C. glutamicum</i> Δ P _{pck} ::P _{dapA} -A16 IDH ^{R453C} and <i>C. glutamicum</i> Δ ramB Δ P _{pck} ::P _{dapA} -A16	[240]
pK19mobsacB- Δ P _{pck} ::P _{dapA} -A8	pK19mobsaB cut with EcoRI and BamHI	Flank1 Amplified with Oligos 7 + 8 from gDNA of <i>C. glutamicum</i> . Flank2 Amplified with Oligos 9 + 10 from gDNA of <i>C. glutamicum</i> . Promoter Fragment Amplified with Oligos 11 + 12 from pK19mobsacB- Δ P _{gltA} ::P _{dapA} -A8	Construction of <i>C. glutamicum</i> Δ P _{pck} ::P _{dapA} -A8 IDH ^{R453C}	[240]
pK19mobsacB- Δ P _{pck} ::P _{dapA} -C5	pK19mobsaB cut with EcoRI and BamHI	Flank1 Amplified with Oligos 7 + 8 from gDNA of <i>C. glutamicum</i> . Flank2 Amplified with Oligos 9 + 10 from gDNA of <i>C. glutamicum</i> . Promoter Fragment Amplified with Oligos 11 + 12 from pK19mobsacB- Δ P _{gltA} ::P _{dapA} -C5	Construction of <i>C. glutamicum</i> Δ P _{pck} ::P _{dapA} -C5 IDH ^{R453C}	[240]
pK19mobsacB- Δ P _{pck} ::P _{dapA} -C7	pK19mobsaB cut with EcoRI and BamHI	Flank1 Amplified with Oligos 7 + 8 from gDNA of <i>C. glutamicum</i> . Flank2 Amplified with Oligos 9 + 10 from gDNA of <i>C. glutamicum</i> . Promoter Fragment Amplified with Oligos 11 + 12 from pK19mobsacB- Δ P _{gltA} ::P _{dapA} -C7	Construction of <i>C. glutamicum</i> P _{pck} ::P _{dapA} -C7 IDH ^{R453C}	[240]
pK19mobsacB-CgLP12::P _{tuf} -malEcad _{opt}	pK19mobsaB cut with EcoRI and BamHI	Flank1 Amplified with Oligos 33 + 34 from gDNA of <i>C. glutamicum</i> . Flank2 Amplified with Oligos 35 + 36 from gDNA of <i>C. glutamicum</i> . <i>tuf</i> Promoter Amplified with Oligos 37 + 31 from gDNA of <i>C. glutamicum</i> . <i>malEcad</i> _{opt} Amplified with Oligos 32 + 38 from pEKEx2- <i>malEcad</i> _{opt}	Construction of <i>C. glutamicum</i> CgLP12::P _{tuf} -malEcad _{opt} , <i>C. glutamicum</i> IDH ^{R453C}	This work
pK19mobsacB-CgLP4::P _{tacM} -malEcad _{opt}	pK19mobsaB cut with EcoRI and BamHI	Flank1 Amplified with Oligos 23 + 24 from gDNA of <i>C. glutamicum</i> . Flank2 Amplified with Oligos 25 + 26 from gDNA of <i>C. glutamicum</i> . <i>malEcad</i> _{opt} Amplified with Oligos 27 + 28 from pEKEx2- <i>malEcad</i> _{opt}	Construction of <i>C. glutamicum</i> Δ ramB Δ gdh CgLP12::P _{tacM} -malEcad _{opt}	This work

Table A6 continued.

Name	Backbone	Insert	Intended use	Source/Ref.
pK19 <i>mobsacB</i> - <i>CgLP4</i> :: <i>P_{tuf}</i> - <i>malEcad_{opt}</i>	pK19 <i>mobsaB</i> cut with EcoRI and BamHI	Flank1 Amplified with Oligos 23 + 29 from gDNA of <i>C. glutamicum</i> . Flank2 Amplified with Oligos 25 + 26 from gDNA of <i>C. glutamicum</i> . <i>tuf</i> Promoter Amplified with Oligos 30 + 31 from gDNA of <i>C. glutamicum</i> . <i>malEcad_{opt}</i> Amplified with Oligos 32 + 28 from pEKEx2- <i>malEcad_{opt}</i>	Construction of <i>C. glutamicum CgLP4</i> :: <i>P_{tuf}</i> - <i>malEcad_{opt}</i>	This work
pK19 <i>mobsacB</i> -IDH ^{A94D}	-	-	Construction of <i>C. glutamicum</i> IDH ^{A94D}	[242]
pK19 <i>mobsacB</i> -IDH ^{A94D} _{ATG::GTG}	-	Whole Plasmid PCR of pK19 <i>mobsacB</i> -IDH ^{A94D} with Oligos 41 + 42	Construction of <i>C. glutamicum</i> IDH ^{A94D} _{ATG::GTG}	This work
pK19 <i>mobsacB</i> -IDH ^{A94D} _{ATG::TTG}	-	Whole Plasmid PCR of pK19 <i>mobsacB</i> -IDH ^{A94D} with Oligos 43 + 44	Construction of <i>C. glutamicum</i> IDH ^{A94D} _{ATG::TTG}	This work
pK19 <i>mobsacB</i> -IDH _{ATG::GTG}	-	Whole Plasmid PCR of pK19 <i>mobsacB</i> -IDH ^{G407S} and pK19 <i>mobsacB</i> -IDH ^{R453C} with Oligos 41 + 42.	Construction of <i>C. glutamicum</i> IDH ^{G407S} _{ATG::GTG} and <i>C. glutamicum</i> IDH ^{R453C} _{ATG::GTG}	This work
pK19 <i>mobsacB</i> -IDH _{ATG::TTG}	-	Whole Plasmid PCR of pK19 <i>mobsacB</i> -IDH ^{G407S} and pK19 <i>mobsacB</i> -IDH ^{R453C} with Oligos 43 + 44.	Construction of <i>C. glutamicum</i> IDH ^{G407S} _{ATG::TTG} and <i>C. glutamicum</i> IDH ^{R453C} _{ATG::TTG}	This work
pK19 <i>mobsacB</i> -IDH ^{G407S}	-	-	Construction of <i>C. glutamicum</i> IDH ^{G407S}	[242]
pK19 <i>mobsacB</i> -IDH ^{R453C}	-	-	Construction of <i>C. glutamicum</i> IDH ^{R453C}	[242]
pMK- <i>ipt1</i>	-	-	Plasmid with Codon Optimized Version of <i>ipt1</i>	This work, Synthesized by GeneArts
pMK- <i>msfA</i>	-	-	Plasmid with Codon Optimized Version of <i>msfA</i>	This work, Synthesized by GeneArts

Appendix

Table A7: Primers and Oligonucleotides Used in this Study.

The table lists the primers used in this study and their intended use. Primers were ordered from Sigma-Aldrich Chemie GmbH; Taufkirchen, Germany. Binding regions are shown in bold.

No.	Sequence	Intended use
1	TGAAGTCCCCACTGGTGTAAAGAATTCCTGCAGAAGGAGATCAGT GGA-TACCCAGCGGATTAAG	Gibson Primer, Amplification of <i>ramA</i>
2	GCTGTAAAACGACGGCCAGTGAATTC TAAAGGCAGGCGCCGATCC	Gibson Primer, Amplification of <i>ramA</i>
3	TGAAGTCCCCACTGGTGTAAAGAGCTCGAAAGGAGAGGATTGAT GGAT-CAGGCAGATCACTC	Gibson Primer, Amplification of <i>itp1</i>
4	CTGTAAAACGACGGCCAGTGAATTC TAGGAGTGCTTGCGTGCTGCC	Gibson Primer, Amplification of <i>itp1</i>
5	TGAAGTCCCCACTGGTGTAAAGAGCTCGAAAGGAGAGGATTGAT GTCC-CACGGCGATAC	Gibson Primer, Amplification of <i>msfA</i>
6	CTGTAAAACGACGGCCAGTGAATTC TACTGAGTTGGCATGTTGAAG	Gibson Primer, Amplification of <i>msfA</i>
7	CAGGTGCACTCTAGAGGATCCT TGCCCTCTGGGTTGATC	Gibson Primer, Amplification of <i>pck</i> Flank 1
8	TAAGACCGGAGCCGCTCGAGAAATCT GAGAGAAGTAATGACTACTG	Gibson Primer, Amplification of <i>pck</i> Flank 1
9	TAAGTGCAGAACCAATGCATCT GCCATCACAATCCAAGC	Gibson Primer, Amplification of <i>pck</i> Flank 2
10	GAGCTCGGTACCCGGGGATCC CACAACAATAAATCCCCACAG	Gibson Primer, Amplification of <i>pck</i> Flank 2
11	TGCTTGGATTGTGATGGCAGATGC ATTGGTTCTGCAGTTATC	Gibson Primer, Amplification of <i>P_{dapA}-A8/A16/C5/C7</i>
12	GTCATTACTTCTCAGATTTCT CGAGCGGCTCCG	Gibson Primer, Amplification of <i>P_{dapA}-A8/A16/C5/C7</i>
13	TGAAGTCCCCACTGGTGTAAAGAATTCGAAAT GAAAATCGTAGTTATCG-GTACG	Gibson Primer, Amplification of <i>noxE</i>
14	GCTGTAAAACGACGGCCAGTGAATTTTT TGCATTTAAAGCTGCAAC	Gibson Primer, Amplification of <i>noxE</i>
15	TTGGGGCTCCCACCACCTAC AGCTTCTCCCCTCCTTC	Gibson Primer, Amplification of <i>glnE</i> Flank 1
16	CCTGCAGGTCGACTCTAGAGGATC ATGCGCTCACCATGGCCGACAAC	Gibson Primer, Amplification of <i>glnE</i> Flank 1
17	GATGAAGGAGGGGAGAAGCT GTAGGTGGTGGGAGCC	Gibson Primer, Amplification of <i>glnE</i> Flank 2
18	GTTGTAAAACGACGGCCAGTGAAT ATCAGATGCTTCATCCAGC	Gibson Primer, Amplification of <i>glnE</i> Flank 2
19	GCCTGCAGGTCGACTCTAGAGGATCC GCACGGTGTGGAACG	Gibson Primer, Amplification of <i>acnR</i> Flank 1
20	AAGTGTGAATCAGGGTCTG TAATGTACTCCTATGGAATAAGCG	Gibson Primer, Amplification of <i>acnR</i> Flank 1
21	ATTTCCATAGGAGTACATT ACGACCCCTGATTCACAC	Gibson Primer, Amplification of <i>acnR</i> Flank 2
22	GTTGTAAAACGACGGCCAGTGAATC AGCTCTGGGAGTTGGTG	Gibson Primer, Amplification of <i>acnR</i> Flank 2
23	CCTGCAGGTCGACTCTAGAGGATC AAAGGCACTGCCCACTATG	Gibson Primer, Amplification of <i>CgLP4</i> Flank1
24	TTTTAATTCTGTTTCTGTGTGAAATTTGTTATCCGCTCACAAATCCACAC- ATGGTACCACACGATGATTAATTGTCAACAGCTCACATCAAAAATCC- GCCGTTCC	Gibson Primer, Amplification of <i>CgLP4</i> Flank1
25	CGTTTCTACAAACTCTTTT GACTAAGTGAGTTTGGATGCG	Gibson Primer, Amplification of <i>CgLP4</i> Flank2
26	GAGCTCGGTACCCGGGGATC GAGAGCTTCCATAACCAGC	Gibson Primer, Amplification of <i>CgLP4</i> Flank2
27	GGATAACAATTTACACAGGAAACAGAATTAAGATATGACCATGAT- TACGCCAAGCTTGCATGC CTCGCAAAGGAGAGGATTGATGAAAACCT- GAAGAAGGTAACCTGG	Gibson Primer, Amplification of <i>malEcad_{opt}</i>
28	CGCATCCAAACTCACTTAGT CAAAAGAGTTTGTAGAAACGC	Gibson Primer, Amplification of <i>malEcad_{opt}</i>
29	AACTACCAGCTACCCTGTGGC ATCAAAAATCCGCCGTTCC	Gibson Primer, Amplification of <i>CgLP4</i> Flank1
30	GGAACGGCGGATTTTTT GATGCCACAGGGTAGCTGGTAG	Gibson Primer, Amplification of <i>P_{tuf}</i>
31	GTTTACCTTCTTCAGTTTT CATTGTATGTCCTCCTGGACTTC	Gibson Primer, Amplification of <i>P_{tuf}</i>
32	CCACGAAGTCCAGGAGGACATACA TGAAAACCTGAAGAAGGTAAC	Gibson Primer, Amplification of <i>malEcad_{opt}</i>
33	CCTGCAGGTCGACTCTAGAGGATC GACACCCTGATGTTACCG	Gibson Primer, Amplification of <i>CgLP12</i> Flank1
34	AACTACCAGCTACCCTGTGGA AATATGCCGATTGCAAGAAACG	Gibson Primer, Amplification of <i>CgLP12</i> Flank1
35	CGTTTCTACAAACTCTTTT GCACTCAAAAATGTTGAAATCAG	Gibson Primer, Amplification of <i>CgLP12</i> Flank2
36	GAGCTCGGTACCCGGGGATC CTCCTCGTTGTTCCGAGC	Gibson Primer, Amplification of <i>CgLP12</i> Flank2
37	CGTTTCTTGAATCGGCATATT CCACAGGGTAGCTGGTAG	Gibson Primer, Amplification of <i>P_{tuf}</i>
38	GATTTCAACATTTTT TGACTGCAAAAGAGTTTGTAGAAACGC	Gibson Primer, Amplification of <i>malEcad_{opt}</i>
39	AAAACGACGGCCAGTGAATC TAGCGCTCCTCGCG	Gibson Primer, Amplification of <i>gltA</i>
40	GAAGTCCCCACTGGTGTAAAGAGCTCGAAAGGAGAGGATTGAT GTTTG- AAAGGGATATCGTGG	Gibson Primer, Amplification of <i>gltA</i>

Table A7 continued.

No.	Sequence	Intended use
41	CGGGTCCAGATGATCTTAGCCACGAGTCTCCTTGGTTG	Amplification of pK19 <i>mobsacB</i> -IDH ^{A94D} , pK19 <i>mobsacB</i> -IDH ^{G407S} and pK19 <i>mobsacB</i> -IDH ^{R453C} , Start Codon Mutation ATG::GTG
42	ATCAACCAAGGAGACTCGTGGCTAAGATCATCTGGACCCG	Amplification of pK19 <i>mobsacB</i> -IDH ^{A94D} , pK19 <i>mobsacB</i> -IDH ^{G407S} and pK19 <i>mobsacB</i> -IDH ^{R453C} , Start Codon Mutation ATG::GTG
43	CGGGTCCAGATGATCTTAGCCAGAGTCTCCTTGGTTGATG	Amplification of pK19 <i>mobsacB</i> -IDH ^{A94D} , pK19 <i>mobsacB</i> -IDH ^{G407S} and pK19 <i>mobsacB</i> -IDH ^{R453C} , Start Codon Mutation ATG::TTG
44	ATCAACCAAGGAGACTCTGGCTAAGATCATCTGGACCCGC	Amplification of pK19 <i>mobsacB</i> -IDH ^{A94D} , pK19 <i>mobsacB</i> -IDH ^{G407S} and pK19 <i>mobsacB</i> -IDH ^{R453C} , Start Codon Mutation ATG::TTG
45	CCTGCAGGTCGACTCTAGAGGATCACTTAAGGGTATGGTTCCATTAC	Gibson Primer, Amplification of cg0354 Flank1
46	CACAGCGGTTTCGAGGTCATTTGTTTTCTACATTCTGCCATTTTC	Gibson Primer, Amplification of cg0354 Flank1
47	GGCAGGAATGTAGAAAACAAATGACCTCGAAACCGCTG	Gibson Primer, Amplification of cg0354 Flank2
48	GAGCTCGGTACCCGGGGATCTAGATCGTTCGATTTTAGGC	Gibson Primer, Amplification of cg0354 Flank2
49	ACGAGGAGAGGAAGCACACGCTAACCAGACAACGCGG	Gibson Primer, Amplification of cg3290 Flank1
50	CCTGCAGGTCGACTCTAGAGGATCCGGTGAGTGGGCATTTTC	Gibson Primer, Amplification of cg3290 Flank1
51	TCACCGCGTTGTCTGGTTAGCGTGTGCTTCTCTCTCTC	Gibson Primer, Amplification of cg3290 Flank2
52	GAGCTCGGTACCCGGGGATCACGTCGTGCGGGC	Gibson primer, amplification of cg3290 Flank2
53	CCTGCAGGTCGACTCTAGAGATAACGAATGCGTAATTAACCAC	Gibson primer, amplification of cg3412 Flank1
54	TCAGGACTTCCCATGAGTGAAGATGCTTCTCGACGC	Gibson primer, amplification of cg3412 Flank1
55	TTTGCCTCGAGAAGCATCTTCACTCATGGGAAGTCTTG	Gibson primer, amplification of cg3412 Flank2
56	GAGCTCGGTACCCGGGGATCTCGATATTTGGGGCGACG	Gibson primer, amplification of cg3412 Flank2
57	CCTGCAGGTCGACTCTAGAGGGTCTAGTGTGTGTTTCATGATC	Gibson primer, amplification of cg1423 Flank1
58	AAGTGTGTTGATGGGTTAGTGTGCTCAGTTTGTCTCG	Gibson primer, amplification of cg1423 Flank1
59	AACGAGACAACTGAGCACACTAACCATCAACATCAGTTTG	Gibson primer, amplification of cg1423 Flank2
60	GAGCTCGGTACCCGGGGATCGCAAAGTGTCCAGTTGAATG	Gibson primer, amplification of cg3412 Flank2
61	AAGCTTGCATGCCTGCAGGTCGAGAAGGAGATCAATGACAAGCAGTG-CAAAGTG	Gibson Primer, Amplification of cg0354
62	GAGCTCGGTACCCGGGGATCTTACGCATTCTGCAGCG	Gibson Primer, Amplification of cg0354
63	AAGCTTGCATGCCTGCAGGTCGAGAAGGAGATCAATGTGCGAAGGTAT-ACGTGTCC	Gibson Primer, Amplification of cg3290
64	GAGCTCGGTACCCGGGGATCTTAGTCTGGGAGGTGATG	Gibson Primer, Amplification of cg3290
65	AAGCTTGCATGCCTGCAGGTCGAGAAGGAGATCAATGAGTGAGTTTG-GCCTG	Gibson Primer, Amplification of cg3412
66	GAGCTCGGTACCCGGGGATCTTAAAAACGACGTTGACCAG	Gibson Primer, Amplification of cg3412
67	AAGCTTGCATGCCTGCAGGTCGAGAAGGAGATCAATGGCTGTCATGG-CATATC	Gibson Primer, Amplification of cg1423
68	GAGCTCGGTACCCGGGGATCTTAGTTTTGCGGGTTTTGG	Gibson Primer, Amplification of cg1423
69	CAAGCTTGCATGCCTGCAGGTCGACCTGCAGAAGGAGATCAATGAAC-AACTTTAATCTGCACACC	Gibson Primer, Amplification of <i>yqhD</i>
70	AATTCGAGCTCGGTACCCGGGGATCCTTAGCGGGCGGCTTC	Gibson Primer, Amplification of <i>yqhD</i>
71	CAAGCTTGCATGCCTGCAGGTCGACCTGCAGAAGGAGATCAATGTCT-GTTGTGGGTACCG	Gibson Primer, Amplification of <i>dkgA</i>
72	AATTCGAGCTCGGTACCCGGGGATCCCTAGTTCAGATCATTGGGTG	Gibson Primer, Amplification of <i>dkgA</i>
73	CAAGCTTGCATGCCTGCAGGTCGACCTGCAGAAGGAGATCAATGACT-GTTCAAACAAGTAAAAATCC	Gibson Primer, Amplification of <i>hchA</i>
74	AATTCGAGCTCGGTACCCGGGGATCCTTAAACCGCGTAAGCTGC	Gibson Primer, Amplification of <i>hchA</i>
75	CAAGCTTGCATGCCTGCAGGTCGACCTGCAGAAGGAGATCAGTGCCA-ACAAGTTTAAAAGATACTG	Gibson Primer, Amplification of <i>yvgN</i>
76	AATTCGAGCTCGGTACCCGGGGATCCTTAAACAGAAAGCTCATCAGG	Gibson Primer, Amplification of <i>yvgN</i>
77	CAAGCTTGCATGCCTGCAGGTCGACCTGCAGAAGGAGATCAATGTCA-GTACCCGTTCAAC	Gibson Primer, Amplification of <i>aldA</i>
78	AATTCGAGCTCGGTACCCGGGGATCCTTAAAGACTGTAAATAAACAC-CTGG	Gibson Primer, Amplification of <i>aldA</i>

Appendix

Table A7 continued.

No.	Sequence	Intended use
79	CAAGCTTGCATGCCTGCAGGTCGACCTGCAGAAGGAGATCAATGACG- CAACCAGGACAG	Gibson Primer, Amplification of <i>dld</i>
80	AATTCGAGCTCGGTACCCGGGGATCCTTAGGCCAGTCTCTGTG	Gibson Primer, Amplification of <i>dld</i>
81	CAAGCTTGCATGCCTGCAGGTCGACCTGCAGAAGGAGATCAATGAAA- CTCGCGGTTTATAGC	Gibson Primer, Amplification of <i>ldhA</i>
82	AATTCGAGCTCGGTACCCGGGGATCCTTAAACCAGTTCGTTCCGGG	Gibson Primer, Amplification of <i>ldhA</i>
83	CTTGCATGCCTGCAGGTCGAGAAGGAGATCAATGCGCGTAGCTATGA- TTCC	Gibson Primer, Amplification of <i>mshA</i>
84	GGATTTTTACTTGTGTTGAACAGTCATTGATCTCCTTCTCGACCTGCAGG- CTTAGCCGTGATGCGTTTCAC	Gibson Primer, Amplification of <i>mshA</i>
85	GTGAAACGCATCACGGCTAAGCCTGCAGGTCGAGAAGGAGATCAATG- ACTGTTCAAACAAGTAAAAATCC	Gibson Primer, Amplification of <i>hchA</i>
86	GAGCTCGGTACCCGGGGATCCTTAAACCAGTTCGTTCCGGG	Gibson Primer, Amplification of <i>hchA</i>
87	CTTGCATGCCTGCAGGTCGAGAAGGAGATCAATGAAAATCGTAGTTA- TCGGTACG	Gibson Primer, Amplification of <i>noxE</i>
88	CCAACAACGGTAACCTTTCATTGATCTCCTTCTGCAGGTCGTTATTTTGC- ATTTAAAGCTGCAAC	Gibson Primer, Amplification of <i>noxE</i>
89	GTTGCAGCTTTAAATGCAAATAACGACCTGCAGAAGGAGATCAATGA- AAGTACCGTTGTTGG	Gibson Primer, Amplification of <i>TPnox</i>
90	GAGCTCGGTACCCGGGGATCCTTACTCGAGTGCATTAACGCTC	Gibson Primer, Amplification of <i>TPnox</i>
91	CTTGCATGCCTGCAGGTCGAGAAGGAGATCAATGTCTGTTGTGGGTA- CCGG	Gibson Primer, Amplification of <i>dkgA</i>
92	GGTGTGCAGATTAAGTTGTTTCATTGATCTCCTTCTGCAGGTCGACCT- GCAGGCCTAGTTTCAGATCAATCGGGTGTG	Gibson Primer, Amplification of <i>dkgA</i>
93	AAGGAGATCAATGAACAACCTTAATCTGCACACC	Gibson Primer, Amplification of <i>yqhD</i>
94	TCGACCTGCAGGCTTAGCGGGCGGGTTCG	Gibson Primer, Amplification of <i>yqhD</i>
95	CGAAGCCGCCCGCTAAGCCTGCAGGTCGACCTGCAGAAGGAGATCAA- TGAAAGTTACCGTTGTTGG	Gibson Primer, Amplification of <i>TPnox</i>
96	CTTGCATGCCTGCAGGTCGAGAAGGAGATCAATGGACCGCATTATTC- AATCACC	Gibson Primer, Amplification of <i>gldA</i>
97	GGATGTTGAACGGGACTGACATTGATCTCCTTCTGCAGGTCGTTATT- CCCCTTTGCAGGAAACG	Gibson Primer, Amplification of <i>gldA</i>
98	CGTTTCCTGCAAGAGTGGGAATAACGACCTGCAGAAGGAGATCAATG- TCAGTACCCGTTCAACATCC	Gibson Primer, Amplification of <i>aldA</i>
99	GGTTCGTACCGATAACTACGATTTTCATTGATCTCCTTCTGCAGGTCGT- TAAGACTGTAATAAACCCACCTGGGTC	Gibson Primer, Amplification of <i>aldA</i>
100	GACCCAGGTGGTTTATTTACAGTCTTAACGACCTGCAGAAGGAGATCA- ATGAAAATCGTAGTTATCGGTACGAACC	Gibson Primer, Amplification of <i>noxE</i>
101	GAGCTCGGTACCCGGGGATCCTTATTTGCATTTAAAGCTGCAACAGTC	Gibson Primer, Amplification of <i>noxE</i>
102	CACCTCCTTCATGGTGTC	Sequencing <i>mfsA</i>
103	TCCGCAATCGCAATTGG	Sequencing <i>itp1</i>
104	CACTCCGTTCTGGATAATG	Sequencing pEKEx2
105	GCTACGGCGTTTCACTTCTG	Sequencing pEKEx2
106	TCAGTGAGCGAGGAAGCG	Sequencing pK19 <i>mobsacB</i>
107	ATGACCATGATTACGCCAAGCTTG	Sequencing pK19 <i>mobsacB</i>
108	TTAGCAGCCCTGCGCC	Sequencing pK19 <i>mobsacB</i>
109	CGTTACCCCAAAGGTTATATCC	Sequencing of <i>pck</i> promoter
110	GGATATAACCTTTGGGGTAACG	Sequencing of <i>pck</i> promoter
111	GTTGATGGATCCCAGGCTGAGTG	Validation of <i>pck</i> deletion
112	GAACTGGCTGTGAACCTCTGCAG	Validation of <i>pck</i> deletion
113	AGCAAGAGTGAATAATTGCAGG	Sequencing <i>noxE</i>
114	CGGTCGCCCAATTGAGGAG	Validation of <i>gdh</i> deletion
115	TTCCAGTCAGCGCAAAGGG	Validation of <i>gdh</i> deletion
116	TACTGCGGTGATCAACG	Sequencing <i>malEcad_{opt}</i>
117	TGGTGCCCCAACTTTTGG	Sequencing <i>CgLP12</i>
118	CTGGAGCTCTACCTGGCTCT	Sequencing <i>CgLP4</i>
119	CTCACGCCGCGCCATTTTT	Validation <i>CgLP4</i>
120	GCAAATCATCTTGAAGATGCTTGATCTC	Validation <i>CgLP4</i>
121	ATCCTCAAGCTGCAGAACAC	Validation <i>CgLP12</i>

Table A7 continued.

No.	Sequence	Intended use
122	AAGAGGAGATCCGAGAGAAGGTC	Validation <i>CgLP12</i>
123	ACCTGATTA AAAACAAACAC	Sequencing <i>malEcad_{opt}</i>
124	ATGACCAAGCAGTCCGCAGA	Sequencing <i>malEcad_{opt}</i>
125	TGCACCCAGGCATGCGGTCT	Sequencing <i>malEcad_{opt}</i>
126	ATCTGCGGACTGCTTGGTCAT	Sequencing <i>malEcad_{opt}</i>
127	GAACGCATCCTGCACAAGTACC	Sequencing <i>malEcad_{opt}</i>
128	TTTTGGCGGATGAGAGAAGATTTTC	Sequencing pEKE _{x2}
129	TTGTGCAATTTGACACGC	Sequencing <i>aldA</i>
130	TGGTTCTGGAAAATGCGC	Sequencing <i>gldA</i>
131	CGCTGAACGTTTGATTGG	Sequencing <i>yqhD</i>
132	TTACTTCTTCAGTGCCTCAACG	Sequencing <i>icd</i>
133	ATGGCTAAGATCATCTGGACC	Sequencing <i>icd</i>
134	TGTAGTCACGCAGAACGTTACC	Sequencing <i>icd</i>
135	TCTTTAATGTCGTA CTGCGG	Sequencing <i>malEcad_{opt}</i>
136	GTTGTCGCGGCAATGATTGACG	Validation cg2115 (<i>sugR</i>) deletion
137	CTCACCACATCCACAAACCACGC	Validation cg2115 (<i>sugR</i>) deletion

Appendix

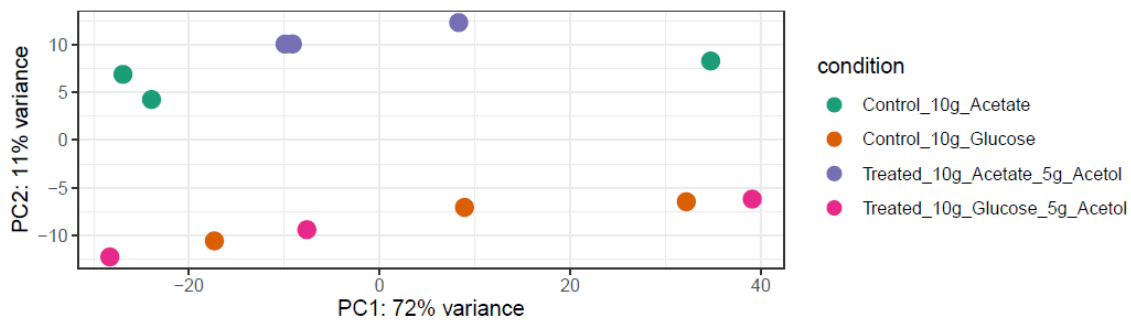


Figure A1: Principal Component Analysis Plot of Transcriptome Sequencing.

The plot of principal component analysis was generated and provided by Dr. Richa Bharti (TUM Campus Straubing; Straubing, Germany). Each point refers to a single biological replicate, cultured under the respective conditions indicated in the legend on the right side.

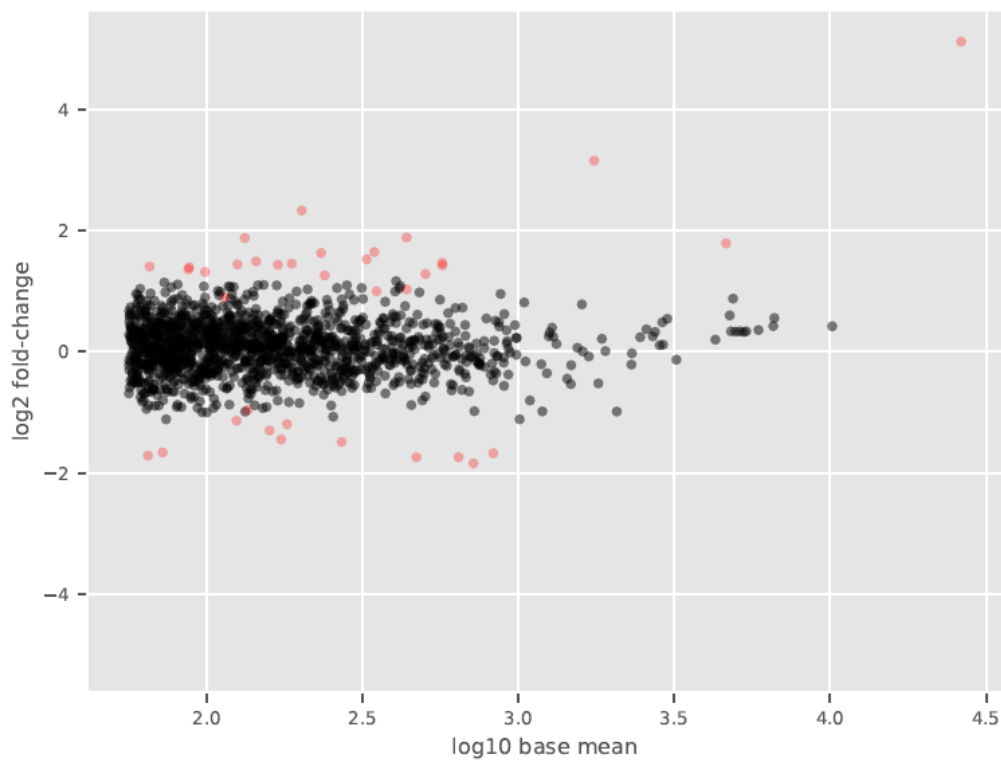


Figure A2: MA Plot of Acetate vs Glucose.

MA plot was generated and provided by Dr. Richa Bharti (TUM Campus Straubing; Straubing, Germany). Each point refers to the changes in the expression of one gene. Red points mark genes with log₂ fold-change ± 1 and (adjusted) p-value of < 0.05 .

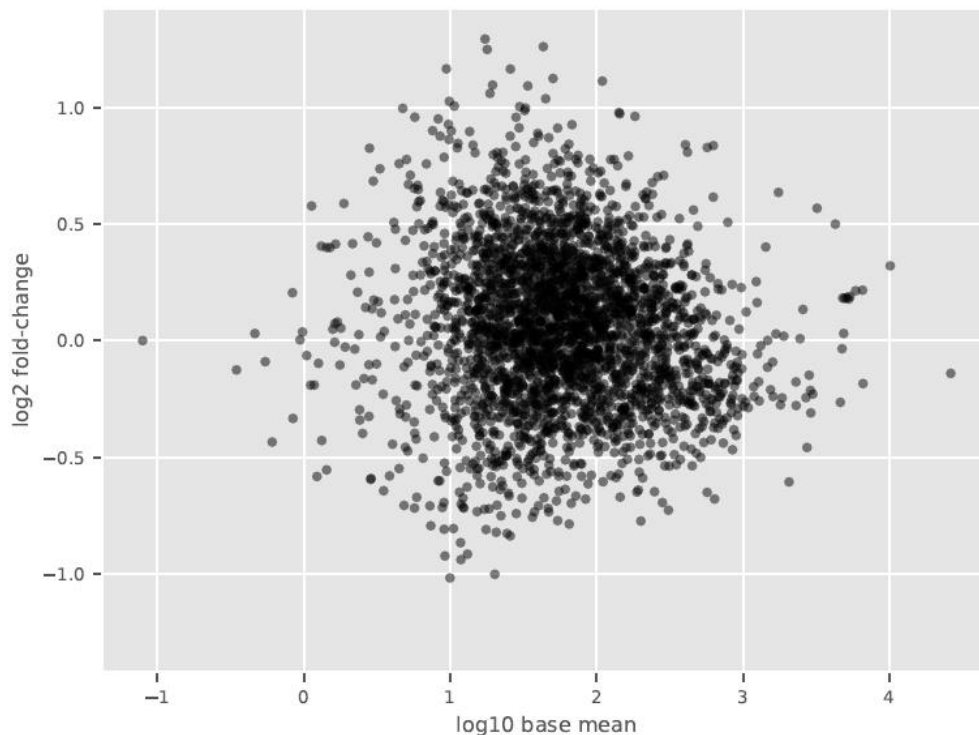


Figure A3: MA Plot of Acetate vs Acetate plus Acetol.

MA plot was generated and provided by Dr. Richa Bharti (TUM Campus Straubing; Straubing, Germany). Each point refers to the changes in the expression of one gene. Red points mark genes with $\log_2(\text{fold-change}) \pm 1$ and (adjusted) p-value of < 0.05 .

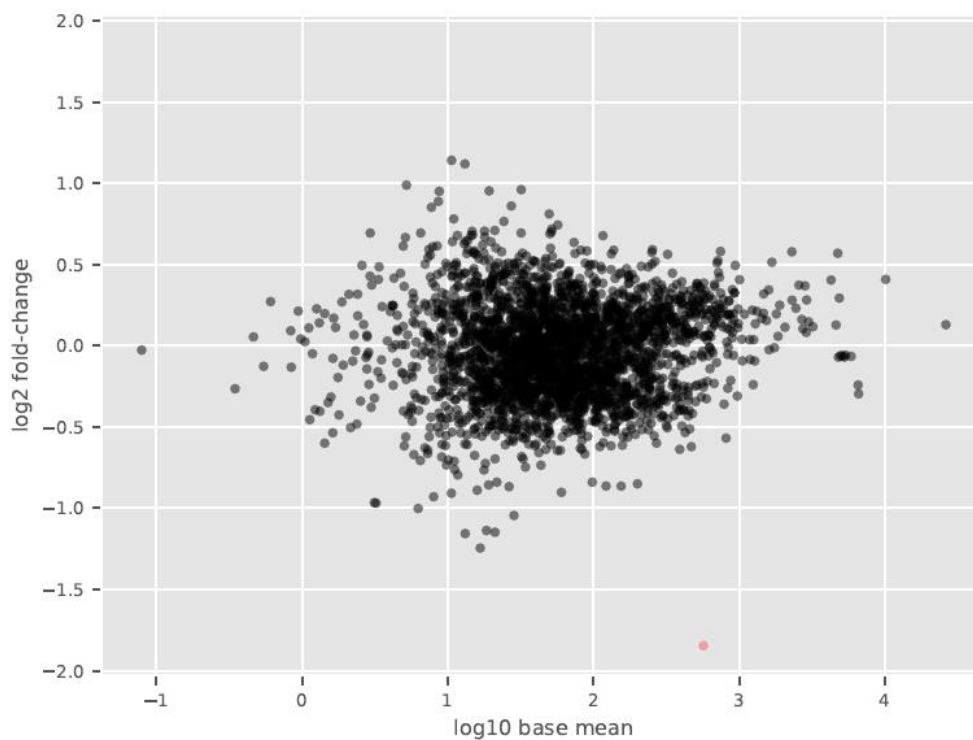


Figure A4: MA Plot of Glucose vs Glucose plus Acetol.

MA plot was generated and provided by Dr. Richa Bharti (TUM Campus Straubing; Straubing, Germany). Each point refers to the changes in the expression of one gene. Red points mark genes with $\log_2(\text{fold-change}) \pm 1$ and (adjusted) p-value of < 0.05 .